Randall-Sundrum Models vs. Supersymmetry: the Different Flavor Signatures

Dissertation von

Stefania Gori

Juli 2010

Lehrstuhl T31 Prof. A. J. Buras
Technische Universität München
Physik Department
James-Franck-Strasse 2
D-85748, Garching

Max-Planck-Institut für Physik
Werner-Heisenberg-Institut
Föhringer Ring 6
D-80805, München

TECHNISCHE UNIVERSITÄT MÜNCHEN

Lehrstuhl T31 Prof. A. J. Buras
Physik Department
James-Franck-Strasse 2
D-85748, Garching

Max-Planck-Institut für Physik
Werner-Heisenberg-Institut
Föhringer Ring 6
D-80805, München

Randall-Sundrum Models vs. Supersymmetry: the Different Flavor Signatures

Stefania Gori

Vollständiger Abdruck der von der Fakultät für Physik der Technischen Universität München zur Erlangung des akademischen Grades eines

Doktors der Naturwissenschaften (Dr. rer. nat.)

genehmigten Dissertation.

Vorsitzender:	Univ.-Prof. Dr. Stephan Paul
Prüfer der Dissertation:	1. Univ.-Prof. Dr. Andrzej J. Buras
	2. Hon.-Prof. Dr. Wolfgang F. L. Hollik

Die Dissertation wurde am 06.07.2010 bei der Technischen Universität München eingereicht und durch die Fakultät für Physik am 19.07.2010 angenommen.

Preface

Abstract

The Minimal Supersymmetric Standard Model based on flavor symmetries and models with a warped extra dimension as first proposed by Randall and Sundrum represent two of the best founded theories beyond the Standard Model. They provide two appealing solutions both to the gauge hierarchy problem and to the Standard Model flavor hierarchy problems. In this thesis we focus on a particular Randall-Sundrum model based on the custodial symmetry $SU(2)_L \times SU(2)_R \times P_{LR}$ in the bulk and on two Supersymmetric flavor models: the one based on a $U(1)$ abelian flavor symmetry, the other on a $SU(3)$ non abelian flavor symmetry. We first analyze and compare the flavor structure of the two frameworks, showing two possible ways to address the New Physics flavor problem: warped geometry and custodial protection vs. flavor symmetry. Subsequently, we study the impact of the new particles (Kaluza-Klein states in the Randall-Sundrum model and superpartners in Supersymmetry) in the K and B meson mixings and rare decays. We perform a global numerical analysis of the new physics effects in the models in question and we show that it is possible to naturally be in agreement with all the available data on $\Delta F = 2$ observables, even fixing the energy scale of the models to the TeV range, in order to have new particles in the reach of the LHC. We then study distinctive patterns of flavor violation which can enable future experiments to distinguish the two frameworks. In particular, the specific correlations between the CP violating asymmetry in the $B_s^0 - \bar{B}_s^0$ system, the rare decays $B_{s,d} \to \mu^+\mu^-$ and $K \to \pi\nu\bar{\nu}$ allow in principle for an experimental test of the Randall-Sundrum model and of the two Supersymmetric flavor models and a clear distinction between the two frameworks, once new data will be available.

Zusammenfassung

Minimale Supersymmetrische Erweiterungen des Standard Modells mit Flavor Symmetrien und Modelle mit einer gekrümmten Extradimension, wie sie zuerst von Randall und Sundrum vorgeschlagen wurden, stellen zwei der am besten motivierten Theorien jenseits des Standard Models dar. Sie bieten attraktive Lösungen sowohl für das Eichhierarchieproblem als auch für die Flavorhierarchieprobleme des Standard Models. In dieser Doktorarbeit konzentrieren wir uns auf ein bestimmtes Randall-Sundrum Modell, das auf der kustodialen $SU(2)_L \times SU(2)_R \times P_{LR}$ Symmetrie in der Extradimension basiert, und auf zwei supersymmetrische Flavormodelle: eines, das auf einer abelschen $U(1)$ Flavorsymme-

trie basiert und ein anderes, das auf einer nicht-abelschen $SU(3)$ Flavorsymmetrie basiert. Wir untersuchen und vergleichen zuerst die Flavorstrukturen beider Modelle und zeigen zwei Möglichkeiten auf, das sogenannte "Flavorproblem von neuer Physik" zu behandeln: eine gekrümmte Extradimension und kustodialer Schutz auf der einen Seite, Flavorsymmetrien auf der anderen Seite. Anschließend untersuchen wir den Einfluss der neuen Teilchen (Kaluza-Klein Teilchen in Fall des Randall-Sundrum Modells und Superpartner in Fall von Supersymmetrie) auf K und B Meson Mischung und auf seltene Zerfälle. Wir führen eine umfassende numerische Analyse der neuen Physik Effekte in den untersuchten Modellen durch und zeigen, dass es in beiden Modellen möglich ist, auf natürliche Art und Weise mit den zu Verfügung stehenden Daten zu $\Delta F = 2$ Observablen übereinzustimmen. Dies gilt, obwohl wir die Energieskala der Modelle auf den TeV Bereich setzen, um die neuen Teilchen in der Reichweite des LHCs zu haben. Im Anschluss untersuchen wir die charakteristischen Muster von Flavorverletzung, die es zukünftigen Experimenten erlauben, die beiden Modelle zu unterscheiden. Insbesondere die Korrelationen zwischen der CP verletzenden Asymmetrie im $B_s^0 - \bar{B}_s^0$ System und den seltenen Zerfällen $B_{s,d} \to \mu^+\mu^-$ und $K \to \pi\nu\bar{\nu}$ erlauben es im Prinzip, das Randall-Sundrum Modell und die zwei supersymmetrischen Flavormodelle experimentell zu testen. Eine klare Unterscheidung zwischen den Modellen wird möglich sein, sobald neue Daten zu Verfügung stehen werden.

Acknowledgement

I would like to thank all the people of the research group T31 to have given me the opportunity to complete this PhD work.

First of all, a warm thank you to my supervisor Prof. Andrzej Buras. I would like to thank you for all the suggestions you gave me, for all the interesting discussions we had and for the opportunity you gave me to work in a very active and lively research atmosphere. Not lastly, I also would like to thank you for involving me in very interesting research projects and of course for reading and commenting this PhD thesis. Thanks also for the "easy going atmosphere" you created in our research group.

I am very grateful to Wolfgang Hollik and the Max Planck Institut für Physik in Munich, for having offered me a scholarship during my PhD and for having financed very many conferences and workshops, as well as the travel to Chicago last November. I also thank Professor Hollik for having agreed to be the second reviewer of this PhD thesis.

A particular thank to all my colleagues with whom I collaborated in the last three years. Thank you to Monika Blanke, Björn Duling, Katrin Gemmler and Andi Weiler for the Randall-Sundrum project. Many thanks to Wolfgang Altmannshofer, Paride Paradisi and David Straub for the Susy flavor models project. Thanks to Maria Valentina Carlucci and to Gino Isidori for the two Higgs doublet model project. An additional big thanks to Roberto Franceschini for the heavy Higgs project. It was nice to collaborate with all of you!

Many thanks also to my diploma supervisor Riccardo Barbieri for the many helpful advices, in physics and beyond, and suggestions for the heavy Higgs project.

Additionally, I would like to thank Stefan Recksiegel for technical assistance: with you, computers are always working! Thank you also to Thorsten Feldmann and Christoph Promberger with whom I did exercises for the course of Quantum Field Theory II, last semester.

Zum Ende, einen persönlichen Dank an David Straub für die sehr gute Büroatmosphäre, an Michael Wick für die gesprächigen Kaffee Pausen und an Wolfgang Altmannshofer für zu viele Grunde, als dass sie hier geschrieben werden könnten.

Contents

Chapter 1

Introduction

The idea for a Large Hadron Collider (LHC) was born at CERN already in the early 1980s. After a long period of work by more than 10,000 scientists, coming from more than 40 different countries, LHC is now finally running. High hopes rest on the experiment that, for the first time in the history of particle physics, will test energies considerably higher than the electroweak (EW) scale. Several fundamental questions are waiting for the results of the LHC: is the Higgs mechanism for generating elementary particle masses via electroweak symmetry breaking (EWSB) indeed realized in nature? What is the nature of the Dark Matter? And also, *is the Standard Model (SM) the complete theory of nature? Is supersymmetry, an extension of the Standard Model and Poincaré symmetry, realized in nature, implying that all known particles have supersymmetric partners? Are there extra dimensions?*

The Standard Model augmented by neutrino masses provides a remarkably successful description of presently known phenomena, except gravity. Given the striking success of the SM why are we not satisfied with that theory? The main reason is that there are strong conceptual indications for physics beyond the SM (BSM).

The computed behavior of the $SU(3)_c \times SU(2)_L \times U(1)_Y$ couplings with energy clearly points towards the unification of the electroweak and strong forces (Grand Unified Theories (GUTs)) at energy scales $M_{\rm GUT} \sim 10^{16}$ GeV. It is quite unlikely that the SM without New Physics (NP) is valid up to such large energies, because of the so called *hierarchy problem* [1, 2] that is related to the presence of light elementary scalar fields in the theory with quadratic mass divergences and no protective extra symmetry at low energy. Hence, already the hierarchy problem would hint towards a theory beyond the Standard Model that is able to stabilize the electroweak scale and that arises, consequently, at an energy just above that scale. This is the strongest theoretical motivation which leads us to believe that there is New Physics beyond the Standard Model.

The hierarchy problem is certainly not the only conceptual problem of the SM. We should also mention the problem of the unification of the coupling constants, the proliferation of parameters and the mysterious pattern of fermion masses and mixings (the so called *SM flavor problem*). But differently from the gauge hierarchy problem and the problem of the unification, the SM flavor problem can be postponed to the final theory that will take over at very large energies, and not at a low scale of $\mathcal{O}(1\,\text{TeV})$.

Finally also experiments seem to hint towards the presence of New Physics. First of all, there is a solid astrophysical and cosmological evidence that most of the matter in the universe is *dark*, namely does not emit electromagnetic radiation. However the SM does not contain any particle with the right properties to form dark matter. Moreover, the simple fact that neutrino masses vanish in the Standard Model implies that the experimental evidence for neutrino oscillations, and hence for massive neutrinos, indicates the existence of New Physics beyond the Standard Model. Additionally, also Baryogenesis cannot occur in the framework of the Standard Model, since the CP violation of the Standard Model is far too weak to explain the process; additional sources of CP violation would be required. Finally there is a good experimental evidence that in the first fraction of a second of the big bang the universe went through a stage of extremely rapid expansion called *inflation*. The fields responsible for the process cannot be Standard Model fields and hence also the process of inflation hints towards the presence of New Physics.

With all these motivations at hand, we consider worth to analyze theories beyond the Standard Model, that try to solve, or at least to address, some of the aforementioned open issues. Probably this is one of the most exciting time to perform this kind of investigation, since the TeV scale, namely the energy scale at which we indeed expect New Physics, is exactly the energy scale that LHC will probe within the next several years.

Presently, at the dawn of the LHC, great importance is given to the study of the possibility to directly detect the Higgs boson and additional new particles not present in the framework of the Standard Model. *What is then the role of flavor physics in this era?*

As we have already mentioned, the Standard Model flavor sector suffers of a conceptual problem: the SM flavor problem. Additionally, comparing the huge amount of data on flavor observables and the corresponding SM predictions, small discrepancies arise. Moreover, low energy precision experiments test the predictions of the Standard Model and of theories beyond to a high level of accuracy, putting stringent constraints on the possible forms of New Physics. They can in fact reveal the main properties of the new particles, thanks to the study of their footprints in low energy processes in which they are involved. In this sense, the indirect searches are complementary to the direct searches of new particles at the LHC, even if the former can in principle be sensitive to much shorter scales than the latter.

In the future, once new data from LHC will be available, it will be necessary to have tools to disentangle between the several theories beyond the Standard Model. Presently, in fact, there are very many BSM theories that are collecting a large interest and that are addressing some of the main problems of the SM, like the gauge hierarchy problem: Supersymmetric theories [3], theories with extra dimensions both with flat metric and warped metric [4, 5], theories based on Technicolor [6], the Little and Littlest Higgs models [7, 8].

In this thesis we will analyze the quark flavor sector of two of the most accredited models BSM: *the Minimal Supersymmetric Standard Model (MSSM) (for an extensive review see [9]) and the Randall-Sundrum (RS) Model [5].* The main aim will be to show the power of flavor physics in supplying a tool to distinguish between the two frameworks through the different pattern of predictions of the MSSM and of the RS model in flavor observables.

The thesis is organized as follows. In **Chapter 2**, we first explain in detail the flavor puzzle and subsequently we introduce the two NP frameworks: Sec. 2.2 is dedicated to the Randall-Sundrum model with custodial protection, Sec. 2.3 to two Susy flavor models, the one based on a $U(1)$ flavor symmetry, the other on a $SU(3)$ flavor symmetry. The two sections are organized in an analogous manner: we first show how to address two of the main problems of the Standard Model, the gauge hierarchy problem and the SM flavor puzzle and, secondly, we present the details of the models analyzed, focusing particularly on the quark flavor sector. In **Chapter 3**, we explain how to limit the (in general too large) NP effects on flavor changing neutral currents (FCNCs), first (Sec. 3.1) in the RS model with custodial protection, and secondly (Sec. 3.2) in Susy flavor models. We will show in fact the big role of the RS-GIM mechanism and of the enlarged gauge group of the RS model in protecting flavor changing neutral vertices from being too large. Thanks to these protection mechanisms, the model can be in agreement with the experimental data on quark flavor observables, in spite of the flavor changing neutral currents arising already at the tree level. In parallel, we will demonstrate the importance of flavor symmetries in reducing the NP effects in flavor changing neutral couplings in the framework of Susy. **Chapter 4** is devoted to the analysis of the impact of the flavor changing neutral currents previously studied, first (Sec. 4.1) on K and B meson oscillation observables, and secondly (Sec. 4.2) on rare B and K decays. We will study the effective Hamiltonians responsible for the several processes, putting a particular attention on the comparison between the different NP contributions and on the understanding of the theoretical structure of the two frameworks responsible for the several results for the $\Delta F = 2$ and $\Delta F = 1$ observables. Each section is concluded by a brief discussion of the present experimental status of the measurements and of the corresponding SM predictions. Already from this chapter we can get a feeling for the expected relative size of NP effects in the several flavor transitions. The expectations will be confirmed in **Chapter 5** that is dedicated to our numerical analysis. In Sec. 5.1 we present the details of our numerical investigation, specifying the particular scan we performed for the two NP frameworks. Secondly, in Sec 5.2, we analyze, both in the RS model and in the two Susy flavor models, the constraints we have to impose on the parameter space, in order to be in agreement with all the well measured $\Delta F = 2$ observables. After having restricted the parameter space of the two theories, we examine the possibility to obtain large NP contributions in the CP violating asymmetry of the $B_s^0 - \bar{B}_s^0$ meson system, $S_{\psi\phi}$. That observable is in fact a golden channel for flavor physics, since present experiments seem to show a discrepancy at the level of 3σ with the SM prediction. In Sec. 5.3, we will turn our attention to the numerical analysis of rare K and B decays. A significant part of our study is dedicated to the investigation of possible correlations between different flavor channels, since these can be seen as parameter independent signatures of the two models. Particular attention is dedicated to the rare decay mode $B_s \to \mu^+\mu^-$ and to its correlation with $S_{\psi\phi}$, since also this B_s decay is one of the golden channels to be explored at the LHC. Finally, in Sec. 5.4 we will summarize how to distinguish the two NP frameworks through a comparative study of the flavor channels analyzed in this thesis, once that new data will be available. Our conclusions are reported in **Chapter 6** and some technical details are relegated to the **Appendices**.

Chapter 2

The two models

2.1 The flavor problem

This thesis is dedicated to flavor physics, namely to the study of the interactions and of the masses of the fermions of the SM. Consequently, we should first justify *for which reason flavor physics is interesting.*

We have to mention that the flavor sector of the SM has a conceptual problem: the *SM flavor problem*. The large hierarchies between the several masses and mixings of the SM fermions are still a mystery. This puzzle became even more severe after the measurement of the very small neutrino masses and mixings, since the SM does not predict any particular structure for the free parameters neither in the quark nor in the lepton flavor sector.

Still the interest in flavor physics goes beyond this only motivation

- CP violation is closely related to flavor physics. Within the Standard Model, there is a single CP violating parameter, the Kobayashi-Maskawa phase $\delta_{\rm KM}$ [10] (in addition to the QCD $\bar{\theta}$ term). Baryogenesis tells us, however, that there must exist new sources of CP violation. Measurements of CP violation in flavor changing processes might provide evidence for these new sources.

- Past experiments showed the important role of flavor precision tests in probing New Physics:

  - The smallness of $\frac{\Gamma(K_L \to \mu^+\mu^-)}{\Gamma(K^+ \to \mu^+\nu)}$ led to predict a fourth (the charm) quark [11].
  - The size of the mass difference ΔM_K led to a successful prediction of the charm mass [12].
  - The size of the mass difference ΔM_d led to a successful prediction of the top mass (for a review [13]).
  - The measurement of the CP violating observable ε_K led to the prediction of the existence of a third generation quarks [10].

- Present experiments of specific flavor observables show small discrepancies with the SM predictions at the level of $(2-3)\sigma$. Two of the most relevant examples are the discrepancy in the anomalous magnetic moment of the muon ($(g-2)_\mu$) (see [14]

for an updated discussion) and in the time dependent CP asymmetry in $B_s \to \psi\phi$, $S_{\psi\phi}$ [15, 16].

These arguments emphasize the important role covered by flavor physics and in particular by the study of flavor physics in theories BSM. However, the SM Cabibbo-Kobayashi-Maskawa (CKM) [10,17] picture of flavor and CP violation has been very well experimentally established in the last decades. Present experiments overconstrain the four parameters of the CKM matrix and lead to a mainly consistent[1] determination of the CKM free parameters [22, 23]. Consequently, New Physics theories are strongly constrained in the flavor sector by the experimental data.

Let us take a generic beyond the Standard Model theory. We can adopt a general bottom-up approach for the analysis, namely we can assume that the new degrees of freedom are heavier than SM fields, we can integrate them out, and describe the NP effects by means of an effective gauge invariant non-renormalizable Hamiltonian. Since the method of effective Hamiltonians is quite relevant for this thesis, we discuss it now briefly.

The flavor transitions involve at least two different energy scales: the electroweak scale, relevant for the flavor changing weak transition, and the scale of strong interactions Λ_{QCD}. Using the method of *Operator Product Expansion* (OPE) [24, 25], these processes can be described by effective weak Hamiltonians where all the particles heavier than the W boson are eliminated as dynamical degrees of freedom from the theory [26–31] (integration out of the heavy particles). The effect of particles heavier than M_W enters only through the Wilson coefficients (WCs) c_i, namely the effective couplings multiplying the operators of the effective Hamiltonian.

In all generality, the effective Hamiltonian will look like

$$\mathcal{H}_{\text{eff}} = \mathcal{H}_{\text{SM}} + \sum_i \frac{c_i^{(d)}}{\Lambda_{\text{NP}}^{(d-4)}} \mathcal{O}_i^{(d)} \,, \tag{2.1}$$

where the operators $\mathcal{O}_i^{(d)}$ have dimension $d > 4$ and they are constructed in terms of the SM fields, and Λ_{NP} is the NP scale at which the new degrees of freedom arise.

Some of the non-renormalizable operators in (2.1) can mediate flavor transitions. Hence the experimental constraints on flavor observables can be summarized in terms of constraints on the $c_i^{(d)}$ parameters, as functions of the NP scale Λ_{NP}. Let us consider for instance the subset of left handed operators (present already in the SM) which mediate transitions of two units of flavor, namely

$$\Delta\mathcal{H}_{\Delta F=2} = \frac{c_{sd}^{(2)}}{\Lambda_{\text{NP}}^2}(\bar{s}_L\gamma^\mu d_L)^2 + \frac{c_{bd}^{(2)}}{\Lambda_{\text{NP}}^2}(\bar{b}_L\gamma^\mu d_L)^2 + \frac{c_{bs}^{(2)}}{\Lambda_{\text{NP}}^2}(\bar{b}_L\gamma^\mu s_L)^2 + \frac{c_{cu}^{(2)}}{\Lambda_{\text{NP}}^2}(\bar{c}_L\gamma^\mu u_L)^2 \,. \tag{2.2}$$

Each of these terms contributes to the mass splitting between the corresponding neutral mesons. For example, the term $(\bar{b}_L\gamma^\mu d_L)^2$ contributes to ΔM_d, the mass difference between the two neutral B_d mesons.

[1] Note however the existence of small tensions as pointed out in [18, 19] and in [20, 21].

If the New Physics has a generic flavor structure, namely $c_{ij}^{(2)} = \mathcal{O}(1)$, the constraints from $\Delta F = 2$ observables (see also Tab. 4.5 for a list of the several constraints coming from $\Delta F = 2$ observables in the meson system) impose a lower bound on the scale of New Physics [32], as shown in the second column of Tab. 2.1. From the numbers collected, it is evident that, in the hypothesis of a generic flavor structure, the scale of NP for flavor cannot be the TeV scale, as for the electroweak sector. This gives rise to the *NP flavor problem*, namely the problem in explaining the hierarchy between the two scales of NP, the one for the EW sector and the other for the flavor sector.

The problem can be also rephrased imposing the NP scale $\Lambda_{\rm NP}$ to be around the TeV scale. The third column of Tab. 2.1 shows the upper bounds on the parameters $c_{ij}^{(2)}$ in that specific case. It is obvious that, if we insist that the New Physics emerges in the TeV region, we have to conclude that it possesses a highly non-generic flavor structure.

Operator	Bounds on $\Lambda_{\rm NP}$ in TeV		Bounds on $c_{ij}^{(2)}$		Observables
	Re	Im	Re	Im	
$(\bar{s}_L\gamma^\mu d_L)^2$	9.8×10^2	1.6×10^4	9.0×10^{-7}	3.4×10^{-9}	ΔM_K; ε_K
$(\bar{b}_L\gamma^\mu d_L)^2$	5.1×10^2	9.3×10^2	3.3×10^{-6}	1.0×10^{-6}	ΔM_d; $S_{\psi K_S}$
$(\bar{b}_L\gamma^\mu s_L)^2$	1.1×10^2		7.6×10^{-5}		ΔM_s
$(\bar{c}_L\gamma^\mu u_L)^2$	1.2×10^3	2.9×10^3	5.6×10^{-7}	1.0×10^{-7}	ΔM_D; $\lvert q/p\rvert, \phi_D$

Table 2.1: Bounds on the dimension-six $\Delta F = 2$ operators listed in (2.2). Bounds on $\Lambda_{\rm NP}$ are quoted assuming couplings $c_{ij}^{(2)} = 1$, or, alternatively, the bounds on the respective $c_{ij}^{(2)}$'s are set assuming $\Lambda_{\rm NP} = 1$ TeV [32]. Observables related to CP violation (CPV) are separated from the CP conserving (CPC) ones with semicolons. In the B_s system we only quote a bound on the modulo of the NP amplitude derived from ΔM_s. The motivation will become clear in Sec. 4.1.6.

In this thesis we will review different mechanisms to protect BSM theories from having too large NP effects in flavor observables, still maintaining a NP scale around the TeV. More precisely we will investigate the role of

- Warped Geometry and custodial symmetry $SU(2)_L \times SU(2)_R \times P_{LR}$ in the context of the RS model (Secs. 3.1.3 - 3.1.4);
- Degeneracy and Alignment of squark mass matrices implemented by Susy flavor symmetries in the context of the MSSM (Sec. 3.2.2);
- Sfermion decoupling in the context of the MSSM (Sec. 3.2.2 or also our recent publication for the Next to Minimal Supersymmetric Standard Model (NMSSM) [33]).

2.2 WED with custodial protection

In this section we will analyze the basic theoretical features of the Randall-Sundrum model with custodial protection. At the beginning we will show how to address some of the open

issues of the Standard Model with the use of a five-dimensional (5D) space with warped metric. Afterwards, we will present the particular RS model analyzed in this thesis.

2.2.1 Motivations

In this section we will show in detail how the the Randall-Sundrum model can address some of the most important open issues of the Standard Model: the gauge hierarchy problem and the SM flavor problem. However, a complete review of the virtues of the RS model goes beyond the scope of this work. For this reason we will omit issues like the problem of the gauge coupling unification and the discussion of a dark matter candidate. For the investigation of the problem of the gauge coupling unification, we can refer the reader to [34,35]. For the discussion of a dark matter candidate we refer instead to [35–38].

Energy scales and the gauge hierarchy problem

The idea that nature is composed of more than four dimensions is almost one hundred years old. The first proposal was in 1914 by Nordström, who tried to simultaneously describe electromagnetism and a scalar version of gravity [39]. With the discovery of General Relativity, Kaluza [40] (1919) and Klein [41] (1926) pursued the idea, realizing that the 5D Einstein theory with one spatial dimension compactified on a circle can describe both the 4-dimensional (4D) gravity and electromagnetism. However, it turned out that their theory was not a viable model to describe nature. For many years the idea of extra dimensions was almost forgotten. However, with the developments in supergravity and superstring theories in the late 1970's, 1980's, the concept of additional spatial dimensions had a renewed interest, because of the requirement of extra dimensions by superstring theories. Still the extra dimensions considered by these theories were beyond any possibility of testing, since extremely small, of the order the Planck length.

In the 1990's, the possibility that the extra spatial dimensions show themselves at (or near) the TeV scale was considered. The origin of this idea was in the work of Antoniadis [42] who first proposed to employ a TeV^{-1} - size extra dimension in order to address the problem of the unification of the gauge couplings. Afterward, Arkani-Hamed, Dimopoulos and Dvali (ADD) [4, 43, 44] proposed the use of a large extra dimensional model, in order to address the gauge hierarchy problem.

Just one year after, an alternative approach to solve the problem was proposed by Randall and Sundrum [5]. In that model the metric of the five dimensional space (the bulk) is not factorisable, since multiplied by a *warping factor* which is a rapidly changing function of the additional dimension y

$$ds^2 \equiv g_{MN} dx^M dx^N = e^{-2ky} \eta_{\mu\nu} dx^\mu dx^\nu - dy^2 \,, \tag{2.3}$$

where k is the 5D anti-de-Sitter space (AdS_5) curvature scale, of the order the Planck scale, and $\eta_{\mu\nu}$ is the Minkowski metric $\eta_{\mu\nu} = \mathrm{diag}(-+++)$. Additionaly, the fifth dimension y is orbifolded, modding out the symmetry S^1/Z_2 which leaves the points $y = 0$ and $y = L$ fixed. Consequently, the fifth dimension is limited in the finite interval $0 \leq y \leq L$; the endpoints of this interval are the so called 3-*ultraviolet* (UV) brane and 3-*infrared* (IR) brane, respectively.

In the model, since distances, and hence energy scales, are location dependent, the hierarchy problem can be redshifted away, just for geometrical reasons.
To be more precise, let us consider the action of a scalar Higgs field H, localized on the IR brane

$$S = \int d^4x \int_0^L dy \sqrt{-G_{\rm IR}} \left(g^{\mu\nu}_{\rm IR} \partial_\mu H^\dagger \partial_\nu H - \lambda (H^2 - v_0^2)^2 \right) \delta(y - L) \,, \tag{2.4}$$

where $g^{\mu\nu}_{\rm IR}$ is the metric on the IR brane ($g^{\mu\nu}_{\rm IR} = g^{\mu\nu}(y = L)$) and $G_{\rm IR} = \det(g^{\mu\nu}_{\rm IR}) = -e^{-8kL}$. Performing the integration over the fifth dimension, one should also redefine the H field $H \to e^{kL} H$, in order to get a canonical normalization for the kinetic term

$$S = \int d^4x \left(\partial^\mu H^\dagger \partial_\mu H - \lambda (H^2 - v_0^2 e^{-2kL})^2 \right) \equiv \int d^4x \left(\partial^\mu H^\dagger \partial_\mu H - \lambda (H^2 - v_{0\,IR}^2) \right) . \tag{2.5}$$

The physical mass scales are then set by the symmetry-breaking scale

$$v_{0\,IR} = v_0 e^{-kL} \,. \tag{2.6}$$

Consequently, if the warping factor e^{-kL} is of the order 10^{-16}, the warped geometry produces an EW physical mass scale on the IR brane (also called SM brane) from a fundamental mass scale v_0 of the order the Planck scale ($10^{19}\,\text{GeV}$). Fixing then the product kL to be around 35, allows the fundamental parameters k and v_0 to be of the same order of the Planck scale, still being in agreement with the requirement that the effective scale of the Higgs boson is the electroweak scale. The gauge hierarchy problem is then addressed.

In principle, this geometrical framework (called also RS framework) would have as free parameters, in addition to k and L, also the bulk and brane cosmological constants and the masses of some heavy fields introduced to stabilize the length of the fifth dimension L. However, these additional parameters are not relevant for our purposes: we can simply assume that the combination $f \equiv ke^{-kL}$ is the only free parameter coming from the geometry, since the product kL is fixed to be $kL \sim 35$, in order to address the gauge hierarchy problem. In this thesis we will then treat f for the Kaluza-Klein (KK) mass $M_{\rm KK} \sim 2.45 f$.[2]

Fermion fields and the SM flavor problem

In the original RS model [5] all forces and matter fields, except for the graviton, do not propagate in the bulk, but are localized on the IR brane. However, this localization is in principle, only required for the Higgs field, in order to address the gauge hierarchy problem. In addition, if the matter fields are not allowed to propagate in the bulk, the theory cannot address the flavor problem, since, using the language of the effective operators (see the previous section) the higher dimensional operators in (2.2) would be suppressed just by

[2] In Appendix A, we will show that the KK mass corresponds to a physical mass, more precisely it is the mass of the first KK excitation of a gauge boson with (++) boundary conditions.

the electroweak scale $\Lambda_{\rm NP} = \mathcal{O}(v \equiv v_{0\,IR})$, as in a generic extension of the SM. This, as already observed, would not be sufficient to cure the NP flavor problem[3].

Consequently, models where the several SM fields (both gauge bosons [45, 46] and fermions [47–49]) are allowed to propagate in the bulk are phenomenologically more sound. In fact, by placing the SM matter fields in the bulk, the effective cut-off scale $\Lambda_{\rm NP}$ will depend on the precise localization of the fields and hence can be even significantly larger than the electroweak scale. Therefore, in what it follows, we will restrict our analysis to RS models in which only the Higgs boson is confined on the IR brane, while the fermions and gauge bosons are 5D fields allowed to propagate along the extra dimension.

Now we will demonstrate that the localization of the SM fermions in the bulk can even alleviate the SM flavor problem [47, 49–51].

Neglecting the possible brane kinetic terms for fermions, the action of a free fermion in a warped metric is given by

$$S_\psi = \int d^4\,x \int_0^L dy \sqrt{G}\; \frac{1}{2}\bar{\psi}(i\Gamma^M(\partial_M + \omega_M) - ck)\psi + h.c.\,, \tag{2.7}$$

where Γ^M are the gamma matrices in 5 dimensions, $\Gamma^M = e^A_M \gamma_A$, where e^A_M is the fünfbein defined by $g_{MN} = e^A_M\, e^B_N \eta_{AB}$ and $\gamma_A = (\gamma_\alpha, \gamma_5)$ are the usual gamma matrices in the flat space. G is introduced in order to obtain an invariant integration measure and is given by $G = \det(g_{MN})$, ω_M is the spin connection and c the fermion bulk mass. The variation principle $\delta S_\psi = 0$ yields to the equation of motion [47]

$$\left[-e^{-2ky}\eta^{\mu\nu}\partial_\mu\partial_\nu + e^{ky}\partial_5\left(e^{-ky}\partial_5\right) - c(c \pm 1)k^2\right] e^{-2ky}\psi_{L,R}(x^\mu, y) = 0\,, \tag{2.8}$$

where we have explicitly separated the left and right handed components of the field ($\psi_{L,R} = \pm\gamma_5\psi_{L,R}$) and $c(c \pm 1)k^2$ are the corresponding bulk mass terms.

To solve this differential equation, one can make use of the Kaluza-Klein decomposition for the fields $\psi_{L,R}$, separating the dependence on x^μ and on the fifth component y

$$\psi_{L,R}(x^\mu, y) = \frac{e^{2ky}}{\sqrt{L}} \sum_{n=0}^{\infty} \phi^{(n)}_{L,R}(x^\mu) f^{(n)}_{L,R}(y)\,, \tag{2.9}$$

where $f^{(n)}_{L,R}(y)$ is the so called fermion shape function for a left/right handed fermion. Inserting then inside the equation of motion (2.8), one finds

$$\left[\partial_5^2 - k\partial_5 - \left(c(c \pm 1)k^2 - e^{2ky}m_n^2\right)\right] f^{(n)}_{L,R}(y) = 0\,, \tag{2.10}$$

where m_n is the mass of the n-th KK mode, given by

$$\eta^{\mu\nu}\partial_\mu\partial_\nu\phi^{(n)}(x^\mu) = m_n^2\phi^{(n)}(x^\mu)\,. \tag{2.11}$$

A comment is in order. Differently from the SM, in the RS model (or more generally in all the extra dimensional scenarios [4, 42, 52]), the solution of the equation of motion

[3] The same kind of problem arises from the proton decay rate if the SM fermions are localized on the IR brane.

is not unique. All a *Kaluza-Klein tower of particles* is solution of the same equation of motion. As we will analyze more in detail in the following, all these fields have common quantum numbers, but different masses.

The equation which specifies the shape function of the n-th fermion in the extra dimension (2.10) is a differential equation of the second order; consequently, a solution $f^{(n)}(y)$ is unambiguously determined only after specifying two additional conditions. The two most simple choices, usually adopted in the literature, is to impose at the boundaries of the interval ($y = 0$ and $y = L$)

- *Dirichlet boundary condition* (BC): $f^{(n)}(y)\big|_{\text{brane}} = 0$. Also denoted with $(-)$.
- *Neumann boundary condition* (BC): $(\partial_5 + ck) f^{(n)}(y)\big|_{\text{brane}} = 0$. Also denoted with $(+)$.

This approach of neglecting all interaction terms, in particular the interactions of fermions with the Higgs boson, in the fermion action of Eq. (2.7) and of considering the above BCs is referred to as the *perturbative approach*. In this approach first the solution of the free equation of motions and the KK fermion masses m_n are worked out, secondly the effects of electroweak symmetry breaking are taken into account and treated as small perturbations $\mathcal{O}(v^2/f^2)$ of the previously obtained KK masses[4].

Solving the equation of motion (2.10) with the above BCs, one finds the solutions for the left handed fields [47]

$$f_L^{(0)}(y,c) = \sqrt{\frac{(1-2c)kL}{e^{(1-2c)kL}-1}}\, e^{-cky}\,, \tag{2.12}$$

$$f_L^{(n)}(y,c,\text{BC}) = \frac{e^{ky/2}}{N_n}\left[J_\alpha\left(\frac{m_n}{k}e^{ky}\right) + b_\alpha(m_n) Y_\alpha\left(\frac{m_n}{k}e^{ky}\right)\right] \quad (n = 1,2,...), \tag{2.13}$$

where $\alpha = |c + 1/2|$ and J, Y are the Bessel function of first and second kind, respectively. Some comments are in order

- The zero modes (2.12) turn out to be massless ($m_0 = 0$) and exist only for $(++)$ BCs. Consequently they correspond to the SM fermions.
- The several fermion fields $f_L^{(n)}$, with $n = 0, 1, 2, ...$, satisfy the orthonormality conditions

$$\frac{1}{L}\int_0^L dy e^{ky} f_L^{(n)}(y,c) f_L^{(m)}(y,c) = \delta_{nm}\,, \tag{2.14}$$

  which determine the normalization constants N_n.

[4]Differently, the effects of EWSB can also be treated exactly, introducing in the fermion action the interaction terms with the Higgs boson (see [53–57] for the study of this equivalent approach).

- The functions $b_\alpha(m_n)$ and the masses m_n are determined through the BCs on the two branes (see [47] for additional details or Appendix A where a similar discussion is performed for the gauge bosons). In particular, an approximate expression for the fermion masses, particularly accurate for large n, is given by

$$m_n \simeq \left(n + \frac{1}{2}\left(\left|c + \frac{1}{2}\right| - 1\right) \mp \frac{1}{4}\right)\pi f\,, \tag{2.15}$$

  where the $\mp$ sign corresponds to a $(\pm)$ BC for the left handed fermion mode on the IR brane.

- For right handed fermions the discussion follows the same lines, changing the bulk mass c suitably: $c \to -c$ and taking opposite BCs. For example if the left handed fermion has $(++)$ BCs, then the corresponding right handed fermion will have $(--)$ BCs, and vice versa.

- The bulk masses c are in general 3×3 hermitian matrices in flavor space, not proportional to the identity matrix (flavor non-universality).

- To make the localization of the zero mode more explicit, one can also normalize the fermion fields with respect to the flat metric. The factor e^{ky} in (2.14) is reabsorbed in the shape function of the fermion fields and the zero mode acquires the form

$$\tilde{f}_L^{(0)}(y,c) = \sqrt{\frac{(1-2c)kL}{e^{(1-2c)kL}-1}}\, e^{(\frac{1}{2}-c)ky}\,, \tag{2.16}$$

  which shows the relevance of the bulk mass c in the localization of the zero mode in the bulk. In Figure 2.1 the dependence of the zero mode shape function on the parameter c is shown: for $c > 1/2$ the fermion is localized towards the UV brane, for $c < 1/2$ towards the IR brane.

One consequence of allowing SM fermions to be localized anywhere in the bulk is that Yukawa coupling hierarchies are naturally generated by separating the SM fermions from the Higgs on the IR brane. The SM flavor problem is then addressed.

Indeed, since the Higgs boson is forced to be localized on (or near) the IR brane, to address the gauge hierarchy problem, we can parametrize its shape function normalized with respect to the warped metric as

$$\mathcal{H}(x^\mu, y) = \frac{1}{\sqrt{L}} H(x^\mu) h(y) = H(x^\mu) e^{ky} \delta(y - L)\,. \tag{2.17}$$

Some comments are in order. In the bulk Higgs scenario, one could take into account the KK decomposition also for the scalar particles. The shape functions of the several Higgs bosons then can be found analyzing an equation of motion similar to Eq. (2.10) obtained for fermions, obtaining for the zero mode

$$\hat{\mathcal{H}}(x^\mu, y) = \frac{1}{\sqrt{L}} H(x^\mu) \hat{h}(y) = \frac{1}{L} H(x^\mu) \sqrt{\frac{2kL(\beta-1)}{e^{2kL(\beta-1)}-1}}\, e^{\beta k y}\,, \tag{2.18}$$

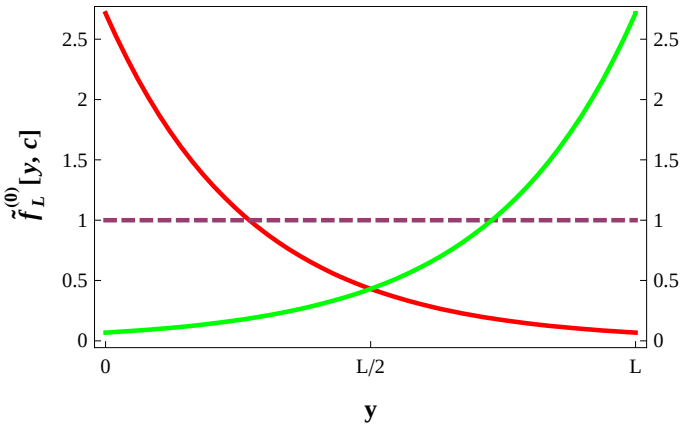

Figure 2.1: Localization of the fermion zero modes in the bulk for different values of the c parameter: $c = 0.6$ in red, $c = 0.5$ dashed and $c = 0.4$ in green.

where β is a free parameter. Then, one forces the Higgs to be localized towards the IR brane, choosing the limit $\beta \to \infty$. However, for our purposes, it is sufficient to use the limiting case (2.17), placing the Higgs directly on the IR brane and reducing the KK tower of scalar particles to the SM Higgs only.

The effective 4D Yukawa matrices Y_{ij} for zero modes are then proportional to

$$Y_{ij} \propto \int_0^L \frac{dy}{kL^{3/2}} \lambda_{ij} h(y) f_L^{(0)}(y, c^i) f_R^{(0)}(y, c^j)\,, \tag{2.19}$$

where λ_{ij} are the fundamental 5D Yukawa couplings and $f_L^{(0)}$, $f_R^{(0)}$ the SM left handed and right handed fermion shape functions, normalized with respect to the warped metric. Replacing, then, inside these couplings the shape function of the Higgs boson (2.17) and the shape functions of the two fermions (2.12), we find the simple expression

$$Y_{ij} \propto \frac{e^{kL}}{kL} f_L^{(0)}(L, c^i)\, \lambda_{ij}\, f_R^{(0)}(L, c^j) \sim \frac{\lambda_{ij}}{kL} e^{kL(1-c^i+c^j)}\,. \tag{2.20}$$

We notice that, in order to reproduce the hierarchies between the different elements of the Yukawa coupling matrices, it is not necessary to have hierarchical 5D Yukawas. Large hierarchies in the elements Y_{ij} are generated, even for totally anarchical and $\mathcal{O}(1)$ λ_{ij}, if the bulk mass parameters c^i and c^j are chosen to be just slightly different. Hence, localizing the quark zero modes in a flavor dependent manner in the bulk[5] (light quarks towards the UV brane, heavy quarks towards the IR brane) the flavor problem can be addressed. Still the RS model does not actually solve the SM flavor problem, since a more fundamental theory would be required to predict the values of the bulk masses and in particular the small differences between the several bulk masses that originate in the large hierarchies in the 4D Yukawas.

[5]It is interesting to notice the apparent analogy between the aforementioned manner of addressing the flavor problem and the proposal by Froggatt and Nielsen [58] (see also our Sec. 2.3.1). See [57, 59] for a detailed analysis of the analogy, in spite of the very different physical framework.

The next natural step would be to discuss the more general NP flavor problem in the framework of the RS model. Since the problem is non-trivial and needs some more basic knowledge about the model, we postpone the analysis to Sec. 3.1.5.

2.2.2 The gauge group

In this thesis we discuss a particular RS model with the gauge group in the bulk given by [60–67]

$$G_{\rm bulk} = SU(3)_c \times O(4) \times U(1)_X \sim SU(3)_c \times SU(2)_L \times SU(2)_R \times U(1)_X \times P_{LR}\,, \quad (2.21)$$

where the symmetry group P_{LR} is the discrete symmetry interchanging the two $SU(2)$ groups[6].

To justify the particular choice of the gauge group, few comments on how the RS model developed are worth. In the original RS model, the gauge group of the bulk was the Standard Model $SU(3)_c \times SU(2)_L \times U(1)_Y$. However, it was realized that this particular RS model had very stringent constraints arising especially from the electroweak observables, in particular from the Peskin-Takeuchi parameters [70] S [60] and T [54, 71–73] and from the anomalous $Zb_L\bar{b}_L$ coupling [60].

The usual "model-building rule" to protect the T parameter is to ensure that the Higgs sector, when considered in isolation from gauge and fermion fields, has a custodial isospin symmetry after EWSB. Consequently, since putting in the bulk an additional gauge $SU(2)_R$ symmetry implies the existence of an unbroken custodial $SU(2)_V$ symmetry in the Higgs sector, the T parameter is protected from too large contributions in the case of a $SU(2)_L \times SU(2)_R$ gauge symmetry. Enlarging the gauge group in the bulk with an extra $SU(2)$ symmetry weakens the bound on the KK mass $M_{\rm KK}$ arising from the T parameter from ~ 10 TeV to $(2-3)$ TeV [73].

The S parameter on the other hand is not protected by the custodial symmetry and depends weakly on the details of the particular gauge group. In RS models, the bound on the KK scale given by S is always around $(2-3)$ TeV [74].

As far as the anomalous coupling $Zb_L\bar{b}_L$ is concerned, it was found that the model needs an additional symmetry to suppress unwanted large corrections: the discrete P_{LR} symmetry [64]. Let us consider in a generic theory the coupling of the Z boson with $b\bar{b}$,

$$g_Z = \frac{g}{\cos\theta_W}(Q_L^3 - Q\sin^2\theta_W)\,, \quad (2.22)$$

where Q_L^3 and Q are respectively the 3rd-component $SU(2)_L$ charge and the electric charge of the left handed bottom quark and θ_W is the Weinberg angle. Since the electric charge is conserved, possible modifications to the coupling $Zb_L\bar{b}_L$ can only arise from corrections to Q_L^3. Before EWSB $Q_L^3 = T_L^3$, but this relation is not guaranted after EWSB anymore. In particular, the Vacuum Expectation Value (VEV) of the Higgs boson is responsible for the breaking $SU(2)_L \times SU(2)_R \times P_{LR} \to SU(2)_V \times P_{LR}$. Most importantly, the subgroup

[6] We refer the reader to [57, 68, 69] for the study of a RS model based on the SM gauge group in the bulk.

$U(1)_V \times P_{LR}$ remains unbroken: this is the symmetry group responsible for the protection of the $Zb_L\bar{b}_L$ coupling. In fact, by $U(1)_V$ invariance, we have that $\delta Q^3_V = \delta Q^3_L + \delta Q^3_R = 0$, and, by P_{LR} invariance, we have $\delta Q^3_L = \delta Q^3_R$. The two conditions imply that $\delta Q^3_L = 0$, or, in other words, that, thanks to the symmetry $SU(2)_L \times SU(2)_R \times P_{LR}$, the coupling $Zb_L\bar{b}_L$ is protected.

It is evident that this principle is applicable to all the couplings of the Z boson with a fermion eigenstate of the symmetry $SU(2)_L \times SU(2)_R \times P_{LR}$, namely with a fermion which satisfies the conditions[7]

$$T_L = T_R\,, \quad T^3_L = T^3_R\,. \tag{2.23}$$

In Sec. 3.1.4 we will show indeed the generalization of the protection to a larger groups of fermions, which couplings with the Z boson turn out to be SM-like. This completes our brief discussion of the gauge group of our theory.

In the development of this thesis, we will show how the aforementioned choice of the gauge group in the bulk has profound consequences in the phenomenology of the model, not only concerning electroweak observables, but also on flavor observables.

2.2.3 The field content

The gauge sector

The gauge group introduced in (2.21) is broken on the two branes in order to have viable phenomenological predictions. In particular, on the IR brane, the Higgs mechanism breaks G_{bulk} to

$$SU(3)_c \times SU(2)_L \times SU(2)_R \times U(1)_X \times P_{LR} \to SU(3)_c \times SU(2)_V \times U(1)_{em}\,. \tag{2.24}$$

Additionally, since LEP2 and Tevatron did not discover additional relatively light gauge bosons, the gauge group $SU(2)_R$ should be broken. One possibility is to break it on the UV brane through appropriate BCs (see the definition of gauge boson BCs in Appendix A) of the gauge bosons of the theory

$$\begin{aligned} G^A_\mu(++)\,, \quad W^a_{L\mu}(++)\,, \quad B_\mu(++)\,, \\ W^\beta_{R\mu}(-+)\,, \quad Z_{X\mu}(-+)\,, \end{aligned} \tag{2.25}$$

where $A = 1, ..., 8$, $a = 1, 2, 3$ and $\beta = 1, 2$. The fields B_μ and Z_{X_μ} are orthogonal combinations of the original fields

$$Z_{X_\mu} = \cos\phi W^3_{R\mu} - \sin\phi X_\mu\,, \tag{2.26}$$

$$B_\mu = \sin\phi W^3_{R\mu} + \cos\phi X_\mu\,, \tag{2.27}$$

[7] In [64] it is shown that the theorem is also valid for the coupling of a fermion with $T^3_L = T^3_R = 0$, even if not eigenstate of the symmetry $SU(2)_L \times SU(2)_R \times P_{LR}$.

with the mixing angle ϕ given by

$$\cos\phi = \frac{g}{\sqrt{g^2 + g_X^2}}\,, \tag{2.28}$$

where, thanks to the P_{LR} invariance, we could define the unique 5-dimensional $SU(2)$ coupling constant $g_L = g_R \equiv g$,[8] that is related to the measured 4-dimensional coupling constant by $g = \sqrt{L}\, g^{4D}$.

The assignment of BCs (2.25) explicitly breaks both $SU(2)_R$ and $U(1)_X$ on the UV brane (see also Fig. 2.2)

$$SU(3)_c \times SU(2)_L \times SU(2)_R \times U(1)_X \times P_{LR} \to SU(3)_c \times SU(2)_L \times U(1)_Y\,. \tag{2.29}$$

From the discussion in Appendix A, it follows that only the fields G_μ^A, $W_{L\mu}^a$ and B_μ (which have (++) BCs) have a massless zero mode which corresponds to a SM gauge field. The KK tower of the remaining fields ($W_{R\mu}^\beta$ and Z_{X_μ}) starts from the first excited state, with a mass given by $\sim 2.40 f$ (see Eq. (A.12)).

Before finishing this section, it is useful to define the following fields for later purposes [75]

$$W_{L\mu}^\pm = \frac{W_{L\mu}^1 \mp i W_{L\mu}^2}{\sqrt{2}}\,, \qquad W_{R\mu}^\pm = \frac{W_{R\mu}^1 \mp i W_{R\mu}^2}{\sqrt{2}}\,, \tag{2.30}$$

and

$$Z_\mu = \cos\psi\, W_{L\mu}^3 - \sin\psi\, B_\mu\,, \tag{2.31}$$

$$A_\mu = \sin\psi\, W_{L\mu}^3 + \cos\psi\, B_\mu\,, \tag{2.32}$$

where ψ is given in terms of the angle ϕ already defined in (2.28) by

$$\cos\psi = \frac{1}{\sqrt{1 + \sin^2\phi}}\,. \tag{2.33}$$

The fermion sector

In this section we present briefly the particular fermion representation of the RS model analyzed by us. The main motivations for the specific choice are also listed.

The SM fermions are embedded in full representations of the bulk gauge group $O(4) \times U(1)_X$. In all generality, there are only three possible representations of $SU(2)_L \times SU(2)_R$: $(\mathbf{2},\mathbf{2})$, $(\mathbf{1},\mathbf{1})$ and $(\mathbf{3},\mathbf{1}) \oplus (\mathbf{1},\mathbf{3})$. Phenomenology provides guidelines towards which multiplets to choose for which field.

In order to have a custodial protection of the $Zb_L\bar{b}_L$ coupling, the choice $b_L \in (\mathbf{2},\mathbf{2})$ with $T_L^3 = T_R^3$ has to be enforced. Additionally, also the left handed top quark should

[8] See Sec. 5.1.1 for a discussion of the value of the several 5D couplings g, g_X.

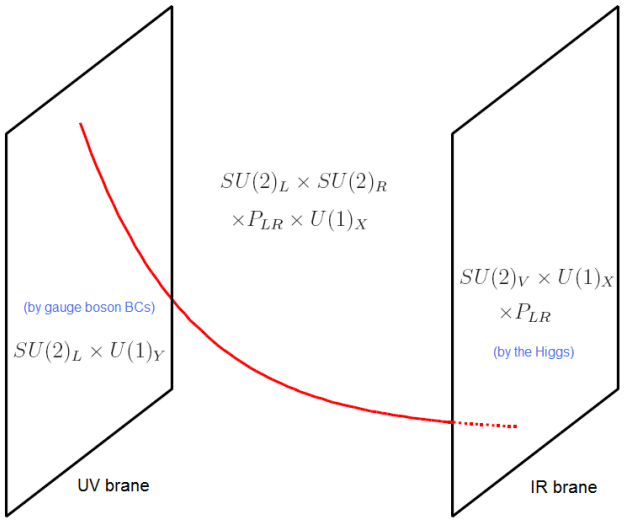

Figure 2.2: EW gauge symmetry group in the bulk and on the two branes.

belong to the same bidoublet, since left handed quarks must transform as doublets of $SU(2)_L$. Although in order to satisfy EW precision measurements only the third quark generation needs to preserve the P_{LR} symmetry, the incorporation of CKM mixing requires the same choice of $O(4)$ representation also for the first two quark generations. Therefore, we embed the entire SM $SU(2)_L$ doublet into the representation $(\mathbf{2},\mathbf{2})$.

As far as the right handed quarks are concerned, in principle two possible choices are available: $(\mathbf{1},\mathbf{1})$ and $(\mathbf{3},\mathbf{1}) \oplus (\mathbf{1},\mathbf{3})$. However, the only choice compatible with the gauge invariance of the Yukawa couplings (see in the following the representation of the Higgs field) and with the electric charge of the several quarks, is given by $b_R \in (\mathbf{3},\mathbf{1}) \oplus (\mathbf{1},\mathbf{3})$ and $t_R \in (\mathbf{1},\mathbf{1})$. Hence, the fermion representation is given by [63, 65, 76, 77]

$$\xi^i_{1L} = \begin{pmatrix} \chi^{u_i}_L(-+)_{5/3} & \mathbf{q^{u_i}_L}(++)_{2/3} \\ \chi^{d_i}_L(-+)_{2/3} & \mathbf{q^{d_i}_L}(++)_{-1/3} \end{pmatrix}_{2/3}, \tag{2.34}$$

$$\xi^i_{2R} = \mathbf{u^i_R}(++)_{2/3}\,, \tag{2.35}$$

$$\xi^i_{3R} = T^i_{3R} \oplus T^i_{4R} = \begin{pmatrix} \psi'^i_R(-+)_{5/3} \\ U'^i_R(-+)_{2/3} \\ D'^i_R(-+)_{-1/3} \end{pmatrix}_{2/3} \oplus \begin{pmatrix} \psi''^i_R(-+)_{5/3} \\ U''^i_R(-+)_{2/3} \\ \mathbf{D^i_R}(++)_{-1/3} \end{pmatrix}_{2/3}, \tag{2.36}$$

where $SU(2)_L$ acts vertically while $SU(2)_R$ acts horizontally. To these fields we have also to add the corresponding with opposite chirality and hence opposite BCs. The subscript of a multiplet denotes the $U(1)_X$ charge and the subscript of the individual fields corresponds to the electric charge determined by the relation

$$Q = T^3_L + T^3_R + X\,. \tag{2.37}$$

Some comments are in order. From our discussion of Sec. 2.2.1, it follows that, before EWSB, only the fields written in boldface q^{d_i,u_i}_L, u^i_R and D^i_R have a massless zero mode

which corresponds to a SM fermion field. In the spectrum, one needs also to add additional up, down and charge 5/3 vector-like fields to fill the three representations of $O(4)$ (the ones with BCs $(-+)$). As shown in Eq. (2.15), choosing a KK scale at the level of $(2-3)$ TeV[9], the first excited state of these exotic fermions would be at the TeV scale and in principle could be a smoking gun signature of the model at the LHC.

Finally, from the discussion of Sec. 2.2.2, we expect that the left handed couplings of the SM Z boson with the down quarks $q_L^{d_i}$ and the right handed couplings of the SM Z boson with the up quarks u_R^i are all SM-like, since all the fermion fields $q_L^{d_i}$ and u_R^i are P_{LR} eigenstates. The discussion will be detailed in Sec. 3.1.4.

The electroweak symmetry breaking

The study of the Higgs sector of the theory is beyond the scope of our analysis. However, it is worth to study the effects of the EWSB on gauge and fermion fields, which cover a central role in our analysis of the flavor phenomenology.

In order to preserve the custodial symmetry, the Higgs field needs to transform as a self-dual bi-doublet under the electroweak gauge group of the bulk

$$\mathcal{H} = \begin{pmatrix} \pi^+/\sqrt{2} & -(h^0 - i\pi^0)/2 \\ (h^0 + i\pi^0)/2 & \pi^-/\sqrt{2} \end{pmatrix}_0 , \tag{2.38}$$

where $\pi^{\pm,0}$ are Goldstone bosons and h^0 is the physical Higgs boson whose VEV leads to EWSB.

The interaction between the gauge bosons and the Higgs field are then through the kinetic terms of the Higgs field

$$S_{\text{Higgs}} = \int d^4x \int_0^L dy \, \sqrt{G} \, \text{Tr} \left[(D_M \mathcal{H})^\dagger (D^M \mathcal{H}) \right] , \tag{2.39}$$

with D_M the covariant derivative of the Higgs bidoublet.

With the breaking of the electroweak symmetry through the Higgs VEV ($v = 246$ GeV)

$$\langle \mathcal{H} \rangle = \begin{pmatrix} 0 & -v/2 \\ v/2 & 0 \end{pmatrix} , \tag{2.40}$$

a mixing between the several gauge bosons with the same electric charge is induced. In particular, neglecting the mixing with the excited states heavier than the first KK excitation

[9] As we have already discussed, a KK scale of $(2-3)$ TeV is not disfavored by the EWPTs in our particular model with an enlarged gauge group in the bulk. In Sec. 5.2 we will investigate the consequences of a relatively low KK scale in flavor physics.

$$\left(W_L^{(0)+} \quad W_L^{(1)+} \quad W_R^{(1)+}\right) \mathcal{M}^2_{\text{charged}} \begin{pmatrix} W_L^{(0)-} \\ W_L^{(1)-} \\ W_R^{(1)-} \end{pmatrix} , \tag{2.41}$$

$$\frac{1}{2}\left(Z^{(0)} \quad Z^{(1)} \quad Z_X^{(1)}\right) \mathcal{M}^2_{\text{neutral}} \begin{pmatrix} Z^{(0)} \\ Z^{(1)} \\ Z_X^{(1)} \end{pmatrix} . \tag{2.42}$$

The process of EWSB induces $\mathcal{O}(v^4/M_{\text{KK}}^2)$ corrections to the elements of the initial mass matrices $\mathcal{M}^2_{\text{charged},\,0} = \mathcal{M}^2_{\text{neutral},\,0} = \text{diag}(0, (2.45f)^2, (2.40f)^2)$, with $M_{\text{KK}} \simeq 2.45f$, as already mentioned.

Additionally, since the symmetries $SU(3)_c$ and $U(1)_{em}$ must not be broken, the gluons and the photons (both zero and excited modes) neither mix nor acquire mass through EWSB. Therefore, the theory will have in the spectrum massless zero modes of gluons and of the photon and first excited with mass $M_{A^{(1)}} = M_{G^{(1)}} \sim 2.45f$, coming from the geometry.

To conclude, we list the several mass eigenstates of gauge bosons after EWSB (this notation will be used throughout the thesis)

$$\begin{aligned} &A^{(0)}\,, G^{(0)}\,, A^{(1)}\,, G^{(1)}\,, \\ &W^{\pm}\,, W_H^{\pm}\,, W'^{\pm} \qquad \text{(obtained diagonalizing } M_{\text{charged}} \text{ in (2.41))}\,, \\ &Z\,, Z_H\,, Z' \qquad\quad \text{(obtained diagonalizing } M_{\text{neutral}} \text{ in (2.42))}\,. \end{aligned} \tag{2.43}$$

The discussion of the interaction of the quarks with the Higgs boson follows the same lines. For the several fermion fields (both zero and KK modes) we expect 4D Yukawas of the type in (2.19). To be more specific the most general Yukawa coupling action of the three quark field representations in (2.34)-(2.36) is given by

$$S_{\text{Y}} = \int d^4x \int_0^L dy\, \sqrt{G}\ \text{Tr} \sum_{i,j=1}^{3} \sqrt{2}\Big[-\lambda^u_{ij}\, \bar{\xi}^i_1 H \xi^j_2 + \sqrt{2}\lambda^d_{ij} \left(\bar{\xi}^i_1\, \tau^c\, T^j_3 H + \bar{\xi}^i_1\, \tau^\gamma\, T^j_4 H\right) + h.c.\Big]\,, \tag{2.44}$$

where τ^α are the Pauli matrices and T^i_3, T^i_4 are given in terms of the fields in (2.36)

$$T^i_3 = \begin{pmatrix} \frac{1}{\sqrt{2}}(\psi'^i + D'^i) \\ \frac{i}{\sqrt{2}}(\psi'^i - D'^i) \\ U'^i \end{pmatrix} , \quad T^i_4 = \begin{pmatrix} \frac{1}{\sqrt{2}}(\psi''^i + D^i) \\ \frac{i}{\sqrt{2}}(\psi''^i - D^i) \\ U''^i \end{pmatrix} . \tag{2.45}$$

After EWSB, the several quarks of the same electric charge mix and their mass matrices receive corrections of $\mathcal{O}(v^2/M_{\text{KK}})$, to be added to the initial diagonal mass matrices with diagonal elements given by 0 in the case of SM fermions , and by $\sim f$ in the case of KK excitations (see also Eq. (2.15)).

The details of the computation of 4D Yukawas and mass matrices for gauge bosons and fermions go beyond the scope of this thesis. We refer the reader to [78].

2.3 Susy flavor models

In this section we will analyze the basic theoretical features of Supersymmetry. At the beginning we will present briefly how to address some of the open issues of the Standard Model with the use of symmetry arguments. Afterwards, we will introduce the particular Susy flavor models analyzed in this thesis.

2.3.1 Motivations

In this section we will discuss two of the main motivations for which Supersymmetry is a well founded theory: it can address the gauge hierarchy problem and the SM flavor problem. The argument is quite well known in the literature and we treat it here briefly with the main aim to show the different approach of Susy and of the RS model in solving the open issues of the Standard Model: the "RS approach" is based on geometrical arguments; the "Susy approach" on symmetry principles.

Superpartners and the gauge hierarchy problem

$N = 1$ supersymmetry [79–81] makes the gauge hierarchy of the Standard Model natural, by relating bosonic and fermionic degrees of freedom. Supersymmetry in fact implies equal masses for SM bosons and corresponding superpartners and it can thus protect small scalar masses if the associated fermion mass is protected by a chiral symmetry. Indeed, supersymmetry eliminates all quadratic divergences from the theory at all orders in perturbation theory, leaving only logarithmic wave function renormalization [82]. Hence the corrections to the Higgs mass (or to the EW scale) will be just logarithmic in the GUT scale and consequently the gauge hierarchy problem discussed in the Introduction is addressed.

Even in the process of Susy breaking, these nice properties are not spoiled, as long as the breaking is done softly [83], namely preserving the cancellation of the quadratic divergences.

Flavor symmetries and the SM flavor problem

A viable way to address the SM flavor problem is to relate the origin of both the hierarchies and the smallness of the quark masses and mixing angles to a symmetry principle. In fact, as articulated by 't Hooft [84], small numbers are natural only if an exact symmetry is acquired when they are set to zero (*naturalness principle*).

The first in pursuing this possibility were Froggatt and Nielsen [58] who introduced a $\mathcal{G}_F = U(1)$ flavor symmetry in the SM to explain the origin of the large quark mass ratios. They assume that at high energy $M \gg 1$ TeV there are additional quarks, interacting with the SM ones, that transform non-trivially under the flavor group $\mathcal{G}_F$ and that acquire a mass of order M. The SM quarks are instead massless at the high scale M. When the heavy quarks are integrated out, higher dimensional operators are generated in the Lagrangian

$$Y^U_{ij}\bar{Q}_i u_j H\left(\frac{\Phi}{M}\right)^{n_{ij}} + Y^D_{ij}\bar{Q}_i d_j H^\dagger\left(\frac{\Phi}{M}\right)^{n'_{ij}}, \tag{2.46}$$

where H is the SM Higgs field (neutral under $\mathcal{G}_F$), Φ is a scalar field (+1) charged under $\mathcal{G}_F$ (the flavon) and the Yukawa couplings $Y^{U,D}$ are naturally assumed to be of $\mathcal{O}(1)$. The eight free parameters n_{ij} and n'_{ij} are function of the $\mathcal{G}_F$ charges of the SM quarks

$$n_{ij} = Q_F(Q_i) - Q_F(u_j)\,, \quad n'_{ij} = Q_F(Q_i) - Q_F(d_j)\,. \tag{2.47}$$

The flavor symmetry is spontaneously broken through the VEV of the flavon, and, consequently, canonical Yukawa couplings are generated in the Lagrangian. Finally, at the EW scale, masses and mixings of the SM quarks are generated (together with their hierarchies) as function of the small $\mathcal{G}_F$ breaking parameter $\frac{\langle\Phi\rangle}{M}$, that is assumed to be of $\mathcal{O}(\lambda)$ (with λ the Cabibbo angle $\lambda \sim 0.22$) in order to reproduce the observed expansion in λ of the CKM matrix elements and of the quark masses.

How predictive is this framework? To define the theory, eight charges have to be fixed by hand. The model then explains the order of magnitude of nine parameters: the four of the CKM matrix and the five ratios of quark masses. Consequently the model predicts a single order of magnitude relation. Usually one quotes as prediction of the model the ratio $|V_{ub}/V_{cb}|$ that is predicted to be [85]

$$\left|\frac{V_{ub}}{V_{cb}}\right| \sim |V_{us}|\,, \tag{2.48}$$

showing a potential weakness of the original Froggatt-Nielsen (FN) model, since experimentally[10] $|V_{ub}/V_{cb}| \sim \lambda^2$ and instead $|V_{us}| \sim \lambda$ [85]. In spite of the fact that the original FN model is experimentally ruled out, the idea of implementing a flavor symmetry to predict the pattern of the SM quark masses and mixing angles is still adopted even in models beyond the Standard Model. A relevant example is Supersymmetry. In the literature there are many different proposals to implement a flavor symmetry in the framework of Susy.

Before entering into the details of two particular Susy flavor models (see Sec. 2.3.4 and 2.3.5), we need to introduce the basics of Supersymmetry.

2.3.2 The MSSM Lagrangian

We start this section with a brief description of the MSSM and with establishing our notation and conventions which will be used throughout this thesis. The MSSM gauge group is the one of the SM, namely $SU(3)_c \times SU(2)_L \times U(1)_Y$. The matter content can be written in the form of $SU(3)_c \times SU(2)_L \times U(1)_Y$ representations

[10] This is a numerical approximation, in spite of the fact that the Wolfenstein parametrization [86] would predict this ratio to be indeed of order λ.

$(1,2,-\frac{1}{2})$	$(1,1,1)$	$(3,2,\frac{1}{6})$	$(\bar{3},1,\frac{1}{3})$	$(\bar{3},1,-\frac{2}{3})$	$(1,2,-\frac{1}{2})$	$(1,2,\frac{1}{2})$
L^I	E^I	Q^I	D^I	U^I	H^1	H^2
$\Psi^I_{_L}$	$\Psi^I_{_E}$	$\Psi^I_{_Q}$	$\Psi^I_{_D}$	$\Psi^I_{_U}$	$\Psi^1_{_H}$	$\Psi^2_{_H}$

where capital letters in the second row denote complex scalar fields and the fields in the third row are left handed fermions. The upper index $I = 1, 2, 3$ labels the generation.

The supersymmetric part of the Lagrangian is expressed by the most general renormalizable superpotential that is invariant under the R parity[11]

$$\tilde{W} = \mu H^1 H^2 + Y_e^{IJ} H^1 L^I E^J + Y_d^{IJ} H^1 Q^I D^J + Y_u^{IJ} H^2 Q^I U^J \,, \tag{2.49}$$

where, in all generality, μ is a complex parameter and $Y_{e,d,u}$ are complex 3×3 matrices in flavor space, the supersymmetric Yukawa couplings. From this expression, it is evident that in Susy two Higgs doublets $(H^1\,,\, H^2)$ are needed in order to give mass to both up and down quarks, still maintaining an analytic superpotential[12].

The remaining part of the MSSM Lagrangian consists of the soft supersymmetry breaking terms: gaugino masses (first line), scalar masses (second and third line) and trilinear scalar interactions (fourth line)

$$\begin{aligned}
\mathcal{L}_{\rm soft} \;=\; & -\frac{1}{2}\Big(M_3 \tilde{g}^{a\,T} (\tilde{g}^a)^C + M_2 \tilde{W}^{i\,T} (\tilde{W}^i)^C + M_1 \tilde{B}^T \tilde{B}^C \;+\; \text{h.c.}\Big) \\
& - M^2_{H^1} H^{1\,\dagger} H^1 - M^2_{H^2} H^{2\,\dagger} H^2 - L^{I\dagger} (M^2_L)^{IJ} L^J - E^{I\dagger} (M^2_E)^{IJ} E^J \\
& - Q^{I\dagger} (M^2_Q)^{IJ} Q^J - D^{I\dagger} (M^2_D)^{IJ} D^J - U^{I\dagger} (M^2_U)^{IJ} U^J + \big(B\mu H^1 H^2 + \text{h.c.}\big) \\
& + \big(A^{IJ}_E H^1 L^I E^J + A^{IJ}_D H^1 Q^I D^J + A^{IJ}_U H^2 Q^I U^J \;+\; \text{h.c.}\big) \,,
\end{aligned} \tag{2.50}$$

where ϕ^C indicates the charged conjugate of the field ϕ. M_3, M_2, and M_1 are the gluino, wino, and bino mass terms, respectively. Each matrix in the second and third line is a 3×3 hermitian matrix in family space and can have complex entries. B is, without loss of generality, a real parameter. Finally in the last line the trilinear terms appear as complex 3×3 matrices in family space.

After electroweak symmetry breaking, the several quarks and leptons mix, giving rise to the physical mass eigenstates that are obtained by the rotations (see e.g., [88] for a review of the flavor sector of the MSSM)

$$\begin{aligned}
& \Psi_{_{L_1}} \to V^\nu_L \Psi_{_{L_1}} \,,\;\; \Psi_{_{L_2}} \to V^E_L \Psi_{_{L_2}} \,,\;\; \Psi^c_{_E} \to V^E_R \Psi^c_{_E} \,,\;\; \Psi_{_{Q_1}} \to V^U_L \Psi_{_{Q_1}} \,,\;\; \Psi_{_{Q_2}} \to V^D_L \Psi_{_{Q_2}} \,, \\
& \Psi^c_{_D} \to V^D_R \Psi^c_{_D} \,,\;\; \Psi^c_{_U} \to V^U_R \Psi^c_{_U} \,,
\end{aligned} \tag{2.51}$$

from where we can define the CKM matrix $V \equiv V^U_L V^{D\,\dagger}_L$.

[11] The discrete R parity is defined such that a field with B baryon number, L lepton number and S spin has an R parity equal to $(-1)^{3B+L+2S}$ [87].

[12] Also the requirement of cancellation of the anomalies implies the presence of two Higgs doublets.

In "parallel" also the squarks and sleptons are rotated with the same rotation matrices to a basis $(\tilde{\nu}, \tilde{L}, \tilde{U}, \tilde{D})$ called the *super CKM (SCKM)* basis

$$\tilde{\nu} = V_L^\nu L_1, \quad \tilde{L} = \begin{pmatrix} V_L^E L_2 \\ V_R^E E \end{pmatrix}, \quad \tilde{U} = \begin{pmatrix} V_L^U Q_1 \\ V_R^U U \end{pmatrix}, \quad \tilde{D} = \begin{pmatrix} V_L^D Q_2 \\ V_R^D D \end{pmatrix}. \tag{2.52}$$

In the study of flavor transitions the mass matrices of the latter three multiplets in (2.52) are essential[13]. For this reason we give here the explicit form of the three 6×6 mass matrices

$$\begin{aligned}
\mathcal{M}^2_{\tilde{L}} &= \begin{pmatrix} (M^2_{\tilde{L}})^T_{LL} + m_l^2 + \frac{\cos 2\beta}{2}(M_Z^2 - 2M_W^2)\mathbb{1} & (M^2_{\tilde{L}})^*_{LR} - \tan\beta\mu^* m_l \\ (M^2_{\tilde{L}})^T_{LR} - \tan\beta\mu\, m_l & (M^2_{\tilde{L}})^T_{RR} + m_l^2 - \cos 2\beta M_Z^2 \sin^2\theta_W \mathbb{1} \end{pmatrix}, \\
\mathcal{M}^2_{\tilde{U}} &= \begin{pmatrix} (M^2_{\tilde{U}})^T_{LL} + m_u^2 - \frac{\cos 2\beta}{6}(M_Z^2 - 4M_W^2)\mathbb{1} & (M^2_{\tilde{U}})^*_{LR} - \cot\beta\mu^* m_u \\ (M^2_{\tilde{U}})^T_{LR} - \cot\beta\mu\, m_u & (M^2_{\tilde{U}})^T_{RR} + m_u^2 + \frac{2\cos 2\beta}{3} M_Z^2 \sin^2\theta_W \mathbb{1} \end{pmatrix}, \\
\mathcal{M}^2_{\tilde{D}} &= \begin{pmatrix} (M^2_{\tilde{D}})^T_{LL} + m_d^2 - \frac{\cos 2\beta}{6}(M_Z^2 + 2M_W^2)\mathbb{1} & (M^2_{\tilde{D}})^*_{LR} - \tan\beta\mu^* m_d \\ (M^2_{\tilde{D}})^T_{LR} - \tan\beta\mu\, m_d & (M^2_{\tilde{D}})^T_{RR} + m_d^2 - \frac{\cos 2\beta}{3} M_Z^2 \sin^2\theta_W \mathbb{1} \end{pmatrix},
\end{aligned} \tag{2.53}$$

where the masses $m_{u,d,l}$ are the diagonal 3×3 SM fermion masses, and $\mathbb{1}$ stands for the 3×3 unit matrix. Finally the flavor changing entries are given by

$$\begin{aligned}
&(M^2_{\tilde{L}})_{LL} = V_L^E M_L^2 V_L^{E\dagger} \qquad (M^2_{\tilde{L}})_{RR} = V_R^E M_E^{2T} V_R^{E\dagger} \qquad (M^2_{\tilde{L}})_{LR} = -\tfrac{v\cos\beta}{\sqrt{2}} V_L^E A_E^* V_R^{E\dagger} \\
&(M^2_{\tilde{U}})_{LL} = V_L^U M_Q^2 V_L^{U\dagger} \qquad (M^2_{\tilde{U}})_{RR} = V_R^U M_U^{2T} V_R^{U\dagger} \qquad (M^2_{\tilde{U}})_{LR} = -\tfrac{v\sin\beta}{\sqrt{2}} V_L^U A_U^* V_R^{U\dagger} \\
&(M^2_{\tilde{D}})_{LL} = V_L^D M_Q^2 V_L^{D\dagger} \qquad (M^2_{\tilde{D}})_{RR} = V_R^D M_D^{2T} V_R^{D\dagger} \qquad (M^2_{\tilde{D}})_{LR} = -\tfrac{v\cos\beta}{\sqrt{2}} V_L^D A_D^* V_R^{D\dagger},
\end{aligned} \tag{2.54}$$

where β is defined through the VEVs of the two Higgs doublets H^1 and H^2: $\langle H_0^1 \rangle = v\cos\beta\,, \langle H_0^2 \rangle = v\sin\beta$.

As we will analyze more in detail in the following, flavor changing neutral current processes are sensitive to particular entries in the above nine matrices. It is useful to parametrize the squark and slepton mass matrices as [89]

$$\mathcal{M}^2_{\tilde{L}} = \mathrm{diag}(\tilde{m}^2) + \tilde{m}^2 \delta_\ell\,, \quad \mathcal{M}^2_{\tilde{U}} = \mathrm{diag}(\tilde{m}^2) + \tilde{m}^2 \delta_u\,, \quad \mathcal{M}^2_{\tilde{D}} = \mathrm{diag}(\tilde{m}^2) + \tilde{m}^2 \delta_d\,, \tag{2.55}$$

where $\tilde{m}^2$ is an average squark and slepton mass. The corrections to the leading term $\mathrm{diag}(\tilde{m}^2)$, also called Mass Insertions (MIs), are then further decomposed according to the "chirality" of the squarks and sleptons

$$\delta = \begin{pmatrix} \delta^{LL} & \delta^{LR} \\ \delta^{RL} & \delta^{RR} \end{pmatrix}. \tag{2.56}$$

[13] From here on we will discuss only the massive fermions of the SM and the corresponding sfermions, neglecting the details about neutrinos and their superpartners that are not relevant for the scope of this work.

It is also convenient to define the trilinear terms $A_{e,u,d}$ in terms of the trilinear terms appearing in the Lagrangian (2.50) $A_{E,U,D}$, following the convention of [90]

$$Y_e A_e \equiv V_L^{E*} A_E V_R^{ET} \ , \quad Y_u A_u \equiv V_L^{U*} A_U V_R^{UT} \ , \quad Y_d A_d \equiv V_L^{D*} A_D V_R^{DT} \, , \tag{2.57}$$

so that we can write the LR MIs for the third generation squarks and sleptons as

$$\begin{aligned} &\tilde{m}^2 (\delta_\ell^{LR})_{33} = -m_\tau \left(A_\tau + \mu^* t_\beta \right) , \ \tilde{m}^2 (\delta_u^{LR})_{33} = -m_t \left(A_t + \mu^* / t_\beta \right) \ , \\ &\tilde{m}^2 (\delta_d^{LR})_{33} = -m_b \left(A_b + \mu^* t_\beta \right) \ , \end{aligned} \tag{2.58}$$

where we have shortened $t_\beta \equiv \tan\beta$.

This completes our very brief presentation of the MSSM, mainly focused on the flavor sector of the theory (for an extensive Susy review see [91]).

2.3.3 The MSUGRA hypothesis

Unlike the supersymmetry preserving part of the MSSM Lagrangian, the soft breaking Lagrangian (2.50) introduces many new free parameters that were not present in the ordinary Standard Model. A careful count [92] reveals that there are 110 masses, phases and mixing angles in the flavor sector of the MSSM Lagrangian that cannot be rotated away by redefining the quark and lepton supermultiplets, and that have no counterpart in the ordinary Standard Model. Thus, in principle, supersymmetry breaking (as opposed to supersymmetry itself) appears to introduce a tremendous arbitrariness in the Lagrangian.

A way to escape this proliferation of free parameters is the class of models in which at the Planck scale the soft parameters obey some very simple relation

$$M_3 = M_2 = M_1 = m_{1/2} \, , \tag{2.59}$$

$$M_Q^2 = M_U^2 = M_D^2 = M_L^2 = M_E^2 = m_0^2 \mathbb{1} \, , \tag{2.60}$$

$$M_{H^1}^2 = M_{H^2}^2 = m_0^2 \, , \tag{2.61}$$

$$A_U = A_0 Y_u \, , \quad A_D = A_0 Y_d \, , \quad A_E = A_0 Y_e \, , \tag{2.62}$$

where the three free parameters $m_{1/2} \, , m_0 \, , A_0$ are the universal mass scales of fermion and scalar masses and of the trilinear terms, respectively. An additional free parameter of the MSUGRA scenario is $\tan\beta$, while the absolute value of μ is determined by the requirement of a correct EWSB: $v = 246$ GeV. Thanks to the very few free parameters, the framework described just above is highly predictive. It is referred to as the *minimal supergravity* (MSUGRA) scenario [93].

Evidently the conditions (2.59)-(2.62) are not valid at the EW scale. The soft parameters are in fact affected by the renormalization group (RG) running from the Planck scale to the EW scale, that alters their relations [94]. A popular approximation (that we will also perform in our analysis) is to start this RG running from the unification scale $M_{\rm GUT}$ instead of from the Planck scale. The reason for this is more practical than principled:

the apparent unification of gauge couplings gives us a strong hint that we know something about how the RG equations behave up to $M_{\rm GUT}$, but unfortunately gives us little guidance about what to expect at scales between $M_{\rm GUT}$ and $M_{\rm Planck}$.

As we will show with two explicit examples in the next two sections, Susy flavor models predict deviations from this simplified setup, since several off-diagonal soft masses are predicted to be non-zero, and several trilinear terms not proportional to the corresponding Yukawa couplings. However, we will adopt an "MSUGRA working hypothesis" at the GUT scale, namely we will assume the conditions (2.59) and (2.61) and, in addition, two common mass scales m_0 and A_0 for sfermion soft masses and trilinear terms, respectively (see Sec. 5.1.2 for an accurate discussion of the scan we performed on the several free parameters in our numerical analysis).

2.3.4 The abelian flavor model

As we have mentioned in the previous section, implementing a flavor symmetry á la Froggatt-Nielsen in the Susy framework introduces deviations from the simple relations (2.59)-(2.62) for the soft parameters of the MSSM Lagrangian at the Planck (or GUT) scale. In particular in this section we present a flavor model by Agashe and Carone (AC) based on the abelian flavor symmetry $U(1)$ embedded in a non-trivial extra-dimensional topography [95], putting a special attention on the predictions of the model for the soft Lagrangian. Before entering into the details of the model, we have to warn the reader that this kind of Susy models based on a single $U(1)$ flavor symmetry are usually disfavored by constraints on FCNC processes [96–98]. More successful models are realized through the abelian flavor group $U(1)_{F1} \times U(1)_{F2}$ [96]. However, thanks to the use of a particular localization of the fermions in the extra dimensions, also the model [95] analyzed in this section can fulfil the constraints from FCNCs, as we will also prove in our Sec. 5.2.4.

In the AC model, two extra spatial dimensions, compactified on the orbifold $(S^1/Z^2)^2$ with the same compactification radius R, are assumed. The MSSM fields are localized as shown in Fig. 2.3. In this particular topography, the $\mathcal{G}_F = U(1)$ flavor symmetry group is introduced at the high scale M, that is assumed to be equal to the GUT scale $M_{\rm GUT}$. The flavor symmetry is then broken by means of the VEV of a flavon, as in the Froggatt-Nielsen model, with

$$\frac{\langle \Phi \rangle}{M} = \lambda \sim 0.22\,. \tag{2.63}$$

With the particular $U(1)$ charge assignments of the matter supermultiplets

$$\begin{array}{ll} Q^I \sim (-3, -2, 0), & D^I \sim (-3, -2, -2), \\ U^I \sim (-5, -2, 0), & H^1, H^2 \sim 0\,, \end{array} \tag{2.64}$$

one can compute the masses and mixings of the SM quarks, obtaining the experimental measured hierarchies between quark masses and mixing angles. The off-diagonal entries of the soft masses and trilinear terms at the GUT scale are also predicted by the model as function of the Cabibbo angle λ

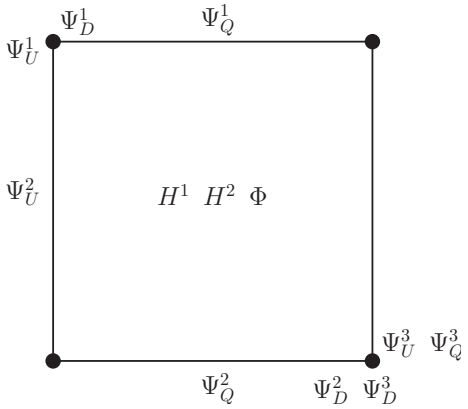

Figure 2.3: Extra-dimensional topography of the AC model.

$$\delta_d^{LL} \simeq \begin{pmatrix} \star & 0 & 0 \\ 0 & \star & \lambda^2 \\ 0 & \lambda^2 & \star \end{pmatrix} \ , \ \ \delta_d^{RR} \simeq \begin{pmatrix} \star & 0 & 0 \\ 0 & \star & e^{i\phi_R} \\ 0 & e^{-i\phi_R} & \star \end{pmatrix} \ , \tag{2.65}$$

$$(\delta_u^{LL})_{12} \simeq \lambda \, , \ \ (\delta_u^{RR})_{12} \simeq \lambda^3 \ , \tag{2.66}$$

where we have suppressed the $\mathcal{O}(1)$ real coefficients which multiply the individual elements of the matrices and where ϕ_R is a free parameter. Additionally, we mention that the chirality-flipping LR MIs are vanishing.

It is interesting to note that a $\mathcal{O}(\lambda)$ $(\delta_u^{LL})_{12}$ is not a peculiar feature of the abelian model analyzed by us, but a common characteristic of all the models based on abelian flavor symmetries. Indeed, abelian symmetries do not imply any pattern for the diagonal entries of the squark mass matrices. The diagonal soft masses are hence naturally split. This mass splitting unavoidably implies the $1 \leftrightarrow 2$ flavor transition in the up squark sector of order $(\delta_u^{LL})_{21} \sim \lambda$ of Eq. (2.66).

This can be easily understood by recalling that the $SU(2)_L$ gauge symmetry relates the left-left blocks of up and down squark matrices, i.e. $(M^2_{\tilde{U}})_{LL}$ and $(M^2_{\tilde{D}})_{LL}$, in such a way that $(M^2_{\tilde{U}})_{LL} = V^*(M^2_{\tilde{D}})_{LL}V^{\mathrm{T}}$. In turn, the expansion of this relation at the first order in λ implies that

$$(M^2_{\tilde{U}})^{21}_{LL} = \left[V^*(M^2_{\tilde{D}})_{LL}V^{\mathrm{T}}\right]^{21} \simeq (M^2_{\tilde{D}})^{21}_{LL} + \lambda\left(\tilde{m}^2_{\tilde{c}_L} - \tilde{m}^2_{\tilde{u}_L}\right) \ , \tag{2.67}$$

where $\tilde{m}_{\tilde{u}_L}$ and $\tilde{m}_{\tilde{c}_L}$ are the masses of left handed up squarks of first and second generation, respectively. Thus, even for $(M^2_{\tilde{D}})^{21}_{LL} = 0$, which is approximately satisfied in abelian flavor models, there are irreducible flavor violating terms in the up squark sector driven by the CKM matrix as long as the left handed squarks are split in mass.

2.3.5 The non abelian flavor model

In addition to the abelian flavor symmetry $U(1)$, there are many candidates for the flavor symmetry group $\mathcal{G}_F$, each having several distinct symmetry breaking patterns. In general,

$\mathcal{G}_F$ must be contained in the full global symmetry group of the SM in the limit of vanishing Yukawa couplings, $U(3)^5$. In particular, concerning non abelian flavor symmetries, a great attention is received by models with a $U(2)$ symmetry [99–102] acting on the lightest two generations and also models with $SU(3)$ symmetry [103–106]. The former are motivated by the large top mass, the latter by the observed neutrino mixings; they are indeed able to naturally predict an almost maximal atmospheric neutrino mixing angle $\theta_{23} \approx 45^\circ$ and to suggest a near maximal solar mixing angle $\theta_{12} \approx 30^\circ$.

In this section, we will present a particular non abelian flavor model based on a $SU(3)$ symmetry, the RVV model (from *Ross, Velasco-Sevilla, Vives*, the names of the authors) [105]. The detailed presentation of the model goes beyond the scope of this thesis. However we mention briefly few theoretical aspects. Thanks to the large symmetry group, the pattern of flavor symmetry breaking is more involved than in the case of the $U(1)$ flavor symmetry. Two flavons θ_3 and θ_{23} (respectively a $\bar{\mathbf{3}}$ and a $\mathbf{3}$ of $SU(3)$) are needed. They break $SU(3)$ in two steps

$$SU(3) \xrightarrow{\langle\theta_3\rangle} SU(2) \xrightarrow{\langle\theta_{23}\rangle} \text{nothing}\,. \tag{2.68}$$

The corresponding two expansion parameters, ε and $\bar{\varepsilon}$, are fixed to be $\varepsilon \sim 0.05$ and $\bar{\varepsilon} \sim 0.15$ at the symmetry breaking scale (that is taken approximately equal to $M_{\rm GUT}$), in order to fit the SM quark masses and mixing angles.

The particular flavor symmetry breaking fixes the superpotential, however the Kahler potential is not uniquely defined and, hence, the soft sector is not unambiguously determined. In the following, we will analyze a particular case of the RVV model to which we refer to as RVV2 model [107]. At the GUT scale, again suppressing the $\mathcal{O}(1)$ coefficients, the expressions for the flavor off-diagonal entries in the soft mass matrices read [107][14]

$$\delta_d^{RR} \simeq \begin{pmatrix} \star & -\bar{\varepsilon}^3\, e^{i\omega_{us}} & -\bar{\varepsilon}^2\, y_b^{0.5} e^{i(\omega_{us}-\chi+\beta_3)} \\ -\bar{\varepsilon}^3\, e^{-i\omega_{us}} & \star & \bar{\varepsilon}\, y_b^{0.5} e^{-i(\chi-\beta_3)} \\ -\bar{\varepsilon}^2\, y_b^{0.5} e^{-i(\omega_{us}-\chi+\beta_3)} & \bar{\varepsilon}\, y_b^{0.5} e^{i(\chi-\beta_3)} & \star \end{pmatrix}, \tag{2.69}$$

$$\delta_d^{LL} \simeq \begin{pmatrix} \star & -\varepsilon^2\bar{\varepsilon}\, e^{i\omega_{us}} & \varepsilon\bar{\varepsilon}\, y_t^{0.5} e^{i(\omega_{us}-2\chi+\beta_3)} \\ -\varepsilon^2\bar{\varepsilon}\, e^{-i\omega_{us}} & \star & \varepsilon\, y_t^{0.5} e^{-i(2\chi-\beta_3)} \\ \varepsilon\bar{\varepsilon}\, y_t^{0.5} e^{-i(\omega_{us}-2\chi+\beta_3)} & \varepsilon\, y_t^{0.5} e^{i(2\chi-\beta_3)} & \star \end{pmatrix}, \tag{2.70}$$

where $y_{t,b}$ are the top and bottom Yukawas, respectively, and the phases ω_{us}, χ and β_3 are set, to a large extent, by the requirement of reproducing the CKM phase; in particular, it turns out that $\omega_{us} \approx -\lambda$ and $(\chi, \beta_3) \approx (20^\circ, -20^\circ)$ (or any other values obtained by adding 180° to each). Additionally, it is found that the up quark MIs are given by [107]

$$(\delta_u^{LL})_{12} \simeq \lambda^4, \;\; (\delta_u^{RR})_{12} \simeq \lambda^6\,. \tag{2.71}$$

Differently from the abelian model, here the $(\delta_u^{LL})_{12}$ (as well as $(\delta_u^{RR})_{12}$) MI is quite small. This is, in fact, a general feature of non abelian flavor models based on a $SU(3)$

[14] Compared to the original RVV2 model [107], in (2.69), (2.70) we have set to zero an extra CPV phase, β_2' that is not constrained by the requirement of reproducing a correct CKM matrix. This simplifying assumption will turn out to be useful, once we will study the flavor phenomenology of the model, since this additional phase β_2' could bring unwanted accidental cancellations among different phases.

flavor symmetry. $SU(3)$ implies, indeed, an approximate degeneracy of the three generation squarks and, hence, large $(\delta_u^{LL})_{12}$ MIs cannot be generated because of $SU(2)$ gauge invariance, as instead it is the case of abelian flavor models.

The trilinear couplings follow the same symmetries as the Yukawas. In the SCKM basis, after rephasing the fields, the trilinears lead to the following flavor off-diagonal LR MIs [107]

$$\delta_d^{LR} \simeq \begin{pmatrix} \star & \bar{\varepsilon}^3\, e^{-i\omega_{us}} & \bar{\varepsilon}^3\, e^{-i\omega_{us}} \\ \bar{\varepsilon}^3\, e^{-i\omega_{us}} & \star & \bar{\varepsilon}^2 \\ \bar{\varepsilon}^3\, e^{i(\omega_{us}+2\beta_3-2\chi)} & \bar{\varepsilon}^2\, e^{2i(\beta_3-\chi)} & \star \end{pmatrix} \frac{A_0}{m_0^2}\, m_b\,. \tag{2.72}$$

Differently from the abelian models, the RVV model is embedded in a $SO(10)$ Susy GUT model, and thus correlations between flavor violating processes in the lepton and in the quark sector naturally occur, making additional tests of the model possible.

In particular, the flavor off-diagonal soft breaking terms of the leptonic sector arising in the RVV2 model are given by [107]

$$\delta_\ell^{RR} \simeq \begin{pmatrix} \star & -\frac{1}{3}\bar{\varepsilon}^3 & -\frac{1}{3}\bar{\varepsilon}^2\, y_b^{0.5} e^{i(-\chi+\beta_3)} \\ -\frac{1}{3}\bar{\varepsilon}^3 & \star & \bar{\varepsilon}\, y_b^{0.5} e^{-i(\chi-\beta_3)} \\ -\frac{1}{3}\bar{\varepsilon}^2\, y_b^{0.5} e^{i(\chi-\beta_3)} & \bar{\varepsilon}\, y_\tau^{0.5} e^{i(\chi-\beta_3)} & \star \end{pmatrix}, \tag{2.73}$$

$$\delta_\ell^{LL} \simeq \begin{pmatrix} \star & -\frac{1}{3}\varepsilon^2\bar{\varepsilon} & \frac{1}{3}\varepsilon\bar{\varepsilon}\, y_t^{0.5} e^{i(-2\chi+\beta_3)} \\ -\frac{1}{3}\varepsilon^2\bar{\varepsilon} & \star & \varepsilon\, y_t^{0.5} e^{-i(2\chi-\beta_3)} \\ \frac{1}{3}\varepsilon\bar{\varepsilon}\, y_t^{0.5} e^{i(2\chi-\beta_3)} & \varepsilon\, y_t^{0.5} e^{i(2\chi-\beta_3)} & \star \end{pmatrix}, \tag{2.74}$$

while the leptonic off-diagonal LR MIs have the following structure

$$\delta_\ell^{LR} \simeq \begin{pmatrix} \star & \bar{\varepsilon}^3 & \bar{\varepsilon}^3 \\ \bar{\varepsilon}^3 & \star & 3\bar{\varepsilon}^2 \\ \bar{\varepsilon}^3\, e^{i(2\beta_3-2\chi)} & 3\bar{\varepsilon}^2\, e^{2i(\beta_3-\chi)} & \star \end{pmatrix} \frac{A_0}{m_0^2}\, m_\tau\,. \tag{2.75}$$

2.3.6 The running of the parameters of the Lagrangian

As specified in the previous two sections, flavor models predict the pattern of the several MIs as function of one (or more) small expansion parameter, at a scale that is quite higher than the EW scale. Thus, to obtain reliable predictions on the phenomenology, one should keep into account the running of the several parameters from the high energy scale (in the case of the aforementioned flavor models, from the GUT scale) to the low energy scale at which the physical observables are defined. In this subsection we are interested in answering to the crucial question:

Are the textures of the squark mass matrices predicted by a flavor model RG stable?

In this discussion we will disregard off-diagonalities in the trilinear couplings, i.e. LR and RL MIs, since they are in general suppressed with respect to the LL and RR MIs by the factor M_Z/m_0 (as shown explicitly in (2.72) for the RVV2 model).

A close inspection of the RG equations (RGEs) [94] relevant for the RR sector shows that the RR MIs are approximately not generated at the low energy scale through the running, if they are not present already at the high energy scale. In fact, neglecting 1st and 2nd generation Yukawa couplings, the RGEs for the off-diagonal elements of $M^2_{U,D}$ of Eq. (2.50) read at the one loop level

$$16\pi^2 \frac{d}{dt}(M^2_U)_{ij} \overset{i\neq j}{\sim} 2\left(y_t^2\right)(M^2_U)_{ij}(\delta_{i3}+\delta_{j3})\,, \tag{2.76}$$

$$16\pi^2 \frac{d}{dt}(M^2_D)_{ij} \overset{i\neq j}{\sim} 2\left(y_b^2\right)(M^2_D)_{ij}(\delta_{i3}+\delta_{j3})\,, \tag{2.77}$$

where $t = \log(\mu/\mu_0)$. As can be easily observed, $(M^2_{U,D})_{12}$ are RG invariant in this approximation; we have checked that this holds numerically to an excellent approximation even if light generation Yukawas and LR-RL MIs are taken into account[15]. Concerning the entries which involve the third generation squarks, we observe that their values are affected by the running. Including also light generation Yukawas and LR-RL MIs, we find that between the GUT scale and the low energy scale (of the order 1 TeV) they are reduced by at most 15%.

The situation in the LL sector is different; there, also mixing with the RR sector and between different generations takes place. Consequently, the elements can be generated by RG effects even if they vanish at the GUT scale. Of course, both these effects are suppressed by combinations of CKM elements, since they would be absent if the CKM matrix was diagonal. Neglecting the LR and RL MIs, the RG equation for the off-diagonal elements of M^2_Q reads

$$\begin{aligned} 16\pi^2 \frac{d}{dt}(M^2_Q)_{ij} \overset{i\neq j}{\sim}\; & 2\left(y_{d,i}\, y_{d,j}\right)(M^2_D)_{ji} + \left(y_b^2\right)(M^2_Q)_{ij}(\delta_{i3}+\delta_{j3}) + y_t^2(M^2_Q)_{ik}\lambda_{kj} + \\ & + y_t^2(M^2_Q)_{kj}\lambda_{ik} + 2y_t^2 m^2_{H^2}\lambda_{ij} + 2y_t^2(M^2_U)_{33}\lambda_{ij}\,, \end{aligned} \tag{2.78}$$

where $\lambda_{ij} = V^*_{ti}V_{tj}$ and we have neglected light generation Yukawas, except in the first term, which in the case of $(ij) = (23)$ is only suppressed by y_s/y_b, but unsuppressed by CKM angles and can therefore be comparable in size to the remaining terms. One should notice that in the RGE just presented, some of the terms are inducing a mixing among the LL elements (see for example the term $y_t^2(M^2_Q)_{ik}\lambda_{kj}$), some others describe the CKM-induced generation of LL MIs, which takes place even in a completely flavor blind situation at the GUT scale (see for example the term $2y_t^2 m^2_{H^2}\lambda_{ij}$).

Finally, let us also mention that the attained values for the MIs defined in (2.55) are renormalization scale dependent mainly because of the fact that the diagonal elements of the soft mass matrices are strongly affected by RG effects (see [94]).

[15] The invariance under RGE of the RR MIs for the first two generations is approximately valid also at the two loop level.

Chapter 3

The New Physics flavor problem

In this chapter we discuss the theoretical features of the flavor sector of the RS model with custodial protection and of Susy flavor models. For both frameworks, at first sight, the NP flavor problem seems to be particularly grave, because of the too large new physics contributions to flavor observables, or, in the language of effective Hamiltonians (see Sec. 2.1), because of the too large Wilson coefficients corresponding to operators mediating flavor changing neutral current processes. However, both models exhibit mechanisms suitable to protect the flavor transitions from too large NP effects. The main focus of the chapter is indeed on the discussion of the several protection mechanisms that allow the frameworks to have the possibility to be consistent with the experiments on flavor observables, still having a NP energy scale of $\mathcal{O}(1\,\text{TeV})$, as hinted by the gauge hierarchy problem.

3.1 Flavor changing transitions in the RS model

3.1.1 Flavor changing neutral currents at the tree level

The RS model shows several characteristic features in the flavor sector. Among the most relevant, one should number the appearance of flavor changing neutral currents already at the tree level, due to the non-universality of the couplings of the several SM fermions with the gauge bosons. These non-universalities are arising mainly because of two effects:

- The non-uniform localization of the gauge bosons (both KK and the zero modes) in the bulk [47, 50, 59, 108];
- The mixing of the fermion zero modes with the KK excitations with the same electric charge, through EWSB [109, 110].

We now review in detail the two effects responsible of FCNCs at the tree level in the RS framework. In the discussion, as also anticipated in Sec. 2.2.3, we will not take into account the presence of fermion and gauge boson excitations heavier than the first.

Gauge boson mixing impact on FCNCs

In Sec. 2.2.1 we have shown that the bulk profiles of the zero mode fermions are not flat along the fifth dimension, but depend exponentially on the respective bulk mass parameters c_i (Eq. (2.12) and Fig. 2.1). Before EWSB the KK gauge bosons, namely the gluons $G_\mu^{(1)A}$, the EW gauge boson Z_{X_μ} in (2.25) and the KK excitation of the Z boson and of the photon A_μ in (2.31) and (2.32), have a shape function peaked towards the IR brane (see Eq. (A.7)). The couplings of the zero mode fermions with the KK gauge bosons with BCs $(++)$ and $(-+)$ are then proportional to

$$\varepsilon^+_{L,R}(c_\psi) = \frac{1}{L}\int_0^L dy\, \tilde{f}^{(0)}_{L,R}(y,c_\psi)^2 g(y)\,, \qquad \varepsilon^-_{L,R}(c_\psi) = \frac{1}{L}\int_0^L dy\, \tilde{f}^{(0)}_{L,R}(y,c_\psi)^2 \tilde{g}(y)\,, \tag{3.1}$$

respectively, where $g(y)$ and $\tilde{g}(y)$ are the shape functions of the KK gauge boson with BCs $(++)$ and $(-+)$, respectively (reported in Appendix A) and $\tilde{f}^{(0)}_{L,R}(y,c_\psi)$ are the shape functions of a SM left handed and right handed fermion, normalized with respect to the flat metric (reported in Eq. (2.16)).

Since the bulk masses c_ψ are flavor dependent, in the flavor basis the couplings of the zero mode fermions together with the KK gauge bosons will be diagonal but *flavor non-universal*. This will give rise to off-diagonal couplings of the SM fermions with KK gauge bosons, once that we rotate to the mass eigenstate basis for fermions. These off-diagonalities are an intrinsic feature of the model and they cannot be rotated away by a redefinition of the fermion fields. Going then to the mass eigenstate basis also for gauge bosons, tree level flavor changing neutral vertices, of the type in the left panel of Fig. 3.1, appear.

On the other hand, in Appendix A (Eq. (A.6)) we show that, before EWSB, the shape function of the SM gauge boson Z_μ (defined in Eq. (2.31)) is flat along the fifth dimension. Consequently we do not expect FCNCs at the tree level involving Z_μ. However, with the breaking of the electroweak symmetry, the SM gauge boson mix with its KK excitation $Z_\mu^{(1)}$ and with the gauge bosons Z_{X_μ} coming from the additional $SU(2)_R$ symmetry (see Eq. (2.42)), developing also a non-flat shape function. In conclusion, thanks to the EWSB, also the SM gauge boson Z_μ acquires flavor changing neutral vertices at the tree level, as represented in the right panel of Fig. 3.1.

Finally the zero modes of the gluons $G_\mu^{(0)A}$ and of the photon $A_\mu^{(0)}$ do not have flavor changing neutral couplings, because they do not experience EWSB.

This concludes the explanation of the first effect that induces FCNCs at the tree level in the RS model.

KK fermion impact on FCNCs

Up to now, we have neglected the mixing between the zero mode fermions $f^{(0)}_{L,R}$ and the KK excitations with the same charge, induced by EWSB (see also end of Sec. 2.2.3). In the following we will analyze in detail this second source of tree level flavor changing neutral vertices of the SM Z boson following closely our analysis in [110].

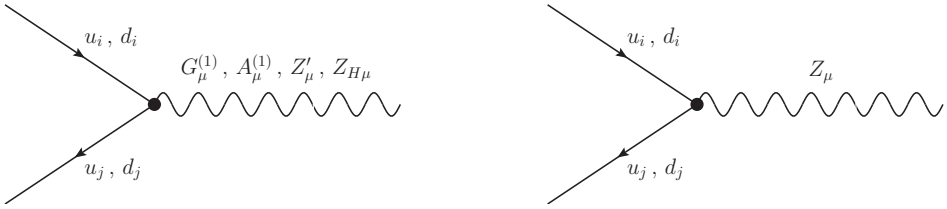

Figure 3.1: Flavor changing ($i \neq j$) vertices allowed at the tree level in the RS model.

A particular suitable way to investigate the effects of mixing of the fermion zero modes with the KK excitations is to write down the effective Hamiltonian generated at the TeV scale, after having integrated out the vector-like heavy fermions [111, 112] (see also [113] for a more general analysis).

We start in all generality with a model-independent analysis. We take a theory which resembles the SM, but which has in the spectrum $N + M$ additional vector-like quarks: N of charge $2/3$ and M of charge $-1/3$ (in the particular case of the RS model, $N = 5$ and $M = 3$)

$$\begin{aligned} \Psi_L^T(2/3) &= \left(u_L,\, U_L^1,\, U_L^2, \ldots,\, U_L^N\right) , \\ \Psi_R^T(2/3) &= \left(u_R,\, U_R^1,\, U_R^2, \ldots,\, U_R^N\right) , \\ \Psi_L^T(-1/3) &= \left(d_L,\, D_L^1,\, D_L^2, \ldots,\, D_L^M\right) , \\ \Psi_R^T(-1/3) &= \left(d_R,\, D_R^1,\, D_R^2, \ldots,\, D_R^M\right) , \end{aligned} \tag{3.2}$$

where with $u_{L,R}$ and $d_{L,R}$ we indicate the SM fermions and with $U_{L,R}^i$ and $D_{L,R}^i$ the heavy fermions. All the flavor indices are suppressed.

It is important to notice that this kind of theory mimics exactly the RS model for all our purposes: in fact the charge $5/3$ quarks present in the RS model do not mix with the SM fermions through EWSB and hence are not relevant for the corrections to gauge bosons-SM fermions vertices.

Before integrating out the heavy degrees of freedom, the fundamental EW Lagrangian relevant for our analysis[1] is given by

$$\mathcal{L} = \mathcal{L}_{\rm kin} + \mathcal{L}_{\rm mass} + \mathcal{L}_{\rm Yuk} + \mathcal{L}_W + \mathcal{L}_Z \,. \tag{3.3}$$

Neglecting for the moment the couplings with the gauge bosons, the canonically normalized kinetic terms for all the quarks of the theory are given by

[1] More specifically, $\mathcal{L}_Z$ and $\mathcal{L}_W$ indicate the terms of the Lagrangian arising from the couplings between quarks and two linear combinations of gauge fields that, after EWSB, will be identified with the Z and $W^\pm$ bosons, respectively. The term $\mathcal{L}_W$ will not be analyzed in detail, since we are interested only to the flavor changing neutral currents of the theory. We refer the reader to the original paper [110] where also $\mathcal{L}_W$ is discussed, in view of the analysis of the unitarity of the CKM matrix in the RS model with custodial protection.

$$\begin{aligned}\mathcal{L}_{\rm kin} &= \bar{\Psi}_L(2/3)i\partial\!\!\!/\Psi_L(2/3) + \bar{\Psi}_R(2/3)i\partial\!\!\!/\Psi_R(2/3) \\ &+ \bar{\Psi}_L(-1/3)i\partial\!\!\!/\Psi_L(-1/3) + \bar{\Psi}_R(-1/3)i\partial\!\!\!/\Psi_R(-1/3)\,, \end{aligned} \tag{3.4}$$

to which we have to add the interactions of the quarks with the (neutral and charged) gauge bosons

$$\begin{aligned}\mathcal{L}_Z &= \Big(\bar{\Psi}_L(2/3)\gamma_\mu \mathcal{A}_L^{2/3}(Z)\Psi_L(2/3) \\ &+ \bar{\Psi}_R(2/3)\gamma_\mu \mathcal{A}_R^{2/3}(Z)\Psi_R(2/3) \\ &+ \bar{\Psi}_L(-1/3)\gamma_\mu \mathcal{A}_L^{-1/3}(Z)\Psi_L(-1/3) \\ &+ \bar{\Psi}_R(-1/3)\gamma_\mu \mathcal{A}_R^{-1/3}(Z)\Psi_R(-1/3)\Big)\, Z^\mu\,, \end{aligned} \tag{3.5}$$

where the matrices $\mathcal{A}_{L,R}^{2/3}(Z)$ and $\mathcal{A}_{L,R}^{-1/3}(Z)$ are $3(N+1)\times 3(N+1)$ and $3(M+1)\times 3(M+1)$ real diagonal matrices respectively, and

$$\begin{aligned}\mathcal{L}_W &= \big(\bar{\Psi}_L(2/3)\gamma_\mu \mathcal{G}_L(W^+)\Psi_L(-1/3) \\ &+ \bar{\Psi}_R(2/3)\gamma_\mu \mathcal{G}_R(W^+)\Psi_R(-1/3)\big)\, W^{\mu\pm}\,, \end{aligned} \tag{3.6}$$

where $\mathcal{G}_{L,R}(W^+)$ are $3(N+1)\times 3(M+1)$ real matrices.

Additionally, the couplings of the several quarks with the Higgs boson are given by

$$\begin{aligned}\mathcal{L}_{\rm Yuk} &= -\Phi\,\big(\bar{\Psi}_L(2/3)\mathcal{Y}(2/3)\Psi_R(2/3) \\ &+ \bar{\Psi}_L(-1/3)\mathcal{Y}(-1/3)\Psi_R(-1/3) + \text{ h.c.}\big)\,, \end{aligned} \tag{3.7}$$

where $\mathcal{Y}(2/3)$ and $\mathcal{Y}(-1/3)$ are $3(N+1)\times 3(N+1)$ and $3(M+1)\times 3(M+1)$ complex matrices, respectively, and Φ is the Higgs doublet.

If the theory contained only chiral fermions, then, before EWSB, the fermion Lagrangian would be the sum of the terms (3.4)-(3.7), only. However, the additional heavy fermions are assumed to be vectorial, so, even before EWSB, the theory has two non-trivial mass terms

$$\mathcal{L}_{\rm mass} = -\bar{\Psi}_L(2/3)\tilde{\mathcal{M}}(2/3)\Psi_R(2/3) - \bar{\Psi}_L(-1/3)\tilde{\mathcal{M}}(-1/3)\Psi_R(-1/3) + h.c.\,, \tag{3.8}$$

where $\tilde{\mathcal{M}}(2/3)$ and $\tilde{\mathcal{M}}(-1/3)$ are $3(N+1)\times 3(N+1)$ and $3(M+1)\times 3(M+1)$ diagonal matrices, respectively. The first three entries correspond to SM quark masses and hence vanish before EWSB, while the remaining entries are of the order $\tilde{f}$, the New Physics scale at which the new quarks arise $(\tilde{f} > v)$[2].

[2]In the RS model $\tilde{f} = M_{\rm KK}$.

At this point, we have all the elements to integrate out the heavy fermions at the tree level, using their equations of motion. Expanding then in powers of $v/\tilde{f}$, we can get the effective Lagrangian at the low scale, where the only degrees of freedom are the SM quarks (and gauge bosons).

To be more specific, after the process of integrating out the heavy quarks, we will get, as effective Lagrangian, the SM Lagrangian and, in addition, several operators of dimension $D = 6$ (keeping terms until the order $v^2/\tilde{f}^2$ in the expansion) corresponding to the corrections due to the interaction between SM fields and the new heavy fermions. Performing then EWSB implies the replacement of Φ with its VEV $\Phi = \frac{v}{\sqrt{2}}$. Making this replacement in the effective Lagrangian allows to find the corrections to the SM couplings that result from the mixing with heavy vector-like fermions. Worth to notice is that, in order to get a canonical propagator of the SM quarks, one should guarantee the canonical form of their kinetic terms, after the integrating out of the heavy degrees of freedom. Operatively, one can achieve that, simply redefining suitably the SM quarks.

In the next step, we want to analyze, how relevant are these corrections, in terms of FCNCs. To simplify the notation, we will denote the 3×3 matrices in flavor space that build up the several matrices $\mathcal{A}_{L,R}$, $\mathcal{G}_{L,R}$ and $\mathcal{Y}$ (introduced in (3.5)-(3.7)) by $(A_{L,R})_{\alpha\beta}$, $(G_{L,R})_{\alpha\beta}$ and $Y_{\alpha\beta}$ respectively, where $\alpha, \beta = 0, 1, ..., N$ (or M). In particular, for $\alpha = \beta = 0$ we have exactly the coupling matrices of the SM quarks in the absence of heavy vector-like states.

The same comment is also valid for the mass matrices. However, at this stage after EWSB, we are not dealing with the matrices in (3.8) containing just vector-like masses anymore, but with the mass matrices M which take into account also the mass terms arising from the Higgs mechanism. In fact, once that the Higgs field is replaced by its VEV, $\mathcal{L}_{\text{Yuk}}$ in (3.7) brings new contributions to the mass matrices (we refer the reader to [78] for the explicit form of the two mass matrices after EWSB). Consequently the matrices $M_{\alpha\beta}$ will have the properties

1. $M_{kk} = \mathcal{O}(\tilde{f})$, with $k \neq 0$;
2. $M_{00} = \mathcal{O}(v)$;
3. M_{ij} with $i \neq j$ are $\mathcal{O}(v)$ but could also vanish;
4. M_{0k} and M_{k0} are generally $\mathcal{O}(v)$ but if $M_{0k} \neq 0$ then $M_{k0} = 0$ and vice versa. This follows from the known property that only one of the chiralities of each vector-like fermion couples to the SM quarks through mass terms [114].

In [110] we studied in detail the corrections to the couplings between SM left and right handed quarks and the neutral Z gauge bosons. We found that, after the integrating out of the heavy fermions

$$
\begin{aligned}
A_L(Z) &= [A_L(Z)]_{00} + M_{0k}M_k^{-1}\,[A_L(Z)]_{kk}\,M_k^{-1}M_{0k}^\dagger \\
&- \frac{1}{2}M_{0k}M_k^{-2}M_{0k}^\dagger\,[A_L(Z)]_{00} \\
&- \frac{1}{2}\,[A_L(Z)]_{00}\,M_{0k}M_k^{-2}M_{0k}^\dagger\,, \qquad (3.9)
\end{aligned}
$$

$$
\begin{aligned}
A_R(Z) &= [A_R(Z)]_{00} + M_{k0}^\dagger M_k^{-1}\,[A_R(Z)]_{kk}\,M_k^{-1}M_{k0} \\
&- \frac{1}{2}M_{k0}^\dagger M_k^{-2}M_{k0}\,[A_R(Z)]_{00} \\
&- \frac{1}{2}\,[A_R(Z)]_{00}\,M_{k0}^\dagger M_k^{-2}M_{k0}\,, \qquad (3.10)
\end{aligned}
$$

where we have denoted $M_{kk} \equiv M_k$ ($k \neq 0$) for the 3×3 mass matrices with identical indices, and summation over repeated indices is understood. We note that these formulae are valid both for charge $+2/3$ and charge $-1/3$ quarks, changing suitably the mass matrices and the couplings $[A_{L,R}(Z)]_{\alpha\beta}$ involved in the expressions.

The structure of the interaction of left and right handed SM quarks with the Z bosons looks very similar: both couplings have a leading term $(A_{L,R}(Z))_{00}$ to which one has to add three corrections of $\mathcal{O}\left(\frac{v^2}{f^2}\right)$. The first originates in the interactions of the heavy fermion fields with the SM gauge bosons and the remaining terms are consequence of the redefinitions of the light SM fields, to maintain canonically normalized kinetic terms[3].

Finally, one has to express the result in the mass eigenstate basis for the SM quarks. For that purpose, one has to write down the two effective 3×3 up and down mass matrices and diagonalize them. More in details, following the procedure discussed above, namely, integrating out the heavy fermions and defining the SM quarks in such a way that their kinetic terms are canonically normalized, one finds for the mass terms of the SM quarks

$$
\begin{aligned}
M &= M_{00} + M_{0k}M_k^{-1}M_{kj}M_j^{-1}M_{j0} \\
&- \frac{1}{2}\left[M_{0k}M_k^{-2}M_{0k}^\dagger M_{00} + M_{00}M_{k0}^\dagger M_k^{-2}M_{k0}\right]\,, \qquad (3.11)
\end{aligned}
$$

with $k \neq j$, valid for both up and down quarks.

These two mass matrices are diagonalized by means of two suitable rotations of the left handed and right handed SM quarks

$$
\begin{aligned}
M_{\rm diag}(-1/3) &= \mathcal{D}_L^\dagger\,M(-1/3)\,\mathcal{D}_R\,, \qquad (3.12) \\
M_{\rm diag}(2/3) &= \mathcal{U}_L^\dagger\,M(2/3)\,\mathcal{U}_R\,. \qquad (3.13)
\end{aligned}
$$

Finally, in the mass eigenstate for SM quarks, the couplings with the Z boson are given by

[3] In the following section we will investigate the importance of this second kind of contribution in the particular case of the RS model with custodial protection.

	(0,0)	(1,1)	(2,2)	(3,3)
$A_L^{-1/3}$	$g_{Z,L}^{4D}(d)$	$g_{Z,L}^{4D}(d)$	$g_Z^{4D}(D')$	$g_{Z,R}^{4D}(d)$
$A_R^{-1/3}$	$g_{Z,R}^{4D}(d)$	$g_{Z,L}^{4D}(d)$	$g_Z^{4D}(D')$	$g_{Z,R}^{4D}(d)$

Table 3.1: Weak charges in the coupling matrices of down quarks to the Z gauge boson.

	(0,0)	(1,1)	(2,2)	(3,3)	(4,4)	(5,5)
$A_L^{2/3}$	$g_{Z,L}^{4D}(u)$	$g_{Z,L}^{4D}(u)$	$g_Z^{4D}(U')$	$g_Z^{4D}(U'')$	$g_Z^{4D}(\chi^d)$	$g_{Z,R}^{4D}(u)$
$A_R^{2/3}$	$g_{Z,R}^{4D}(u)$	$g_{Z,L}^{4D}(u)$	$g_Z^{4D}(U')$	$g_Z^{4D}(U'')$	$g_Z^{4D}(\chi^d)$	$g_{Z,R}^{4D}(u)$

Table 3.2: Weak charges in the coupling matrices of up quarks to the Z gauge boson.

$$\left[A_{L,R}^{-1/3}(Z)\right]_{\text{mass}} = \mathcal{D}_{L,R}^{\dagger}\, A_{L,R}^{-1/3}(Z)\, \mathcal{D}_{L,R}\,, \tag{3.14}$$

$$\left[A_{L,R}^{2/3}(Z)\right]_{\text{mass}} = \mathcal{U}_{L,R}^{\dagger}\, A_{L,R}^{2/3}(Z)\, \mathcal{U}_{L,R}\,. \tag{3.15}$$

This ends our model-independent analysis of the effects of heavy vectorial fermions on the couplings of the SM quarks with the Z gauge boson. Now we can apply our formalism to the RS model in which the quark field content (3.2) is explicitly given by

$$\begin{aligned}
\Psi_L^T(-1/3) &= \left(q_L^{d_i(0)},\, q_L^{d_i},\, D_L'^i,\, D_L^i\right)\,, \\
\Psi_R^T(-1/3) &= \left(D_R^{i(0)},\, q_R^{d_i},\, D_R'^i,\, D_R^i\right)\,, \\
\Psi_L^T(2/3) &= \left(q_L^{u_i(0)}, q_L^{u_i}, U_L'^i, U_L''^i, \chi_L^{d_i}, u_L^i\right)\,, \\
\Psi_R^T(2/3) &= \left(u_R^{i(0)}, q_R^{u_i}, U_R'^i, U_R''^i, \chi_R^{d_i}, u_R^i\right)\,,
\end{aligned} \tag{3.16}$$

and the scale at which the heavy fermions arise is given by $\tilde{f} = M_{\text{KK}}$.

The block coupling matrices of the several quarks with the Z boson $(A_{L,R})_{\alpha\beta}$ are proportional to 3×3 unit matrices with proportionality factors collected in Tabs. 3.1 and 3.2 and given explicitly in Appendix B.

We can finally adapt Eqs. (3.9) and (3.10) for the effective Z couplings to this particular model, finding for the charge $-1/3$ quarks the corrected couplings (the values of the several weak charges given in Appendix B are already replaced inside the expressions for the couplings)

$$A_L^{-1/3}(Z) = g_{Z,L}^{4D}(d)\mathbb{1} + \frac{1}{2}\frac{g^{4D}}{\cos\psi}\left(M_{03}\frac{1}{M_3^2}M_{03}^{\dagger} - M_{02}\frac{1}{M_2^2}M_{02}^{\dagger}\right)\,, \tag{3.17}$$

and

$$A_R^{-1/3}(Z) = g_{Z,R}^{4D}(d)\mathbb{1} - \frac{g^{4D}}{\cos\psi}\left(\frac{1}{2}M_{10}^\dagger\frac{1}{M_1^2}M_{10} + M_{20}^\dagger\frac{1}{M_2^2}M_{20}\right), \tag{3.18}$$

where the values of $g_{Z,R}^{4D}(d)$ and $g_{Z,L}^{4D}(d)$ are listed in Appendix B.

Analogously, using Tab. 3.2 with the corresponding values for the up-weak charges, we find for the couplings of the SM up quarks with the Z gauge boson

$$A_L^{2/3}(Z) = g_{Z,L}^{4D}(u)\mathbb{1} - \frac{1}{2}\frac{g^{4D}}{\cos\psi}\left(M_{02}\frac{1}{M_2^2}M_{02}^\dagger + M_{03}\frac{1}{M_3^2}M_{03}^\dagger + M_{05}\frac{1}{M_5^2}M_{05}^\dagger\right), \tag{3.19}$$

and

$$A_R^{2/3}(Z) = g_{Z,R}^{4D}(u)\mathbb{1} + \frac{1}{2}\frac{g^{4D}}{\cos\psi}\left(M_{10}^\dagger\frac{1}{M_1^2}M_{10} - M_{40}^\dagger\frac{1}{M_4^2}M_{40}\right), \tag{3.20}$$

where the values of $g_{Z,R}^{4D}(u)$ and $g_{Z,L}^{4D}(u)$ are listed in Appendix B[4].

With all these formulae at hand, we can now compare the impact of the mixing of the SM fermions with the lightest KK fermions with the impact of gauge boson mixing on the (flavor changing) neutral couplings of the SM fermions with the Z boson, and identify the dominant contribution. Namely, we are now ready to compare the relevance of the two sources of FCNCs, listed at the beginning of this section.

To simplify the discussion we denote the contribution to FCNC couplings from gauge boson mixing presented at the beginning of this section as Δ_G^{ij} and the contributions from KK fermion mixing as $\Delta_{\rm KK}^{ij}$. We can then write for a generic coupling of a SM quark with the Z boson the two contributions as

$$|A_{L,R}^Q(Z)|_{\rm G} = K_{L,R}^Z\left(\mathbb{1} + \frac{v^2}{M_{\rm KK}^2}|\Delta_{L,R}^Q(Z)|_{\rm G}\right), \tag{3.21}$$

$$|A_{L,R}^Q(Z)|_{\rm KK} = K_{L,R}^Z\left(\mathbb{1} + \frac{v^2}{M_{\rm KK}^2}|\Delta_{L,R}^Q(Z)|_{\rm KK}\right), \tag{3.22}$$

where $K_{L,R}^Z$ is the coupling constant of the SM field in question with the Z boson, in the absence of New Physics.

As an example, in Fig. 3.2 we compare the contributions from gauge boson mixing and KK fermion mixing that enter the flavor violating $Zt_L\bar{c}_L$ and $Zs_R\bar{d}_R$ couplings. We present the couplings in two density plots: lighter colors correspond to higher densities of points, darker colors to the lower densities. The plots are obtained for a set of parameter points that reproduces the quark masses and mixings as well as the well measured observables in $K^0 - \bar{K}^0$ and $B_{s,d}^0 - \bar{B}_{s,d}^0$ oscillations (see also Secs. 5.2.1, 5.2.2). From the figure it is evident that the KK fermion contribution is generally smaller than the contribution arising from gauge boson mixing for a majority of points in the parameter space, and in particular for those points that produce the largest effects in the respective coupling.

[4]To note that the last term in (3.17)-(3.20) arises because of the redefinition of the SM quark fields to maintain canonically normalized kinetic terms.

We have checked that this feature is totally general, independently of the two quarks involved in the coupling with the Z boson; indeed, what we have presented in Fig. 3.2 is the most unfortunate case in which the contribution from the KK fermion mixing is not fully negligible, as instead it is in many other cases, like for all the couplings of the type $Zd_L^i d_L^j$ and $Zu_R^i u_R^j$ (see also Sec. 3.1.4).

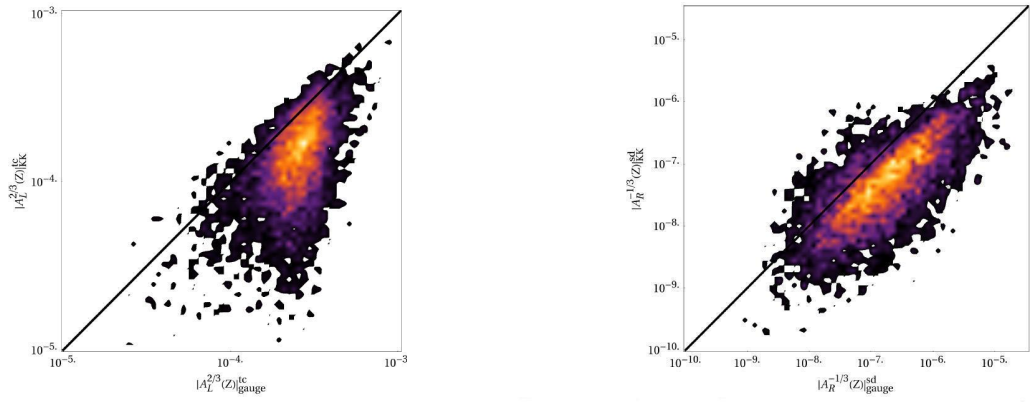

Figure 3.2: Comparison of contributions from KK fermion mixing and gauge boson mixing to the $Zt_L\bar{c}_L$ (left panel) and to the $Zs_R\bar{d}_R$ (right panel) coupling.

In conclusion, in view of this investigation and in view of the many uncertainties in the calculation of the several $\Delta F = 2$ flavor observables in Secs. 5.2.1, 5.2.2, as well as of the several branching ratios of rare B and K decays of Secs. 5.3.1 - 5.3.3, we consider safe not to take into account further the contributions of the KK fermion mixings to FCNC processes. Therefore all the phenomenology of Chapter 5 will be developed, not taking into account the presence of KK fermions.

Independently of the source of flavor changing neutral interaction, the main conclusion of this section is that the model shows FCNCs already at the tree level. Consequently, using the effective field theory language, once that the gauge bosons mediating the FCNC interactions are integrated out, we expect operators of the type (2.2) with an effective coupling $c_i^{(2)}$ that is not suppressed by one loop factors, but is typically of $\mathcal{O}(1)$. Therefore, following the discussion of Sec. 2.1, we can expect that either the NP scale $\Lambda_{\rm NP}$ (which corresponds to $M_{\rm KK}$ in the RS model) is quite high, or the model is not in agreement with the experimental constraints on flavor transition observables. Due to the FCNCs at the tree level, the NP flavor problem seems particularly grave in the RS model.

Fortunately, this is just a naive conclusion: in Secs. 3.1.3 and 3.1.4, indeed, we will study the mechanisms which weaken the NP flavor problem, in spite of the tree level flavor changing couplings. We will show that the Wilson coefficients $c_i^{(2)}$ are not naturally of $\mathcal{O}(1)$, but smaller.

3.1.2 Higgs mediated flavor changing neutral currents

Recently, the study of the effects of FCNCs due to the exchange at the tree level of one (or more) Higgs boson generated a lot of interest, both in the context of Two Higgs Doublet Models (2HDMs) (see e.g. our recent work [115]) and in the context of composite Higgs models [116] and hence also in the RS model [117, 118].

Let us analyze the main features of the Higgs mediated FCNCs in the RS framework. In addition to FCNCs at the tree level due to the exchange of gauge bosons, the warped extra dimensional (WED) structure of the model can also lead to Higgs mediated FCNCs at the tree level. In fact, quark masses and Yukawa couplings can be not aligned.

Focusing for simplicity on the down quark sector, the main source of misalignment is represented in Fig. 3.3 in the mass insertion approximation (see also Sec. 3.2.1 for a pedagogical explanation of the mass insertion approximation in the framework of Susy). The second diagram in the figure affects masses and Yukawa couplings in a different manner since its contribution to the Yukawa couplings arises setting only two of the three Higgs to the VEV v and hence, contrary to the contribution to the masses, a combinatorical factor of three appears.

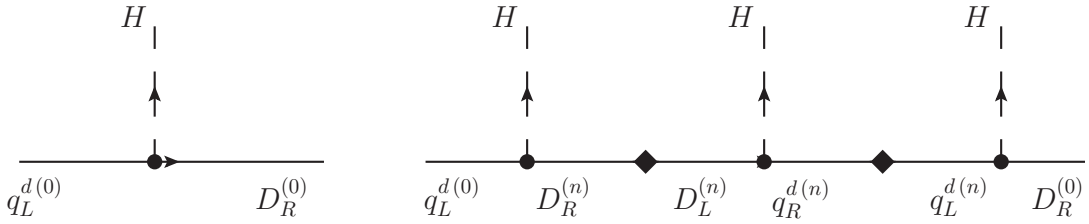

Figure 3.3: Contributions to masses and Yukawa couplings of SM down fermions using the mass insertion approximation (the mass insertions are denoted with a diamond ⧫).

In [117] it was pointed out that the misalignment is indeed non-vanishing, in spite of the Dirichlet boundary conditions on the IR brane of the fields D_L and q_R^d (see also the field representation in Eqs. (2.34)-(2.36)). In fact, their profiles do not exactly vanish on the IR brane but display a small discontinuity that is proportional to the Higgs VEV[5]. After regularizing this discontinuity and summing over the infinite tower of fermion KK modes it is found that a non-vanishing misalignment between quark masses and Yukawa couplings is generated by the above diagram.

More specifically, using the notation of [117], if one defines the misalignment for the i-th flavor as

$$\Delta_i^d \equiv m_{i\,\mathrm{SM}}^d - y_{i\,\mathrm{SM}}^d v\,, \tag{3.23}$$

then, after the sum over the entire KK tower of fermions

$$\Delta_i^d = \frac{(Y_1^2 Y_2)_{ii} v^2}{M_{\mathrm{KK}}^2}\,, \tag{3.24}$$

[5]The tiny discontinuity does not appear in our perturbative approach (see Sec. 2.2.1).

where $Y_{1,2}$ are the two Yukawa couplings for down quarks defined by

$$S_{\rm Yuk} = \int d^4x \int_0^L dy \sqrt{G}\ {\rm Tr} \sum_{i,j=1}^{3} \sqrt{2}\mathcal{H}\Big[Y_1\, \bar{q}^d_L D_R + Y_2\, \bar{q}^d_R D_L + h.c.\Big]\,. \tag{3.25}$$

Rotating then to mass eigenstates for SM fermions, the several misalignments produce flavor changing neutral couplings of the SM fermions with the Higgs boson, that could be in principle competitive with the flavor changing neutral couplings of SM down quarks with gluons [117], that we have presented in the previous section.

One should however notice that this conclusion does not apply to the particular RS model that we are studying in this thesis. Analyzing in fact the structure of the Yukawa couplings just mentioned, we note the appearance of an additional Yukawa coupling matrix (Y_2) that is not required for generating the SM fermion masses. Hence, as also shown by the Yukawa couplings of the model analyzed by us in Eq. (2.44), one could simply put that matrix to zero. Keeping this approach, the aforementioned contribution to FCNCs would vanish.

Finally, to conclude the discussion of the Higgs mediated FCNCs, one should also mention another source of misalignment between SM quark masses and corresponding Yukawa couplings: the modification of the kinetic terms by the mixing of SM quarks and KK quarks after EWSB, that we have analyzed in the previous section. Indeed, these flavor-dependent corrections to the kinetic terms make redefinitions of the SM quark fields necessary to keep canonically normalized kinetic terms, which in turn give rise to an additional shift between quark masses and Yukawa couplings. In [110] we have found that the contribution is negligible for the first two generation quarks, but not for the third generation.

In our numerical analysis of Chapter 5 we will not include these effects, that in any case would not spoil the overall picture of the phenomenology studied by us.

3.1.3 The RS-GIM mechanism

In the Standard Model the FCNC processes are kept under control by the so called Glashow-Iliopoulos-Maiani (GIM) mechanism [11]. GIM implies the absence of flavor changing neutral transitions at the tree level thanks to the unitarity of the CKM matrix. Additionally, if the masses of quarks were equal, GIM would also imply that flavor changing neutral transitions are not present at one loop either. However, as it is well known, the quark masses are different, leading to the breaking at one loop of GIM and consequently to the appearance of FCNC transitions in the SM.

In the RS model a suppression of flavor changing neutral currents is due to a similar mechanism, hence called the *RS-GIM* mechanism [51, 119].

As already anticipated at the beginning of Sec. 3.1.1, in the flavor eigenstate basis, the coupling of a SM quark with a gauge boson with BCs $(++)$ or $(-+)$, can be expressed by the flavor dependent overlap integrals $\varepsilon^{\pm}_{L,R}$ in (3.1). In order to go to mass eigenstates for quarks (neglecting, as already explained, the mixing with the heavy KK fermions), the 3×3 diagonal matrices formed by the flavor dependent terms $\varepsilon^{\pm}_{L,R}$ on the diagonal should

be rotated with biunitary transformations, similarly to what we have seen in (3.14)-(3.15). In particular, for up and down quarks, dropping the $\pm$ sign indicating the BCs of the gauge boson involved in the coupling, we have

$$\Delta_{L,R}^{-1/3} = D_{L,R}^{\dagger}\,\varepsilon_{L,R}^{-1/3}\,D_{L,R}\,, \tag{3.26}$$

$$\Delta_{L,R}^{2/3} = U_{L,R}^{\dagger}\,\varepsilon_{L,R}^{2/3}\,U_{L,R}\,, \tag{3.27}$$

where with $D_{L,R}$ and $U_{L,R}$ we denote the rotation matrices that diagonalize the SM quark mass matrices (namely, the matrices $D_{L,R}$ and $U_{L,R}$ which diagonalize the mass matrices M_{00} for down and up quarks in (3.11)).

It is clear that if the couplings $\varepsilon_{L,R}$ were proportional to the identity matrix, then, because of the unitarity of the matrices $U_{L,R}$ and $D_{L,R}$, $\Delta_{L,R}^{Q}$ would be diagonal and hence the model would not have FCNCs at the tree level. The RS-GIM mechanism would then be exact. However, the several elements of the couplings $\varepsilon_{L,R}$ depend on the bulk masses c_{ψ}^{i}, that are flavor non-universal, because of the requirement to reproduce the different quark masses (see also Eq. (2.44) after EWSB). Consequently, FCNCs at the tree level arise.

But how large can they be?

Let us take first a heavy KK gauge boson. As discussed in Appendix A, the KK gauge boson is mainly localized towards the IR brane. Hence the couplings of the zero mode fermions to the KK gauge bosons are roughly proportional to the square of the shape function of the fermions computed on the IR brane (see Eq. (3.1)). In particular for the quark $SU(2)_L$ doublet and the up and down singlet we can write, respectively

$$\left(\varepsilon_{L}^{2/3\,,-1/3}\right)_{ii} \propto \tilde{f}_{L}^{(0)}(L, c_{Q}^{i})^{2}\,, \tag{3.28}$$

$$\left(\varepsilon_{R}^{2/3}\right)_{ii} \propto \tilde{f}_{R}^{(0)}(L, c_{u}^{i})^{2}\,, \tag{3.29}$$

$$\left(\varepsilon_{R}^{-1/3}\right)_{ii} \propto \tilde{f}_{R}^{(0)}(L, c_{d}^{i})^{2}\,. \tag{3.30}$$

These couplings depend strongly on the bulk masses $c_{Q,u,d}^{i}$, and so, in principle, flavor is strongly violated. However, the first two generations of quarks are mainly localized towards the UV brane, because of their lightness. Consequently, their overlap with the gauge boson shape function, namely $\left(\varepsilon_{L,R}^{2/3,-1/3}\right)_{ii}$ with $i \neq 3$, will be quite small. Performing then the rotation to the mass eigenstate basis for SM quarks (3.26)-(3.27), the resulting off-diagonal elements, corresponding to the first two generations, will be small as well. The RS-GIM mechanism works quite well for the first two light generations, resembling hence the GIM mechanism of the SM.

The third generation of quark merits a different treatment. Because of the heaviness of the top quark, third generation quarks (both up and down) cannot be localized near the UV brane. Consequently for the third generation, we do not expect small couplings $\varepsilon_{L,R}$,

namely a strong suppression of flavor changing neutral couplings because of the RS-GIM mechanism, that is now strongly violated by the top mass (once more resembling the SM GIM mechanism).

Still, the RS-GIM mechanism can be regarded as one of the reasons for which the RS framework may avoid the severe constraints from FCNC processes even with a quite low KK scale, alleviating in such a way (especially for the first two generation quarks) the NP flavor problem. We can compare this setup with the flat extra dimensional model, which does not have an analog of the GIM mechanism and which consequently naturally requires KK masses as high as $\mathcal{O}(1000\,\text{TeV})$ [51] to satisfy FCNC constraints.

Until now we have just considered the couplings of KK gauge bosons with the SM quarks. An analogous discussion holds also for the SM Z boson. In fact, after EWSB, the Higgs VEV mixes zero and KK modes of Z with the $SU(2)_R$ gauge boson Z_X (see Eq. (2.42)), leading in the interaction basis to a non-universal shift of the coupling of the SM quarks to the physical Z. It is straightforward to prove, in terms of overlap integrals, that this shift will be quite small for the first two generations quarks and larger for the third generation, showing the impact of the RS-GIM mechanism. In conclusion, also for the SM Z gauge boson we can conclude that the RS-GIM mechanism helps in reducing the flavor changing neutral couplings and consequently in alleviating the NP flavor problem in the RS framework.

3.1.4 The custodial protection

In the RS model with enlarged gauge group, it turns out that the RS-GIM mechanism is not the only mechanism for keeping under control the flavor changing neutral current effects. In this section, we will show how some of the flavor changing neutral couplings are protected simply by the enlarged gauge group of the model and by the particular fermion representations.

In Sec. 2.2.2 we have learned that in the RS model, as well as in all models containing in the gauge group the symmetry $SU(2)_L \times SU(2)_R \times P_{LR}$, a fermion with quantum numbers which obey the relations

$$T_L = T_R\,, \quad T_L^3 = T_R^3\,, \tag{3.31}$$

has SM-like couplings (or does not couple, if it is not a SM fermion) with the SM Z boson. As we mentioned briefly in that section, the authors of [64] have also noticed that for a fermion with $T_L \neq T_R$ satisfying

$$T_L^3 = T_R^3 = 0\,, \tag{3.32}$$

the Z couplings are protected as well.

As pointed our first by us in [59, 110], the custodial protection generalizes also to off-diagonal Z couplings. In other words, if a fermion F satisfies one of the conditions (3.31)-(3.32), then, indicating with F^i the i-th flavor, all the couplings of the type ZF^iF^j with also $i \neq j$ are either SM-like (in the case of F a SM fermion) or 0 (in the case of F a KK fermion). In [59, 110] we pointed out the relevance of the protection of the several flavor changing neutral couplings in flavor transitions.

Now we want to demonstrate pedagogically the previous statement, writing in all the details the several couplings that we expect to be protected. We restrict our analysis to the couplings of the SM fermions; the discussion of the couplings of the heavy fermions follows in a straightforward manner.

After EWSB, the NP corrections to the couplings of the Z boson with a left or right handed SM quark (i, j are flavor indices) are given by

$$\Delta^{ij}_{L,R}(Z) = \frac{M_Z^2}{M_{\rm KK}^2}\left[-\mathcal{I}_1^+ \hat{\Delta}^{ij}_{L,R}(Z^{(1)}) + \mathcal{I}_1^- \cos\phi\, \cos\psi \hat{\Delta}^{ij}_{L,R}(Z_X^{(1)})\right] + \Delta^{ij}_{L,R}(Z)_{\text{KK-fermions}}\,, \tag{3.33}$$

where the angles ϕ and ψ are defined in (2.28) and (2.33) respectively, and the two overlap integrals $\mathcal{I}_1^{\pm}$ of the Higgs boson with gauge bosons with $(++)$ and $(-+)$ BCs are defined as

$$\mathcal{I}_1^+ = \frac{1}{L}\int_0^L dy\, e^{-2ky} g(y) h(y)^2\,, \tag{3.34}$$

$$\mathcal{I}_1^- = \frac{1}{L}\int_0^L dy\, e^{-2ky} \tilde{g}(y) h(y)^2\,, \tag{3.35}$$

with the Higgs boson shape function given in (2.17) and the gauge boson shape functions $g(y)$, $\tilde{g}(y)$ reported in Appendix A.

For the time being, we will just analyze the contributions within the square brackets; the last contribution arising from the mixing between SM and KK fermions will be discussed afterwards. To simplify the notation, we simply consider the couplings of a left handed fermion. For right handed ones, the discussion is exactly the same: one has only to change the chirality indices.

The two $\hat{\Delta}^{ij}_L(V)$ with $V = Z^{(1)}, Z_X^{(1)}$ represent the coupling of the quark with the gauge bosons $Z^{(1)}$ and $Z_X^{(1)}$ before EWSB

$$\hat{\Delta}_L(V) = D_L^\dagger \hat{\varepsilon}_L(V) D_L \qquad \left(V = Z^{(1)}, Z_X^{(1)}\right)\,, \tag{3.36}$$

if the SM quark is of down type, and

$$\hat{\Delta}_L(V) = U_L^\dagger \hat{\varepsilon}_L(V) U_L \qquad \left(V = Z^{(1)}, Z_X^{(1)}\right)\,, \tag{3.37}$$

if the SM quark is of up type. The rotation matrices U_L and D_L were already introduced after Eqs. (3.26) and (3.27), and the overlap integrals $\hat{\varepsilon}_L(V)$ are proportional to the $\varepsilon_L^{\pm}$ integrals in (3.1) and are given by

$$\hat{\varepsilon}_L(Z^{(1)}) = g_Z^{4D}\cdot\varepsilon_L^+ = g_Z^{4D}\frac{1}{L}\int_0^L dy\, \tilde{f}_L^{(0)}(y, c_\psi)^2 g(y)\,, \tag{3.38}$$

$$\hat{\varepsilon}_L(Z_X^{(1)}) = \kappa_Z^{4D}\cdot\varepsilon_L^- = \kappa_Z^{4D}\frac{1}{L}\int_0^L dy\, \tilde{f}_L^{(0)}(y, c_\psi)^2 \tilde{g}(y)\,. \tag{3.39}$$

Additionally, g_Z^{4D} and κ_Z^{4D} are the 4 dimensional charge factors of the SM fermion examined. More specifically, if the fermion has got quantum numbers T_L^3, T_R^3 and Q then[6]

$$g_Z^{4D}(F) = \frac{g^{4D}}{\cos\psi}\left[T_L^3 - (\sin\psi)^2 Q\right] , \tag{3.40}$$

$$\kappa_Z^{4D}(F) = \frac{g^{4D}}{\cos\phi}\left[T_R^3 - (Q - T_L^3)\sin^2\phi\right] . \tag{3.41}$$

Now we have all the ingredients to show the custodial protection of some of the Z boson couplings.

To simplify still a bit the notation, from now on we will restrict our analysis to a down type fermion. The generalization to up quarks is straightforward: one has just to replace the correct quantum numbers and the rotation matrix properly.

If the symmetry P_{LR} is unbroken, then the relations $\mathcal{I}_1^+ = \mathcal{I}_1^-$ and $\varepsilon_L^- = \varepsilon_L^+$ hold, since the shape functions $g(y)$ and $\tilde{g}(y)$ correspond to a $SU(2)_L$ and a $SU(2)_R$ gauge boson, respectively, and hence are equal in the limit of exact symmetry. Consequently, one can write the contributions in the bracket of Eq. (3.33) as

$$\left(\Delta_L^{ij}(Z)\right)_{\text{gauge}} = \frac{M_Z^2}{M_{\text{KK}}^2} D_L^\dagger \varepsilon_L^+ \left(-g_Z^{4D} + \cos\phi\cos\psi\kappa_Z^{4D}\right) D_L \mathcal{I}_1^+ . \tag{3.42}$$

This expression is proportional to the so called "magic combination"

$$g_Z^{4D}(F) - \cos\phi\cos\psi\kappa_Z^{4D}(F) , \tag{3.43}$$

that is exactly zero for a fermion obeying the condition $T_L^3 = T_R^3$, as can be easily seen from Eqs. (3.40), (3.41), once that the relation between the angles ψ and ϕ in Eq. (2.33) is employed.

As we have anticipated at the beginning of the proof, the protection of the Z couplings with P_{LR} eigenstate fermions is also valid for KK fermions: their couplings with the Z boson will be exactly zero for an unbroken P_{LR} symmetry.

To conclude, we have demonstrated that both flavor conserving and flavor violating Z couplings with a SM (or KK) quark which respects the condition $T_L^3 = T_R^3$ do no receive any NP contribution, in the hypothesis that the symmetry P_{LR} is unbroken.

Looking at the fermion representation (2.34)-(2.36), it is clear that the coupling $Zb_L\bar{b}_L$ is not the only one to be protected. All the following Z couplings, both flavor conserving and flavor violating with

1. left handed couplings of SM down quarks,

2. right handed couplings of SM up quarks,

[6] In Appendix B we report the explicit form of the couplings g_Z^{4D} and κ_Z^{4D} of all the quarks of the theory.

3. couplings of $\chi^{u^i}_{L,R}$,

4. couplings of $U'^i_{L,R}$ and of $U''^i_{L,R}$

are protected and do not experience NP contributions if the symmetry P_{LR} is unbroken. We note that this implies that the KK fields $\chi^{u^i}_{L,R}, U'^i_{L,R}, U''^i_{L,R}$ do not couple at all with Z, in that hypothesis.

It remains to prove that this conclusion is not spoiled by the mixing between SM and KK fermions, namely that also the last term in (3.33) is zero, for quarks satisfying the condition $T^3_L = T^3_R$. In other words, we have to demonstrate that all the couplings of SM right handed up quarks and of SM left handed down quarks with the Z boson do not receive NP corrections because of the mixing with KK fermions, in the limit of exact P_{LR} symmetry.

In Sec. 3.1.1 we have already obtained the general formulae for the couplings of the SM fermions with the Z boson in terms of the elements of the mass matrices (Eqs. (3.17)-(3.20)), in the presence of the first excited KK fermions. Now we analyze the impact of the symmetry P_{LR} on the two protected couplings (point 1. and 2. listed above).

- Couplings of the right handed up quarks (Eq. (3.20)): the custodial symmetry P_{LR} acts on the quark fields as $P_{LR}(q^u_R) = \chi^d_R$. This relation guarantees that also the corresponding mass matrix elements have to be equal, namely

$$|M_{10}| = |M_{40}| \,, \quad M_1 = M_4 \,. \tag{3.44}$$

  Inserting these relations in (3.20), one finds that the last two terms cancel. One should notice the relevance of the term coming from the redefinition of the SM fields, to maintain canonically normalized kinetic terms. Without this contribution the cancellation would not be possible. Consequently, all the couplings of the right handed up quarks with the Z boson do not receive any NP contributions coming from the mixing between SM and KK fermions, thanks to the symmetry P_{LR}.

- Couplings of the left handed down quarks (Eq. (3.17)): the custodial symmetry P_{LR} acts on the quark fields as $P_{LR}(D_L) = D'_L$. This relation guarantees that also the corresponding mass matrix elements have to be equal, namely

$$|M_{03}| = |M_{02}| \,, \quad M_3 = M_2 \,. \tag{3.45}$$

  Inserting these relations in (3.17), one finds that the last two terms cancel (thanks still to the redefinition of the SM fermion fields to maintain canonically normalized kinetic terms). Consequently, all the couplings of the left handed down quarks with the Z boson do not receive any NP contributions coming from the mixing between SM and KK fermions, thanks to the symmetry P_{LR}.

In conclusion, we have demonstrated explicitly that, thanks to the underlying P_{LR} symmetry, the protection of the flavor conserving and flavor violating $Zu^i_R\bar{u}^j_R$, $Zd^i_L\bar{d}^j_L$ couplings is not spoiled by the mixing of the SM quarks with the KK fermions.

Up to now we have performed the analysis in the hypothesis of an unbroken P_{LR} symmetry. However in the model the parity symmetry is broken because of the boundary conditions of the gauge bosons on the UV brane (see Eq. (2.25) for the fields $W^a_{L\mu}$ and $W^\beta_{R\mu}$).

Indeed, including the effects of the breaking of the custodial symmetry P_{LR} our two statements in the boxes are not valid anymore: non-trivial NP effects arise also for the protected couplings. However, we checked that the NP contributions coming from the mixing between SM and KK fermions are still negligibly small. As far as the effects coming from the mixing of gauge bosons after EWSB concern, they are not negligible, but still smaller than the NP contributions of the couplings that are not protected. In Sec. 4.2.9, we will analyze their importance for flavor transitions, and in particular for the rare decays of K and B mesons.

As an example, in Fig. 3.4 we compare the flavor changing protected couplings $Zs_L\bar{d}_L$ and $Zb_L\bar{s}_L$ with the unprotected ones $Zs_R\bar{d}_R$ and $Zb_R\bar{s}_R$. The points in blue represent the points that we obtain in the custodial protected model, once that we have fitted the quark masses and mixings, and the well measured observables of the $K^0-\bar{K}^0$ and $B^0_{s,d}-\bar{B}^0_{s,d}$ systems (see also Secs. 5.2.1, 5.2.2). The mixing between SM and KK fermions is neglected. It is evident that the unprotected couplings are larger than the protected ones by two (in the case of $s\bar{d}$) or one (in the case of $b\bar{s}$) orders of magnitude.

In the same figure, we present in purple how our results would look like if the protection of the left handed Z couplings to down type quarks was not present. In order to get a rough idea we simply removed the contributions of the $Z^{(1)}_X$ gauge boson to the Z couplings that are generated in the process of electroweak symmetry breaking (Eq. (3.33))[7]. From the purple points we observe that the hierarchies of the several couplings completely change: $\Delta^{sd}_L(Z)$ tends now to be larger than $\Delta^{sd}_R(Z)$, while $\Delta^{bs}_L(Z)$ fully dominates over $\Delta^{bs}_R(Z)$, as it was expected from the fact that the relevant left handed down modes belong to the same representation of the left handed up modes and hence are localized closer towards the IR brane than the right handed down modes.

Before finishing this section, it is also of interest to have a brief look at the couplings of the SM quarks with the heavy Z' gauge boson (the heaviest of the neutral gauge bosons arising from the mixing (2.42)) and with Z_H. Neglecting the mixing with the KK fermions, the couplings of Z' to up and down quarks are given by

$$\Delta^{ij}_{L,R}(Z') = \frac{1}{\sqrt{2}\cos\psi}\left[-\hat{\Delta}^{ij}_{L,R}(Z^{(1)}) + \cos\phi\,\cos\psi\hat{\Delta}^{ij}_{L,R}(Z^{(1)}_X)\right]. \tag{3.46}$$

[7]The points in blue in the figure can fit, in addition to quark masses, CKM matrix and $\Delta F = 2$ observables, also constraints coming from EWPTs. The removal of the custodial protection as done here in general can lead to tensions with EWPTs. For a more detailed analysis one should take these constraints into account as well.

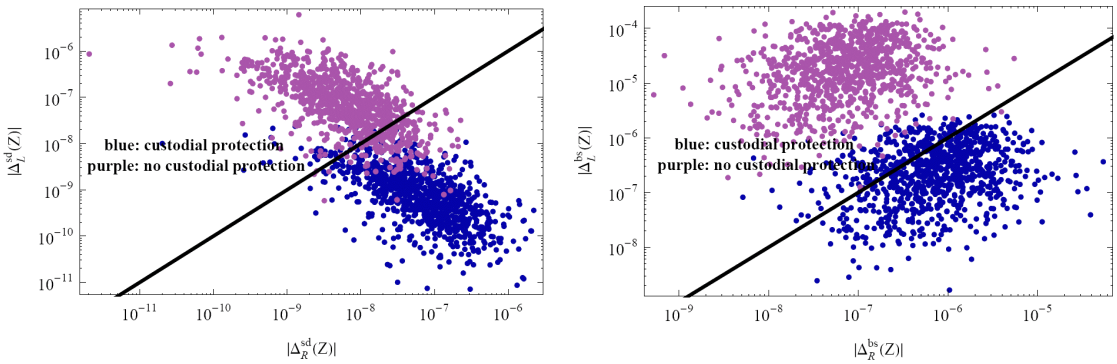

Figure 3.4: $|\Delta_L^{ij}(Z)|$ versus $|\Delta_R^{ij}(Z)|$ for $ij = sd$ (left) and $ij = bs$ (right). The blue points are obtained in the custodially protected model after fitting SM quark masses and mixings and after imposing all constraints from $\Delta F = 2$ observables (see also Secs. 5.2.1, 5.2.2). The purple points show the effect of removing the custodial protection. The solid lines display the equality $|\Delta_L^{ij}(Z)| = |\Delta_R^{ij}(Z)|$.

In the case of $P_{L,R}$ symmetry these couplings are proportional to the combination present already in the couplings of the SM quarks with the Z boson (3.33). Thus, also all the diagonal and off-diagonal couplings $Z' u_R^i \bar{u}_R^j$ and $Z' d_L^i \bar{d}_L^j$ are protected by the custodial symmetry P_{LR}. Based on analogous considerations we can conclude that also the couplings of Z' with the heavy fermions $U'_{L,R}$, $U''_{L,R}$ and $\chi_{L,R}^{u_i}$ are protected.

Differently, none of the couplings of the Z_H boson with SM (or heavy KK) quarks are protected by the custodial symmetry P_{LR}, since they are given by the combination

$$\Delta_{L,R}^{ij}(Z_H) = \frac{1}{\sqrt{2}\cos\psi}\left[\cos\phi\,\cos\psi\hat{\Delta}_{L,R}^{ij}(Z^{(1)}) + \hat{\Delta}_{L,R}^{ij}(Z_X^{(1)})\right] . \tag{3.47}$$

3.1.5 The NP flavor problem

We come back to the NP flavor problem, mentioned already at the end of Sec. 2.1. At first sight, the RS model seems to introduce a severe flavor problem, because of the presence of flavor changing neutral currents already at the tree level, which could be disastrous for the model when compared with the flavor observable measurements. As already discussed at the end of Sec. 3.1.1, one would in fact expect that the RS model is ruled out by flavor precision experiments because of the too large NP contributions to the flavor observables that are well in agreement with the SM, unless it holds at a very high energy scale $M_{\rm KK}$, not addressing consequently the gauge hierarchy problem.

However, in the last two sections of this thesis, we saw that this conclusion is not necessarily true. In fact, the RS model with custodial protection develops also protection mechanisms which weaken the potential huge NP effects in flavor observables. We have presented in detail the RS-GIM mechanism, which protects mainly the flavor transitions involving the first two families of quarks, and the custodial protection, due to the P_{LR} symmetry which protects some (flavor changing) couplings of the SM Z boson and of the heavy Z' boson. These protection mechanisms decrease the natural expectation for

the Wilson coefficients c_i of Eq. (2.1) that are not expected to be naturally of $\mathcal{O}(1)$. Consequently, we expect that the model can be a viable model of flavor, even with a not too large $M_{\rm KK}$ scale. Indeed, it was found that, assuming $\mathcal{O}(1)$ entries for the 5D Yukawa couplings (defined in (2.44)), $M_{\rm KK}$ has a lower bound of roughly $M_{\rm KK} \geq 20$ TeV [120]. This result has been confirmed by us in [59] and will be presented in this thesis in Sec. 5.2.1.

In addition to the RS-GIM mechanism and to the custodial protection, in the literature several other alternatives to protect the model from too large NP contributions to flavor transitions are studied. Contrary to our simple assumption of completely anarchical 5D Yukawas, all these approaches incorporate some sort of flavor symmetry.

One possible set up is to protect the model from all tree level FCNCs by incorporating a $U(3)^3$ flavor symmetry, so that all flavor mixing is generated by kinetic terms on the UV brane [121]. A more recent proposal postulates that the only sources of flavor breaking are the two anarchical Yukawa spurions, implementing hence the Minimal Flavor Violation (MFV) principle (see also Sec. 3.2.2 for a detailed explanation of the MFV ansatz) in the five dimensional theory [122]. Finally, another recent approach [123] is based on two horizontal $U(1)$ flavor symmetries, which force the alignment of bulk masses and down Yukawas and hence strongly suppress FCNCs in the down sector. FCNCs in the up sector, however, can be close to the experimental limits.

All these approaches based on flavor symmetries enforce the final statement

In addition to the SM flavor puzzle, the RS model can alleviate also the NP flavor problem.

This statement is in any case valid even for the original RS model (without any imposition of flavor symmetries) that we will be analyzed in this thesis.

3.2 Flavor changing transitions in Susy flavor models

In parallel with what we have shown in the previous section for the RS model with custodial protection, we want now to analyze in detail the NP flavor problem in Susy flavor models. First, we will show how serious is the problem in the general MSSM. Secondly, we will discuss what are the protection mechanisms that can be implemented in the MSSM to ameliorate the problem. Particular relevance is devoted to the role of flavor symmetries. This should be regarded as a different approach, when compared to the "geometrical approach" adopted in the RS model.

3.2.1 Large one loop flavor changing neutral currents

Contrary to the Randall-Sundrum model, Supersymmetry does not contain quark and lepton flavor changing neutral vertices at the tree level, thanks to the Susy-GIM mechanism, which resembles closely the GIM mechanism of the SM. FCNC processes arise only at the one loop level and are very sensitive to the soft parameters in (2.50). In particular the most relevant vertices for our discussion of quark flavor violation are the ones in which

both quarks and squarks are present. There are three types of such vertices: $f\tilde{f}\chi^-$, $f\tilde{f}\chi^0$ and $f\tilde{f}\tilde{g}$, where we have indicate with f ($\tilde{f}$) a generic mass eigenstate fermion (sfermion), with χ^- (χ^0) a mass eigenstate chargino (neutralino) and with $\tilde{g}$ a gluino. In Fig. 3.5 we show as an example one of these three classes of vertices, the one with the gluino. The other two types of vertices are perfectly analogous and hence will not be listed here.

Figure 3.5: Gluino-quark-squark vertices. $i\,, j$ are the flavor indices, α, β the $SU(3)_c$ indices.

One indeed can work in mass eigenstates, as shown in Fig. 3.5, but the expressions for the elementary vertices containing neutralinos and charginos are then quite complicated. Additionally, in the mass eigenstate basis, flavor transition amplitudes often look highly non-transparent. For this reason, it is often convenient to work in the SCKM basis defined in Eq. (2.52). In this basis, all the couplings of fermions and sfermions to neutral gauginos are flavor diagonal, while the flavor changing is introduced by the non-diagonality of the sfermion propagators. This procedure is justified as long as the several MIs defined in (2.55) are significantly smaller than one and the diagonal entries in the soft terms $\left(M^2_{\tilde{U},\tilde{D}}\right)_{AB}$ ($AB = LL, RR, LR, RL$) in Eq. (2.54) are approximately degenerate[8]. In that case the sfermion propagators can be expanded as a series of the several MIs, as shown explicitly in Fig. 3.6 for the $K^0 - \bar{K}^0$ mixing (see also Sec. 4.1.4). This method of computing flavor transitions is often called Mass Insertion Approximation (MIA) [125].

Two main advantages come from the use of the MIA: first of all, one does not need the full diagonalization of the sfermion mass matrices to perform a test of the Susy model under consideration in the FCNC sector. In addition the formulae are much simpler and hence transparent, allowing to identify easier the main properties of the flavor transition, as we will show in Secs. 4.1, 4.2. At the same time, the limiting aspect is that the MIA breaks down when the sfermion flavor violating mixing angles are of $\mathcal{O}(1)$, as it is indeed predicted by many flavor models, as the ones we have presented in Secs. 2.3.4 - 2.3.5. Indeed our numerical analysis of those models will be performed exactly, working with mass eigenstate fermions (see Chapter 5).

In spite of the fact that the Susy contributions to flavor observables are only at the one loop level, the NP flavor problem in Susy is not weaker than in the RS model. In fact, precise measurements of FCNC transitions put severe upper bounds on the several entries of the sfermion mass matrices in (2.54) at the low energy. The common approach to set

[8]The phenomenological implications of a highly hierarchical sfermion scenario have been recently addressed in [124].

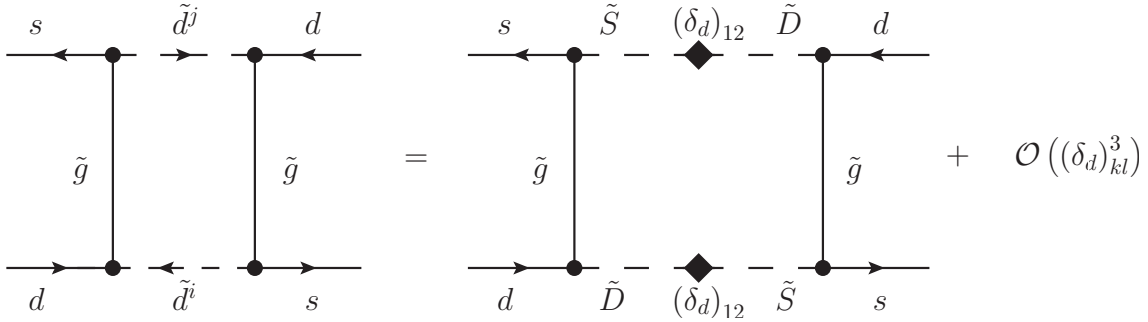

Figure 3.6: Mass Insertion Approximation applied to the gluino contribution to the $K^0-\bar{K}^0$ meson mixing system. $\tilde{f}$ indicates a mass eigenstate sfermion, $\tilde{F}$ indicates a sfermion in the SCKM basis, as introduced in (2.52). The several Mass Insertions are represented with a diamond ⧫.

bounds on the MIs is to switch on only one MI at a time, in order to avoid accidental unnatural cancellations between different Susy contributions [126].

In [90] we have performed an extensive study of the bounds on the several deltas. Here we cite just one of the results, in order to show how severe is the Susy flavor problem. In our numerical investigation we set at the GUT scale an MSUGRA spectrum, as explained in Sec. 2.3.3, and at the EW scale we switch on only one MI at a time. In Fig. 3.7 we show the bounds we obtain on the element 21 of the MI LL (in the left panel) and LR (in the right panel) of the down sector, namely we present the bound on the LL soft mass and trilinear term connecting the first two generations of down squarks.

From Fig. 3.7 we can observe that the bounds on the MIs are quite strict, when compared to the expected $\mathcal{O}(1)$ MI parameters. One notes also that the bound is particularly severe for a phase in the MIs of $\pi/4$, for which the constraint from the CP violating observable ε_K is quite strict. Vice versa, for a phase equal to zero or $\pi/2$, the bound is looser, since the CP conserving observable ΔM_K provides only a mild constraint (see also Sec. 4.1.4 for the discussion of the two observables of the K system). The bounds can be of course weakened by choosing heavier soft masses m_0 and $m_{1/2}$, that in any case are forced to be at around the TeV scale in order to address the gauge hierarchy problem (see Introduction). The main conclusion will not change: *to naturally satisfy the bounds on FCNCs coming from the experiments, one has to implement in Susy a "protection mechanism", preserving the MIs from being too large.* Indeed in Secs. 2.3.4 - 2.3.5 we have shown with two explicit examples that abelian and non abelian flavor symmetries can accomplish this requirement, since they predict MIs suppressed by powers of small flavor symmetry breaking parameters. Studying the phenomenology of these two models (Secs. 5.2.4, 5.2.5) in the $\Delta F = 2$ meson sector, we will show in detail which are the constraints arising to satisfy the several FCNC constraints.

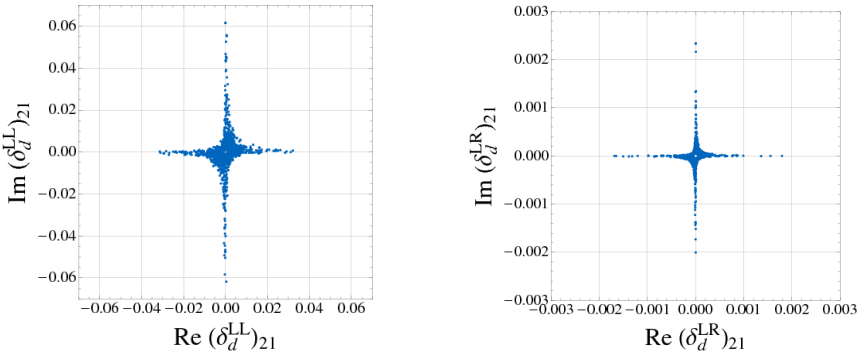

Figure 3.7: Bounds on the MIs $(\delta_d^{LL})_{21}$ (in the left panel) and $(\delta_d^{LR})_{21}$ (in the right panel) as obtained by imposing the experimental constraints from the well measured $\Delta F = 2$ observables (see Tab. 4.5), in particular from ε_K and ΔM_K. The scan is performed on the MSUGRA parameters $m_{1/2} \leq 200$ GeV, $m_0 \leq 300$ GeV, $|A_0| \leq 3m_0$ and $5 \leq \tan\beta \leq 15$. For further details see [90].

3.2.2 The Susy protection mechanisms

In this section we want to overview the main protection mechanisms that can be implemented in Susy[9] in order to protect the theory from too large NP contributions to the well measured flavor observables.

- *Degeneracy.* At a high energy scale, e.g. the GUT scale, squark mass eigenstates are approximately degenerate in mass. This leads naturally to a strong GIM suppression of the off-diagonal MIs in the SCKM basis. Since the most severe constraints are coming from 1-2 transitions, one can also soften the requirement, imposing it to the first two generation squarks only.

  It was found that bounds on the squark mass degeneracy are in the range of few percents (and hence not highly strict), even for the first two generations, as long as their masses are around 1 TeV [127].

  Such degeneracy could naturally arise from models with gauge-mediated supersymmetry breaking (GMSB) in which the masses of squarks (and sleptons) depend only on their gauge quantum numbers and hence are naturally degenerate [128]. In addition also Susy flavor models based on *non abelian* flavor symmetries can achieve that scope. In fact, as also explained in Sec. 2.3.5, an unbroken $SU(3)$ or $U(2)$ flavor symmetry would imply at the high energy scale the degeneracy of at least the first two families and hence the absence of the corresponding off-diagonal MIs. The NP flavor contributions would arise just as symmetry breaking effects and hence would be naturally suppressed.

- *Alignment.* Quark-squark alignment is a different idea which relies on a strong correlation between fermion and sfermion mass generation. At the high energy scale

[9] The last two mechanisms in the list are usually applied also to other models beyond the Standard Model, in order to suppress FCNCs.

it exists a basis (the SCKM basis) in which both the down type squark mass matrix, the down trilinear terms and the down quark mass matrix are diagonal [96]. Hence at that scale all the off-diagonal terms $\left(\delta_d^{AB}\right)_{ij}$ with $AB = (LL, RR, LR)$ would be zero.

The alignment cannot be valid also for up type quarks-squarks. The $SU(2)_L$ gauge symmetry relates in fact the left-left block of up and down squark matrices, i.e. $(M^2_{\tilde{U}})^{LL}$ and $(M^2_{\tilde{D}})^{LL}$ respectively, in such a way that $(M^2_{\tilde{U}})^{LL} = V^*(M^2_{\tilde{D}})^{LL}V^{\mathrm{T}}$.

Consequently, it is not possible to diagonalize the down squark mass matrix $M^2_{\tilde{D}}$ and the up squark mass matrix $M^2_{\tilde{U}}$ simultaneously in the same basis, if the left handed squarks are non-degenerate in mass, as it is natural in this class of models.

Such alignment could naturally arise from models with abelian flavor symmetries [85, 96], in which the contributions of misalignment arise only as flavor symmetry breaking effects. In particular models based on the flavor group $\mathcal{G}_F = U(1) \times U(1)$ and with expansion parameters fixed to be $\varepsilon_1 = \lambda$ and $\varepsilon_2 = \lambda^2$ [85] lead to a satisfactory alignment between down quark and squark mass matrices and hence suppression of the NP effects in FCNC transitions in the down sector.

- *MFV principle.* The several off-diagonal MIs could be different from zero but dependent only on some particular combination of the off-diagonal CKM elements and hence small. This turns out to be the result of the Minimal Flavor Violation principle applied to Susy flavor models [129, 130].

  In the Standard Model, switching off the Yukawa couplings, the quark flavor symmetry is given by $U(3)^3$ [131, 132]. The only source of flavor symmetry breaking are the Yukawa couplings. Models with Minimal Flavor Violation resemble the SM in the sense that the dynamics of flavor violation is completely determined by the structure of the two ordinary Yukawa couplings. In this class of models one can restore the $U(3)^3$ flavor invariance by promoting the Yukawas to spurions with quantum numbers

$$Y_u \sim (3, \bar{3}, 1)_{\mathrm{SU}(3)^3_q}\,, \quad Y_d \sim (3, 1, \bar{3})_{\mathrm{SU}(3)^3_q}\,. \tag{3.48}$$

  Following this prescription, one can write the several soft masses and trilinear terms presented in (2.50) as series in the spurion fields $Y_{u,d}$ that are invariant under the $U(3)^3$ flavor symmetry. In particular, restricting only to the first terms of the expansion [129] we have

$$M_Q^2 = \tilde{m}^2 \left(a_1 \mathbb{1} + b_1 Y_u Y_u^\dagger + b_2 Y_d Y_d^\dagger + b_3 Y_d Y_d^\dagger Y_u Y_u^\dagger + b_3^* Y_u Y_u^\dagger Y_d Y_d^\dagger \right) , \quad (3.49)$$

$$M_U^2 = \tilde{m}^2 \left(a_2 \mathbb{1} + b_4 Y_u^\dagger Y_u \right) , \quad (3.50)$$

$$M_D^2 = \tilde{m}^2 \left(a_3 \mathbb{1} + b_5 Y_d^\dagger Y_d \right) , \quad (3.51)$$

$$A_U = A \left(a_4 \mathbb{1} + b_6 Y_d Y_d^\dagger \right) Y_u , \quad (3.52)$$

$$A_D = A \left(a_5 \mathbb{1} + b_7 Y_u Y_u^\dagger \right) Y_d , \quad (3.53)$$

where a_i and b_i are unknown order one coefficients ($a_{1,2,3}$, $b_{1,2,4,5}$ real and $a_{4,5}$, $b_{3,6,7}$ in general complex [133]). To obtain Eqs. (3.49)-(3.53), high order contributions in the small first two generation Yukawas are neglected.

Thanks to the smallness of the Yukawa couplings of the first two generations, also the off-diagonal MIs turn out to be naturally small in the MFV framework. The same conclusion holds when the soft masses and trilinear terms are rotated to the SCKM basis. The off-diagonal MIs will be given in terms of the (small) off-diagonal CKM elements and hence will be suppressed.

- *Decoupling.* The decoupling hypothesis is a completely different approach. The protection of the flavor transitions does not rely anymore on a symmetry principle, but on the fact that the sfermion mass scale $\tilde{m}$ is taken to be very high. This usually brings an unwanted high level of fine-tuning of the theory, since the lightest Higgs mass (or equivalently the EW scale) receives huge one loop corrections proportional to the factor $\log\left(\frac{m_{\tilde{t}_1} m_{\tilde{t}_2}}{m_t^2}\right)$, where $m_{\tilde{t}_{1,2}}$ are the masses of the two stops. However a "hybrid" scenario in which the first two generation squarks are heavy and split from the third generation that arises at the EW scale could ameliorate the fine-tuning problem just mentioned [134–136][10].

  The encouraging feature of this framework is that, in spite of the heaviness of the superpartners, such a scenario may be probed at the LHC through non-decoupling effects such as the super-oblique parameters [138].

[10] For an alternative solution of the fine-tuning problem in Supersymmetry see also our recent work [33] and [137].

Chapter 4

Impact on flavor observables

At present, at the dawn of the LHC, great interest is given to the study of the properties of new particles not present in the Standard Model that could be detected directly by the machine, establishing hence the presence of NP. While direct detection of new particles will be the main avenue at the LHC, indirect searches will provide precious complementary information. In particular, precision measurements and computations in the realm of flavor physics are expected to play a key role in constraining the unknown parameters of the Lagrangian of any NP model.

In this chapter we will pursue the indirect approach for the two models that we have already introduced in Chapter 2. We first investigate the flavor observables arising from the mixing of meson and corresponding antimeson, and secondly we analyze some decays of B and K mesons that are highly suppressed in the SM: rare B and K meson decays into purely leptonic states (such as $B_{s,d} \to \mu^+\mu^-$ or $K_L \to \mu^+\mu^-$) or into semileptonic states (such as $K \to \pi\nu\bar{\nu}$).

Since the chapter is relatively long, we consider it worth to present here a brief summary. The chapter is composed of two sections structured in an analogous manner.

The first section deals with the $\Delta F = 2$ transitions. First the SM effective Hamiltonians for the K and B system are presented (Sec. 4.1.1); then, restricting to the K system (we comment on how to generalize the formulae to the $B_{s,d}$ systems), the NP contributions to the effective Hamiltonian are worked out in both the RS (Secs. 4.1.2, 4.1.3) and the Susy (Secs. 4.1.4, 4.1.5) frameworks. Finally in Sec. 4.1.6 we review the formulae for the several $\Delta F = 2$ observables and we end with a brief summary of the experimental status and the comparison with the SM predictions.

The second section deals with selected rare K and B decays. We present the effective Hamiltonian for the elementary process $s \to d\nu\bar{\nu}$ first in the SM (Sec. 4.2.1) and secondly in the RS (Sec. 4.2.2) and Susy (Sec. 4.2.3) frameworks. Subsequently, in Sec. 4.2.4 we present the general formulae for the branching ratios of the $K^+ \to \pi^+\nu\bar{\nu}$ and $K_L \to \pi^0\nu\bar{\nu}$ decay modes, valid both in the RS model and in Susy. Afterwards, we present first the most general effective Hamiltonian for the elementary processes $s \to d\ell^+\ell^-$ and $b \to (s,d)\ell^+\ell^-$ first in the SM (Sec. 4.2.5) and secondly the new physics contributions arising from the RS

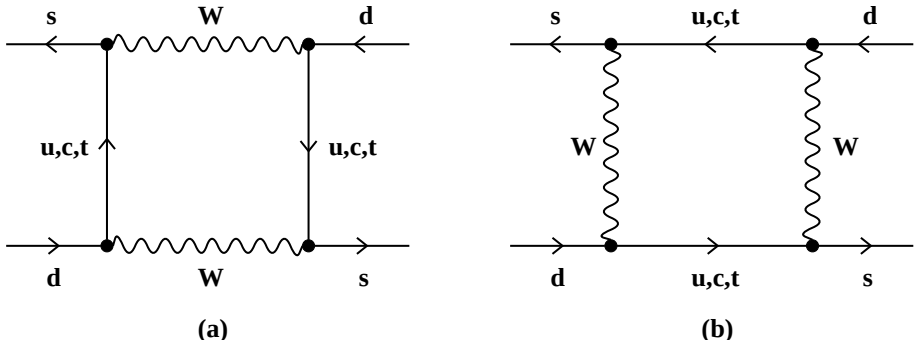

Figure 4.1: Box diagrams contributing to $K^0 - \bar{K}^0$ mixing in the Standard Model [31].

model (Sec. 4.2.6) and from supersymmetry (Sec. 4.2.7)[1]. In Sec. 4.2.8 we discuss then the formulae for the branching ratios of $B_{s,d} \to \mu^+\mu^-$ (in the RS model and in Susy) and of $K_L \to \mu^+\mu^-$ (in the RS model). In Sec. 4.2.9 it follows a discussion of the anatomy of the NP contributions to the several decays in the RS model (we do not perform the anatomy also for the Susy flavor models, since in that framework it is quite clear which are the main contributions) and finally we end the section with a small review of the experimental status of the rare B and K decays analyzed in this thesis and of the SM predictions for their branching ratios (Sec. 4.2.10).

4.1 Operator structure for $\Delta F = 2$ transitions

Particle-antiparticle mixing has always been of fundamental importance in testing the Standard Model and represents often a serious constraint to satisfy for theories beyond the Standard Model. In the past it was a very successful tool to test heavy flavor physics: to mention some of the main examples, from the calculation of the $K_L - K_S$ mass difference, Gaillard and Lee [12] could estimate the value of the charm quark mass before the charm discovery; $B_d^0 - \bar{B}_d^0$ mixing [139, 140] gave the first indication of a large top quark mass.

4.1.1 $\Delta F = 2$ processes in the SM

We apply the method of *operator product expansion*, already introduced in Sec. 2.1, to the case of particle-antiparticle mixing ($K^0 - \bar{K}^0$, $B_{s,d}^0 - \bar{B}_{s,d}^0$). In the Standard Model, the effective Hamiltonian responsible for the $\Delta F = 2$ flavor transitions is particularly simple, since it just contains one operator, that is arising from the box diagrams shown in Fig. 4.1. In the case of Kaon mixing, at scales μ below the charm threshold $\mu_c = \mathcal{O}(m_c)$, we can write the effective Hamiltonian as [30]

[1] We restrict only to the case of the elementary process $b \to s\ell^+\ell^-$, since the other two are perfectly analogous.

$$\begin{aligned}\left[\mathcal{H}_{\rm eff}^{\Delta S=2}\right]_{\rm SM} &= \frac{G_{\rm F}^2}{16\pi^2} M_W^2 \left[\lambda_c^{(K)\,2}\eta_1 S_0(x_c) + \lambda_t^{(K)\,2}\eta_2 S_0(x_t) + 2\lambda_c^{(K)}\lambda_t^{(K)}\eta_3 S_0(x_c,x_t)\right] \times \\ &\times \left[\alpha_s^{(3)}(\mu)\right]^{-2/9}\left[1+\frac{\alpha_s^{(3)}(\mu)}{4\pi}J_3\right] Q(\Delta S=2) + h.c.\,, \end{aligned} \tag{4.1}$$

where $\lambda_i^{(K)} = V_{is}^* V_{id}$, $\alpha_s^{(3)}(\mu)$ is the strong coupling constant at an energy μ at which the number of "effective" flavors is given by 3. The renormalization scheme dependent J_3 is given in the NDR scheme by $J_3 = 1.895$ [30] and the correction factors η_1, η_2 and η_3 keep into account the short-distance (SD) QCD effects and are given at the next to leading order (NLO) by [141–143]

$$\eta_1 = 1.44 \pm 0.35, \qquad \eta_2 = 0.57 \pm 0.01, \qquad \eta_3 = 0.47 \pm 0.05. \tag{4.2}$$

Finally the functions $S_0(x)$, $S_0(x,y)$ are smooth functions of the ratios $x_{t,c} = m_{t,c}^2/M_W^2$ and can be found in Appendix C. As we can note from Eq. (4.1), the effective Hamiltonian for the mixing of $K^0 - \bar{K}^0$ consists of a single four-quark operator

$$Q(\Delta S=2) \equiv (\bar{s}d)_{V-A}(\bar{s}d)_{V-A} \equiv [\bar{s}\gamma_\mu(1-\gamma_5)d] \otimes [\bar{s}\gamma^\mu(1-\gamma_5)d]\ , \tag{4.3}$$

and the Wilson coefficient is proportional to $G_F^2/(16\pi^2)$ indicating that the effect arises only at the one loop level.

An analogous result holds also for $B_{s,d}^0 - \bar{B}_{s,d}^0$ meson mixing, for which, neglecting both the long-distance (LD) and the charm quark contributions, the effective Hamiltonian is given by

$$\left[\mathcal{H}_{\rm eff}^{\Delta B=2}\right]_{\rm SM} = \frac{G_{\rm F}^2}{16\pi^2} M_W^2 \left(\lambda_t^{(s,d)}\right)^2 \eta_B S_0(x_t) \left[\alpha_s^{(5)}(\mu_b)\right]^{-\frac{6}{23}}\left[1+\frac{\alpha_s^{(5)}(\mu_b)}{4\pi}J_5\right] Q(\Delta B=2) + h.c.\,, \tag{4.4}$$

with $\eta_B = 0.55 \pm 0.01$ [142], $\lambda_t^{(s,d)} = V_{tb}^* V_{t(s,d)}$ and $\alpha_s^{(5)}(\mu_b)$ is the strong coupling constant at an energy μ_b at which the number of "effective" flavors is given by 5. $J_5 = 1.627$ in the NDR scheme [144] and the scale μ_b is of $\mathcal{O}(m_b)$. The only operator involved is now given by

$$Q(\Delta B=2) \equiv (\bar{b}(s,d))_{V-A}(\bar{b}(s,d))_{V-A} \equiv \left[\bar{b}\gamma^\mu(1-\gamma_5)(s,d)\right] \otimes \left[\bar{b}\gamma^\mu(1-\gamma_5)(s,d)\right]\ . \tag{4.5}$$

From the two effective Hamiltonians (4.1) and (4.4), it is easy to compute the contribution to the off-diagonal mixing amplitude $M_{12}^{K,s,d}$ defined in the case of $K^0 - \bar{K}^0$ mixing as

$$2m_K (M_{12}^K)_{\rm SM}^* = \langle \bar{K}^0 | \left[\mathcal{H}_{\rm eff}^{\Delta S=2}\right]_{\rm SM} | K^0 \rangle\,, \tag{4.6}$$

and analogously for the $B_{s,d}$ systems. Computing the matrix elements, one finds

$$\left(M_{12}^K\right)_{\rm SM} = \frac{G_{\rm F}^2}{12\pi^2} F_K^2 \hat{B}_K m_K M_W^2 \left[\lambda_c^{(K)\,2}\eta_1 S_0(x_c) + \lambda_t^{(K)\,2}\eta_2 S_0(x_t) + 2\lambda_c^{(K)}\lambda_t^{(K)}\eta_3 S_0(x_c,x_t)\right]^*, \tag{4.7}$$

where the renormalization group invariant parameter $\hat{B}_K$ is defined by

$$\hat{B}_K = B_K(\mu)\left[\alpha_s^{(3)}(\mu)\right]^{-2/9}\left[1 + \frac{\alpha_s^{(3)}(\mu)}{4\pi}J_3\right], \tag{4.8}$$

and the decay constant F_K by

$$\langle \bar{K}^0|(\bar{s}d)_{V-A}(\bar{s}d)_{V-A}|K^0\rangle \equiv \frac{8}{3}B_K(\mu)F_K^2 m_K^2\,, \tag{4.9}$$

with m_K the mass of the Kaon.

For the mixing in the $B_{s,d}$ systems, we have completely analogous formulae

$$\left(M_{12}^{s,d}\right)_{\rm SM} = \frac{G_F^2}{12\pi^2}F_{B_{s,d}}^2 \hat{B}_{B_{s,d}} m_{B_{s,d}} M_W^2 \left[\left(\lambda_t^{(s,d)*}\right)^2 \eta_B S_0(x_t)\right], \tag{4.10}$$

where the renormalization group invariant parameters $\hat{B}_{B_{s,d}}$ are defined as

$$\hat{B}_{B_{s,d}} = B_{B_{s,d}}(\mu)\left[\alpha_s^{(5)}(\mu)\right]^{-6/23}\left[1 + \frac{\alpha_s^{(5)}(\mu)}{4\pi}J_5\right], \tag{4.11}$$

and the decay constants $F_{B_{s,d}}$ by

$$\langle \bar{B}_q^0|(\bar{b}q)_{V-A}(\bar{b}q)_{V-A}|B_q^0\rangle \equiv \frac{8}{3}B_{B_{s,d}}(\mu)F_{B_{s,d}}^2 m_{B_{s,d}}^2\,, \tag{4.12}$$

with m_{B_s} (m_{B_d}) the mass of the meson B_s (B_d).

4.1.2 $\Delta F = 2$ processes in the RS model: operator structure

In the RS model, the effective Hamiltonians characterizing the particle-antiparticle mixings get new contributions, thanks to the flavor changing neutral vertices present in the theory already at the tree level (see Fig. 3.1). The first complete analysis of all these new contributions, including those arising from the exchange of the EW gauge bosons, was performed by us in [59]. Previous studies can be found in [51, 55, 119, 120, 145–147]. In the following we will focus on the $K^0 - \bar{K}^0$ mixing system (that will turn out to give the most relevant constraints in the RS model); the corresponding formulae for the $B_{s,d}^0 - \bar{B}_{s,d}^0$ systems can be easily obtained by properly adjusting all the flavor indices.

The new tree level contributions from the exchange of KK gluons, EW gauge bosons (Z_H, Z' and Z) and the KK photon $A^{(1)}$ lead to the Hamiltonian

$$\left[\mathcal{H}_{\rm eff}^{\Delta S=2}\right]_{\rm KK} = C_1^{VLL}\mathcal{Q}_1^{VLL} + C_1^{VRR}\mathcal{Q}_1^{VRR} + C_1^{LR}\mathcal{Q}_1^{LR} + C_2^{LR}\mathcal{Q}_2^{LR}\,, \tag{4.13}$$

that is valid at energy scales $\mathcal{O}(M_{\rm KK})$, at which the Wilson coefficients C_i are evaluated. We perform the analysis in the operator basis introduced in [148] defined as

$$\begin{aligned}
\mathcal{Q}_1^{VLL} &= (\bar{s}^\alpha \gamma_\mu P_L d^\alpha)\left(\bar{s}^\beta \gamma^\mu P_L d^\beta\right), \\
\mathcal{Q}_1^{VRR} &= (\bar{s}^\alpha \gamma_\mu P_R d^\alpha)\left(\bar{s}^\beta \gamma^\mu P_R d^\beta\right), \\
\mathcal{Q}_1^{LR} &= (\bar{s}^\alpha \gamma_\mu P_L d^\alpha)\left(\bar{s}^\beta \gamma^\mu P_R d^\beta\right), \\
\mathcal{Q}_2^{LR} &= (\bar{s}^\alpha P_L d^\alpha)\left(\bar{s}^\beta P_R d^\beta\right), \qquad (4.14)
\end{aligned}$$

where α, β are color indices and $P_{L,R} = (1 \mp \gamma_5)/2$ are the chirality projectors. We note the presence of 3 additional operators when compared to the case of the SM, where the only operator is, apart from a numerical factor, given by $\sim \mathcal{Q}_1^{VLL}$. The Wilson coefficients at the scale $M_{\rm KK}$ are given by the sum

$$C_i(M_{\rm KK}) = C_i(M_{\rm KK})^G + C_i(M_{\rm KK})^A + C_i(M_{\rm KK})^{Z_H, Z', Z}, \qquad (4.15)$$

where the superscripts indicate the gauge boson responsible for the contribution. We now briefly recall the main features of the several terms. We want in particular to show the importance of the EW gauge boson contribution, especially in the $B_{s,d}$ systems. Indeed, at odds with what we found, in the most part of the literature the contribution $C_i(M_{\rm KK})^G$ due to the exchange of KK gluons was assumed to yield the dominant effect not only in the $K^0 - \bar{K}^0$ system but also in the $B^0_{s,d} - \bar{B}^0_{s,d}$ systems [51, 55, 119, 120, 145–147].

The KK gluon contribution

Using Fierz transformations, we can easily compute the Wilson coefficients $C_i(M_{\rm KK})^G$, corresponding to the basis presented in (4.14). In the absence of brane kinetic terms we obtain (see the original paper [59] for a brief discussion of the effect of the brane kinetic terms on the $\Delta F = 2$ Wilson coefficients)

$$\begin{aligned}
C_1^{VLL}(M_{\rm KK})^G &= \frac{1}{6M_{\rm KK}^2}\left(\hat{\Delta}_L^{sd}(G^{(1)})\right)^2, \\
C_1^{VRR}(M_{\rm KK})^G &= \frac{1}{6M_{\rm KK}^2}\left(\hat{\Delta}_R^{sd}(G^{(1)})\right)^2, \\
C_1^{LR}(M_{\rm KK})^G &= -\frac{1}{6M_{\rm KK}^2}\hat{\Delta}_L^{sd}(G^{(1)})\hat{\Delta}_R^{sd}(G^{(1)}), \\
C_2^{LR}(M_{\rm KK})^G &= -\frac{1}{M_{\rm KK}^2}\hat{\Delta}_L^{sd}(G^{(1)})\hat{\Delta}_R^{sd}(G^{(1)}), \qquad (4.16)
\end{aligned}$$

where the flavor violating couplings $\hat{\Delta}_{L,R}^{sd}(G^{(1)})$ are defined as function of the overlap integrals $\varepsilon_{L,R}^{+}$ defined already in (3.1). More precisely, dropping the flavor indices, we have the relations

$$\hat{\Delta}_L(G^{(1)}) = \frac{g_s}{\sqrt{L}} D_L^\dagger \varepsilon_L^+(c_1) D_L = g_s^{4D} D_L^\dagger \varepsilon_L^+(c_1) D_L \,, \tag{4.17}$$

$$\hat{\Delta}_R(G^{(1)}) = \frac{g_s}{\sqrt{L}} D_R^\dagger \varepsilon_R^+(c_3) D_R = g_s^{4D} D_R^\dagger \varepsilon_R^+(c_3) D_R \,, \tag{4.18}$$

where the rotation matrices $D_{L,R}$ are those which diagonalize the 3×3 down type mass matrix, as introduced in Eq. (3.26), and g_s is the fundamental 5D strong coupling which, at the tree level and in the absence of brane kinetic terms, is related to the experimentally determined 4D strong coupling by $g_s = \sqrt{L} g_s^{4D}$.

Comparing this result with the Wilson coefficient present in the SM (Eq. (4.1)), it is evident that the NP contributions do not have any suppression by the loop factor $G_F^2/(16\pi^2)$, indicating that the effects are already arising at the tree level. Instead, we have a suppression by the factor $M_W^2/M_{\rm KK}^2$ because of the exchange of heavy particles, instead of the W boson.

The KK photon contribution

We find the following Wilson coefficients

$$\begin{aligned}
C_1^{VLL}(M_{\rm KK})^A &= \frac{1}{2M_{\rm KK}^2} \left[\hat{\Delta}_L^{sd}(A^{(1)})\right]^2 \,, \\
C_1^{VRR}(M_{\rm KK})^A &= \frac{1}{2M_{\rm KK}^2} \left[\hat{\Delta}_R^{sd}(A^{(1)})\right]^2 \,, \\
C_1^{LR}(M_{\rm KK})^A &= \frac{1}{M_{\rm KK}^2} \left[\hat{\Delta}_L^{sd}(A^{(1)})\right] \left[\hat{\Delta}_R^{sd}(A^{(1)})\right] \,, \\
C_2^{LR}(M_{\rm KK})^A &= 0 \,,
\end{aligned} \tag{4.19}$$

where the couplings $\hat{\Delta}_L^{sd}(A^{(1)})$ are defined analogously to the case of the KK gluons, but with the strong coupling replaced by the fundamental 5D electric charge Qe, related to the experimentally measured 4D electric charge by $Qe = \sqrt{L} Q e^{4D}$. Already from the expressions of these Wilson coefficients, two observations are evident

- We expect that the contribution of the KK photon is quite suppressed when compared to the contribution of the KK gluons, because of the suppression by the ratio $\alpha_{\rm QED}/\alpha_s(M_{\rm KK})$ and by the charge factor 1/9. These suppressions are partially compensated by the absence of the 1/3 color factors in (4.19). This suppression will be confirmed in our numerical analysis.

- Without $\mathcal{O}(\alpha_s)$ corrections (see also next section) to the tree level exchange of the KK photon, the coefficient $C_2^{LR}(M_{\rm KK})^A$ vanishes. Strictly speaking for a NLO-QCD analysis the $\mathcal{O}(\alpha_s)$ corrections to the result (4.19) should be included. But as these corrections are small we can neglect them.

The EW gauge boson contribution and the role of the custodial symmetry

While the KK gluon and photon contributions are universal for all the RS models with bulk fermions, the contributions due to the EW gauge bosons Z_H, Z' and Z depend sensitively on the EW gauge group and on the choice of fermion representation. Consequently we do not expect to obtain the same results obtained in the RS model without custodial protection studied for example in [57,69]. Similarly to the computation of the contribution of the KK photon, we can work out the contribution to the several Wilson coefficients from the exchange of the heavy EW gauge bosons Z_H and Z'. Adding the two contributions we find

$$\begin{aligned}
C_1^{VLL}(M_{\rm KK})^{Z_H,Z'} &= \frac{1}{2M_{\rm KK}^2}\left[\left(\hat{\Delta}_L^{sd}(Z^{(1)})\right)^2+\left(\hat{\Delta}_L^{sd}(Z_X^{(1)})\right)^2\right], \\
C_1^{VRR}(M_{\rm KK})^{Z_H,Z'} &= \frac{1}{2M_{\rm KK}^2}\left[\left(\hat{\Delta}_R^{sd}(Z^{(1)})\right)^2+\left(\hat{\Delta}_R^{sd}(Z_X^{(1)})\right)^2\right], \\
C_1^{LR}(M_{\rm KK})^{Z_H,Z'} &= \frac{1}{M_{\rm KK}^2}\left[\hat{\Delta}_L^{sd}(Z^{(1)})\hat{\Delta}_R^{sd}(Z^{(1)})+\hat{\Delta}_L^{sd}(Z_X^{(1)})\hat{\Delta}_R^{sd}(Z_X^{(1)})\right], \\
C_2^{LR}(M_{\rm KK})^{Z_H,Z'} &= 0\,, \qquad (4.20)
\end{aligned}$$

where the two coupling $\hat{\Delta}_{L,R}(Z^{(1)})$ and $\hat{\Delta}_{L,R}(Z_X^{(1)})$ have been already defined in (3.36). At this level, without considering RG running, the operator $\mathcal{Q}_2^{LR}$ is not generated. Additionally, even if not observable from the structure of the Wilson coefficients (4.20) where we summed up the contributions of Z_H and Z', the effect of Z' is smaller than the effect of Z_H because of the suppression of the left handed couplings due to the custodial symmetry P_{LR} (see also Sec. 3.1.4).

Finally, it remains to discuss the contribution of the light Z boson. Naively, one could expect that this contribution dominates the contribution of the heavy EW gauge bosons, because of the light propagator present in the Feynman diagram responsible for the process (suppression by a factor $1/M_Z^2$, instead of by $1/M_{\rm KK}^2$). However, examining the expressions for the couplings of the Z boson with down type quarks (Eq. (3.33)), one can notice the additional suppression by the factor $M_Z^2/M_{\rm KK}^2$ with respect to the mediation of the heavy EW gauge bosons, due to the fact that the Z boson does not have FCNCs before EWSB. In addition, in Sec. 3.1.4 we have demonstrated that the Z flavor violating couplings to left handed down quarks vanish in the limit of exact P_{LR} symmetry. For these reasons one could neglect the contribution of the Z boson in $\Delta F = 2$ processes[2]. Still we would like to point out that, even in the case of a RS model without custodial protection, we do not expect a non-negligible Z contribution, because of the suppression factor $M_Z^2/M_{\rm KK}^2$ discussed just above.

[2] In Sec. 4.2.9 we will show however that the statement is not valid for $\Delta F = 1$ transitions, for which the Z contribution turns out to be the dominant effect.

Adding all contributions

Having all contributions to the $\Delta S = 2$ effective Hamiltonian at hand, we can now add them up, using Eq. (4.15), and compare the size of the contributions arising from the exchange of the KK gluons and of the EW gauge bosons. For that scope, we factor out all the couplings and charge factors from the several $\hat{\Delta}^{sd}_{L,R}$ couplings. Neglecting then the small effects of P_{LR} symmetry breaking due to the different boundary conditions of $Z^{(1)}$ and $Z^{(1)}_X$ on the UV brane, the remaining $\tilde{\Delta}^{sd}_{L,R}$ are universal. Indeed the inclusion of the breaking would amount only to some percent effects, so, at this level of discussion, it is safe to neglect it (in our numerical analysis of Secs. 5.2.1 - 5.2.3 also the symmetry breaking effects will be included). In that approximation we find

$$\begin{aligned}
C_1^{VLL}(M_{\rm KK}) &\approx \frac{1}{4M^2_{\rm KK}}(0.67+0.02+0.56)(\tilde{\Delta}^{sd}_L)^2\,,\\
C_1^{VRR}(M_{\rm KK}) &\approx \frac{1}{4M^2_{\rm KK}}(0.67+0.02+0.98)(\tilde{\Delta}^{sd}_R)^2\,,\\
C_1^{LR}(M_{\rm KK}) &\approx \frac{1}{4M^2_{\rm KK}}(-0.67+0.04+1.13)(\tilde{\Delta}^{sd}_L\tilde{\Delta}^{sd}_R)\,,\\
C_2^{LR}(M_{\rm KK}) &\approx \frac{1}{4M^2_{\rm KK}}(-4+0+0)(\tilde{\Delta}^{sd}_L\tilde{\Delta}^{sd}_R)\,,
\end{aligned} \tag{4.21}$$

where, as indicated in Eq. (4.15), the first contribution is due to the exchange of KK gluons, the second of the KK photon and the third of the EW gauge bosons.

From these expressions, we can conclude that at the high energy scale $M_{\rm KK}$ the EW gauge boson contributions to the Wilson coefficients C_1^{VLL}, C_1^{VRR} and C_1^{LR} (but not to C_2^{LR}) are of the same order of the KK gluon contributions and have to be taken into account, to have a reliable phenomenological prediction of the model. On the other hand the KK photon contributions turn out to be negligible in all cases, being suppressed by the small electric charge of down type quarks.

This terminates the study of the effective Hamiltonian at the high energy scale $M_{\rm KK}$ responsible for the $\Delta F = 2$ transitions in the RS framework.

To further investigate which is the main contribution responsible for $\Delta F = 2$ transitions, we have to examine the QCD renormalization group effects and the chiral enhancement of the hadronic matrix elements.

4.1.3 Chiral enhancement and renormalization group effects (1)

We now perform the renormalization group evolution of the effective Hamiltonian obtained in the previous section down to the low energy scale μ_0, depending on the system analyzed: $\mu_0 \equiv \mu_L \simeq 2$ GeV for the K system and $\mu_0 \equiv \mu_b \simeq 4.6$ GeV for the $B_{s,d}$ systems.

In all generality, independently of the system analyzed, the SM $(V-A)\otimes(V-A)$ operator $(\bar{s}d)_{V-A}(\bar{s}d)_{V-A}$ (and the analogous ones for the $B_{s,d}$ systems) can be renormalized separately from the operators present in the NP effective Hamiltonian $\left[\mathcal{H}_{\rm eff}^{\Delta S=2}\right]_{\rm KK}$. We recall indeed that the operator $\mathcal{Q}_1^{VLL}$ (as well as its "chirality partner" operator $\mathcal{Q}_1^{VRR}$) renormalizes without mixing with the other $\Delta F = 2$ operators [148–150]. Consequently,

we can first deal with the renormalization of the NP effective Hamiltonian in (4.13) (and the corresponding for the $B_{s,d}$ systems), and afterwards add the contribution coming from the SM effective Hamiltonian in (4.1) (or (4.4) for the $B_{s,d}$ systems).

In order to investigate which are the main contributions to the $\Delta F = 2$ observables, both in terms of operators and of gauge bosons exchanged, few observations on the renormalization group running are worth [148–150]

- $\mathcal{Q}_1^{VLL}$ and $\mathcal{Q}_1^{VRR}$ do not mix with the other operators and their anomalous dimensions are the same, since QCD is a chirality blind theory.
- $\mathcal{Q}_1^{LR}$ and $\mathcal{Q}_2^{LR}$ mix under renormalization so that their RG evolution operator is a 2×2 matrix. The running of these operators is in general stronger than the one experienced by $\mathcal{Q}_1^{VLL}$ and $\mathcal{Q}_1^{VRR}$. At the low scale μ_0 the $\mathcal{Q}_1^{LR}$ and $\mathcal{Q}_2^{LR}$ Wilson coefficients are strongly enhanced, contrary to those of the two operators $\mathcal{Q}_1^{VLL}$ and $\mathcal{Q}_1^{VRR}$, which are instead weakly suppressed.
- Comparing the K and the $B_{s,d}$ systems, we notice that in the former the RG enhancement is a bit larger than in the latter, since the relevant scale in K physics is lower than the one in B physics.

We can then finally write the effective Hamiltonian for the $K^0 - \bar{K}^0$ mixing at the low scale μ_L[3]

$$\left[\mathcal{H}_{\rm eff}^{\Delta S=2}\right]_{\rm KK}^{\mu_L} = C_1^{VLL}(\mu_L)\mathcal{Q}_1^{VLL} + C_1^{VRR}(\mu_L)\mathcal{Q}_1^{VRR} + C_1^{LR}(\mu_L)\mathcal{Q}_1^{LR} + C_2^{LR}(\mu_L)\mathcal{Q}_2^{LR}\,, \quad (4.22)$$

and analogous expressions for the $\Delta B = 2$ Hamiltonians at the low energy μ_b.

It remains then to compute the contribution to the off-diagonal mixing amplitude $(M_{12}^K)_{\rm KK}$, that will be then added to the corresponding contribution already obtained in the SM (4.7)

$$2m_K \left(M_{12}^K\right)_{\rm KK}^* = \langle \bar{K}^0 | \left[\mathcal{H}_{\rm eff}^{\Delta S=2}\right]_{\rm KK}^{\mu_L} | K^0 \rangle = \sum_i C_i(\mu_L) \langle \bar{K}^0 | \mathcal{Q}_i | K^0 \rangle\,. \quad (4.23)$$

The hadronic matrix elements $\langle \bar{K}^0 | \mathcal{Q}_i | K^0 \rangle$ can be parametrized as follows, with explicit dependence on the low energy scale μ_L

$$\langle \bar{K}^0 | \mathcal{Q}_1^{VLL} | K^0 \rangle = \langle \bar{K}^0 | \mathcal{Q}_1^{VRR} | K^0 \rangle = \frac{2}{3} m_K^2 F_K^2 B_1^{VLL}(\mu_L)\,, \quad (4.24)$$

$$\langle \bar{K}^0 | \mathcal{Q}_1^{LR} | K^0 \rangle = -\frac{1}{3} R^K(\mu_L) m_K^2 F_K^2 B_1^{LR}(\mu_L)\,, \quad (4.25)$$

$$\langle \bar{K}^0 | \mathcal{Q}_2^{LR} | K^0 \rangle = \frac{1}{2} R^K(\mu_L) m_K^2 F_K^2 B_2^{LR}(\mu_L)\,, \quad (4.26)$$

where the decay constant F_K was already defined in Eq. (4.9) and the $B_i(\mu_L)$ parameters are known from lattice calculations. Their numerical results calculated in the $\overline{\rm MS}$-NDR scheme are given in Tab. 4.1.

[3] See [148] for the explicit expressions of the renormalized Wilson coefficients $C_i(\mu_L)$.

Finally the chiral enhancement factor $R^K(\mu_L)$ of the chirality-flipping operators $\mathcal{Q}_{1,2}^{LR}$ is given by

$$R^K(\mu_L) = \left(\frac{m_K}{m_s(\mu_L) + m_d(\mu_L)}\right)^2 . \tag{4.27}$$

This factor is responsible for a $\mathcal{O}(20)$ enhancement of the $\mathcal{Q}_{1,2}^{LR}$ contributions, with respect to $\mathcal{Q}_1^{VLL}$ and $\mathcal{Q}_1^{VRR}$.

	B_1^{VLL}	B_1^{LR}	B_2^{LR}	μ_0
K^0-$\bar{K}^0$	0.57	0.56	0.81	2.0 GeV
B^0-$\bar{B}^0$	0.87	1.73	1.15	4.6 GeV

Table 4.1: Values of the B_i parameters in the $\overline{\text{MS}}$-NDR scheme obtained in [151] (K^0-$\bar{K}^0$) and [152] (B^0-$\bar{B}^0$). The scale μ_0 at which B_i are evaluated is given in the last column. For $\hat{B}_K$ in (4.8) and for $\hat{B}_{B_{s,d}}$ in (4.11) we use $\hat{B}_K = 0.724 \pm 0.008 \pm 0.028$ [153] and $\hat{B}_{B_{s,d}} = 1.22 \pm 0.12$ [154] respectively.

We can now write the NP tree level contribution to the off-diagonal mixing amplitude $(M_{12}^K)_{\text{KK}}$

$$\begin{aligned}\left(M_{12}^K\right)_{\text{KK}} &= \frac{1}{3} m_K F_K^2 \Big[\left(C_1^{VLL}(\mu_L) + C_1^{VRR}(\mu_L)\right) B_1^{VLL}(\mu_L) \\ &- \frac{1}{2} R^K(\mu_L) C_1^{LR}(\mu_L) B_1^{LR}(\mu_L) + \frac{3}{4} R^K(\mu_L) C_2^{LR}(\mu_L) B_2^{LR} \Big]^* . \end{aligned} \tag{4.28}$$

Analogous expressions can be derived for $(M_{12}^{s,d})_{\text{KK}}$ for the $B_{s,d}$ systems

$$\begin{aligned}\left(M_{12}^{s,d}\right)_{\text{KK}} &= \frac{1}{3} m_{B_{s,d}} F_{B_{s,d}}^2 \Big[\left(C_1^{VLL}(\mu_b) + C_1^{VRR}(\mu_b)\right) B_1^{VLL}(\mu_b) \\ &- \frac{1}{2} R^{s,d}(\mu_b) C_1^{LR}(\mu_b) B_1^{LR}(\mu_b) + \frac{3}{4} R^{s,d}(\mu_b) C_2^{LR}(\mu_b) B_2^{LR}(\mu_b) \Big]^* , \end{aligned} \tag{4.29}$$

where now the chiral enhancement is given by

$$R^{s,d}(\mu_b) = \left(\frac{m_{B_{s,d}}}{m_b(\mu_b) + m_{s,d}(\mu_b)}\right)^2 , \tag{4.30}$$

that is much smaller than in the K system (only $\sim \mathcal{O}(1)$) because of the suppression by the heavy bottom quark mass.

To avoid ambiguities, we have to notice that the values of the Wilson coefficients C_i in (4.29) differ from those in (4.28) as different couplings $\hat{\Delta}^{ij}$ are involved and also the scales μ_L and μ_b are different. Similarly the B_i parameters in (4.29) differ from the ones in (4.28) as now hadronic matrix elements between $B_{s,d}$ and $\bar{B}_{s,d}$ are evaluated (see Tab. 4.1 for a collection of the B_i parameters).

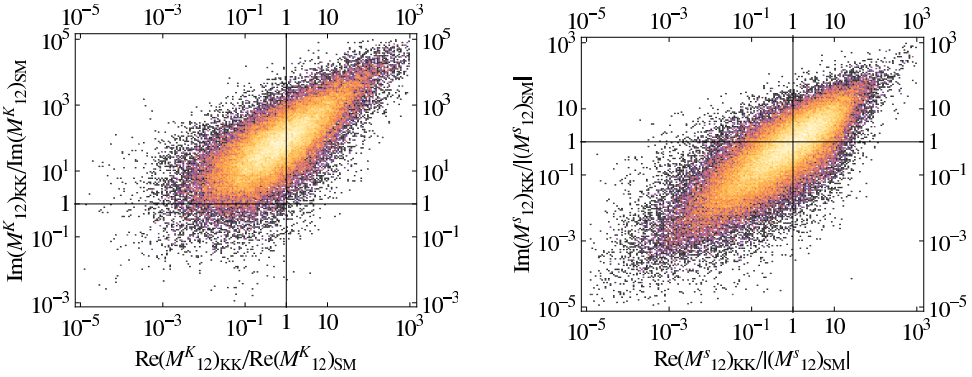

Figure 4.2: Left: $\mathrm{Re}(M_{12}^K)_{\mathrm{KK}}/\mathrm{Re}(M_{12}^K)_{\mathrm{SM}}$ and $\mathrm{Im}(M_{12}^K)_{\mathrm{KK}}/\mathrm{Im}(M_{12}^K)_{\mathrm{SM}}$, plotted on logarithmic axes. Right: $\mathrm{Re}(M_{12}^s)_{\mathrm{KK}}$ and $\mathrm{Im}(M_{12}^s)_{\mathrm{KK}}$, normalized to $|(M_{12}^s)_{\mathrm{SM}}|$ and plotted on logarithmic axes. Lighter colors correspond to higher densities of points.

Finally, the results for M_{12}^K, M_{12}^d and M_{12}^s, which govern the analysis of the $\Delta F = 2$ transitions in the RS model with custodial protection, are given by

$$M_{12}^i = \left(M_{12}^i\right)_{\mathrm{SM}} + \left(M_{12}^i\right)_{\mathrm{KK}} \qquad (i = K, d, s)\,, \tag{4.31}$$

with $\left(M_{12}^i\right)_{\mathrm{SM}}$ given in (4.7), (4.10) and $\left(M_{12}^i\right)_{\mathrm{KK}}$ in (4.28), (4.29).

We now estimate the size of the NP effects in $M_{12}^{K,s,d}$, when compared to the SM values. In Fig. 4.2 the complex $(M_{12}^K)_{\mathrm{KK}}$ and $(M_{12}^s)_{\mathrm{KK}}$ planes are shown. In particular, in the left panel of Fig. 4.2, we show in a density plot $\mathrm{Im}(M_{12}^K)_{\mathrm{KK}}/\mathrm{Im}(M_{12}^K)_{\mathrm{SM}}$ as a function of $\mathrm{Re}(M_{12}^K)_{\mathrm{KK}}/\mathrm{Re}(M_{12}^K)_{\mathrm{SM}}$. We observe that while $\mathrm{Re}(M_{12}^K)_{\mathrm{KK}}$ is typically of the order of the SM contribution, the KK contribution to $\mathrm{Im}(M_{12}^K)$ typically exceeds the SM by two orders of magnitude (to recall that lighter colors correspond to higher densities of points). This is due to the fact that, while we expect $\mathrm{Im}(M_{12}^K)_{\mathrm{KK}} \sim \mathrm{Re}(M_{12}^K)_{\mathrm{KK}}$, in the SM $\mathrm{Im}(M_{12}^K)_{\mathrm{SM}}$ is suppressed with respect to $\mathrm{Re}(M_{12}^K)_{\mathrm{SM}}$ by roughly a factor 100 (see Eq. (4.7))[4].

Analogously, in the right panel of Fig. 4.2, we show $\mathrm{Re}(M_{12}^s)_{\mathrm{KK}}$ and $\mathrm{Im}(M_{12}^s)_{\mathrm{KK}}$, normalized to $|(M_{12}^s)_{\mathrm{SM}}|$. We observe that the KK gauge boson contribution tends to be of roughly the same size as the SM contribution, and that, contrary to the SM, $\mathrm{Re}(M_{12}^s)_{\mathrm{KK}}$ and $\mathrm{Im}(M_{12}^s)_{\mathrm{KK}}$ are generically of the same size, so that an $\mathcal{O}(1)$ new physics phase can be expected. For completeness we mention that the results for M_{12}^d are very similar to those for M_{12}^s, and hence we do not show them here.

We postpone to Sec. 5.2 the numerical analysis of the $\Delta F = 2$ transitions described by the off-diagonal mixing amplitudes $M_{12}^{K,s,d}$. However, here we want to get a feeling for the importance of the various operators. Therefore in Fig. 4.3 we show the ratio of the $\mathcal{Q}_2^{LR}$ and $\mathcal{Q}_1^{VLL}$ operator contributions to $(M_{12}^K)_{\mathrm{KK}}$ in the left panel and to $(M_{12}^s)_{\mathrm{KK}}$ in the right panel. In the K system, as we already expected from the analysis of QCD renormalization effects and chiral enhancement, we observe that the LR operator contribution is by far

[4] In Sec. 5.2.1 we will show that this leads to a strong constraint on the parameter space, coming from the CP violating observable ε_K but not from the mass difference ΔM_K.

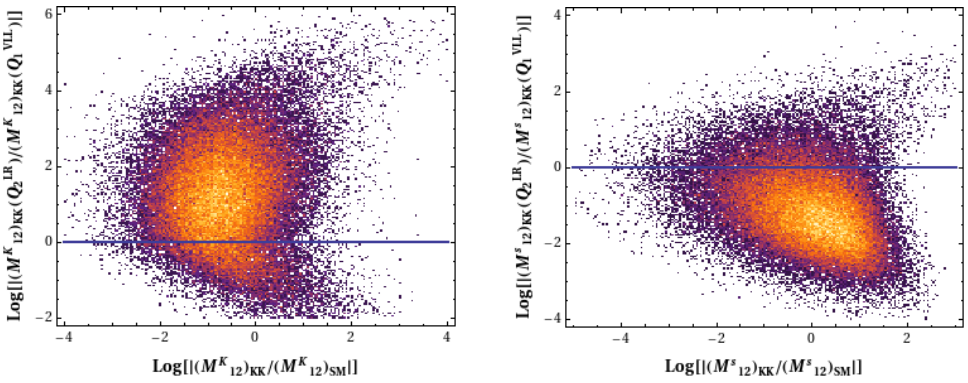

Figure 4.3: The ratio of the contribution of the operator $\mathcal{Q}_2^{LR}$ and $\mathcal{Q}_1^{VLL}$ to $(M_{12}^K)_{\rm KK}$ (left panel) and to $(M_{12}^s)_{\rm KK}$ (right panel), as a function of $(M_{12}^i)_{\rm KK}/(M_{12}^i)_{\rm SM}$ $(i = K\,, s)$ plotted in logarithmic scale. In the two plots, the blue lines indicate an equal contribution of the two operators $\mathcal{Q}_2^{LR}$ and $\mathcal{Q}_1^{VLL}$.

the dominant one, while the LL contribution is typically below 10%. Differently, in the B_s system the $\mathcal{Q}_1^{VLL}$ and $\mathcal{Q}_2^{LR}$ operator contributions turn out to be competitive in size, and in most cases $\mathcal{Q}_1^{VLL}$ even yields the dominant contribution. Additionally we have found that the results for the B_d system are very similar to those of the B_s system. This different feature of the K and $B_{s,d}$ systems is due to the absence of the chiral enhancement in the $B_{s,d}$ system and to the weaker renormalization group QCD enhancement, experienced by the B systems.

From the left panel, we can also conclude that in the K system the KK gluons, which are, at the tree level, the only responsible for the operator $\mathcal{Q}_2^{LR}$, bring the main contribution. Vice versa, from the right panel we deduce that in the B_s (and B_d) system the EW gauge bosons are competitive with the KK gluons, since the operator $\mathcal{Q}_1^{VLL}$, which is also due to the exchange of EW gauge bosons, brings an important contribution.

In Fig. 4.3 we have not shown the contribution of the operator $\mathcal{Q}_1^{VRR}$. Indeed, we have investigated numerically that it is negligibly small. Naively we would have expected to find a contribution of the same size of the one coming from its "chirality partner" $\mathcal{Q}_1^{VLL}$. This conclusion works roughly for the K system, where, as we have analyzed above, the contribution of the operator LL is in any case subleading, but not for the B system for which quarks of the third generation are involved. We have in fact to recall that the Wilson coefficient of the RR operator depends on the off-diagonal couplings $\hat{\Delta}_R^{ij}(Z^{(1)}, Z_X^{(1)})$ (Eq. (4.20)) and that these couplings are much smaller than the corresponding with the opposite chirality $\hat{\Delta}_L^{ij}(Z^{(1)}, Z_X^{(1)})$. In fact, the SM right handed down quark b_R, contrary to the left handed b_L, does not belong to the same representation of the SM left handed up quark t_L (Eqs. (2.34)-(2.36)) and hence has a different bulk mass. In order to reproduce a large top mass, t_L (as well as b_L) has to be localized towards the IR brane, while the right handed field b_R is UV localized. Equivalently, the couplings of the left handed down quarks with KK gauge bosons is much larger than the corresponding couplings of the right handed down quarks.

	K system RG	K system: Chiral	B system: RG	B system: Chiral	KK gluons	EW bosons
$\mathcal{Q}_1^{VLL}$					✓	✓
$\mathcal{Q}_1^{VRR}$					✓	✓
$\mathcal{Q}_1^{LR}$	✓	✓	$\sim$		✓	✓
$\mathcal{Q}_2^{LR}$	✓	✓	$\sim$		✓	

Table 4.2: Summary of the main features of the four quark operators involved in $\Delta F = 2$ transitions in the RS model with custodial protection. In the first four columns we indicate with a ✓a strong effect of enhancement, and with a $\sim$ if the enhancement is present but not particularly relevant. In the last two columns we indicate which are the gauge bosons responsible for the several operators.

As conclusion of this section, in Tab. 4.2 we summarize the main features of the operators involved in $\Delta F = 2$ transitions, both in the K system (first two columns) and in the B system (second two columns). In Sec. 4.1.5 we will generalize this table, including also the $\Delta F = 2$ operators arising in Susy.

4.1.4 $\Delta F = 2$ processes in the Susy flavor models: operator structure

In Susy, the effective Hamiltonians characterizing the particle-antiparticle mixings get contribution from additional operators not present in the RS model effective Hamiltonians. To provide a direct comparison with the formulae reported for the RS framework, we pursue here the study of the $K^0 - \bar{K}^0$ mixing system. A comparison with the features of the $B_{s,d}$ meson mixing systems will be also performed.

Within the MSSM, the effective Hamiltonian in the basis defined in [126][5] has the form

$$\left[\mathcal{H}_{\rm eff}^{\Delta S=2}\right]_{\rm SUSY} = \sum_{i=1}^{5} C_i Q_i + \sum_{i=1}^{3} \tilde{C}_i \tilde{Q}_i \ + \text{h.c.} \ , \tag{4.32}$$

with the operators Q_i given by

$$\begin{aligned}
Q_1 &= (\bar{s}^\alpha \gamma_\mu P_L \, d^\alpha)\,(\bar{s}^\beta \gamma^\mu P_L \, d^\beta) = \mathcal{Q}_1^{VLL} \ , \\
Q_2 &= (\bar{s}^\alpha P_L \, d^\alpha)\,(\bar{s}^\beta P_L \, d^\beta) \ , \\
Q_3 &= (\bar{s}^\alpha P_L \, d^\beta)\,(\bar{s}^\beta P_L \, d^\alpha) \ , \\
Q_4 &= (\bar{s}^\alpha P_L \, d^\alpha)\,(\bar{s}^\beta P_R \, d^\beta) = \mathcal{Q}_2^{LR} \ , \\
Q_5 &= (\bar{s}^\alpha P_L \, d^\beta)\,(\bar{s}^\beta P_R \, d^\alpha) = -\frac{\mathcal{Q}_1^{LR}}{2} \ .
\end{aligned} \tag{4.33}$$

[5] Commonly in Susy the operator basis presented in (4.14) for the RS model is not adopted. For this reason we decided to perform our analysis in the usual basis presented in Eq. (4.33), implementing then explicitely a comparison with the operators present in the RS model (reported in blue in Eq. (4.33)).

The operators $\tilde{Q}_{1,2,3}$ are obtained from $Q_{1,2,3}$ by the replacement $L \leftrightarrow R$ ($\tilde{Q}_1 = \mathcal{Q}_1^{VRR}$). Comparing to the effective Hamiltonian of the RS framework, we notice that the MSSM effective Hamiltonian for $\Delta S = 2$ transitions has four additional operators ($Q_{2,3}$ and the corresponding ones with opposite chirality). We write in blue the operators also present in the RS model (see Eq. (4.14)).

The process receives contributions from box diagrams with the exchange of gluinos $\tilde{g}$ [126], charginos $\tilde{\chi}^{\pm}$, neutralinos $\tilde{\chi}^0$, mixed neutralino/gluino and charged Higgs, and from double penguins [155, 156] with the exchange of the neutral Higgs $H^0\,, A^0$. However in models with non-MFV, the contribution arising from chargino, neutralino, neutralino/gluino and charged Higgs boxes are usually subdominant, when compared to the other two contributions. Thus, in the following we will discuss in detail only the contributions of gluino boxes and double Higgs penguins. The several Wilson coefficients will be given by the sum

$$C_i \cong C_i^{\tilde{g}} + C_i^H\,, \qquad\qquad \tilde{C}_i \cong \tilde{C}_i^{\tilde{g}} + \tilde{C}_i^H\,. \tag{4.34}$$

We now recall the main features of the several contributions at the high scale, making use of the MIA (Sec. 3.2.1). Subsequently, the effects of the RG running to the low energy scale and of the chiral enhancement are discussed.

The gluino contribution

Four different gluino-down squark boxes contribute to the $\Delta S = 2$ flavor transition. In order to facilitate the comprehension of the results of the corresponding Wilson coefficients we represent the gluino Feynman diagrams, showing only the leading contributions in the MIA, in Fig. 4.4.

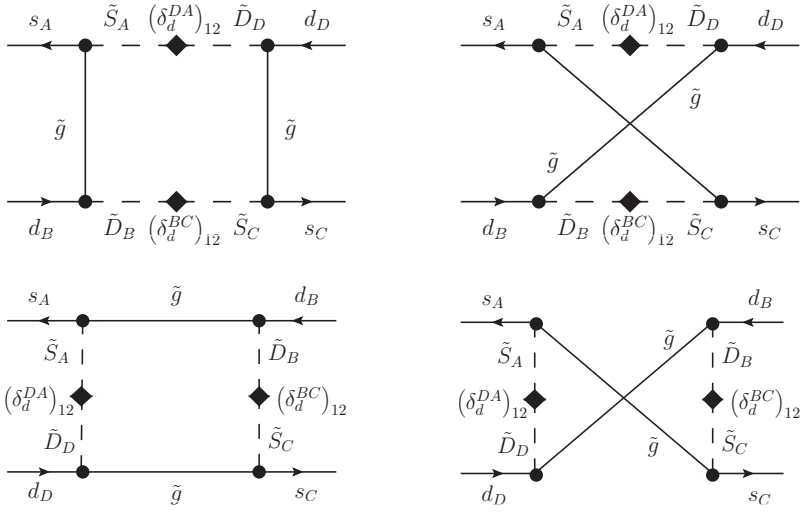

Figure 4.4: Gluino contributions to the $\Delta S = 2$ transition. $A, B, C, D = \{L, R\}$.

The Wilson coefficients arising from these diagrams are given by

$$
\begin{aligned}
C_1^{\tilde{g}} &\simeq -\frac{\alpha_s^2}{\tilde{m}^2}\left[(\delta_d^{LL})_{12}\right]^2 g_1(x_g)\ , \\
C_2^{\tilde{g}} &\simeq -\frac{\alpha_s^2}{\tilde{m}^2}\left[(\delta_d^{RL})_{12}\right]^2 g_2(x_g)\ , \\
C_3^{\tilde{g}} &\simeq -\frac{\alpha_s^2}{\tilde{m}^2}\left[(\delta_d^{RL})_{12}\right]^2 g_3(x_g)\ , \\
C_4^{\tilde{g}} &\simeq -\frac{\alpha_s^2}{\tilde{m}^2}\left[(\delta_d^{LL})_{12}(\delta_d^{RR})_{12}\ g_4(x_g) + (\delta_d^{RL})_{12}(\delta_d^{LR})_{12}\ g_4'(x_g)\right]\ , \\
C_5^{\tilde{g}} &\simeq -\frac{\alpha_s^2}{\tilde{m}^2}\left[(\delta_d^{LL})_{12}(\delta_d^{RR})_{12}\ g_5(x_g) + (\delta_d^{RL})_{12}(\delta_d^{LR})_{12}\ g_5'(x_g)\right]\ ,
\end{aligned}
\tag{4.35}
$$

where $x_g = M_{\tilde{g}}^2/\tilde{m}^2$ ($M_{\tilde{g}}$ is the gluino mass) and the analytic expressions for the loop functions $g_{1,2,3,4,5}$, and $g'_{4,5}$ can be found in Appendix C. It is important to notice that the loop function g_4 entering the expression of the Wilson coefficient $C_4^{\tilde{g}}$ (corresponding to the operator Q_4, or, in the language of the RS model, to the operator $\mathcal{Q}_2^{LR}$) is roughly a factor 30 larger than the one entering the expression of the Wilson coefficient of the SM operator Q_1 (or $\mathcal{Q}_1^{VLL}$ in the language of the RS model). Finally, the Wilson coefficients of the $\tilde{Q}_i$ operators are obtained from the $C_i^{\tilde{g}}$ Wilson coefficients with the exchange $L \leftrightarrow R$, applied to the several MIs. As a final observation, one should note the decoupling of the Wilson coefficients with the Susy mass scale $\tilde{m}$.

The Wilson coefficients for the $B_{s,d}$ systems can be obtained straightforwardly from (4.35), changing properly the flavor indices.

Higgs contribution

Three different neutral Higgs two loops Feynman diagrams contribute to the $\Delta S = 2$ flavor transition at the second order in the MIA. In order to facilitate the comprehension of the results for the corresponding Wilson coefficients we represent the double Higgs penguin Feynman diagrams in Fig. 4.5.

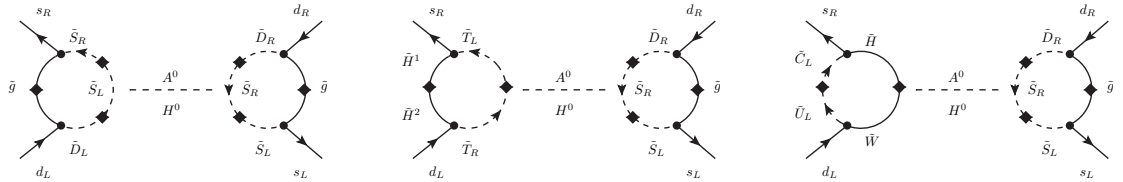

Figure 4.5: Feynman diagrams responsible for the dominant Higgs mediated contributions to the $\Delta S = 2$ transition. The leading contribution proportional to $\tan^4\beta$ comes from the self-energy corrections in diagrams where the Higgs propagators are attached to the external quark legs.

In the regime of large $\tan\beta$, the Feynman diagrams in Fig. 4.5 contribute only to the operator Q_4 in (4.33). In particular, taking into account both gluino and chargino loops we have

$$
\begin{aligned}
C_4^H &\simeq -\frac{\alpha_s^2\alpha_2}{4\pi}\frac{m_s^2}{2M_W^2}\frac{t_\beta^4}{|1+\epsilon t_\beta|^4}\frac{|\mu|^2 M_{\tilde g}^2}{M_A^2\tilde m^4}(\delta_d^{LL})_{12}(\delta_d^{RR})_{12}\left[h_1(x_g)\right]^2 \\
&+ \frac{\alpha_2^2\alpha_s}{4\pi}\frac{m_s^2}{2M_W^2}\frac{t_\beta^4}{|1+\epsilon t_\beta|^4}\frac{|\mu|^2}{M_A^2\tilde m^2}\times\left[\frac{m_t^2}{M_W^2}\frac{A_t M_{\tilde g}}{\tilde m^2}h_1(x_g)h_3(x_\mu)(\delta_d^{RR})_{12}V_{td}V_{ts}^*\right. \\
&+ \left.\frac{M_2 M_{\tilde g}}{\tilde m^2}(\delta_u^{LL})_{12}(\delta_d^{RR})_{12}h_1(x_g)h_4(x_2,x_\mu)\right] , \qquad (4.36)
\end{aligned}
$$

where the mass ratios $x_\mu = |\mu|^2/\tilde m^2$, $x_2 = |M_2|^2/\tilde m^2$ (M_A is the mass of the neutral pseudoscalar Higgs boson) and to simplify the notation we adopted again the abbreviation $t_\beta \equiv \tan\beta$. The loop functions $h_{1,3,4}$ are reported in Appendix C. Finally, ϵ is the well known resummation factor arising from non-holomorphic (t_β enhanced) threshold corrections (see e.g. [157, 158]). The dominant gluino contribution reads

$$
\epsilon \simeq \frac{2\alpha_s}{3\pi}\frac{\mu M_{\tilde g}}{\tilde m^2}f(x_g) , \qquad (4.37)
$$

with the loop function f given in Appendix C.

We stress that the contribution in (4.36) is suppressed by the square of the small strange quark mass m_s and hence negligible, contrary to what instead happens for the $B_{s,d}$ system contributions where the suppression is given by m_b^2.[6] We know that instead in MFV scenarios the double penguin contributions are suppressed by $m_s m_d$, $m_b m_d$, $m_b m_s$, respectively. In the presence of RR mass insertions instead, this strong suppression is lifted and replaced by the proportionality to m_b^2 in the case of $B_{s,d}^0 - \bar B_{s,d}^0$ mixing. For the K system, the most relevant effect coming from the neutral Higgs exchange arises only at the fourth order in the MI expansion, where the $s \to d$ transition is generated by a double $(s \to b)(b \to d)$ flavor-flip. The corresponding contribution is also proportional to m_b^2. We find the following expression

$$
(C_4^H)_2 \simeq -\frac{\alpha_s^2\alpha_2}{4\pi}\frac{m_b^2}{2M_W^2}\frac{t_\beta^4}{(1+\epsilon t_\beta)^4}\frac{|\mu|^2 M_{\tilde g}^2}{M_A^2\tilde m^4}(\delta_d^{LL})_{32}(\delta_d^{LL})_{13}(\delta_d^{RR})_{32}(\delta_d^{RR})_{13}h_2(x_g)^2 , \qquad (4.38)
$$

with h_2 given in Appendix C.

Comparing the Wilson coefficient arising from the exchange of a neutral Higgs boson C_4^H and the one from the exchange of gluinos $C_4^{\tilde g}$, some observations should be pointed out

- The Higgs contributions are in general suppressed compared to the gluino contributions, since the former are a two loop effect (suppression by $\alpha_s^2\alpha_2/4\pi$) and the latter are arising already at the one loop level (suppression by α_s^2).

[6] The double Higgs penguin contribution to the B_s (and B_d) meson mixing systems is given by Eq. (4.36), once that the flavor indices (including the masses) are changed accordingly.

- However, in the regime of large $\tan\beta$ the Higgs contributions can dominate, or at least compete, with the gluino contributions. We note in fact the enhancement of the Higgs contributions by the fourth power of $\tan\beta$ [156].
- Also for a quite heavy Susy mass scale $\tilde{m}$, we can expect that the Higgs contributions are relevant. We note in fact that the gluino contributions decouple with the Susy scale, contrary to what happens to the Higgs contributions which are suppressed just by the Higgs mass M_A.

4.1.5 Chiral enhancement and renormalization group effects (2)

Now that we have the effective Hamiltonian responsible for the meson-antimeson mixing at the high scale in Susy, we have to study the renormalization group evolution of the several operators, exactly as we performed in Sec. 4.1.3 for the operators present in the RS model effective Hamiltonian (Eq. (4.13)).

As far as the operators Q_1, Q_4 and Q_5 are concerned, we refer the reader to Sec. 4.1.3. In fact, as already noticed, these operators are exactly the operators present in the RS model ($\mathcal{Q}_1^{VLL}$, $\mathcal{Q}_2^{LR}$ and $\mathcal{Q}_1^{LR}$, respectively).

On the contrary, the operators Q_2 and Q_3 merit a careful analysis. Analogously to the operators Q_4 and Q_5, the two new operators mix under renormalization so that the RG evolution operator is a 2×2 matrix. Q_2 and Q_3 experience a strong running, even if a bit weaker than the one which involves the operators $Q_{4,5}$ [148–150]. As a result the operators Q_2 and Q_3 are quite enhanced by the running between the GUT scale and the μ_0 low energy scale[7].

We can now write at the low scale μ_L the effective Hamiltonian responsible for the K meson mixing. We have

$$\left[\mathcal{H}_{\rm eff}^{\Delta S=2}\right]_{\rm SUSY}^{\mu_L} = \sum_{i=1}^{5} C_i(\mu_L) Q_i + \sum_{i=1}^{3} \tilde{C}_i(\mu_L) \tilde{Q}_i \ + \text{h.c.} \ , \tag{4.39}$$

from where we can compute the contribution to the off-diagonal K meson mixing amplitude $\left(M_{12}^K\right)_{\rm SUSY}$

$$\begin{aligned} 2m_K \left(M_{12}^K\right)_{\rm SUSY}^* &= \langle \bar{K}^0 | \left[\mathcal{H}_{\rm eff}^{\Delta S=2}\right]_{\rm SUSY}^{\mu_L} | K^0 \rangle = & (4.40) \\ &= \sum_{i=1}^{5} C_i(\mu_L) \langle \bar{K}^0 | Q_i | K^0 \rangle + \sum_{i=1}^{3} \tilde{C}_i(\mu_L) \langle \bar{K}^0 | \tilde{Q}_i | K^0 \rangle \, . & (4.41) \end{aligned}$$

In Sec. 4.1.3 we have already computed the hadronic matrix elements of the operators $Q_{1,4,5}$ and $\tilde{Q}_1$ (Eqs. (4.24)-(4.26)). Now it remains only to parametrize the matrix elements $\langle \bar{K}^0 | Q_{2,3} | K^0 \rangle$ and the corresponding with opposite chirality. We have [159]

[7] Notice that the same observations are also valid for the operators $\tilde{Q}_2$ and $\tilde{Q}_3$ since QCD is a chirality blind theory.

$$\langle \bar{K}^0|Q_2|K^0\rangle = \langle \bar{K}^0|\tilde{Q}_2|K^0\rangle = -\frac{5}{12}R^K(\mu_L)m_K^2F_K^2B_2(\mu_L)\,, \tag{4.42}$$

$$\langle \bar{K}^0|Q_3|K^0\rangle = \langle \bar{K}^0|\tilde{Q}_3|K^0\rangle = \frac{1}{12}R^K(\mu_L)m_K^2F_K^2B_3(\mu_L)\,, \tag{4.43}$$

where $R^K(\mu_L)$ is the chiral enhancement already defined in (4.27) and F_K the decay constant defined in (4.9). Finally the values of the $B_i(\mu_L)$ parameters, known from lattice calculation, are reported in Tab. 4.3, which generalizes Tab. 4.1 presented for the RS model. It is important to note that the operators $Q_{2,3}$ (and the corresponding $\tilde{Q}_{2,3}$) experience the same chiral enhancement exhibited by the operators $Q_{4,5}$ (see Eqs. (4.25)-(4.26)).

Quite analogous expressions hold also for the contribution of Q_2 and Q_3 to the off-diagonal B_s and B_d meson mixing amplitudes $\left(M_{12}^{s,d}\right)_{\rm SUSY}$, even if the chiral enhancement is much weaker, as already discussed for the operators Q_4 and Q_5 in Sec. 4.1.3.

	B_1^{VLL}	B_2	B_3	B_1^{LR}	B_2^{LR}	μ_0
K^0-$\bar{K}^0$	0.57	0.68	1.06	0.56	0.81	2.0 GeV
B^0-$\bar{B}^0$	0.87	0.83	0.90	1.73	1.15	4.6 GeV

Table 4.3: Complete table of the values of the B_i parameters in the $\overline{\rm MS}$-NDR scheme obtained in [151] (K^0-$\bar{K}^0$) and [152] (B^0-$\bar{B}^0$). The scale μ_0 at which B_i are evaluated is given in the last column. For $\hat{B}_K$ in (4.8) and for $\hat{B}_{B_{s,d}}$ in (4.11) we use $\hat{B}_K = 0.724 \pm 0.008 \pm 0.028$ [153] and $\hat{B}_{B_{s,d}} = 1.22 \pm 0.12$ [154], respectively. For completeness we repeat in blue the values of B_1^{VLL}, $B_{1,2}^{LR}$ already discussed in Tab. 4.1.

To conclude this section, we now summarize in Tab. 4.4 the several virtues of the operators present in the $\Delta F = 2$ Hamiltonians (both in the K and in the B system) in the Susy framework. Already from the table, we can observe that the operator Q_4 has the potentiality to be the most important operator in both K and $B_{s,d}$ systems. Thus, the double Higgs penguin diagrams in Fig. 4.5 can be quite relevant.

The running of the parameters of the Lagrangian

Before terminating this section, we want to apply what we have learned about the running of the parameters of the Lagrangian in Sec. 2.3.6, to the two Susy flavor models that we have presented in Secs. 2.3.4 - 2.3.5.

We have already noticed that the operator Q_4 can potentially give the largest contribution to K and B meson mixings. However, from the expressions in (4.35) and (4.36), (4.38) for its WCs, we note that Q_4 is present in the Lagrangian at the TeV scale only if both LL and RR MIs are present. From Sec. 2.3.6 we have also learned that the RR MIs can be present at the low energy scale, only if they are already present at the high energy scale. Therefore, we can conclude that a specific Susy flavor model can have large NP contributions in the K and B meson mixing systems only if the corresponding RR MI is predicted to be sizable at the high energy scale; on the contrary, there are no particular

	K system RG	K system: Chiral	B system: RG	B system: Chiral	Gluino	Higgs boson
$\mathcal{Q}_1$					✓	
$\mathcal{Q}_2$	✓	✓✓	$\sim$		✓	
$\mathcal{Q}_3$	✓	✓✓	$\sim$		✓	
$\mathcal{Q}_4$	✓✓	✓✓	✓		✓✓	✓✓
$\mathcal{Q}_5$	✓✓	✓✓	✓		✓	

Table 4.4: Features of the four quark-operators involved in $\Delta F = 2$ transitions in Susy. In the first four columns we indicate with a ✓✓, if the effect of enhancement is strongly present, with a ✓if the effect is present and with a $\sim$ if the effect is present but not particularly relevant. In the last two columns we indicate which are the particles exchanged in order to generate the several operators.

requirements for the LL MIs, since they can be generated at the low energy scale, even if not present at the high energy scale.

Analyzing the pattern of the MIs of the two flavor models of Secs. 2.3.4 - 2.3.5, we can hence deduce that we expect large NP contributions in the B_s meson system in both models. Smaller effects are instead predicted in the K and B_d systems, especially in the abelian model in which at the GUT scale $\left(\delta_d^{RR}\right)_{12} = \left(\delta_d^{RR}\right)_{13} = 0$.

4.1.6 $\Delta F = 2$ Observables: compendium of formulae

This section is a brief compendium of the formulae for the $\Delta F = 2$ observables that we will use in our numerical analysis of Sec. 5.2. Before starting, we would like to emphasize that, although physical observables are phase convention independent, some of the formulae collected in this section depend on the phase convention chosen for the CKM matrix and yield correct results only if the standard phase convention [160] is used consistently.

Let us start with the CP conserving observables: the mass differences of the $K^0 - \bar{K}^0$ and $B^0_{s,d} - \bar{B}^0_{s,d}$ systems

$$\Delta M_K = 2\left[\mathrm{Re}\left(M_{12}^K\right)_{\mathrm{SM}} + \mathrm{Re}\left(M_{12}^K\right)_{\mathrm{NP}}\right], \tag{4.44}$$

$$\Delta M_q = 2\left|(M_{12}^q)_{\mathrm{SM}} + (M_{12}^q)_{\mathrm{NP}}\right| \qquad (q = d, s), \tag{4.45}$$

where $(M_{12})_{\mathrm{NP}}$ is the NP contribution to M_{12}, namely $(M_{12})_{\mathrm{KK}}$ in the RS model and $(M_{12})_{\mathrm{SUSY}}$ in Susy flavor models.

As far as the CP violating observables concern, in the K system ε_K is given by

$$\varepsilon_K = \frac{\kappa_\epsilon e^{i\varphi_\epsilon}}{\sqrt{2}(\Delta M_K)_{\mathrm{exp}}}\left[\mathrm{Im}\left(M_{12}^K\right)_{\mathrm{SM}} + \mathrm{Im}\left(M_{12}^K\right)_{\mathrm{NP}}\right], \tag{4.46}$$

where $\varphi_\epsilon = (43.51 \pm 0.05)^\circ$ and $\kappa_\epsilon = 0.94 \pm 0.02$ [18, 161] take into account that $\varphi_\epsilon \neq \pi/4$ and include long-distance contributions to ε_K. $(\Delta M_K)_{\rm exp}$ is the measured value of the mass difference ΔM_K.

Finally for the $B_{s,d}$ systems, let us write the off-diagonal mixing amplitude as [22]

$$M_{12}^q = (M_{12}^q)_{\rm SM} + (M_{12}^q)_{\rm NP} = (M_{12}^q)_{\rm SM}\, C_{B_q} e^{2i\varphi_{B_q}}\,, \tag{4.47}$$

where

$$\left(M_{12}^d\right)_{\rm SM} = \left|\left(M_{12}^d\right)_{\rm SM}\right| e^{2i\beta}\,, \qquad \beta \simeq 22^\circ\,, \tag{4.48}$$

$$(M_{12}^s)_{\rm SM} = |(M_{12}^s)_{\rm SM}|\, e^{2i\beta_s}\,, \qquad \beta_s \simeq -1^\circ\,. \tag{4.49}$$

Here the phases β and β_s are defined as functions of the CKM matrix elements through

$$V_{td} = |V_{td}| e^{-i\beta} \quad \text{and} \quad V_{ts} = -|V_{ts}| e^{-i\beta_s}\,. \tag{4.50}$$

We can then define the CP violating asymmetries of the $B_{s,d}$ systems ($S_{\psi\phi}$ and $S_{\psi K_s}$, respectively) as

$$\frac{\Gamma\left(\bar{B}_d(t) \to \psi K_s\right) - \Gamma\left(B_d(t) \to \psi K_s\right)}{\Gamma\left(\bar{B}_d(t) \to \psi K_s\right) + \Gamma\left(B_d(t) \to \psi K_s\right)} \simeq S_{\psi K_s} \sin(\Delta M_d t)\,, \tag{4.51}$$

$$\frac{\Gamma\left(\bar{B}_s(t) \to \psi \phi\right) - \Gamma\left(B_s(t) \to \psi \phi\right)}{\Gamma\left(\bar{B}_s(t) \to \psi \phi\right) + \Gamma\left(B_s(t) \to \psi \phi\right)} \simeq S_{\psi\phi} \sin(\Delta M_s t)\,, \tag{4.52}$$

where the CP violation in the decay amplitude is set to zero. The two asymmetries are given, in terms of the angles β and β_s by

$$S_{\psi K_S} = \sin(2\beta + 2\varphi_{B_d})\,, \tag{4.53}$$

$$S_{\psi\phi} = \sin(2|\beta_s| - 2\varphi_{B_s})\,. \tag{4.54}$$

Thus in the presence of NP phases φ_{B_d} and φ_{B_s} these two asymmetries do not measure the angles of the CKM matrix elements β and β_s but $(\beta + \varphi_{B_d})$ and $(|\beta_s| - \varphi_{B_s})$, respectively.

Finally, we end this section with the discussion of the semileptonic CP asymmetries $A_{\rm SL}^q$ $(q = s, d)$, defined by

$$A_{\rm SL}^q = \frac{\Gamma(\bar{B}_q \to \ell^+ X) - \Gamma(B_q \to \ell^+ X)}{\Gamma(\bar{B}_q \to \ell^+ X) + \Gamma(B_q \to \ell^+ X)} \qquad (q = s, d)\,. \tag{4.55}$$

One can express these asymmetries as

$$A_{\rm SL}^q = {\rm Im}\left(\frac{\Gamma_{12}^q}{M_{12}^q}\right)^{\rm SM} \frac{\cos 2\varphi_{B_q}}{C_{B_q}} - {\rm Re}\left(\frac{\Gamma_{12}^q}{M_{12}^q}\right)^{\rm SM} \frac{\sin 2\varphi_{B_q}}{C_{B_q}}\,, \tag{4.56}$$

where we have defined with Γ_{12}^q the absorptive part of the $B_q^0 - \bar{B}_q^0$ mixing amplitude in the presence of new CP violating phases beyond the CKM. This expression for the semileptonic asymmetries should be compared with the SM prediction

$$\left(A_{\rm SL}^q\right)^{\rm SM} = {\rm Im}\left(\frac{\Gamma_{12}^q}{M_{12}^q}\right)^{\rm SM} . \tag{4.57}$$

It is important to notice that, since in the SM ${\rm Re}\left(\frac{\Gamma_{12}^q}{M_{12}^q}\right)^{\rm SM} \gg {\rm Im}\left(\frac{\Gamma_{12}^q}{M_{12}^q}\right)^{\rm SM}$, even a small new physics phase φ_{B_q} can induce an order of magnitude enhancement of $A_{\rm SL}^q$ relative to the SM.

For later purposes, we recall also the model-independent correlation between the CP asymmetry $S_{\psi\phi}$ and the semileptonic asymmetry $A_{\rm SL}^s$ involving C_{B_s}, pointed out first in [162]

$$A_{\rm SL}^s = -\left|\frac{\Gamma_{12}^s}{M_{12}^s}\right|^{\rm SM} \frac{1}{C_{B_s}} S_{\psi\phi} \,, \tag{4.58}$$

and investigated model-independently in [163].

In Secs. 5.2.3 and 5.2.4, 5.2.5 we will confirm numerically this correlation in the framework of the RS model and of the two Susy flavor models.

Status of the measurements and comparison with the Standard Model

In the last decade, a huge progress in the experimental determination of $\Delta F = 2$ observables has been achieved. The main result is that for the largest part of the observables the room of New Physics is quite narrow, since the SM prediction is in very good agreement with the measurement. Some hints of New Physics come from the CP violating observable ε_K, that, with the last improved value of the hadronic parameter $\hat{B}_K$ from unquenched lattice QCD [153] and with the additional suppression by the multiplicative factor κ_ε [18, 161], seems to show a small discrepancy between the SM prediction and the experiments [18, 161]. Still the deviation is not a very clear signal of New Physics.

The asymmetry $S_{\psi\phi}$ represents an exception in the pattern of good agreement between the SM predictions and the experimental values. Indeed, CP violation in $b \to s$ transitions is predicted to be very small in the SM, thus, any experimental evidence for sizable enhancements in the B_s system would unambiguously point towards a NP evidence. Relatively recent messages from the CDF and D0 experiments [164–166] seem to indicate that this indeed could be the case [15, 16]. In fact, taking into account the two experiments, the Heavy Flavor Averaging Group (HFAG) collaboration [167] gives the average $S_{\psi\phi} = 0.81^{+0.12}_{-0.32}$, that is roughly 3σ away from the SM prediction. This message has been subsequently confirmed by the very recent measurement by D0 [166], but not by CDF [168].

In Tab. 4.5, we summarize and compare the present status of the several $\Delta F = 2$ observables discussed in this section.

From the table we can observe that, while in ΔM_d there is still room for a NP contribution at the 25% level, scenarios with large new CP violating phases are strongly

Observable	Experiment	SM prediction	Exp./SM
ΔM_K	$(5.292 \pm 0.009) \times 10^{-3}$ ps^{-1} [169]		
$\lvert\varepsilon_K\rvert$	$(2.229 \pm 0.010) \times 10^{-3}$ [169]	$(1.91 \pm 0.30) \times 10^{-3}$	1.17 ± 0.18
ΔM_d	(0.507 ± 0.005) ps^{-1} [167]	(0.51 ± 0.13) ps^{-1}	0.99 ± 0.25
$S_{\psi K_S}$	0.672 ± 0.023 [167]	0.734 ± 0.038	0.92 ± 0.06
$A^d_{\rm SL}$	-0.0047 ± 0.0046 [167]	$-(6.4 \pm 1.4) \cdot 10^{-4}$ [170]	
ΔM_s	(17.77 ± 0.12) ps^{-1} [171]	(18.3 ± 5.1) ps^{-1}	0.97 ± 0.27
$S_{\psi\phi}$	$0.81^{+0.12}_{-0.32}$ [167]	0.0366 ± 0.0015 [172]	22 ± 6
$A^s_{\rm SL}$	-0.0146 ± 0.0075 [166]	$(2.6 \pm 0.5) \cdot 10^{-5}$ [170]	
$\Delta M_d/\Delta M_s$	$(2.85 \pm 0.03) \cdot 10^{-2}$	$(2.85 \pm 0.38) \cdot 10^{-2}$	1.00 ± 0.13

Table 4.5: Experimental values and SM predictions for the $\Delta F = 2$ observables. The SM predictions are obtained using CKM parameters from the NP UTfit [22]. The fourth column shows the ratio of the measured value and the SM prediction, signaling the room left for NP effects in the corresponding observable; in particular in red we show the observables for which one could expect large NP contributions, still being in agreement with the experiments. We do not give a SM prediction for ΔM_K because of unknown long-distance contributions.

constrained by the bound on $S_{\psi K_S}$. Finally we can also note that, contrary to the mass differences ΔM_s and ΔM_d alone, the ratio $\Delta M_d/\Delta M_s$ is also a quite relevant constraint on NP, since its SM prediction is more accurate than the prediction for ΔM_d and for ΔM_s, thanks to the cancellation of the most part of the hadronic uncertainties in the ratio

$$\frac{\Delta M_d}{\Delta M_s} = \frac{m_{B_d}}{m_{B_s}} \left|\frac{V_{td}}{V_{ts}}\right|^2 \frac{1}{\xi^2}\,, \tag{4.59}$$

where ξ is defined as $\xi \equiv \frac{\sqrt{\hat{B}_{B_s}} F_{B_s}}{\sqrt{\hat{B}_{B_d}} F_{B_d}}$ and it is given by the accurate value $\xi = 1.21 \pm 0.04$ [154] (see also Tab. 5.2).

4.2 Operator structure for $\Delta F = 1$ transitions

We now analyze in the context of the RS model with custodial protection and of the two Susy flavor models the rare decays of K and B mesons. We will restrict our analysis to few particular decay channels that will show distinctive patterns, allowing us to give recipes to distinguish the two frameworks with the use of low energy observables. We will discuss the theoretically very clean decays $K \to \pi\nu\bar{\nu}$, the purely leptonic decays $K_L \to \mu^+\mu^-$ and $B_{s,d} \to \mu^+\mu^-$. We refer to [173] and [90] for the analysis of additional rare K and B decays in the RS model with custodial protection and in the Susy flavor models, respectively.

4.2.1 The SM effective Hamiltonian for $s \to d\nu\bar{\nu}$

The $K \to \pi\nu\bar{\nu}$ decays are known to be one of the best probes of NP in the quark flavor sector, since they are very suppressed in the SM and theoretically very clean. In the SM the processes arise only at the one loop level, through penguin and box diagrams with internal charm and top exchanges[8] (see Fig. 4.6). The resulting effective Hamiltonian is given by

$$\left[\mathcal{H}_{\rm eff}^{\nu\bar{\nu}}\right]^K_{\rm SM} = g^2_{\rm SM} \sum_{\ell=e,\mu,\tau} \left[\lambda_c^{(K)} X^{\ell}_{\rm NNL}(x_c) + \lambda_t^{(K)} X(x_t)\right] (\bar{s}d)_{V-A} (\bar{\nu}_\ell \nu_\ell)_{V-A} + h.c.\,, \qquad (4.60)$$

where $x_i = m_i^2/M_W^2$, $\lambda_i^{(K)} = V_{is}^* V_{id}$ and, for convenience, we have introduced the effective coupling $g^2_{\rm SM} \equiv \frac{G_F}{\sqrt{2}} \frac{\alpha}{2\pi \sin^2\theta_W}$. Finally, the function $X(x_t)$, as well as $X^{\ell}_{\rm NNL}(x_c)$, comprises internal top (and charm) quark contribution and it is known to high accuracy including QCD corrections [174–176] (see also Appendix C where it is reported at the leading order).

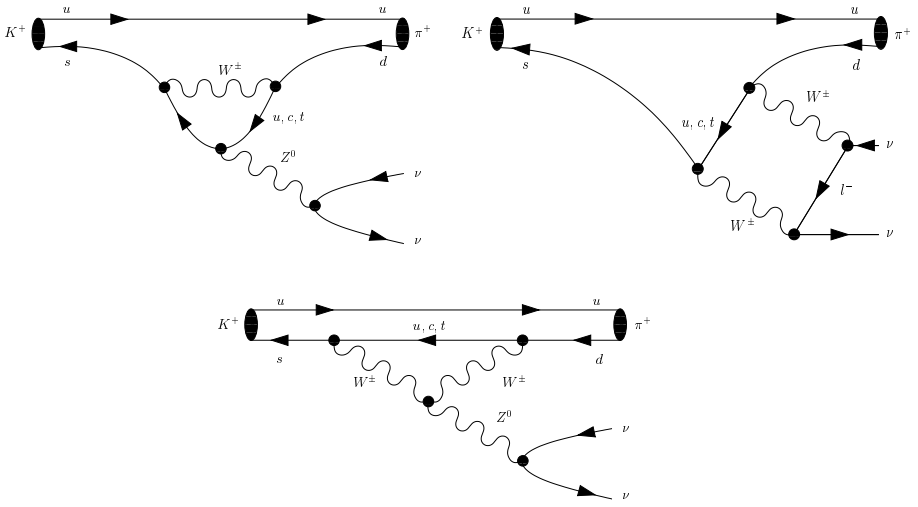

Figure 4.6: The penguin and box diagrams contributing to $K^+ \to \pi^+\nu\bar{\nu}$. For $K_L \to \pi^0\nu\bar{\nu}$ only the spectator quark is changed from u to d. (Diagrams from [177].)

4.2.2 New tree level contributions in the RS model

Thanks to the flavor violating vertices present in the RS model (see Fig. 3.1), $[\mathcal{H}_{\rm eff}^{\nu\bar{\nu}}]^K$ receives tree level contributions from the Z boson and from the heavy neutral gauge bosons Z_H and Z'. Because of these new effects, the effective Hamiltonian will contain new operators when compared to the one of the SM.

[8] The internal up quark contribution is needed only for the GIM mechanism, but can otherwise be neglected.

Combining the three new physics contributions, we find

$$\left[\mathcal{H}_{\rm eff}^{\nu\bar{\nu}}\right]^K_{\rm KK} = g_{\rm SM}^2 \lambda_t^{(K)} \sum_{\ell=e,\mu,\tau} \left[\left(X_K^{V-A}\right)_{\rm KK}\right](\bar{s}d)_{V-A}(\bar{\nu}\nu)_{V-A} + \left[\left(X_K^{V}\right)_{\rm KK}\right](\bar{s}d)_{V}(\bar{\nu}_\ell\nu_\ell)_{V-A} + h.c.\,, \tag{4.61}$$

where the Lorentz structure of the new operator is given by

$$(\bar{s}d)_V(\bar{\nu}\nu)_{V-A} = [\bar{s}\gamma^\mu d] \otimes [\bar{\nu}\gamma_\mu(1-\gamma_5)\nu]\ . \tag{4.62}$$

The functions $X_K^{V-A,V}$ are given by the sums

$$\left(X_K^{V-A}\right)_{\rm KK} = \sum_{i=Z,Z',Z_H} \left((X_i^K)^{V-A}\right)_{\rm KK}\ , \tag{4.63}$$

$$\left(X_K^{V}\right)_{\rm KK} = \sum_{i=Z,Z',Z_H} \left((X_i^K)^{V}\right)_{\rm KK}\ , \tag{4.64}$$

where the several factors are functions of the off-diagonal couplings of the EW gauge bosons with the SM fermions and of their couplings with neutrinos. More specifically, for $i = Z, Z', Z_H$

$$\left((X_i^K)^{V-A}\right)_{\rm KK} = \frac{1}{\lambda_t^{(K)}} \frac{\Delta_L^{\nu\nu}(i)}{4M_i^2 g_{\rm SM}^2} \left[\Delta_L^{sd}(i) - \Delta_R^{sd}(i)\right]\ , \tag{4.65}$$

$$\left((X_i^K)^{V}\right)_{\rm KK} = \frac{1}{\lambda_t^{(K)}} \frac{\Delta_L^{\nu\nu}(i)}{2M_i^2 g_{\rm SM}^2} \Delta_R^{sd}(i)\,, \tag{4.66}$$

where the several off-diagonal couplings $\Delta_{L,R}^{sd}(i)$ ($i = Z, Z', Z_H$) have been already defined in (3.33), (3.46) and (3.47), respectively, and M_i are the masses of the gauge bosons that, in first approximation, are equal to M_Z and to $M_{\rm KK}$ ($= M_{Z'} \sim M_{Z_H} \sim M_{A^{(1)}}$). The flavor universal neutrino couplings $\Delta_L^{\nu\nu}(i)$ are given by

$$\Delta_L^{\nu\nu}(Z) = \frac{g^{4D}}{2\cos\psi}\,, \tag{4.67}$$

$$\Delta_L^{\nu\nu}(Z') = \frac{-g^{4D}}{2\sqrt{2}\cos^2\psi} \left[\varepsilon_L^\nu(Z^{(1)}) + \cos^2\psi\cos^2\phi\,\varepsilon_L^\nu(Z_X^{(1)})\right]\ , \tag{4.68}$$

$$\Delta_L^{\nu\nu}(Z_H) = \frac{g^{4D}\cos\phi}{2\sqrt{2}\cos\psi} \left[\varepsilon_L^\nu(Z^{(1)}) - \varepsilon_L^\nu(Z_X^{(1)})\right]\ , \tag{4.69}$$

where we have defined the overlap integrals between neutrinos and the neutral gauge eigenstates $Z^{(1)}$ and $Z_X^{(1)}$ as in Eq. (3.1) for the quark couplings: $\varepsilon_L^\nu(Z^{(1)}) = \varepsilon_L^+(c_\psi^\nu)$ and $\varepsilon_L^\nu(Z_X^{(1)}) = \varepsilon_L^-(c_\psi^\nu)$, with the suitable choice of the bulk mass c_ψ^ν (see also Sec. 5.1.1 for the discussion of the bulk masses for neutrinos).

It is relevant to note that, contrary to the SM in which the function $X(x_t)$ is flavor universal, here the functions $X^{V-A,V}$ depend on the quark flavors involved, through the flavor indices in the $\Delta_{L,R}^{sd}$ couplings and through the prefactors $1/\lambda_t^{(K)}$.

We conclude this section with the functions that govern the analysis of the $K \to \pi\nu\bar{\nu}$ decays in the RS model with custodial protection

$$X_K^{V-A} = X(x_t) + \left(X_K^{V-A}\right)_{\rm KK} , \tag{4.70}$$

$$X_K^{V} = \left(X_K^{V}\right)_{\rm KK} , \tag{4.71}$$

with $\left(X_K^{V-A}\right)_{\rm KK}$ and $\left(X_K^{V}\right)_{\rm KK}$ given in (4.63)-(4.66).

4.2.3 New one loop contributions in the Susy flavor models

In Susy, the NP contribution to the effective Hamiltonian of the elementary process $s \to d\nu\bar{\nu}$ is still the sum of two operators, as we have already shown in Eq. (4.61) for the RS model

$$\begin{aligned}\left[\mathcal{H}_{\rm eff}^{\nu\bar{\nu}}\right]^K_{\rm SUSY} = g_{\rm SM}^2 \lambda_t^{(K)} \sum_{\ell=e,\mu,\tau} &\left[\left(X_K^{V-A}\right)_{\rm SUSY}\right](\bar{s}d)_{V-A}(\bar{\nu}_\ell\nu_\ell)_{V-A} \\ &+\left[\left(X_K^{V}\right)_{\rm SUSY}\right](\bar{s}d)_{V}(\bar{\nu}_\ell\nu_\ell)_{V-A} + h.c.\,.\end{aligned} \tag{4.72}$$

Sizable contributions to the two functions $\left(X_K^{V-A}\right)_{\rm SUSY}$ and $\left(X_K^{V}\right)_{\rm SUSY}$ can arise only from

- chargino/up squark loops [178–181] (see Fig. 4.7),
- charged Higgs/top quark loops [182] (see Fig. 4.8).

The chargino/up squark loops of Fig. 4.7 give a contribution only to the operator $(\bar{s}d)_{V-A}(\bar{\nu}\nu)_{V-A}$. In particular, the most important contribution arises only at the second order of the MIA and it is given by

$$\left(X_K^{V-A}\right)^{\chi^\pm}_{\rm SUSY} = \frac{1}{8\lambda_t^{(K)}}(\delta_u^{RL})_{32}(\delta_u^{LR})_{13}\ell_C(x_2)\,, \tag{4.73}$$

where the loop function $\ell_C(x)$ is reported in Appendix C and $x_2 = |M_2|^2/\tilde{m}^2$.

One should remark that in principle, in the case of $K \to \pi\nu\bar{\nu}$ decays also other Z penguins and supersymmetric box diagrams could provide effects (see e.g. [183]). However, the remarkable feature of Eq. (4.73) is that it is not explicitly suppressed by the ratio $M_W^2/\tilde{m}^2$, as other contributions are. In conclusion, the only sizable contribution coming from chargino/up squark loops is expressed by Eq. (4.73) and is thus present only in Susy flavor models which predict sizable LR MIs in the up sector.

This requirement seems at odd with the predictions of the two flavor models analyzed in this thesis (see Secs. 2.3.4 and 2.3.5). Indeed, in Sec. 5.3.4 we will confirm numerically that the NP effects coming from chargino/up squarks are quite small.

Concerning the second possible sizable contribution to the two functions X_K^{V-A} and X_K^V, the Z penguin amplitudes generated at the one loop level by charged Higgs/top quark

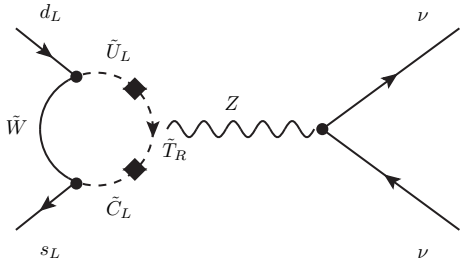

Figure 4.7: Chargino/up squark penguin diagrams contributing to the decays $K \to \pi\nu\bar{\nu}$.

diagrams give only rather small contributions to the functions $X_K^{V-A,V}$, which result to be the sum of terms suppressed either by the second power of $\tan\beta$ or by the light quark masses $m_d \cdot m_s$. Sizable contributions arise only at the three loop level in the presence of $(\delta_d^{RR})_{13}$ and $(\delta_d^{RR})_{32}$ mass insertions, thanks to the diagrams shown in the upper panels of Fig. 4.8. The leading contribution to the effective coupling $H^+ \bar{u}_L^i d_R^j$ (shown with a blue square in the Figure) is given by the gluino loop diagram shown in the lower panel of Fig. 4.8.

Evaluating the charged Higgs/top quark leading contributions to the $K \to \pi\nu\bar{\nu}$ effective Hamiltonian, one finds [182]

$$\left(X_K^V\right)^H_{\rm SUSY} = -2\left(X_K^{V-A}\right)^H_{\rm SUSY} = 2\left[\frac{(\delta_d^{RR})_{13}(\delta_d^{RR})_{32}}{\lambda_t^{(K)}}\right]\frac{m_b^2 t_\beta^2}{2M_W^2}\frac{|\varepsilon_{RR}|^2 t_\beta^2}{|1+\epsilon t_\beta|^4} f_H(y_{tH})\,, \quad (4.74)$$

where $y_{tH} = m_t^2/M_H^2$ (M_H is the mass of the charged Higgs), the loop function $f_H(x)$ is given in Appendix C and the resummation factor ϵ was already introduced in Sec. 4.1.4 (see its approximate expression in Eq. (4.37)). Additionally, to have a compact notation, we have introduced the quantity

$$\varepsilon_{RR} = \frac{2\alpha_s}{3\pi}\frac{\mu}{M_{\tilde{g}}} x_{d_R g} H_3(x_{d_L g}, x_{d_L g}, x_{d_R g})\,, \quad (4.75)$$

where we have defined the ratios $x_{d_{(L,R)}g} = (M^2_{(Q,D)})_{11}/M^2_{\tilde{g}}$ and the loop function H_3 is given in Appendix C.

One should remark that this contribution is sizable only in Susy flavor models which predict down RR MIs in the $(1-3)$ and $(2-3)$ sectors both large.

This requirement seems, once more, at odd with the predictions of the two flavor models analyzed in this thesis (see Secs. 2.3.4 and 2.3.5). Indeed, in Sec. 5.3.4 we will confirm numerically that the NP effects on the $K \to \pi\nu\bar{\nu}$ decays coming from charged Higgs/top quark are quite small.

4.2.4 The decays $K^+ \to \pi^+\nu\bar{\nu}$ and $K_L \to \pi^0\nu\bar{\nu}$

Having at hand the effective Hamiltonian for the $s \to d\nu\bar{\nu}$ transition in the RS model and in Susy flavor models, it is now straightforward to obtain explicit expressions for the

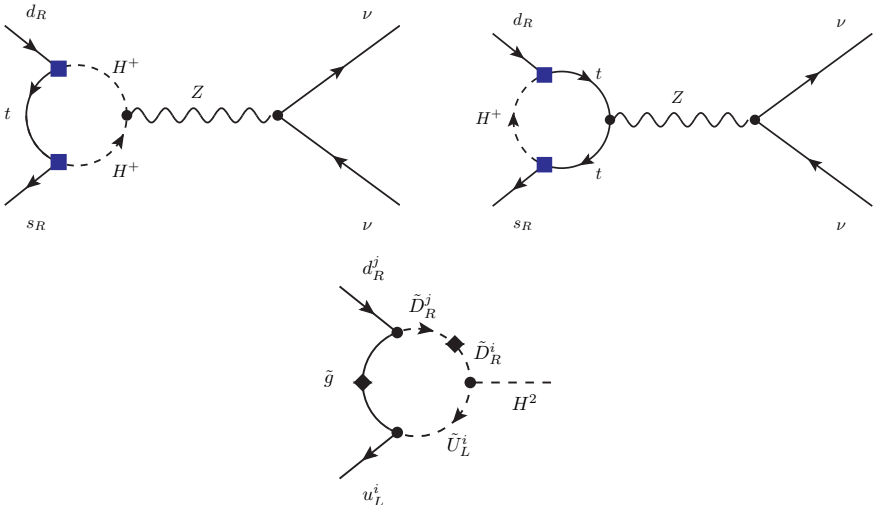

Figure 4.8: First row: Irreducible charged Higgs/top quark one loop diagrams contributing to the decays $K \to \pi\nu\bar{\nu}$. Second row: Effective vertex $H^+\bar{u}_L^i d_R^j$.

branching ratios $\mathrm{Br}(K^+ \to \pi^+\nu\bar{\nu})$ and $\mathrm{Br}(K_L \to \pi^0\nu\bar{\nu})$. Reviews of these two decays can be found in [177, 184, 185].

Since in the two NP frameworks, in addition to the SM operator $(\bar{s}d)_{V-A}(\bar{\nu}\nu)_{V-A}$, also the operator $(\bar{s}d)_V(\bar{\nu}\nu)_{V-A}$ is present, one has to evaluate both matrix elements $\langle\pi|(\bar{s}d)_{V-A}|K\rangle$ and $\langle\pi|(\bar{s}d)_V|K\rangle$. However, since both K and π mesons are pseudoscalars, a simplifying relation holds

$$\langle\pi|(\bar{s}d)_{V-A}|K\rangle = \langle\pi|(\bar{s}d)_V|K\rangle \ . \tag{4.76}$$

This means that effectively, in both models, the effects of NP can be collected in a single function that generalizes the SM $X(x_t)$ function presented in (4.60). We denote this function with

$$X_K \equiv X_K^{V-A} + X_K^V \equiv |X_K| e^{i\,\theta_X^K} \ . \tag{4.77}$$

Note that, in contrast to the real function $X(x_t)$, the new function X_K is in general complex implying new CP violating effects that can be best tested in the very clean CP violating decay $K_L \to \pi^0\nu\bar{\nu}$.

Generalizing then the formulae in [186], we find

$$\mathrm{Br}(K_L \to \pi^0\nu\bar{\nu}) = \kappa_L r_1^2 \left[\sin(\beta_X^K)\right]^2 |X_K|^2 \,, \tag{4.78}$$

$$\mathrm{Br}(K^+ \to \pi^+\nu\bar{\nu}) = \kappa_+ \left[r_1^2|X_K|^2 + 2r_1\bar{P}_c(x)|X_K|\cos(\beta_X^K) + \bar{P}_c^2(x)\right] \,, \tag{4.79}$$

where we have denoted $r_1 = \frac{|V_{ts}||V_{td}|}{\lambda^5}$ and $\beta_X^K = \beta - \beta_s - \theta_X^K$. Additionally we have [187]

$$\kappa_L = (2.31 \pm 0.01)\cdot 10^{-10} \,, \quad \kappa_+ = (5.36 \pm 0.026)\cdot 10^{-11} \,, \tag{4.80}$$

and $\bar{P}_c(x)$ includes both the NNLO corrections [176] and the long-distance contributions [188]

$$\bar{P}_c(x) = \left(1 - \frac{\lambda^2}{2}\right) P_c(x)\,, \quad P_c(x) = 0.42 \pm 0.05\,. \tag{4.81}$$

As we already anticipated, the decay $K_L \to \pi^0\nu\bar{\nu}$ is a very good test of CP violation in rare K decays. In fact the ratio

$$\frac{\mathrm{Br}(K_L \to \pi^0\nu\bar{\nu})}{\mathrm{Br}(K_L \to \pi^0\nu\bar{\nu})_{\mathrm{SM}}} = \left|\frac{X_K}{X(x_t)}\right|^2 \left[\frac{\sin\beta_X^K}{\sin(\beta - \beta_s)}\right]^2 \tag{4.82}$$

is very sensitive to the total phase θ_X^K and is theoretically very clean.

4.2.5 The SM effective Hamiltonian for $s \to d\ell^+\ell^-$ and $b \to (s,d)\ell^+\ell^-$

At the parton level the decays $K_L \to \mu^+\mu^-$ and $B_{s,d} \to \mu^+\mu^-$ are given by analogous transitions: $s \to d\ell^+\ell^-$ for the first and $b \to q\ell^+\ell^-$ $(q = d, s)$ for the second decays. However, as we will learn in Sec. 4.2.8, the two decays are rather different, concerning both the theory and the experimental prospects.

The analysis of the effective Hamiltonian responsible for the short-distance contribution to the process $K_L \to \mu^+\mu^-$ proceeds essentially in the same manner as for the decays $K \to \pi\nu\bar{\nu}$. In particular let us recall that in the SM the top quark contribution to the effective Hamiltonian for $s \to d\ell^+\ell^-$ reads[9]

$$\begin{aligned}\left[\mathcal{H}_{\mathrm{eff}}^{\ell\ell}\right]_{\mathrm{SM}}^{K} &= -g_{\mathrm{SM}}^2 \left[\lambda_t^{(K)} Y(x_t)\right] (\bar{s}d)_{V-A}(\bar{\ell}\ell)_{V-A} \\ &\quad + 4g_{\mathrm{SM}}^2 \sin^2\theta_W \left[\lambda_t^{(K)} Z(x_t)\right] (\bar{s}d)_{V-A}(\bar{\ell}\ell)_{V} + h.c.\,. \end{aligned} \tag{4.83}$$

Here $Y(x_t)$ and $Z(x_t)$ are loop functions, analogous to $X(x_t)$, that result from various penguin and box diagrams (see Appendix C for their expressions, once that the QCD corrections are neglected). The charm contributions and QCD corrections are irrelevant for the discussion presented below and will be included only in the numerical analysis of Chapter 5.

Finally, the effective Hamiltonians for the processes $b \to (s,d)\ell^+\ell^-$ can be obtained from (4.83) by properly adjusting all the flavor indices. In addition, we should remark that in principle also the dipole operators

$$\mathcal{Q}_{7\gamma} = \frac{e}{16\pi^2} m_b \left(\bar{s}\sigma^{\mu\nu} P_R b\right) F_{\mu\nu}\,, \tag{4.84}$$

$$\mathcal{Q}_{8G} = \frac{g_s}{16\pi^2} m_b \left(\bar{s}\sigma^{\mu\nu} T^A P_R b\right) G^A_{\mu\nu} \tag{4.85}$$

[9] In Sec. 4.2.8 we will show that the operator $(\bar{s}d)_{V-A}(\bar{\ell}\ell)_V$ does not contribute to the branching ratio of the decay $K_L \to \mu^+\mu^-$. However in this section we want simply to analyze the full effective Hamiltonian for the elementary process $s \to d\ell^+\ell^-$ (and the corresponding processes $b \to (s,d)\ell^+\ell^-$ for the decays $B_{s,d} \to \mu^+\mu^-$). This more general analysis could be used for the investigation of the decay $K_L \to \pi^0\ell^+\ell^-$ for which the operator $(\bar{s}d)_{V-A}(\bar{\ell}\ell)_V$ plays a central role.

should be included in the Hamiltonian. However, as it turns out, they do not contribute to the decays $B_{s,d} \to \mu^+\mu^-$.

4.2.6 New tree level contributions in the RS model

As we have argued at the beginning of the previous section, the effective Hamiltonians of the elementary processes $s \to d\ell^+\ell^-$, $b \to s\ell^+\ell^-$ and $b \to d\ell^+\ell^-$, contributing to the decays $K_L \to \mu^+\mu^-$ (SD contribution) and to $B_{s,d} \to \mu^+\mu^-$ are perfectly analogous. Therefore we will restrict our discussion to the elementary process $b \to s\ell^+\ell^-$ only.

$\left[\mathcal{H}_{\rm eff}^{\ell\ell}\right]^B$ receives tree level contributions from the exchange of the Z, Z' and Z_H gauge bosons, and, as now charged leptons appear in the final state, also the KK photon $A^{(1)}$ contributes.

Following the same method used for the $K \to \pi\nu\bar{\nu}$ decays, we can write the new physics contributions to the effective Hamiltonian in the compact form

$$\begin{aligned}
\left[\mathcal{H}_{\rm eff}^{\ell\ell}\right]^B_{\rm KK} &= -g_{\rm SM}^2 \left[\lambda_t^{(s)} \left(Y_B^{V-A}\right)_{\rm KK}\right] (\bar{s}b)_{V-A}(\bar{\ell}\ell)_{V-A} \\
&\quad +4g_{\rm SM}^2 \sin^2\theta_W \left[\lambda_t^{(s)} \left(Z_B^{V-A}\right)_{\rm KK}\right] (\bar{s}b)_{V-A}(\bar{\ell}\ell)_{V} \\
&\quad -g_{\rm SM}^2 \left[\lambda_t^{(s)} \left(Y_B^{V}\right)_{\rm KK}\right] (\bar{s}b)_{V}(\bar{\ell}\ell)_{V-A} \\
&\quad +4g_{\rm SM}^2 \sin^2\theta_W \left[\lambda_t^{(s)} \left(Z_B^{V}\right)_{\rm KK}\right] (\bar{s}b)_{V}(\bar{\ell}\ell)_{V} + h.c.\,, \qquad (4.86)
\end{aligned}$$

to which we should add the dipole operators in (4.84), (4.85). We can notice the appearance of two additional operators, when compared to the SM effective Hamiltonian in Eq. (4.86). We have introduced the functions $\left(Y_B^{V-A,V}\right)_{\rm KK}$ and $\left(Z_B^{V-A,V}\right)_{\rm KK}$ defined as:

$$\left(Y_B^{V-A}\right)_{\rm KK} = \sum_{i=Z,Z',Z_H,A^{(1)}} \left((Y_i^B)^{V-A}\right)_{\rm KK}\,, \qquad (4.87)$$

$$\left(Z_B^{V-A}\right)_{\rm KK} = \sum_{i=Z,Z',Z_H,A^{(1)}} \left((Z_i^B)^{V-A}\right)_{\rm KK}\,, \qquad (4.88)$$

$$\left(Y_B^{V}\right)_{\rm KK} = \sum_{i=Z,Z',Z_H,A^{(1)}} \left((Y_i^B)^{V}\right)_{\rm KK}\,, \qquad (4.89)$$

$$\left(Z_B^{V}\right)_{\rm KK} = \sum_{i=Z,Z',Z_H,A^{(1)}} \left((Z_i^B)^{V}\right)_{\rm KK}\,, \qquad (4.90)$$

where the several factors are function of the off-diagonal couplings of the EW gauge bosons with the SM fermions and of their couplings with leptons. In particular, for

$i = Z, Z', Z_H, A^{(1)}$

$$\left((Y_i^B)^{V-A}\right)_{\rm KK} = -\frac{1}{\lambda_t^{(s)}}\frac{\left[\Delta_L^{\ell\ell}(i)-\Delta_R^{\ell\ell}(i)\right]}{4M_i^2 g_{\rm SM}^2}\left[\Delta_L^{sb}(i)-\Delta_R^{sb}(i)\right], \tag{4.91}$$

$$\left((Z_i^B)^{V-A}\right)_{\rm KK} = \frac{1}{\lambda_t^{(s)}}\frac{\Delta_R^{\ell\ell}(i)}{8M_i^2 g_{\rm SM}^2\sin^2\theta_W}\left[\Delta_L^{sb}(i)-\Delta_R^{sb}(i)\right], \tag{4.92}$$

$$\left((Y_i^B)^{V}\right)_{\rm KK} = -\frac{1}{\lambda_t^{(s)}}\frac{\left[\Delta_L^{\ell\ell}(i)-\Delta_R^{\ell\ell}(i)\right]}{2M_i^2 g_{\rm SM}^2}\Delta_R^{sb}(i), \tag{4.93}$$

$$\left((Z_i^B)^{V}\right)_{\rm KK} = \frac{1}{\lambda_t^{(s)}}\frac{\Delta_R^{\ell\ell}(i)}{4M_i^2 g_{\rm SM}^2\sin^2\theta_W}\Delta_R^{sb}(i), \tag{4.94}$$

where the several off-diagonal couplings $\Delta_{L,R}^{sb}(i)$ ($i = Z, Z', Z_H, A^{(1)}$) has been already defined in (3.33), (3.46), (3.47) and below Eq. (4.19), respectively, and M_i are the masses of the gauge bosons that, in first approximation, are equal to M_Z and to $M_{\rm KK}$ ($= M_{Z'} \sim M_{Z_H} \sim M_{A^{(1)}}$). The flavor universal lepton couplings $\Delta_{L,R}^{\ell\ell}(i)$ are given by

$$\Delta_L^{\ell\ell}(Z) = \frac{g^{\rm 4D}}{\cos\psi}\left(-\frac{1}{2}+\sin^2\psi\right), \qquad \Delta_R^{\ell\ell}(Z) = \frac{g^{\rm 4D}}{\cos\psi}\sin^2\psi, \tag{4.95}$$

$$\Delta_L^{\ell\ell}(Z_H) = \frac{g^{\rm 4D}\cos\phi\left(-\frac{1}{2}+\sin^2\psi\right)}{\sqrt{2}\cos\psi}\left[\varepsilon_L^{\ell}(Z^{(1)}) - \frac{1}{2\left(-\frac{1}{2}+\sin^2\psi\right)}\varepsilon_L^{\ell}(Z_X^{(1)})\right], \tag{4.96}$$

$$\Delta_R^{\ell\ell}(Z_H) = \frac{g^{\rm 4D}\cos\phi\sin^2\psi}{\cos\psi}\left[\varepsilon_L^{\ell}(Z^{(1)}) - \frac{1}{\sin^2\psi}\varepsilon_L^{\ell}(Z_X^{(1)})\right], \tag{4.97}$$

$$\Delta_L^{\ell\ell}(Z') = -\frac{g^{\rm 4D}\left(-\frac{1}{2}+\sin^2\psi\right)}{\sqrt{2}\cos^2\psi}\left[\varepsilon_L^{\ell}(Z^{(1)}) + \frac{\cos^2\phi\cos^2\psi}{2\left(-\frac{1}{2}+\sin^2\psi\right)}\varepsilon_L^{\ell}(Z_X^{(1)})\right], \tag{4.98}$$

$$\Delta_R^{\ell\ell}(Z') = -\frac{g^{\rm 4D}\tan^2\psi}{\sqrt{2}}\left[\varepsilon_L^{\ell}(Z^{(1)}) + \frac{\cos^2\phi}{\tan^2\psi}\varepsilon_L^{\ell}(Z_X^{(1)})\right], \tag{4.99}$$

where we have defined the overlap integrals between leptons and the neutral gauge eigenstates $Z^{(1)}$ and $Z_X^{(1)}$ as in Eq. (3.1) for the quark couplings: $\varepsilon_L^{\ell}(Z^{(1)}) = \varepsilon_L^{+}(c_\psi^\ell)$ and $\varepsilon_L^{\ell}(Z_X^{(1)}) = \varepsilon_L^{-}(c_\psi^\ell)$, with the suitable choice of the bulk mass c_ψ^ℓ (see also Sec. 5.1.1 for the discussion of the bulk masses for leptons).

Finally, we can write the functions that govern the analysis of the process $b \to s\ell^+\ell^-$ in the RS model with custodial protection

$$Y_B^{V-A} = Y(x_t) + \left(Y_B^{V-A}\right)_{\rm KK}, \tag{4.100}$$

$$Z_B^{V-A} = Z(x_t) + \left(Z_B^{V-A}\right)_{\rm KK}, \tag{4.101}$$

$$Y_B^{V} = \left(X_B^{V}\right)_{\rm KK}, \tag{4.102}$$

$$Z_B^{V} = \left(Z_B^{V}\right)_{\rm KK}, \tag{4.103}$$

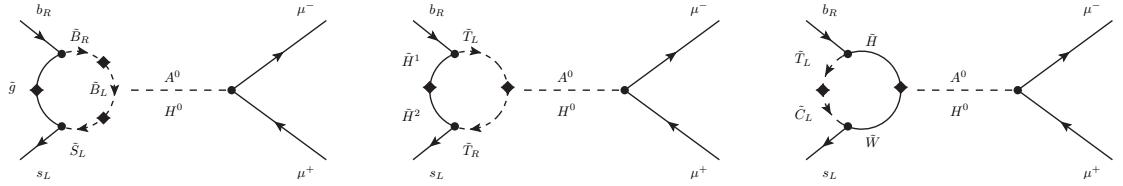

Figure 4.9: Feynman diagrams for the dominant Higgs mediated contributions to $B_s \to \mu^+\mu^-$. The leading contribution to the decay amplitude proportional to $\tan^3\beta$ comes from the self-energy corrections in diagrams where the Higgs propagators are attached to the external quark legs.

with $\left(Y_B^{V-A,V}\right)_{\rm KK}$ and $\left(Z_B^{V-A,V}\right)_{\rm KK}$ given in (4.87)-(4.94).

4.2.7 New one loop contributions in the Susy flavor models

In Susy, the effective Hamiltonian responsible for the process $b \to s\ell^+\ell^-$ includes certainly the two operators already present in the SM (see Eqs. (4.83)-(4.85)). In addition it contains several additional operators, in particular the scalar and the pseudoscalar operators Q_S and Q_P,

$$Q_S = m_b\,(\bar{s}P_R b)\,\left(\bar{\ell}\ell\right) \;\;,\;\; Q_P = m_b\,(\bar{s}P_R b)\,\left(\bar{\ell}\gamma_5\ell\right) \;\;, \tag{4.104}$$

as well as the corresponding $\tilde{Q}_S$ and $\tilde{Q}_P$ that are obtained by the exchange $L \leftrightarrow R$. The main NP contributions come indeed from the scalar and pseudoscalar operators just introduced. For this reason, in this section we will analyze only the corresponding WCs (for a complete analysis see e.g. [189]). We can then write the relevant effective Hamiltonian as

$$\left[\mathcal{H}_{\rm eff}^{\ell\ell}\right]^B_{\rm SUSY} = C_S Q_S + C_P Q_P + \tilde{C}_S \tilde{Q}_S + \tilde{C}_P \tilde{Q}_P \,. \tag{4.105}$$

The main contribution to the Wilson coefficients $C_{S,P}$ (and to the corresponding $\tilde{C}_{S,P}$) is given by the Higgs penguin diagrams shown in Fig. 4.9.

The leading contributions to the Wilson coefficients arising from these diagrams are given, to a very good approximation, by

$$C_P \simeq -C_S \;\;,\;\; \tilde{C}_P \simeq \tilde{C}_S \;\;, \tag{4.106}$$

with

$$\begin{aligned} C_S &= \frac{\alpha_2^2}{M_A^2}\frac{m_\ell}{4M_W^2}\frac{t_\beta^3}{(1+\epsilon t_\beta)^2(1+\epsilon_\ell t_\beta)}\left[\frac{m_t^2}{M_W^2}\frac{A_t\mu}{\tilde{m}^2}V_{tb}V_{ts}^* h_3(x_\mu) + \frac{M_2\mu}{\tilde{m}^2}(\delta_u^{LL})_{32} h_4(x_2,x_\mu)\right] \\ &\quad -\frac{\alpha_2\alpha_s}{M_A^2}\frac{m_\ell}{4M_W^2}\frac{t_\beta^3}{(1+\epsilon t_\beta)^2(1+\epsilon_\ell t_\beta)}\frac{M_{\tilde{g}}\mu}{\tilde{m}^2}(\delta_d^{LL})_{32} h_1(x_g) \;, \end{aligned} \tag{4.107}$$

$$\tilde{C}_S = -\frac{\alpha_2\alpha_s}{M_A^2}\frac{m_\ell}{4M_W^2}\frac{t_\beta^3}{(1+\epsilon t_\beta)^2(1+\epsilon_\ell t_\beta)}\frac{M_{\tilde{g}}\mu^*}{\tilde{m}^2}(\delta_d^{RR})_{32} h_1(x_g) \;, \tag{4.108}$$

where we have included the $\tan\beta$ enhanced non-holomorphic corrections for the lepton Yukawas ϵ_ℓ. In particular, in the limit of degenerate Susy particles it turns out that $\epsilon_\ell \sim -3\alpha_2/16\pi$. Finally, the loop functions h_1, h_3 and h_4 are given in Appendix C and were already introduced in Eq. (4.36) for the double Higgs penguin contribution to the K and $B_{s,d}$ meson mixing. Indeed, already from the comparison of the Feynman diagrams in Fig. 4.9 for the decay $B_s \to \mu^+\mu^-$ and those coming from Fig. 4.5 (changing accordingly the flavor indices) for the $B_s^0 - \bar{B}_s^0$ mixing, one expects a correlation between the branching ratio of $B_s \to \mu^+\mu^-$ and the observables of the B_s meson mixing system, if the double Higgs penguins produce a large contribution to the $B_s^0 - \bar{B}_s^0$ mixing. In Sec. 5.3.4 we will analyze in detail this correlation in the two Susy flavor models of Secs. 2.3.4, 2.3.5.

From the expression for the Wilson coefficients C_S and $\tilde{C}_S$ it is important to notice the enhancement by the third power of $\tan\beta$, that can induce orders of magnitude enhancement in the branching ratio of the decay $B_s \to \mu^+\mu^-$ (and $B_d \to \mu^+\mu^-$). Finally one should also note that the WCs do not decouple with the Susy scale $\tilde{m}$, but with the mass of the Higgs M_A, as also exhibited by the WCs of the double Higgs penguins mediating $\Delta F = 2$ transitions (Eq. (4.36)).

4.2.8 The decays $B_{s,d} \to \mu^+\mu^-$ and $K_L \to \mu^+\mu^-$

In this section, we first discuss the theory and the experimental prospects of the decays $K_L \to \mu^+\mu^-$ and $B_{s,d} \to \mu^+\mu^-$. Secondly, we analyze the several branching ratios.

The rare decay $K_L \to \mu^+\mu^-$ is a CP conserving process and, in addition to its short-distance part, given in the SM by Z penguins and box diagrams, receives important contributions from the two-photon intermediate state. This fact is rather unfortunate because the short-distance part is, similarly to the decays $K \to \pi\nu\bar{\nu}$, almost free of hadronic uncertainties and hence would give a clear test for the theories beyond the Standard Model. Additionally the extraction of the short-distance part from the data is subject to considerable uncertainties.

Concerning the rare B decays, there are many motivations to study $B_{s,d} \to \mu^+\mu^-$. Differently from the $K_L \to \mu^+\mu^-$ decay examined previously, these decays are short-distance dominated and, after the decays $B \to X_s\nu\bar{\nu}$, are the theoretically cleanest decays in the field of rare B decays. Additionally, there are well founded hopes to measure the branching ratio of $B_s \to \mu^+\mu^-$ in the coming years at LHCb and any experimental evidence for sizable NP effects in the $B_{s,d} \to \mu^+\mu^-$ decays would unambiguously point towards a NP evidence, since in the SM their branching ratios receive a strong chiral suppression.

The theoretical computation of the $B_{s,d} \to \mu^+\mu^-$ and $K_L \to \mu^+\mu^-$ branching ratios is analogous. The dipole operators in (4.84)-(4.85) do not contribute. Consequently, the calculation of the two branching ratios requires only the knowledge of the matrix element of the four operators in (4.86) for the RS framework and also of the operators Q_S and Q_P (and the corresponding ones with $L \leftrightarrow R$) in (4.104) for the Susy flavor models.

Two simplifications occur. First, when evaluating the matrix elements $\langle 0|(\bar{q}b)_{V-A}|B_q\rangle$ and $\langle 0|(\bar{q}b)_V|B_q\rangle$ (and the corresponding ones for the K decay) only the $\gamma_\mu\gamma_5$ part contributes because of the pseudoscalar nature of the $B_{s,d}$ (and K) mesons, so that

$$\langle 0|(\bar{q}b)_V|B_q\rangle = 0\,. \tag{4.109}$$

Then, due to the conserved vector current, the vector component of the $\mu\mu$-vertex drops out as well and, as in the SM, only the $\gamma_\mu\gamma_5$ component of the $\mu\mu$-vertex is relevant.

Therefore, we can conclude that

- In the RS model only the SM operator $(V-A)\otimes(V-A)$ contributes to the three branching ratios.
- In Susy in addition to the SM operator also the scalar operators Q_S and Q_P (and the corresponding ones with $L \leftrightarrow R$) contribute to the processes.

In the following we will give first explicit formulae for the branching ratios of $B_{s,d} \to \mu^+\mu^-$ in the two NP frameworks[10]. Secondly, we will restrict ourselves in reporting the expression for the branching ratio of $K_L \to \mu^+\mu^-$ only in the RS model. In Chapter 5 we will in fact show the importance of the decay, but only in the framework of the RS model.

The $B_{s,d} \to \mu^+\mu^-$ decay in the RS model and in Susy

In the RS model, we can define, analogously to what we have performed for the $K \to \pi\nu\bar{\nu}$ decays, the generalization of the SM $Y(x_t)$ function presented in Eq. (4.83)

$$Y_B^q \equiv (Y_B^{V-A})^q\,, \tag{4.110}$$

where we decided to insert an explicit flavor index, not present in the definition of the function Y_B^{V-A} for the process $b \to s\ell^+\ell^-$ in (4.100). The function Y_B^q is in fact flavor non-universal, contrary to what happens in the SM.

Using this function, we can then easily write the branching ratios of $B_q \to \mu^+\mu^-$

$$\frac{\mathrm{Br}(B_q \to \mu^+\mu^-)_{\mathrm{RS}}}{\mathrm{Br}(B_q \to \mu^+\mu^-)_{\mathrm{SM}}} = \frac{|Y_B^q|^2}{Y(x_t)^2}\,, \tag{4.111}$$

where in the SM

$$\mathrm{Br}(B_q \to \mu^+\mu^-)_{\mathrm{SM}} = \frac{G_F^2\tau_{B_q}}{\pi}\left(\frac{\alpha_{\mathrm{QED}}}{4\pi\sin^2\theta_W}\right)^2 F_{B_q}^2 m_{B_q} m_\mu^2 \sqrt{1-\frac{4m_\mu^2}{m_{B_q}^2}}\,|V_{tb}^* V_{tq}|^2\,Y(x_t)^2\,, \tag{4.112}$$

where τ_{B_q} is the life time of the B_q meson.

In Susy instead the expression for the two branching ratios appears a bit more complicated, because of the presence of the two additional operators Q_S and Q_P (and the corresponding ones with tilde). We have

[10] We could simply give the formulae for the branching ratios in Susy, since, as we will show, the results for the RS model are just a particular case of the more general formulae we obtain in the Susy framework. However, for completeness, we will list the formulae for both theories.

$$\mathrm{BR}(B_q \to \mu^+\mu^-)_{\mathrm{SUSY}} = \frac{\tau_{B_q} F_{B_q}^2 m_{B_q}^3}{32\pi}\sqrt{1-4\frac{m_\mu^2}{m_{B_q}^2}}\left(|B|^2\left(1-4\frac{m_\mu^2}{m_{B_q}^2}\right)+|A|^2\right) \ , \quad (4.113)$$

where A and B are given by the two linear combinations of Wilson coefficients

$$A = 4\frac{m_\mu}{m_{B_q}} C_{(V-A)(V-A)} + m_{B_q}\left(C_P - \tilde{C}_P\right) \ , \ B = m_{B_q}\left(C_S - \tilde{C}_S\right) \ , \quad (4.114)$$

where $C_{(V-A)(V-A)}$ is the Wilson coefficient of the SM operator $(V-A)\otimes(V-A)$ that, neglecting the NP contributions, is given by $C_{(V-A)(V-A)} = -g_{\mathrm{SM}}^2 \lambda_t^{(q)} Y(x_t)$ as shown by Eq. (4.83) for the SM effective Hamiltonian (with the suitable change of flavor indices). $C_{S,P}, \tilde{C}_{S,P}$ are given in (4.106)-(4.108).

One should note that this expression for the two branching ratios is nothing other than the generalization of what we have obtained in the RS model (Eqs. (4.111), (4.112)). Indeed, putting to zero the Wilson coefficients of the scalar operators $Q_{S,P}$ (and the corresponding ones with tilde) in (4.113) and changing suitably the Wilson coefficient $C_{(V-A)(V-A)}$, one gets exactly the expression in Eq. (4.111) for the branching ratios.

The $K_L \to \mu^+\mu^-$ decay in the RS model

As we have already discussed, the short-distance contribution to the decay $K_L \to \mu^+\mu^-$ calculated here is only a part of the dispersive contribution to $K_L \to \mu^+\mu^-$ that is by far dominated by the absorptive contribution with two internal photon exchanges. Consequently the SD contribution constitutes only a small fraction of the branching ratio. In the following we will give the expressions for the SD contributions to the branching ratio of $K_L \to \mu^+\mu^-$ in the RS model.

In the RS model, we can define the generalization of the function $Y(x_t)$ present in the SM, analogously to what we have shown just above for the decays $B_q \to \mu^+\mu^-$ (Eq. (4.110)), changing the flavor indices suitably

$$Y_K \equiv Y_K^{V-A} = |Y_K^{V-A}| e^{i\bar{\theta}_Y^K} \ . \quad (4.115)$$

Following [186], we find for the SD contribution

$$\mathrm{Br}(K_L \to \mu^+\mu^-)_{\mathrm{RS}}^{\mathrm{SD}} = 2.08 \cdot 10^{-9}\left[\bar{P}_c\left(Y_K\right) + A^2 R_t \left|Y_K\right| \cos\bar{\beta}_Y^K\right]^2 \ , \quad (4.116)$$

where we have defined

$$\bar{\beta}_Y^K \equiv \beta - \beta_s - \bar{\theta}_Y^K \ , \quad \bar{P}_c\left(Y_K\right) \equiv \left(1-\frac{\lambda^2}{2}\right) P_c\left(Y_K\right) \ , \quad (4.117)$$

with $P_c\left(Y_K\right) = 0.113 \pm 0.017$ [190].

4.2.9 Anatomy of contributions (RS model)

In this section we will compare in the framework of the RS model the several contributions to the rare K and B decays. Through this comparison we can already anticipate some patterns of flavor violation that will be confirmed in our numerical analysis of Secs. 5.3.1-5.3.3.

Contributions of the EW gauge bosons in the RS model

As we have already shown, four EW gauge bosons are contributing to the several K and B decays: Z, Z', Z_H and the photon $A^{(1)}$. However the contribution of the photon turns out to be small (if not absent) in all cases, since it is suppressed by the smallness of the electromagnetic coupling e and the electric quark charge. Let us hence restrict our analysis to the other three EW gauge bosons. Numerically we find the following patterns for their couplings with down quarks (Eqs. (4.118)-(4.119)) and leptons (Eq. (4.120))

$$\Delta_L^{ij}(Z_H) : \Delta_L^{ij}(Z') : \Delta_L^{ij}(Z) \sim \mathcal{O}(10^4) : \mathcal{O}(10^3) : 1\,, \tag{4.118}$$

$$\Delta_R^{ij}(Z_H) : \Delta_R^{ij}(Z') : \Delta_R^{ij}(Z) \sim \mathcal{O}(10^2) : \mathcal{O}(10^2) : 1\,, \tag{4.119}$$

$$\Delta_{L,R}^{\nu\nu,\ell\ell}(Z_H) : \Delta_{L,R}^{\nu\nu,\ell\ell}(Z') : \Delta_{L,R}^{\nu\nu,\ell\ell}(Z) \sim \mathcal{O}(10^{-1}) : \mathcal{O}(10^{-1}) : 1\,, \tag{4.120}$$

where the first two relations hold for the K, B_d and B_s systems likewise, that is for $ij = sd$, $ij = bd$ and $ij = bs$, respectively.

With our knowledge of the flavor sector of the model, we could have already anticipated the most part of the features listed above. In particular

- *As far as* $\Delta_L^{ij}(\alpha)$ *concern,* as presented in Sec. 3.1.4, in the presence of an exact P_{LR} symmetry, the flavor violating couplings $\Delta_L^{ij}(Z)$ and $\Delta_L^{ij}(Z')$ would vanish identically. Taking into account the P_{LR} symmetry breaking effects on the UV brane, the custodial protection mechanism is not exact anymore and the Z and Z' couplings are non-zero. However they are suppressed, when compared to the Z_H couplings. Additionally in the case of Z', the mixing angles for $Z^{(1)}$ and $Z_X^{(1)}$ are modified by roughly 10% when including the violation of the P_{LR}. Accordingly, the protection is weaker for the Z' couplings, when compared to the Z couplings and, in fact, in Eq. (4.118) we read that $\Delta_L^{ij}(Z')$ is suppressed only by one order of magnitude compared to $\Delta_L^{ij}(Z_H)$.

- *As far as* $\Delta_R^{ij}(\alpha)$ *concern,* the suppression of the Z couplings is due to the factor $M_Z^2/M_{\rm KK}^2$ presented in Eq. (3.33). For all these couplings the custodial symmetry P_{LR} is not effective, since the right handed down quarks are not eigenvalues of the symmetry P_{LR}.

- *As far as* $\Delta_{L,R}^{\nu\nu,\ell\ell}(i)$ *concern,* in contrast to Z_H and Z', the Z boson exhibits SM couplings and hence it is expected to dominate over Z_H and Z', that have couplings that are suppressed by overlap integrals[11].

In addition to the several couplings, we have also to keep into account the mass of the particle exchanged in the process. Assuming that the neutral gauge bosons Z_H and Z'

[11] The results in (4.120) are obtained using a bulk mass parameter for neutrinos and leptons equal to ± 0.7 (for left handed and right handed particles respectively). This assumption is in fact motivated by the lightness of the leptons and consequently by their localization towards the UV brane (see also Sec. 5.1.1 for a more detailed discussion).

are degenerate in mass (see also Appendix A), their contribution to rare K and B decays is suppressed by a factor $M_Z^2/M_{\rm KK}^2 \sim \mathcal{O}(10^{-3})$ with respect to the Z contribution.

Now we have all the building blocks to investigate which is the main contribution to the decays in question. Analyzing all the several orders of magnitude in (4.118)-(4.120) and the suppression given by propagator of the gauge boson exchanged, it turns out that the main contribution can come either from the couplings $\Delta_L^{ij}(Z_H)$, that are of the same magnitude of the couplings $\Delta_L^{ij}(Z)$, or from the couplings $\Delta_R^{ij}(Z)$. However we know that, due to the custodial protection and the particular structure of the model, the Z boson couples much more strongly to right handed than to left handed down quarks, $\Delta_R^{ij}(Z) \gg \Delta_L^{ij}(Z)$.

Thus, the main message from our semi-analytic analysis is the following:

> *If the new effects in rare K and B decays are significant, they are dominantly caused by the Z boson coupled to right handed down quarks.*

K physics vs B physics in the RS model

Up to now we have not distinguished between the B and the K system. Now we aim to predict, starting from the flavor structure of the model, the average relative size of NP contributions in the K and B systems and also possible correlations between the NP contributions in the two systems. As the tree level Z contributions turn out to be dominant, from now on we restrict our discussion only to these contributions, if not differently specified.

Having a closer look at the NP contributions $\left((X^i, Y^i, Z^i)^{V-A,V}\right)_{\rm KK}$,$(i = K, d, s)$ listed in (4.65)-(4.66) and in (4.91)-(4.94), we observe that the possible size of NP effects are proportional to the factors

$$\frac{1}{\lambda_t^{(K)}} \sim 2500\,, \quad \frac{1}{\lambda_t^{(d)}} \sim 100\,, \quad \frac{1}{\lambda_t^{(s)}} \sim 25\,, \tag{4.121}$$

for the K, B_d and B_s system, respectively. Therefore, we would naively expect the deviation from the SM functions in the K system to be by an order of magnitude larger than in the B_d system, and even by a larger factor than in the B_s system. However this strong hierarchy in the factors $1/\lambda_t^{(i)}$ is partially compensated by the opposite hierarchy in $\Delta_R^{ij}(Z)$, due to the fact that the third generation quarks is localized closer to the IR brane than the first two generations. Numerically we find as an average on a large number of parameter sets[12]

$$\Delta_R^{sd}(Z) : \Delta_R^{bd}(Z) : \Delta_R^{bs}(Z) \sim 1 : 6 : 9\,. \tag{4.122}$$

Thus, we can conclude that the size of the NP contributions on average drops by a factor of four when going from the K to the B_d system and by another factor of two when going from the B_d to the B_s system.

[12]The parameter sets we are using fit quark masses and mixings, in addition to all the well measured $\Delta F = 2$ observables.

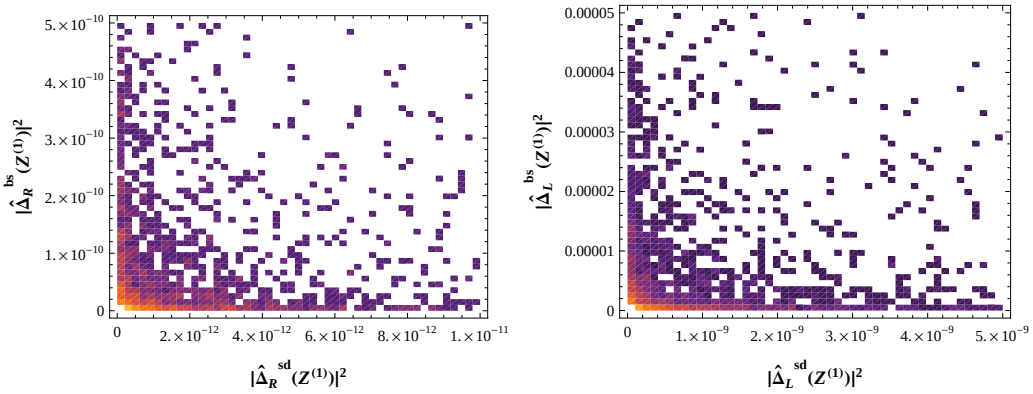

Figure 4.10: Absolute squares of the couplings of the first excitation of the Z boson ($Z^{(1)}$) with quarks down-strange and bottom-strange. In the right panel the right handed couplings are shown, in the left panel the left handed. Lighter colors correspond to higher density of points.

It is of interest to investigate this issue in the case of absence of the custodial protection P_{LR}. Following the same arguments as before, it is easy to find that the left handed Z couplings to down quarks would yield the dominant contribution to tree level rare decays. In addition, using our parameter sets[13] we discover that these couplings exhibit roughly the opposite hierarchies than the ones shown by the CKM elements in (4.121)

$$\Delta_L^{sd}(Z) : \Delta_L^{bd}(Z) : \Delta_L^{bs}(Z) \sim 1 : 30 : 130\,. \tag{4.123}$$

Hence in the RS model without custodial protection we expect the relative NP effects in the K and B rare decays to be roughly of the same size. This is a clear feature that distinguishes the RS model with custodial protection from the model without protection. It will be also confirmed by our numerical analysis in Sec. 5.3.3.

Anticorrelation between different couplings

At present, we have always analyzed the absolute size of the several contributions to rare K and B decays. However, it is relevant also to investigate the relative contributions, namely to examine if several contributions are correlated and in which way. As an example, in Fig. 4.10 we present in two density plots the correlation between different elements of the coupling of the first excitation of the Z boson ($Z^{(1)}$) with left handed and right handed down type quarks: $\hat{\Delta}_R^{sd}(Z^{(1)})$ vs. $\hat{\Delta}_R^{bs}(Z^{(1)})$ (in the right panel) and $\hat{\Delta}_L^{sd}(Z^{(1)})$ vs. $\hat{\Delta}_L^{bs}(Z^{(1)})$ (in the left panel). The figure shows clearly that typically the off-diagonal couplings cannot be simultaneously large. We have investigated and we have found that this feature is totally general, since it is valid also for the KK gauge boson $Z_X^{(1)}$ couplings.

[13] One should note that removing the protection also modifies the predictions for the $\Delta F = 2$ observables, so that the points from our parameter scan do in general not fulfil the associated constraints any more. On the other hand we have seen that the most severe constraint comes from ε_K, which is dominated by KK gluon contributions and thus insensitive to the precise structure of the EW sector. Consequently we do not expect our results to be affected significantly by this simplified working assumption.

This general characteristic of the flavor violating couplings derives from the definition of the couplings in Eq. (3.36) (and the corresponding ones for the right handed quarks). In fact, those expressions imply an upper bound on the sum of off-diagonal terms $|\hat{\Delta}_{L,R}|^2_{21} + |\hat{\Delta}_{L,R}|^2_{31} + |\hat{\Delta}_{L,R}|^2_{32}$ [191]. Hence, typically, two off-diagonal couplings cannot be simultaneously large, as shown by our Fig. 4.10.

This is an important message, since it implies that whenever we find large NP contributions in K physics we cannot have large NP contributions in B physics and vice versa. This feature will be confirmed by our numerical analysis in Sec. 5.3.

4.2.10 Status of the measurements and comparison with the Standard Model

Differently from the $\Delta F = 2$ observables analyzed in Sec. 4.1.6, the branching ratios of the several rare decays analyzed in this thesis are not well measured (most of them are indeed not measured at all). Contrary, from a theoretical point of view, in the SM the branching ratios are accurately predicted[14] and, since they are based on higher order electroweak effects, they are expected to be very small. Consequently, from a theoretical point of view, rare decays of K and B mesons have still a largely open room for NP; from an experimental point of view, an improvement on the measurements of the several branching ratios would be an efficient test of the SM and of the several theories beyond it.

In recent years, many experiments have been performed to precisely measure many Kaon decay parameters. Lifetimes and charge asymmetries have been measured with unprecedented accuracy for K_L and K^+. However, concerning the very rare $K^+ \to \pi^+\nu\bar{\nu}$ and $K_L \to \pi^0\nu\bar{\nu}$ decay modes, only for the charged mode seven candidate events have been found by the E949 [192] experiment at the Alternating Gradient Synchrotron (AGS) of the Brookhaven National Laboratory, implying

$$\mathrm{Br}(K^+ \to \pi^+\nu\bar{\nu})_{\mathrm{exp}} = (1.73^{+1.15}_{-1.05}) \cdot 10^{-10} \,. \tag{4.124}$$

Contrary, for the decay $K_L \to \pi^0\nu\bar{\nu}$ only a very loose upper bound exists. The present bound from E391a at KEK [193] is given by

$$\mathrm{Br}(K_L \to \pi^0\nu\bar{\nu})_{\mathrm{exp}} < 2.6 \cdot 10^{-8} \,, \tag{4.125}$$

that is still larger than the limit of $\mathrm{Br}(K_L \to \pi^0\nu\bar{\nu}) < 12.4 \cdot 10^{-10}$ at 90% CL, arising from the model-independent Grossman-Nir (GN) bound [194]

$$\mathrm{Br}(K_L \to \pi^0\nu\bar{\nu}) < 4.3\, \mathrm{Br}(K^+ \to \pi^+\nu\bar{\nu}) \,. \tag{4.126}$$

The situation of the Standard Model prediction is radically different. The accuracy of the SM prediction for $K_L \to \pi^0\nu\bar{\nu}$ and $K^+ \to \pi^+\nu\bar{\nu}$ has been improved considerably during the last five years. This progress can be traced back mainly to the improved values

[14] For the $K_L \to \mu^+\mu^-$, as already discussed, only the SD contributions are computed precisely in the SM.

of m_t and of $|V_{cb}|$ and to some extent to the inclusion of NLO QCD corrections. In particular we have [176, 195]

$$\begin{aligned} \mathrm{Br}(K_L \to \pi^0 \nu\bar{\nu})_{\mathrm{SM}} &= (2.8 \pm 0.6) \cdot 10^{-11}\,, & (4.127)\\ \mathrm{Br}(K^+ \to \pi^+ \nu\bar{\nu})_{\mathrm{SM}} &= (8.5 \pm 0.7) \cdot 10^{-11}\,. & (4.128) \end{aligned}$$

From these numbers, it is evident that the SM prediction for the K^+ decay is consistent with the experiments and, on the contrary, the prediction for the K_L decay is still far below the experimental results.

Future experiments plan to improve the measurements of the decays $K \to \pi\nu\bar{\nu}$. In particular the NA62 experiment at CERN SPS (see e.g., [196]) has been proposed with the purpose to measure the branching ratio for the rare decay $K^+ \to \pi^+\nu\bar{\nu}$ with a statistical precision of less than 10%. Studies of the K^+ decay are also planned at the J-Parc experiment which has the goal to collect more than 50 $K^+ \to \pi^+\nu\bar{\nu}$ events from K^+ decays at rest [197]. Still at J-Parc, the experiment K0TO is a dedicated experiment to search for the CP violating rare decay mode $K_L \to \pi^0\nu\bar{\nu}$ that also Project-X at Fermilab plans to measure.

Concerning the rare B decays, the situation is quite similar. Up to today there are only experimental upper bounds on the two modes $B_{s,d} \to \mu^+\mu^-$ by CDF [198] and D0 [199] (in parenthesis)[15]

$$\begin{aligned} \mathrm{Br}(B_s \to \mu^+\mu^-)_{\mathrm{exp}} &< 3.3\,(5.3) \cdot 10^{-8}\,, & (4.129)\\ \mathrm{Br}(B_s \to \mu^+\mu^-)_{\mathrm{exp}} &< 1 \cdot 10^{-8}\,, & (4.130) \end{aligned}$$

which are still more than a factor of 10 larger than the respective SM predictions [201][16]

$$\begin{aligned} \mathrm{Br}(B_s \to \mu^+\mu^-)_{\mathrm{SM}} &= (3.2 \pm 0.2) \cdot 10^{-9}\,, & (4.131)\\ \mathrm{Br}(B_d \to \mu^+\mu^-)_{\mathrm{SM}} &= (1.0 \pm 0.1) \cdot 10^{-10}\,. & (4.132) \end{aligned}$$

Searches for $B_s \to \mu^+\mu^-$ are only carried out at hadron machines, whereas $B_d \to \mu^+\mu^-$ is being searched for at the B-factories as well, even if the measurements are no longer competitive with the Tevatron results. The decay $B_s \to \mu^+\mu^-$ is one of the most promising channels for New Physics at LHCb. This experiment will be able to exclude branching ratios above the SM level, with just $2\mathrm{fb}^{-1}$ of data corresponding to one nominal year of data taking. Instead, a 5σ discovery at the SM level will require several years of data taking, since it is only possible after $10\mathrm{fb}^{-1}$ [202].

[15] The numbers given above are updates presented at the EPS-HEP09 conference. More information is given in [200] .

[16] We report here the most updated result for the SM prediction for the two branching ratios. However, to be consistent with the table of input parameters we give for our numerical analysis (Tab. 5.2), we should quote [90] $\mathrm{Br}(B_s \to \mu^+\mu^-) = (3.6 \pm 0.37)10^{-9}$, $\mathrm{Br}(B_s \to \mu^+\mu^-) = (1.08 \pm 0.11) \cdot 10^{-10}$.

LHCb will also perform studies of the decay $B_d \to \mu^+\mu^-$, even if it is not clear yet if it will have the capacity to reach the SM expectation for the branching ratio, that is around one order of magnitude smaller than the one of $B_s \to \mu^+\mu^-$.

Finally, there are several experiments which have measured the rare decay $K_L \to \mu^+\mu^-$, as for example BNL791 [203] and KEK137 [204]. The world average is given by [169]

$$\mathrm{Br}(K_L \to \mu^+\mu^-)_{\mathrm{exp}} = (6.84 \pm 0.11) \cdot 10^{-9} \,. \tag{4.133}$$

More problematic is the comparison between the SM prediction (for the short-distance contribution) and the experiment. In fact, as already discussed, the decay is dominated by the contributions from the two-photon intermediate state (absorbitive part) which are difficult to calculate reliably. Consequently the SD contribution constitutes only a small fraction of the branching ratio. The most recent estimate of the short-distance contribution extracted from the data gives [205]

$$\mathrm{Br}(K_L \to \mu^+\mu^-)^{\mathrm{SD}}_{\mathrm{exp}} < 2.5 \cdot 10^{-9} \,, \tag{4.134}$$

that one should compare with the short-distance contribution computed in the SM. At the NNLO of QCD we have [190]

$$\mathrm{Br}(K_L \to \mu^+\mu^-)^{\mathrm{SD}}_{\mathrm{SM}} = (0.79 \pm 0.12) \cdot 10^{-9} \,. \tag{4.135}$$

We conclude the section with a table which summarizes the present status of the SM predictions and of the measurements of the several K and B rare decay branching ratios presented in this thesis.

Decay	Experiment	SM prediction	Future
$K_L \to \pi^0\nu\bar{\nu}$	$< 2.6 \cdot 10^{-8}$ [193]	$(2.8 \pm 0.60) \cdot 10^{-11}$ [176]	J-Parc, Project-X
$K^+ \to \pi^+\nu\bar{\nu}$	$(1.73^{+1.15}_{-1.05}) \cdot 10^{-10}$ [192]	$(8.5 \pm 0.7) \cdot 10^{-11}$ [195]	NA62, J-Parc
$(K_L \to \mu^+\mu^-)_{\mathrm{SD}}$	$< 2.5 \cdot 10^{-9}$ [205]	$(0.79 \pm 0.12) \cdot 10^{-9}$ [190]	
$B_s \to \mu^+\mu^-$	$< 3.3\,(5.3) \cdot 10^{-8}$ [198, 199]	$(3.2 \pm 0.2) \cdot 10^{-9}$ [201]	LHCb
$B_d \to \mu^+\mu^-$	$< 1 \cdot 10^{-8}$ [198]	$(1.0 \pm 0.1) \cdot 10^{-10}$ [201]	LHCb

Table 4.6: Experimental values and SM predictions for the rare K and B decays analyzed in this thesis. Additionally the last column shows which are the experiments, if any, from which we can expect an improvement in the measurement of the several branching ratios in the coming years. Note: for the SD contribution to the $K_L \to \mu^+\mu^-$ decay we do not have direct experimental access. In the table we put the result of the most recent estimate of the extraction of the SD part from the data [190].

Chapter 5

Numerical analysis

After the discussion of the flavor sector of the RS model and of the two Susy flavor models, and after the analysis of the several flavor observables of the K and B meson mixing systems and of the branching ratios of the rare decays of K and B mesons, we can now perform a global numerical analysis of particle-antiparticle oscillations and rare K and B decays. The main focus will be on the comparison of the three models and on the discussion of the possibility to distinguish them, through the measurement of few flavor observables at upcoming experiments, and in particular at the LHCb. Particular attention will be given to the theoretical understanding of our numerical results, pointing out the main theoretical features of the models which lead to the numerical results.

5.1 Preliminaries

In this section, we summarize how the numerical analysis has been performed. For the RS model, the strategy for the analysis has been developed in [59] (for the $\Delta F = 2$ transitions) and in [173] (for the $\Delta F = 1$ transitions). For the Susy flavor models instead, we refer the reader to [90].

5.1.1 Numerical strategy for the RS model

As we have already discussed in Sec. 2.2.2, the custodial symmetry of the RS model allows consistency with EWPT for masses of the lightest KK states as low a $(2-3)$ TeV, with only moderate constraints on the fermion bulk mass parameters c's. Therefore, throughout our numerical analysis, we set

$$f = 1\,\text{TeV} \quad \Longleftrightarrow \quad M_{\text{KK}} \sim 2.45\,\text{TeV}\,, \tag{5.1}$$

in such a way that the first KK modes of fermions and gauge bosons could be in principle detectable via direct searches at the LHC.

This terminates the discussion of the only free parameter coming from the geometry. The discussion of the constraints on the bulk masses c's is more involved. First of all, we have to remind the number of free parameters coming from the flavor sector (see also [51]).

First, the 3×3 complex 5D Yukawa coupling matrices introduced in (2.44)

$$\lambda^u\,, \qquad \lambda^d \tag{5.2}$$

contain each 9 real parameters and 9 complex phases. This is precisely the case of the SM. New flavor parameters enter through the three hermitian 3×3 bulk mass matrices

$$c_Q\,, \qquad c_u\,, \qquad c_d\,, \tag{5.3}$$

which bring in additional 18 real parameters and 9 complex phases. Altogether this counting leads to 36 real parameters and 27 complex phases. However, not all of them are physical: some can be eliminated thanks to the quark flavor symmetry $U(3)^3$ which, as in the SM (see Sec. 3.2.2), exists in the limit of vanishing $\lambda^{u,d}$ and $c_{Q,u,d}$. 9 real parameters and 17 phases can be eliminated by making use of this symmetry. One phase cannot in fact be removed as it corresponds to the unbroken $U(1)_B$ baryon number. We are then left with 27 real parameters and 10 complex phases: 18 real parameters and 9 phases in addition to the free parameters of the SM in the quark sector.

In our numerical analysis it will be convenient to work in the special basis in which the bulk mass matrices $c_{Q,u,d}$ are diagonal and real and thus comprise only 9 real parameters. The remaining 18 real parameters and 10 physical phases are then collected in the 5D Yukawa coupling matrices λ^u and λ^d. It will be essential to have an efficient parameterization of $\lambda^{u,d}$ in terms of only these physical parameters.

A useful parameterization of $\boldsymbol{\lambda^{u,d}}$

The 5D Yukawa matrices, as every complex 3×3 matrix, can always be singular value decomposed as

$$\lambda^u = e^{i\phi_u} U_u^\dagger D_u V_u\,, \qquad \lambda^d = e^{i\phi_d} U_d D_d V_d\,, \tag{5.4}$$

where the $D_{u,d}$ are real and diagonal and the $U_{u,d}, V_{u,d} \in SU(3)$.

At this stage the decompositions in (5.4) contain each $(0,1) + (3,5) + (3,0) + (3,5) = (9,11)$ parameters, corresponding to 9 real parameters and 11 phases. Two of those phases are of course spurious, since a complex 3×3 matrix is described by $(9,9)$ parameters. In order to find a description in terms of physical parameters only we use the Euler decomposition for $SU(3)$ matrices [206]

$$U(\alpha, a, \gamma, c, \beta, b, \theta, \phi) = e^{i\lambda_3\alpha} e^{i\lambda_2 a} e^{i\lambda_3\gamma} e^{i\lambda_5 c} e^{i\lambda_3\beta} e^{i\lambda_2 b} e^{i\lambda_3\theta} e^{i\lambda_8\phi}\,, \tag{5.5}$$

where λ_i $(i = 1, ..., 8)$ are the Gell-Mann matrices. Additionally a, b, c are real mixing angles and $\alpha, \gamma, \beta, \theta, \phi$ are phases. As we will show in the following, the parameters appearing in this last decomposition are all physical.

In the basis in which $c_{Q,d,u}$ are diagonal and real we have the freedom to make the following diagonal rephasing

$$Q_L \;\to\; e^{i\lambda_3\alpha_{U_d}} e^{-i\lambda_8\phi_{U_u}} Q_L\,, \tag{5.6}$$

$$u_R \;\to\; e^{-i\phi_u} e^{-i\lambda_3\theta_{V_u}} e^{-i\lambda_8\phi_{V_u}} u_R\,, \tag{5.7}$$

$$d_R \;\to\; e^{-i\phi_d} e^{-i\lambda_3\theta_{V_d}} e^{-i\lambda_8\phi_{V_d}} d_R. \tag{5.8}$$

Additionally, the unitary matrices U, V in a singular value decomposition are defined up to an internal diagonal rephasing

$$UDV = (Ue^{i\lambda_3 A + i\lambda_8 B})D(e^{-i\lambda_3 A - i\lambda_8 B}V) = U'DV' \,. \tag{5.9}$$

Using this freedom and an additional rephasing of the quark fields we find the equivalence

$$\begin{aligned} \lambda^u &= U_u^\dagger(0, a_{U_u}, \gamma_{U_u}, c_{U_u}, \beta_{U_u}, b_{U_u}, \theta_{U_u}, 0)\, D_u\, V_u(\alpha_{V_u}, a_{V_u}, \gamma_{V_u}, c_{V_u}, \beta_{V_u}, b_{V_u}, 0, 0) \\ &= U_u^\dagger(0, a_{U_u}, \gamma_{U_u} + r, c_{U_u}, \beta_{U_u} - r, b_{U_u}, \theta_{U_u}, r/\sqrt{3})\, D_u \\ &\qquad V_u(\alpha_{V_u}, a_{V_u}, \gamma_{V_u} + r, c_{V_u}, \beta_{V_u} - r, b_{V_u}, 0, r/\sqrt{3}) \,. \end{aligned} \tag{5.10}$$

The entries $r/\sqrt{3}$ can be again rotated to zero due to the freedom to rephase the quark zero modes. Using this invariance parameterized by r allows us to choose $\gamma_{U_u} = 0$. We can finally define λ^u and λ^d in terms of physical parameters only

$$\lambda^u = U_u^\dagger(0, a_{U_u}, 0, c_{U_u}, \beta_{U_u}, b_{U_u}, \theta_{U_u}, 0)\, D_u\, V_u(\alpha_{V_u}, a_{V_u}, \gamma_{V_u}, c_{V_u}, \beta_{V_u}, b_{V_u}, 0, 0) \,, \tag{5.11}$$

$$\lambda^d = U_d(0, a_{U_d}, \gamma_{U_d}, c_{U_d}, \beta_{U_d}, b_{U_d}, 0, 0)\, D_d\, V_d(\alpha_{V_d}, a_{V_d}, \gamma_{V_d}, c_{V_d}, \beta_{V_d}, b_{V_d}, 0, 0) \,, \tag{5.12}$$

with $D_u = \mathrm{diag}(y_u^1, y_u^2, y_u^3)$ and $D_d = \mathrm{diag}(y_d^1, y_d^2, y_d^3)$. Altogether we find 18 real parameters and 10 physical phases contained in the 5D Yukawas, as already discussed previously.

The parameter scan

The starting point of our numerical analysis is the generation of random 5D Yukawa coupling matrices $\lambda^{u,d}$. The first requirement one has to satisfy is the requirement of perturbativity which forbids the Yukawa couplings $\lambda^{u,d}$ to be arbitrary large (see for example [51, 120, 207]). Imposing that the one loop contribution to the Yukawa couplings with loop momenta cut off at energies as large as the mass of the n-th KK mode is smaller than the tree level term brings the constraint $\langle\lambda^{u,d}\rangle \leq 2\pi/N$, where $\langle\lambda^{u,d}\rangle$ is the typical size of the 5D Yukawas $\lambda^{u,d}$. Hence the loosest constraint we can obtain (for $N = 2$) is given by $\langle\lambda^{u,d}\rangle \lesssim 3$. Consequently, we will perform our scan on

$$0 \leq y_{u,d}^i \leq 3 \qquad (i = 1, 2, 3) \,, \tag{5.13}$$

pursuing hence the idea of completely anarchical and of $\mathcal{O}(1)$ 5D Yukawa couplings.

Additionally, the real mixing angles

$$a_{U_u}, c_{U_u}, b_{U_u}, a_{V_u}, c_{V_u}, b_{V_u}, a_{U_d}, c_{U_d}, b_{U_d}, a_{V_d}, c_{V_d}, b_{V_d} \,, \tag{5.14}$$

and the CP violating phases

$$\beta_{U_u}, \theta_{U_u}, \alpha_{V_u}, \gamma_{V_u}, \beta_{V_u}, \gamma_{U_d}, \beta_{U_d}, \alpha_{V_d}, \gamma_{V_d}, \beta_{V_d}, \tag{5.15}$$

will be varied in their physical ranges given by $[0, \pi/2)$ and $[0, 2\pi)$, respectively. This completes the discussion of the free parameters appearing in the 5D Yukawas $\lambda^{u,d}$, parametrized as in (5.11)-(5.12).

Finally, we have also to discuss the range allowed for the bulk masses c's. Putting together constraints from the electroweak parameters (in particular T) and from perturbativity of the theory, one can find that [64, 76] the bulk mass c_Q^3 has to be close to the conformal point $c_Q^3 \lesssim 0.5$ and that the right handed top quark bulk mass c_u^3 has to be strongly localized towards the IR brane $c_u^3 \gtrsim 0$. For this reason, throughout all the numerical analysis, we will scan in the ranges[1]

$$0.4 \leq c_Q^3 \leq 0.5\,, \qquad c_u^3 \geq 0\,. \tag{5.16}$$

The remaining bulk mass parameters will then be fitted, imposing the constraints coming from quark masses and CKM parameters, listed in Tabs. 5.1, 5.2 at the 2σ level. One should also mention here that, in order not to depend on unphysical phases at this stage, we choose to fit the Jarlskog determinant [208]

$$J_{\rm CP} = {\rm Im}(V_{ud}V_{cs}V_{us}^*V_{cd}^*) \tag{5.17}$$

rather than the CKM angle $\gamma = \arg(V_{ub})$.

For those parameter points that reproduce the SM quark masses and mixing angles we subsequently evaluate the $\Delta F = 2$ observables discussed in Sec. 4.1 and finally the branching ratios of K and B decays analyzed in Sec. 4.2. All the numerical analysis is performed neglecting the mixing between the SM fermion and the KK excitations, analyzed in Sec. 3.1.

	$\mu = 2\,\text{GeV}$	$\mu = 4.6\,\text{GeV}$	$\mu = 172\,\text{GeV}$	$\mu = 3\,\text{TeV}$
$m_u(\mu)$	3.0(10) MeV	2.5(8) MeV	1.6(5) MeV	1.4(5) MeV
$m_d(\mu)$	6.0(15) MeV	4.9(12) MeV	3.2(8) MeV	2.7(7) MeV
$m_s(\mu)$	110(15) MeV	90(12) MeV	60(8) MeV	50(7) MeV
$m_c(\mu)$	1.04(8) GeV	0.85(7) GeV	0.55(4) GeV	0.45(4) GeV
$m_b(\mu)$	—	4.2(1) GeV	2.7(1) GeV	2.2(1) GeV
$m_t(\mu)$	—	—	162(2) GeV	135(2) GeV

Table 5.1: Renormalized quark masses at various scales, evaluated using NLO running. The 1σ uncertainties are given in brackets.

The lepton and the gauge sector

The discussion of the free parameters of the lepton sector is quite less involved than what we have just shown for the quark sector. In fact, for our scopes it is sufficient to neglect the mixings between the several leptons, so that lepton flavor eigenstates coincide with the mass eigenstates and hence to neglect the effects of lepton flavor changing neutral currents. We thus consider degenerate bulk masses for all the SM leptons. Since leptons are significantly lighter than quarks, we have to choose them to be localized towards the UV brane and in our numerical analysis we simply set all the bulk mass parameters

[1] One should mention that this particular range for c_Q^3 and c_u^3 is only viable because of the protection of the Z couplings to the right handed up quarks from large corrections. A localization of the right handed top quark so close to the IR brane would be disastrous in the RS model without custodial protection.

to $c^\ell_\psi = \pm 0.7$ for left and right handed leptons, respectively. This assumption is well motivated by the observation that the flavor conserving couplings of leptons with gauge bosons depend only very weakly on the actual value of c^ℓ_ψ, provided that $c^\ell_\psi > 0.5$. Hence we consider safe not to scan on the parameter c^ℓ_ψ.

The discussion of the free parameters coming from the neutrino sector proceeds on the same lines. Also for (left handed) neutrinos, we simply fix a universal bulk mass given by $c^\nu_\psi = 0.7$.

Also the gauge sector does not show any new free parameter. In fact, in the absence of brane kinetic terms, the 5D EW gauge couplings g and g_X presented first in Sec. 2.2.3 are not dimensionless and are related to the measured 4D couplings as $g_i = \sqrt{L} g_i^{4D}$. The same discussion holds also for the strong 5D coupling g_s that, in the absence of brane kinetic terms, gets the value $g_s = \sqrt{L} g_s^{4D}$. For a discussion of the impact of brane kinetic terms on the gauge couplings and on flavor observables we refer the reader to [59, 120].

parameter	value	parameter	value
$\hat{B}_K$	$0.724 \pm 0.008 \pm 0.028$ [153]	$\alpha_s(M_Z)$	0.118 ± 0.002
F_{B_s}	(245 ± 25) MeV [154]	$\alpha_{\rm em}(M_Z)$	$1/127.9$
F_{B_d}	(200 ± 20) MeV [154]	η_1	1.44 ± 0.35 [141, 209]
F_K	(156.1 ± 0.8) MeV [210]	η_2	0.57 ± 0.01 [142]
$\hat{B}_{B_d}$	1.22 ± 0.12 [154]	η_3	0.47 ± 0.05 [143, 209, 211]
$\hat{B}_{B_s}$	1.22 ± 0.12 [154]	η_B	0.55 ± 0.01 [142, 212]
$F_{Bs}\sqrt{\hat{B}_{Bs}}$	(270 ± 30) MeV [154]	λ	0.2258 ± 0.0014 [213]
$F_{B_d}\sqrt{\hat{B}_{B_d}}$	(225 ± 25) MeV [154]	ξ	1.21 ± 0.04 [154]
V_{cb}	$(41.2 \pm 1.1) \times 10^{-3}$ [169]	$\lvert V_{ub}\rvert$	$(3.8 \pm 0.4) \times 10^{-3}$ [169]

Table 5.2: Input parameters used in the numerical analysis. Note: the input parameters listed here are those used in the chronologically last paper reviewed in this thesis [90] and hence they are slightly different than those used in our papers on the RS model [59, 110, 173].

5.1.2 Numerical strategy for the Susy flavor models

As we have already discussed in Sec. 2.3.3, the MSSM has in the flavor sector a very large number of free parameters, in addition to those already present in the SM: 110. Only in the quark sector we have to number 45 real parameters and 19 phases. Obviously the risk of such a huge parameter space is the weakening of the predictive power of the theory. However, as we will show in our numerical analysis of Secs. 5.2.4, 5.2.5, 5.3.4, the adoption of an "MSUGRA like" spectrum (see Sec. 2.3.3) and of the soft parameters predicted by the two Susy flavor models reduces considerably the number of free parameters of the theory and hence increases strongly its predictive power.

Let us then introduce the free parameters of the two Susy flavor models analyzed. First of all, the MSSM with the MSUGRA hypothesis contains (assuming vanishing flavor blind

phases) five parameters: $m_{1/2}$, m_0, A_0, $\tan\beta$ and the sign of μ. However, a positive μ is preferred by the muon anomalous magnetic moment constraints [14,214,215] and hence, in our numerical analysis we will simply assume $\mu > 0$. Consequently only four parameters are left.

Moreover, the flavor models do not predict the exact value of the off-diagonal soft masses and trilinear terms, but only their order of magnitude, as function of one (AC abelian flavor model, Sec. 2.3.4) or more (RVV2 non abelian flavor model, Sec. 2.3.5) expansion parameters. Consequently, we have as free parameters also the several $\mathcal{O}(1)$ real coefficients multiplying the off-diagonal entries of the soft masses and trilinear terms in (2.65)-(2.66) and (2.69)-(2.75) for the abelian and the non abelian model, respectively. Additionally, in the abelian model (Sec. 2.3.4) it appears also an undetermined phase (ϕ_R) on which we have to scan (see below for the range).

Finally a few words concerning the diagonal entries of soft masses and trilinear terms. In principle, for each 3×3 matrix we would have three independent free parameters on the diagonal of order m_0 (for the soft masses) and A_0 (for the trilinear terms). The abelian and non abelian models show a quite opposite behavior:

- *Abelian Model:* the $U(1)$ flavor symmetry does not imply any pattern for the diagonal entries. The diagonal soft masses are hence naturally split. Consequently, in our numerical analysis, we impose a large mass splitting between the first and the second generation squarks, such that at the GUT scale $m_{\tilde{u}_L} = 2m_{\tilde{c}_L} = 2m_{\tilde{t}_L} = 2m_0$. Additionally we simply assume a common mass scale A_0 in the diagonal trilinear terms.

- *Non abelian Model:* the $SU(3)$ flavor symmetry implies an approximate degeneracy of the three generation squarks. Hence, we simply assume to have an exact degeneracy both in the diagonal soft masses ($= m_0$) and in the diagonal trilinear terms ($= A_0$).

The parameter scan

Having listed the several parameters of the two Susy flavor models, we are now in the position to explain the type of parameter scan we have performed.

First of all, concerning the "MSUGRA parameters", we scan in the following ranges

$$m_0 < 2\,\text{TeV}\,, \quad m_{1/2} < 1\,\text{TeV}\,, \quad |A_0| < 3m_0\,, \quad 5 < \tan\beta < 55\,. \tag{5.18}$$

This particular choice was dictated by the requirement of a not too heavy sparticle spectrum (and hence the upper bound on m_0 and $m_{1/2}$) and by the requirement of vacuum stability (and hence the upper bound on A_0 as a function of m_0). The discussion of the technical details on the bound on the trilinear mass scale A_0 goes beyond the scope of this thesis: see e.g., [216].

Secondly, we scan over the several $\mathcal{O}(1)$ coefficients multiplying the off-diagonal entries of soft masses and trilinear terms, independently, in the range $\pm[0.5, 2]$. Additionally, the undetermined phase ϕ_R appearing in the soft mass matrix δ_d^{RR} of the abelian model (Eq. (2.65)) is varied in the range $[0, 2\pi)$.

We impose then several constraints coming from the experiments:

1. Requirement of a correct electroweak symmetry breaking and vacuum stability;
2. Lower bounds on sparticle masses, coming from direct Susy searches;
3. Agreement with the experiments on electroweak precision observables.
4. Requirement of a neutral lightest Susy particle (i.e. requirement of a dark matter candidate).

For those parameter points that satisfy these four requirements we subsequently evaluate exactly (i.e. not making use of the MIA) the $\Delta F = 2$ observables discussed in Sec. 4.1 and we impose the corresponding bounds listed in Tab. 4.5. We impose then the additional constraints listed in Tab. 5.3 (like $\mathrm{Br}(b \to s\gamma)$, $\mathrm{Br}(B \to \tau\nu)$) and we finally compute the branching ratios of K and B decays analyzed in Sec. 4.2.

5.2 K and B meson oscillation

In this section we will analyze the K and B meson mixing observables first in the RS model with custodial protection, and secondly in the two Susy flavor models. In particular, for both frameworks, we will investigate how strict are the constraints coming from all the several observables, but $S_{\psi\phi}$. Subsequently, once that the constraints are imposed, we analyze the possibility to have large new physics contributions in the phase of the $B_s^0 - \bar{B}_s^0$ system, $S_{\psi\phi}$.

The approach to the analysis is a bit different in the two frameworks: in contrast to the Susy flavor models, in the RS model we study also the fine-tuning required to fit the several observables (see Eq. (5.19) for the definition of fine-tuning).

5.2.1 The ε_K constraint in the RS model

Our analysis of the KK contributions to M_{12}^K of Sec. 4.1.3 already raised the problem of reconcilability of ε_K with the experimental data which agree with the SM value, within uncertainties (see Tab. 4.5). From the left panel of Fig. 4.2 we could already conclude that generically ε_K is more than two orders of magnitude too large. However, from that panel, we could also notice that quite few points of parameter space are able to arrange a value for ε_K in agreement with the experiments.

The issue we want now to analyze is *how large fine-tuning we have to introduce in the model in order to fit the experimental* ε_K. To this end we will use the measure of fine-tuning introduced by Barbieri and Giudice [217] and most commonly used in the literature: the amount of tuning $\Delta_{\mathrm{BG}}(O_i, p_j)$ in an observable O_i with respect to a parameter p_j is defined as the sensitivity of O_i to infinitesimal variations of p_j. Explicitly,

$$\Delta_{\mathrm{BG}}(O_i, p_j) = \left| \frac{p_j}{O_i} \frac{\partial O_i}{\partial p_j} \right| , \tag{5.19}$$

where the normalization factor p_j/O_i appears in order not to have a fine-tuning sensitive to the absolute size of p_j and O_i. The overall fine-tuning in the observable O_i which

depends on m parameters p_j is then given by

$$\Delta_{\rm BG}(O_i) = \max_{j=1,\ldots,m}\{\Delta_{\rm BG}(O_i, p_j)\}\,, \tag{5.20}$$

where the index j runs over all m dimensions of parameter space. Obviously, the larger $\Delta_{\rm BG}(O_i)$, the more sensitive is the value of O_i to small variations in the parameters p_j, i. e. the more fine-tuning is required to keep O_i stable.

In the left panel of Fig. 5.1 we show in a density plot the fine-tuning in ε_K as a function of ε_K normalized to its experimental value. We observe that, while for generic values $\varepsilon_K/(\varepsilon_K)_{\rm exp} \sim \mathcal{O}(100)$ the fine-tuning is typically relatively small, $\Delta_{\rm BG}(\varepsilon_K) \sim 20$, the average required tuning (blue line in the plot) strongly increases with decreasing values of ε_K. Generically for $\varepsilon_K \sim (\varepsilon_K)_{\rm exp}$ a fine-tuning of the order $\Delta_{\rm BG}(\varepsilon_K) \sim 700$ is required, i.e. the amount of fine-tuning increases by roughly a factor $30 - 40$ when going from the generic prediction for ε_K down to values in accordance with the experiments. This high level of average fine-tuning required to fit the experimental ε_K shows the "ε_K problem" of the RS model. Obviously, despite this generic trend, there are areas in parameter space for which ε_K roughly reproduces the experimental value and the required tuning is moderate ($\Delta_{\rm BG}(\varepsilon_K) \lesssim 20$). In particular, for SM-like ε_K roughly 30% of the points lie still in the range with small tuning.

Another way to study the problem is to derive a generic lower bound on the KK scale $M_{\rm KK}$ (that is not fixed anymore to 2.45 TeV as in all the rest of the numerical analysis) arising from the ε_K constraint. In the right panel of Fig. 5.1 we show the average required fine-tuning in ε_K, obtained by taking the arithmetic mean of $\Delta_{\rm BG}(\varepsilon_K)$ on those points that fulfil the ε_K constraint within $\pm 30\%$, as a function of $M_{\rm KK}$. We observe that $\Delta_{\rm BG}(\varepsilon_K)$ decreases roughly as $1/M_{\rm KK}^2$, as expected from the dependence of $(M_{12}^K)_{\rm KK}$ on the KK scale (Eq. (4.28)). From the figure we can derive a bound for $M_{\rm KK}$ dependent on the maximum level of fine-tuning we allow. If we set the maximum tuning to 20, then we obtain the lower bound on the KK scale

$$M_{\rm KK} \gtrsim 18\,{\rm TeV}\,, \tag{5.21}$$

that is roughly in agreement with the previous findings of [120]. The bound shows clearly that, to have a low level of average fine-tuning on ε_K, the $M_{\rm KK}$ scale cannot be fixed to 2.45 TeV as in Eq. (5.1).

However, we would like to stress again, that although this bound can be considered as a naturalness constraint on the theory coming from ε_K, we have found, even for a KK scale as low as 2.5 TeV, regions of parameter space which yield ε_K in rough agreement with the experiments with a moderate amount of fine-tuning. Still one should be aware that, in this particular region of parameter space, loop corrections to the tree level contributions to ε_K could be potentially sizable. Keeping into account also these effects would lead to a modified prediction for ε_K for a given point of the parameter space; however, thanks to the large number of free parameters of the theory, we do not expect the overall picture to be modified at the qualitative level.

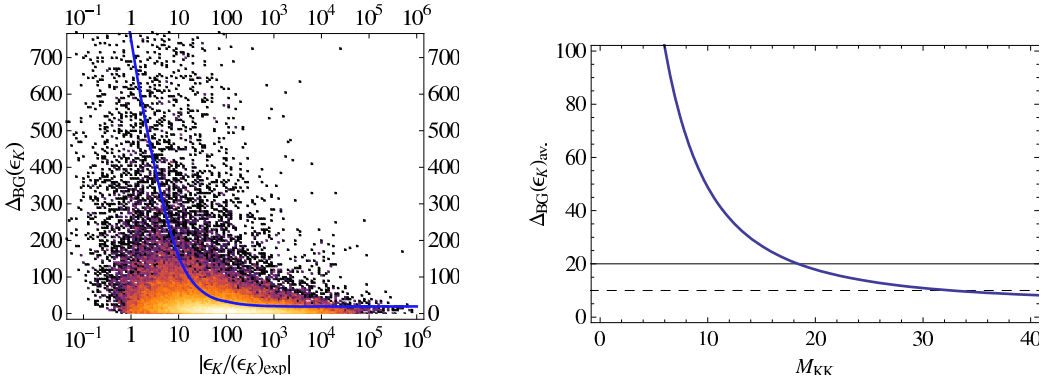

Figure 5.1: Left: the fine-tuning $\Delta_{\rm BG}(\varepsilon_K)$ plotted against ε_K normalized to its experimental value. The blue line displays the average fine-tuning as a function of ε_K. Right: the average required fine-tuning in ε_K as a function of the KK scale $M_{\rm KK}$.

5.2.2 The measured $\Delta F = 2$ observables in the RS model

In the present section we will extend our analysis to the remaining $\Delta F = 2$ observables that have been well measured experimentally (see also Tab. 4.5). The main aim is to investigate if the problem in fitting the observable ε_K is a peculiar problem of ε_K or if it is a general problem for all the well measured $\Delta F = 2$ observables. In the former case, we would like to understand the motivations for which ε_K is special.

We start with the mass difference ΔM_K which is sensitive to the real part of M_{12}^K, the fundamental quantity which is involved also in ε_K. Already from the left panel of Fig. 4.2 we could guess that in average the NP contributions to ΔM_K are not as large as those to ε_K (which depends on the imaginary part of M_{12}^K). Indeed this observation is confirmed by the left panel of Fig. 5.2 which shows the fine-tuning $\Delta_{\rm BG}(\Delta M_K)$ plotted as a function of ΔM_K, with the latter normalized to its experimental value. Contrary to ε_K, the theoretical uncertainties due to the non-perturbative LD contributions to ΔM_K are large. Hence, we consider safe to assume that the computed SD contributions to ΔM_K amount to $(70 \pm 30)\%$ of the measured value only. From the figure, it is evident that, in correspondence of this phenomenologically relevant region, the average fine-tuning turns out to be really small. Indeed the KK scale $M_{\rm KK}$ would not get any relevant lower bound from the constraint $\Delta_{\rm BG}(\Delta M_K) \leq 20$. We thus conclude that the model does not have any problem in fitting ΔM_K with low fine-tuning.

Next we analyze the CP asymmetry $S_{\psi K_s}$ which is sensitive to the CP violating phase in the B_d mixing system (see Eq. (4.53)). In the right panel of Fig. 5.2 we show the fine-tuning $\Delta_{\rm BG}(S_{\psi K_s})$ plotted as a function of $S_{\psi K_s}$. We observe that the RS prediction is generically very close to the SM prediction ($= 0.734 \pm 0.038$, see Tab. 4.5) and slightly larger than the experimental value ($= 0.672 \pm 0.023$, see Tab. 4.5). The average fine-tuning corresponding to the experimental data is quite small, typically smaller than 5.

Finally, we do not show the results for the mass differences ΔM_s and ΔM_d since their plots are very similar to the one for $S_{\psi K_s}$. ΔM_s and ΔM_d are easily fitted in the RS

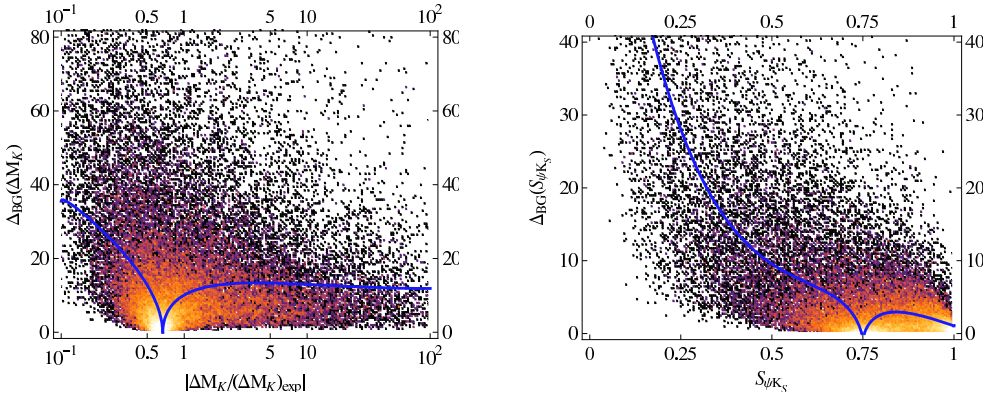

Figure 5.2: Left: The fine-tuning $\Delta_{\rm BG}(\Delta M_K)$ plotted against ΔM_K normalized to its experimental value. Right: the fine-tuning $\Delta_{\rm BG}(S_{\psi K_S})$ plotted against $S_{\psi K_S}$. In both panels the blue line displays the average fine-tuning.

model and the associated average fine-tuning is quite small.

Our analysis of the well measured $\Delta F = 2$ observables showed the facility of the RS model (with custodial protection) in fitting all the several observables, but the CP violating observable ε_K. Thus, a natural question arises:

What are the special features of ε_K, when compared to all the other $\Delta F = 2$ observables?

Here we just summarize the properties of ε_K that have been already mentioned throughout Sec. 4.1.3:

- In the K system, contrary to the $B_{s,d}$ systems, the NP contribution coming from the operator $\mathcal{Q}_2^{LR}$ in (4.14) is quite large (see Fig. 4.3). In the K system, in fact, the chirality-flipping operator experiences a strong chirality enhancement and RG running from the high KK energy scale to the low energy scale of ~ 2 GeV.

- Within the K system, the NP contribution to M_{12}^K obeys naturally to $\mathrm{Im}(M_{12}^K)_{\rm KK} \sim \mathrm{Re}(M_{12}^K)_{\rm KK}$. However, in the SM, because of the small phase of $V_{cs}^* V_{cd}$ in (4.7), $\mathrm{Im}(M_{12}^K)_{\rm SM} \ll \mathrm{Re}(M_{12}^K)_{\rm SM}$ and hence the relative NP contribution to the imaginary part is much larger than the relative NP contribution to the real part (see also left panel of Fig. 4.2), resulting in a strong enhancement of ε_K, but not of ΔM_K.

However, the main message of the section is not the RS "ε_K problem", but the possibility of the model in fitting all the well measured $\Delta F = 2$ observables *simultaneously*, even with a moderate amount of fine-tuning. We have shown indeed that the ε_K constraint is the most severe and its imposition drastically reduces the available parameter space, but still there exists a subspace of parameter space able to satisfy the constraint. In that subspace all the other constraints from the well measured observables are easily satisfied.

In the following, the entire numerical analysis of the RS model will be performed in the region of parameter space which predicts the observables ΔM_K, ΔM_d, ΔM_s, $\Delta M_d/\Delta M_s$,

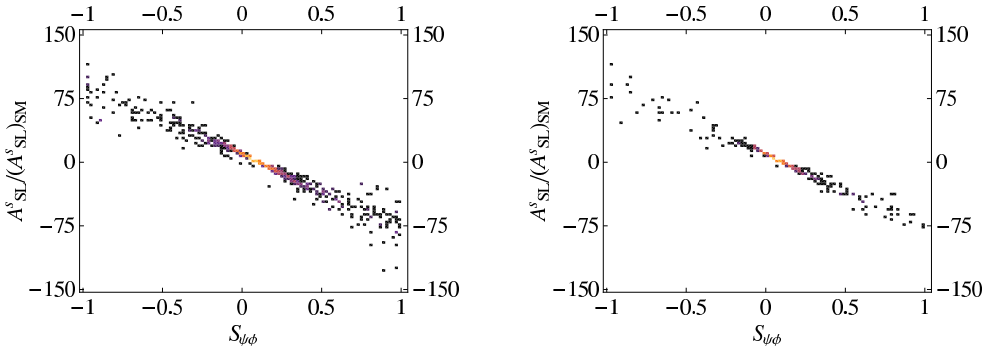

Figure 5.3: Left: The semileptonic asymmetry $A^s_{\rm SL}$, normalized to its SM value, as a function of $S_{\psi\phi}$. In addition to the requirement of correct quark masses and CKM mixings, also the available $\Delta F = 2$ constraints are imposed. Right: The same, but in addition the condition $\Delta_{\rm BG}(\varepsilon_K) < 20$ is imposed.

ε_K and $S_{\psi K_S}$ in agreement with their measurements with at most a deviation of $\pm 50\%$, $\pm 30\%$, $\pm 30\%$, $\pm 20\%$, $\pm 30\%$ and $\pm 20\%$, respectively. We impose rather conservative uncertainties, since we are aware of the theoretical uncertainties entering our analysis due to the several approximations we made. We are indeed taking into account the mixing of the SM gauge bosons with only the first Kaluza-Klein excitation gauge bosons (and not with the entire KK tower of modes) and neglecting the mixing between SM and KK fermions.

5.2.3 The CP violating phase in the B_s system

Having at hand the constrained parameter sets constructed in the previous section, we are now in the position to investigate the possible size of NP effects in the not yet precisely measured CP violating observable of the B_s system, $S_{\psi\phi}$. As described in detail in Sec. 4.1.6, the CP violation in the B_s system is one of the best probes of NP in the quark flavor sector, especially after the new recent data from D0 [166]. Hence we consider it worth to dedicate a section to the study of the CP violation in the $B^0_s - \bar{B}^0_s$ mixing system in the RS model.

In the left panel of Fig. 5.3 we present the correlation between the semileptonic asymmetry $A^s_{\rm SL}$ (see Eq. (4.56)) and $S_{\psi\phi}$ that emerges after imposing all available $\Delta F = 2$ constraints analyzed in the previous two sections. From the density plot, we read that the full range for $S_{\psi\phi}$ is possible. We observe that, while values of this asymmetry close to the SM prediction turn out to be most likely, a sizable amount of points lie also close to the central value $S_{\psi\phi} \sim 0.81$ recently reported by the HFAG collaboration [167][2].

In addition we note the model-independent correlation between $S_{\psi\phi}$ and $A^s_{\rm SL}$ pointed out first in [162] and described by us in Eq. (4.58). Thanks to this strong (model-independent) correlation between the two observables, in correspondence to the central

[2]Presently the central value of $S_{\psi\phi}$ is debated because of the new measurement of D0 [166]. We simply report here the central value valid when we wrote the papers to which we are referring in this thesis (before the D0 measurement).

value for $S_{\psi\phi}$ of 0.81, the semileptonic asymmetry $A^s_{\rm SL}$ would be enhanced by roughly two orders of magnitude relative to its SM value.

In the right panel of Fig. 5.3 we show what changes in the correlation, when we impose on the employed region of parameter space not only to fit the $\Delta F = 2$ observables, but also to exhibit a low level of fine-tuning (< 20) in the observable ε_K. The basic features of the correlation do not change, although the overall number of parameter points shown in the plots of course decreases (by roughly a factor of 3). Still a substantial enhancement of the two asymmetries is possible.

5.2.4 $\Delta F = 2$ transitions in the abelian flavor model

We study now the predictions of the abelian Susy flavor model on the $\Delta F = 2$ transitions, focusing especially on the promising CP violating phase of the B_s system. The analysis will be substantially different than what we have just presented for the RS model, since now we will not perform a study of naturalness, but first an investigation of the main constraints to be imposed on the parameter space and, subsequently, a study of the possibility to achieve a large NP contribution in the CP violating phase of the $B^0_s - \bar{B}^0_s$ mixing system.

Let us start with the $K^0 - \bar{K}^0$ mixing system. The matrices for the soft masses predicted by the abelian flavor model in Eq. (2.65) show that, at the high energy scale both LL and RR mass insertions for the transition $s \leftrightarrow d$ are zero. Thus, at the low energy scale, the model has only a LL mass insertion generated through the RG running (see Sec. 2.3.6) of size $V_{ts}V^*_{td}$ (MFV type MI). We know from the literature [218–220] that the Susy flavor models based on the MFV ansatz predict only small contributions to $\Delta F = 2$ observables. Thus, we can conclude that we expect only tiny NP contributions to ε_K and to ΔM_K since, for those transitions, the model resembles the MSSM with MFV.

To be more specific, we obtain a NP contribution to ε_K at most of the order 10% (for a relatively light Susy spectrum) and hence within the theoretical uncertainty of the prediction of the SM.

It is appealing to note that the smallness of the NP effects in ε_K is a common feature of the abelian flavor models that are indeed built in such a way to contain the NP effects in the $s \leftrightarrow d$ sector [85, 96].

A different trend is exhibited by the constraints coming from the $D^0 - \bar{D}^0$ mixing, that involves a $\Delta F = 2$ transition in the up sector of the type $u \leftrightarrow c$. Already from the predicted MI $(\delta^{LL}_u)_{12} = \lambda$ we could have expected huge NP contributions to the M^D_{12} matrix element. Fortunately, at the low scale, where we evaluate the Susy contributions to the physical observables, $(\delta^{LL}_u)_{21}$ is significantly smaller than λ, thanks to the RG running (for details see [94]), so that the constraints coming from $D^0 - \bar{D}^0$ mixing can be satisfied, even for squark masses of a few hundred GeV. Still the D meson mixing system represents one of the most severe constraints for the abelian model.

It is interesting to notice that the previous observations on the D meson mixing system are not peculiar to the abelian flavor model analyzed by us, but are valid for all the flavor models based on abelian symmetries. In fact, the abelian flavor symmetries do not predict any degeneracy between first and second generation up squarks and hence, as explained

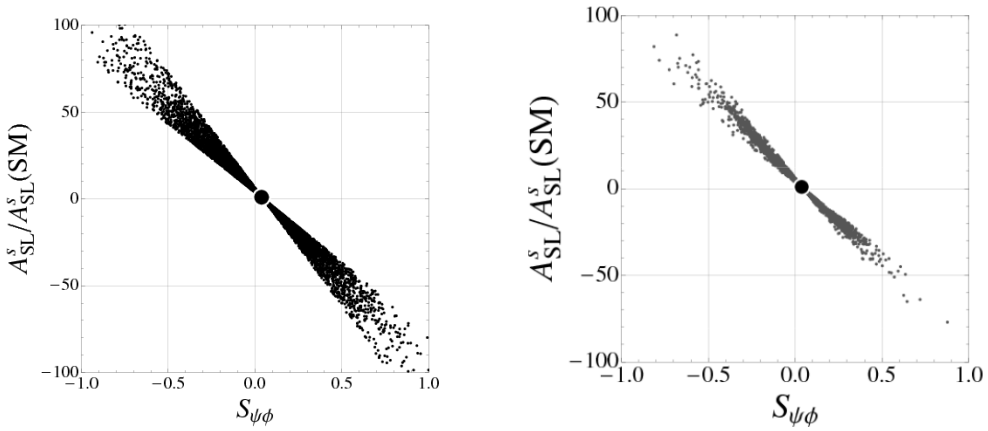

Figure 5.4: Left: correlation between the semileptonic asymmetry $A^s_{\rm SL}$ normalized to its SM prediction and $S_{\psi\phi}$ in the abelian flavor model. Right: the same for the non abelian flavor model. In both panels the dot represents the SM prediction for the two observables.

in Sec. 2.3.4, large $(\delta_u^{LL})_{12}$ MIs are always generated, leading to large NP contributions in the $D^0 - \bar{D}^0$ mixing system.

In our numerical analysis we do not study the several observables in the $D^0 - \bar{D}^0$ mixing system in detail, but we simply imposed the condition [221]

$$\left|M_{12}^D\right|_{\rm SUSY} < 0.02\,{\rm ps}^{-1}\,. \tag{5.22}$$

Finally, constraints coming from the mass differences ΔM_d, ΔM_s and from the ratio $\Delta M_s/\Delta M_d$ are imposed on the parameter space of the theory. In particular, the mass difference in the B_d meson mixing system is a relatively loose constraint to satisfy. Looking at the soft masses predicted by the model (Eq. (2.65)) we can in fact note that at the GUT scale $(\delta_d^{LL})_{13} = (\delta_d^{RR})_{13} = 0$ and hence, exactly as for the $K^0 - \bar{K}^0$ system, the NP contributions in B_d mixing system are MFV like and hence small.

A different behavior is exhibited by ΔM_s and by the ratio $\Delta M_s/\Delta M_d$. At the GUT scale the RR MI for the transition $s \leftrightarrow b$ is in fact sizable ($\left|\delta_d^{RR}\right|_{23} \sim 1$) and induces a large NP contribution to the mass difference of the B_s meson mixing system, thanks to the operator Q_4 defined in Eq. (4.33) that is RG enhanced and multiplied by a large loop function g_4 (see Appendix C for its expression). Effects of $\mathcal{O}(1)$ are possible.

In our numerical analysis we require to the parameter space of the model to fit the several mass differences, both in the B_d and in the B_s systems and the mass ratio $\Delta M_s/\Delta M_d$, at the 2σ level (see also Tab. 4.5).

Having imposed all the $\Delta F = 2$ constraints, it is interesting to investigate if the model has still room for large NP effects in the CP violating phase of the B_s meson mixing system. In the left panel of Fig. 5.4 we present our results for the correlation between the semileptonic asymmetry $A^s_{\rm SL}$ and $S_{\psi\phi}$ in the abelian flavor model analyzed by us.

As also discussed in Sec. 5.1.2, the several points represented in the plot satisfy, in addition to the $\Delta F = 2$ constraints, also the constraints coming from ${\rm Br}(b \to s\gamma)$,

observable	Experiment	SM prediction
$S_{\phi K_S}$	0.44 ± 0.17 [167]	$\sin 2\beta + 0.02 \pm 0.01$ [222]
$S_{\eta' K_S}$	0.59 ± 0.07 [167]	$\sin 2\beta + 0.01 \pm 0.01$ [222]
$\mathrm{Br}(\mu \to e\gamma)$	$< 1.2 \cdot 10^{-11}$ [223]	~ 0
$\lvert d_e \rvert$ $(e\,\mathrm{cm})$	$< 1.6 \times 10^{-27}$ [224]	$\simeq 10^{-38}$ [225]
$\lvert d_n \rvert$ $(e\,\mathrm{cm})$	$< 2.9 \times 10^{-26}$ [226]	$\simeq 10^{-32}$ [225]
$\mathrm{Br}(B \to X_s\gamma)$	$(3.52 \pm 0.25) \cdot 10^{-4}$ [167]	$(3.15 \pm 0.23) \cdot 10^{-4}$ [227]
$\mathrm{Br}(B \to X_s\ell^+\ell^-)$	$(1.59 \pm 0.49) \cdot 10^{-6}$ [228, 229]	$(1.59 \pm 0.11) \cdot 10^{-6}$ [230]
$\mathrm{Br}(B \to \tau\nu)$	$(1.73 \pm 0.35) \cdot 10^{-4}$ [231]	$(1.10 \pm 0.29) \cdot 10^{-4}$ [90]

Table 5.3: Current experimental sensitivities and SM predictions for the observables most relevant for our analysis. The branching ratio of $B \to X_s\ell^+\ell^-$ refers to the low dilepton invariant mass region, $q^2_{\ell^+\ell^-} \in [1, 6]\,\mathrm{GeV}^2$.

$\mathrm{Br}(B \to \tau\nu)$ and $\mathrm{Br}(B \to X_s\ell^+\ell^-)$ that are imposed throughout our analysis at the 2σ level (the detailed analysis of these additional constraints goes beyond the scope of this thesis, see e.g., the original paper [90]). In Tab. 5.3 we report all the additional constraints we imposed on the parameter space (in both abelian and non abelian flavor model).

From the plot, it is evident that the entire range for the asymmetry $S_{\psi\phi}$ can be in principle covered by the model, which hence can easily settle the last results of CDF and D0 [164–166], still being compatible with all the constraints coming from the well measured flavor observables. Finally, due to the strong correlation with A^s_{SL}, the latter asymmetry can be enhanced by as much as two orders of magnitude.

5.2.5 $\Delta F = 2$ transitions in the non abelian flavor model

In this section we want to present an analogous analysis for the non abelian flavor model, still with the aim to answer the question: *How large can the NP effects in the CP violating asymmetry $S_{\psi\phi}$ be, still being in accordance with the several experiments on flavor transitions?*

We start the discussion with the $K^0 - \bar{K}^0$ mixing system. Contrary to what we have shown for the abelian flavor model, in the non abelian framework the LL and RR MIs corresponding to the flavor transition $s \leftrightarrow d$ are relatively large. Indeed, in the SM the typical size of the transition would be $|V_{ts}V^*_{td}| \sim \lambda^5$ and this should be compared with $(\delta^{LL}_d)_{12}$ and $(\delta^{RR}_d)_{12}$ predicted by the model, that are given by $\varepsilon^2\bar{\varepsilon} \sim \lambda^5$ and $\bar{\varepsilon}^3 \sim \lambda^4$, respectively. Hence the constraints arising from the K meson mixing system, especially from the very well measured CP violating observable ε_K, are severe and represent the main source of exclusion of points of parameter space coming from the quark sector.

A different trend is exhibited by the constraints coming from the $D^0 - \bar{D}^0$ mixing. The $SU(3)$ flavor symmetry, on which the model is based, does not lead to any mass splitting

between the first and the second generation squarks, as it was instead the case of the abelian $U(1)$ flavor symmetry. Consequently the $(\delta_u^{LL})_{12}$ MI predicted by the model is very small ($\sim \lambda^4$) and induces only negligible NP contributions to the $D^0 - \bar{D}^0$ system. In conclusion the $D^0 - \bar{D}^0$ system is only a very loose constraint for the non abelian flavor model. This is probably one of the most characteristic features which distinguishes non abelian flavor models from abelian ones.

Finally constraints coming from the mass differences ΔM_d, ΔM_s and from the ratio $\Delta M_s/\Delta M_d$ are imposed on the parameter space of the theory. The mass differences in the $1-3$ and $2-3$ sectors are indeed stringent constraints for the non abelian model which predicts, as shown in Eqs. (2.69), (2.70), LL and RR MIs both sizable in the two sectors, generating hence the very powerful left-right operator Q_4. Effects of the order 10% (for the $1-3$ sector) and 50% (for the $2-3$ sector) are possible.

In our numerical analysis we require the parameter space of the model to fit the several mass differences, both in the B_d and in the B_s systems, at the 2σ level (see also Tab. 4.5).

Having imposed all the constraints, it is interesting to investigate if the model has still room for large NP effects in the CP violating phase of the B_s meson mixing system. In the right panel of Fig. 5.4 we present our results for the correlation between the semileptonic asymmetry $A_{\rm SL}^s$ and $S_{\psi\phi}$ in the non abelian flavor model analyzed by us.

The several points represented in the plot satisfy also the constraint coming from $\mathrm{Br}(b \to s\gamma)$ at the 2σ level. Additionally, since the non abelian model is embedded in a $SO(10)$ Susy GUT model (see Sec. 2.3.5), one should also take into account the constraints coming from lepton flavor violating observables. The most severe to satisfy is the branching ratio of $\mu \to e\gamma$ because of the relatively large MIs in the lepton $1-2$ sector[3]. We impose this additional constraint at the 2σ level (see Tab. 5.3 for the list of the additional constraints imposed on the parameter space).

From the plot, it is evident that large values for $S_{\psi\phi}$ are allowed while being compatible with all the constraints coming from quark and lepton flavor violating observables. However, contrary to the abelian model, the entire range for $S_{\psi\phi}$ cannot be reached (because of the smaller MIs in the $2-3$ sector), however, the central value $S_{\psi\phi} \sim 0.81$ of HFAG [167] can be attained, even if hardly. Accordingly, also the semileptonic asymmetry $A_{\rm SL}^s$ can be enhanced by roughly a factor 50 beyond its SM value.

5.3 Rare decays of K and B mesons

In this section we will discuss, first in the RS model with custodial protection and secondly in the Susy flavor models, the rare K and B decays already analyzed theoretically in Sec. 4.2. Before entering into the details of the discussion, we have to mention that

- In the plots we will show for the RS model, blue points correspond to points of the parameter space which fulfil all the $\Delta F = 2$ constraints presented in Secs. 5.2.1 and 5.2.2 only, orange points instead satisfy also the requirement of a small amount

[3] For a complete analysis of the lepton flavor violating processes in the non abelian Susy framework see the original paper [90].

of fine-tuning ($\Delta_{\rm BG}(\varepsilon_K) < 20$) in ε_K. Only on occasion we will remove the custodial protection from the RS model for the purpose of illustration. In this case, red points correspond to points of the parameter space which fulfil all the $\Delta F = 2$ constraints and green points imply also a small amount of fine-tuning.

- In Susy flavor models only the points satisfying the several constraints mentioned in Secs. 5.2.4 and 5.2.5 are presented.

5.3.1 Rare K decays in the RS model

As discussed in Sec. 4.2.10, the $K \to \pi\nu\bar{\nu}$ decays are theoretically very clean and highly sensitive to NP, thus they can offer an excellent possibility of distinguishing between different BSM frameworks, once both branching ratios $\mathrm{Br}(K^+ \to \pi^+\nu\bar{\nu})$ and $\mathrm{Br}(K_L \to \pi^0\nu\bar{\nu})$ will be accurately measured.

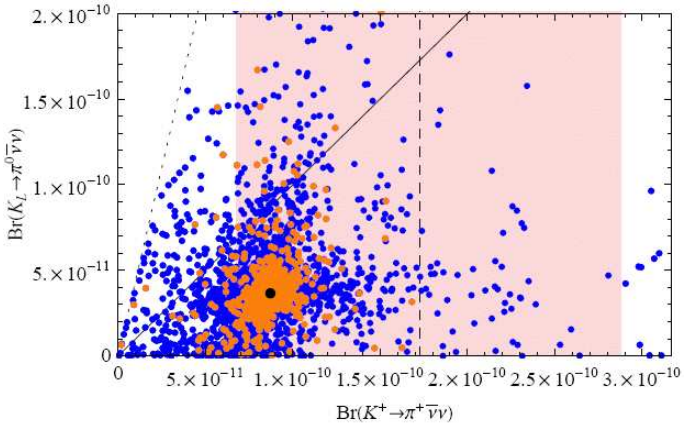

Figure 5.5: $\mathrm{Br}(K_L \to \pi^0\nu\bar{\nu})$ as a function of $\mathrm{Br}(K^+ \to \pi^+\nu\bar{\nu})$. The shaded area represents the experimental 1σ range for $\mathrm{Br}(K^+ \to \pi^+\nu\bar{\nu})$ (the central measured value is represented by a dashed line). The GN bound of Eq. (4.126) is displayed by the dotted line, while the solid line separates the two areas where $\mathrm{Br}(K_L \to \pi^0\nu\bar{\nu})$ is larger or smaller than $\mathrm{Br}(K^+ \to \pi^+\nu\bar{\nu})$. The black point represents the SM prediction (note that they are slightly different than the updated values we put in Tab 4.6; in fact the point in the plot represents the SM prediction at the time of our numerical analysis (Dec 2008)).

Already from the discussion of Sec. 4.2.9, we expect possible large NP contributions for the branching ratios of the two modes in the RS model with custodial protection. This is indeed confirmed by Fig. 5.5 where we show $\mathrm{Br}(K_L \to \pi^0\nu\bar{\nu})$ as a function of $\mathrm{Br}(K^+ \to \pi^+\nu\bar{\nu})$. We observe that the $K^+ \to \pi^+\nu\bar{\nu}$ decay rate can be enhanced by up to a factor ~ 2, reaching the central experimental value of $\sim 1.7 \cdot 10^{-10}$ (see also Tab. 4.6). For the decay $K_L \to \pi^0\nu\bar{\nu}$ the enhancement can be even larger, reaching ~ 3 times the SM prediction, still being consistent with the measured value of $\mathrm{Br}(K^+ \to \pi^+\nu\bar{\nu})$.

From the plot it is evident that no correlation holds between the two branching ratios: for a given value of $\mathrm{Br}(K^+ \to \pi^+\nu\bar{\nu})$ all values for $\mathrm{Br}(K_L \to \pi^0\nu\bar{\nu})$ consistent with the Grossman-Nir bound in (4.126) can be reached. The reason for this non-correlation has been pointed out in [232] and relies upon the importance of the operator $\mathcal{Q}_2^{LR}$ which brings

the largest NP effect to the $K^0 - \bar{K}^0$ mixing system. Because of that operator, the new CP violating phases in $K^0 - \bar{K}^0$ mixing and the rare K decays turn out to be independent of each other, and the ε_K constraint does not enforce any correlation between the neutral and charged $K \to \pi\nu\bar{\nu}$ modes.

Correlation between rare K decays and $S_{\psi\phi}$

We have shown how in principle both the rare decays $K \to \pi\nu\bar{\nu}$ and the CP violating asymmetry $S_{\psi\phi}$ can obtain a large NP contribution in the RS model with custodial protection. It is now interesting to investigate if the NP effects in the two channels are totally uncorrelated or, on the contrary, if there is a precise pattern regulating the two NP contributions.

In Fig. 5.6, we show the correlation between the branching ratio of $K^+ \to \pi^+\nu\bar{\nu}$ and $S_{\psi\phi}$. The most striking feature of the plot is that large enhancements in $\mathrm{Br}(K^+ \to \pi^+\nu\bar{\nu})$ exclude large NP effects in $S_{\psi\phi}$ and vice versa. Therefore, if the present hints for a large value of $S_{\psi\phi}$ by CDF and D0 [164–166] will be confirmed, visible effects in $\mathrm{Br}(K^+ \to \pi^+\nu\bar{\nu})$ in the context of the RS model with custodial protection will most likely be excluded. Vice versa, if future experiments on $S_{\psi\phi}$ will lead to a SM-like $S_{\psi\phi}$, then the room for NP contributions to the rare K^+ decay will be largely open.

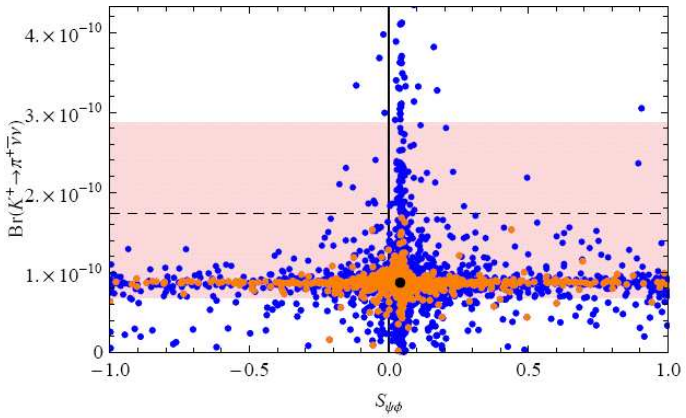

Figure 5.6: $\mathrm{Br}(K^+ \to \pi^+\nu\bar{\nu})$ as a function of $S_{\psi\phi}$. The dashed line represents the central measured value for the branching ratio of $K^+ \to \pi^+\nu\bar{\nu}$. The shaded area represents the experimental 1σ range for $\mathrm{Br}(K^+ \to \pi^+\nu\bar{\nu})$, and the black point the SM prediction (note that they are slightly different than the updated values we put in Tab 4.6; in fact the point in the plot represents the SM prediction at the time of our numerical analysis (Dec 2008)).

The correlation between the CP violating decay branching ratio $\mathrm{Br}(K_L \to \pi^0\nu\bar{\nu})$ and $S_{\psi\phi}$ turns out to be perfectly analogous and hence we do not show it here (see the original paper [173]).

We mention that we could have already anticipated the anticorrelation shown in Fig. 5.6 from Sec. 4.2.9. $S_{\psi\phi}$ and the rare K decays involve in fact two different flavor transitions: $s \leftrightarrow b$ for the first observable and $d \leftrightarrow s$ for the second ones. In Fig. 4.10 has been shown that large flavor changing neutral vertices in one sector ($\hat{\Delta}^{bs}_{L,R}$) preclude the possibility to

have large flavor changing neutral vertices in another sector ($\hat{\Delta}^{sd}_{L,R}$). The anticorrelation shown in Fig. 4.10 for the flavor changing neutral vertices corresponds exactly to what we have obtained in terms of physical observables in Fig. 5.6.

We conclude with the main message of this section. Fig. 5.6 shows the relevance of the next experiments NA62 and LHCb in confirming the pattern between the decays $K \to \pi\nu\bar{\nu}$ and $S_{\psi\phi}$ or in putting the RS model with custodial protection under pressure, in the case of finding large NP contributions in both flavor channels.

5.3.2 Rare B decays in the RS model

We want now to discuss the very promising decays $B_{s,d} \to \mu^+\mu^-$, following the same strategy used in the previous section for the $K \to \pi\nu\bar{\nu}$ modes. $B_s \to \mu^+\mu^-$ is one of the LHCb golden channels, hence it is worth to discuss it in detail in the context of NP models, such as the RS model with custodial protection.

In Sec. 4.2.9 we have already anticipated that the NP contributions to rare B decays are expected to be quite smaller than those entering in the rare K decays. This is indeed confirmed by Fig. 5.7 where we show the correlation between $\mathrm{Br}(B_s \to \mu^+\mu^-)$ and $\mathrm{Br}(B_d \to \mu^+\mu^-)$ in the RS model with custodial protection.

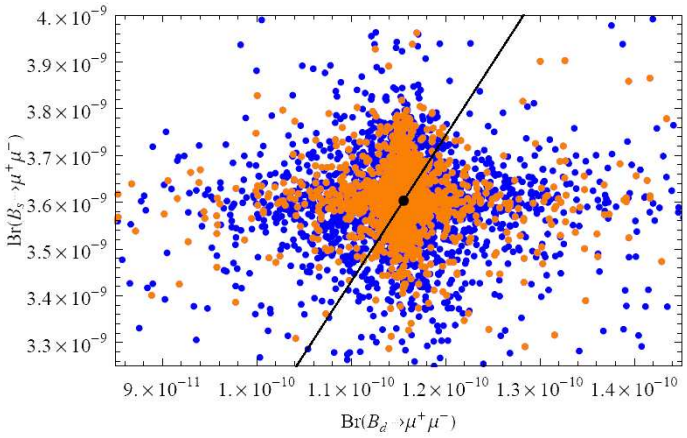

Figure 5.7: $\mathrm{Br}(B_s \to \mu^+\mu^-)$ versus $\mathrm{Br}(B_d \to \mu^+\mu^-)$. The straight line represents the MFV correlation ($r = 1$ in Eq. (5.23)) and the black point is the SM prediction (note that they are slightly different than the updated values we put in Tab 4.6; in fact the point in the plot represents the SM prediction at the time of our numerical analysis (Dec 2008)).

We observe that the NP effects on the two decays are rather small: $B_d \to \mu^+\mu^-$ can get at most a 20% effect compared to the SM prediction and even smaller contributions are shown for the decay $B_s \to \mu^+\mu^-$ that can acquire at most a 10% NP effects. The smallness of the deviations from the SM predictions for the two rare B decays can be traced back to the absence of the scalar operators which could in principle bring large NP effects, and to the custodial protection of the left handed Z couplings being more effective in B than in K physics (see also Sec. 4.2.9). Indeed in the following section we will show how remarkable is the impact of removing the custodial protection on the two rare B

decays.

Finally the straight line drawn in Fig. 5.7 represents the correlation between $\mathrm{Br}(B_s \to \mu^+\mu^-)$ and $\mathrm{Br}(B_d \to \mu^+\mu^-)$ predicted by models with MFV. In those models, the ratio between the two branching ratios is predicted to be equal to the prediction of the SM [233]

$$\frac{\mathrm{Br}(B_s \to \mu^+\mu^-)_{\mathrm{MFV}}}{\mathrm{Br}(B_d \to \mu^+\mu^-)_{\mathrm{MFV}}} = \frac{\hat{B}_{B_d}}{\hat{B}_{B_s}} \frac{\tau_{B_s}}{\tau_{B_d}} \frac{\Delta M_s}{\Delta M_d} r\,, \tag{5.23}$$

with $r = 1$. This MFV correlation is obviously strongly broken in the RS model (see the formulae (4.111), (4.112) for the branching ratios) but still the deviations from the straight line shown in Fig. 5.7 are probably too small to allow LHCb to distinguish between models with MFV and the RS model using these decay modes only[4].

In Fig. 5.8 we confirm this statement, showing the correlation between the quantity r as a function of the CP violating observable $S_{\psi\phi}$. The departure of r from unity measures the violation of the MFV relation ($r = 1$ in Eq. (5.23)) in the framework of the RS model with custodial protection.

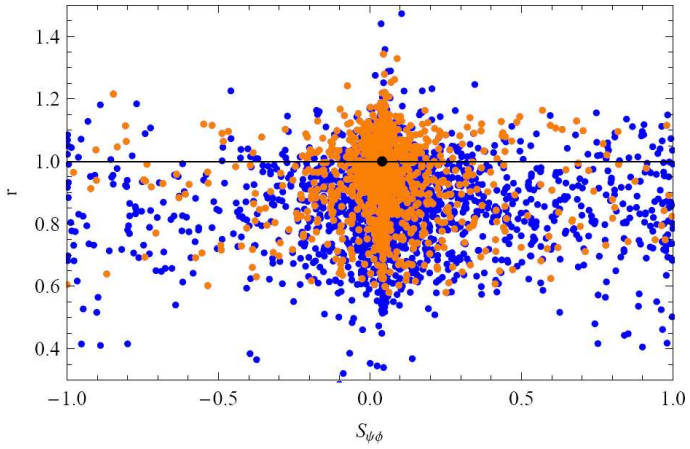

Figure 5.8: r of Eq. (5.23) as a function of $S_{\psi\phi}$. The solid line indicates the MFV prediction and the black dot the SM value.

We observe that most points lie in the range

$$0.60 \leq r \leq 1.35\,, \tag{5.24}$$

with only a mild anticorrelation with $S_{\psi\phi}$.

We conclude this section with the main message coming from Fig. 5.7. The $B_{s,d} \to \mu^+\mu^-$ rare decays do not receive sizable NP contributions in the RS model with custodial protection. It will be very challenging for LHCb to disentangle a possible NP effect coming from the custodially protected RS model in rare B decays. In particular LHCb could in principle put seriously under pressure the model finding a branching ratio for $B_s \to \mu^+\mu^-$ highly deviating from the SM prediction.

[4] In the following section we will present a more effective way to distinguish the RS model from frameworks based on the MFV principle.

5.3.3 RS model vs MFV

In the previous section we have shown how challenging is to distinguish the RS model with custodial protection from models based on the MFV principle, using just rare B decay modes. The reason is that, in spite of the fact that theoretically the RS model is definitely at odds with the MFV framework, the NP effects in rare B decays are small and difficult to be measured by the next experiments.

One possibility to circumvent the problem would be to analyze correlations predicted by the MFV framework that involve both rare K and B decays. The huge NP effects in rare K decays would most probably lead to a hard breaking of those correlations.

As an example, we study here the pattern of correlation between the SD contribution to the branching ratio of $K_L \to \mu^+\mu^-$ and the branching ratio of $B_s \to \mu^+\mu^-$. In models with MFV, the several functions regulating the flavor transitions ($X^{V,V-A}$, $Y^{V,V-A}$ and $Z^{V,V-A}$) are flavor universal, as in the SM. Hence, comparing the formulae for the branching ratios of $B_s \to \mu^+\mu^-$ and $K_L \to \mu^+\mu^-$ presented in (4.111) and in (4.116) respectively, one can deduce that, in the absence of NP phases ($\bar{\theta}_Y^K = 0$), a straight correlation between the two branching ratios exists. In Fig. 5.9 we present the branching ratio of $K_L \to \mu^+\mu^-$ as a function of the $B_s \to \mu^+\mu^-$ branching ratio. The MFV prediction is presented as a solid black line.

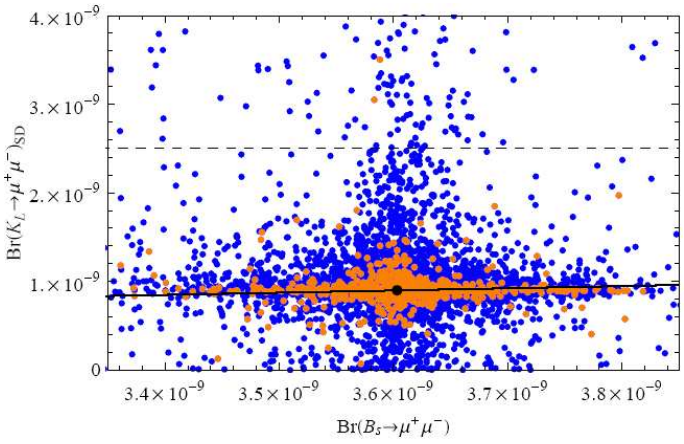

Figure 5.9: $\mathrm{Br}(K_L \to \mu^+\mu^-)_{\mathrm{SD}}$ as a function of $\mathrm{Br}(B_s \to \mu^+\mu^-)$. The dashed line indicates the experimental upper bound on $\mathrm{Br}(K_L \to \mu^+\mu^-)_{\mathrm{SD}}$. The solid line shows the MFV prediction, while the black point represents the SM prediction (note that they are slightly different than the updated values we put in Tab 4.6; in fact the point in the plot represents the SM prediction at the time of our numerical analysis (Dec 2008)).

From the plot we notice that, indeed, the MFV prediction can be strongly violated thanks to the much more pronounced NP effects in $\mathrm{Br}(K_L \to \mu^+\mu^-)_{\mathrm{SD}}$ than in $\mathrm{Br}(B_s \to \mu^+\mu^-)$. In principle, this study could represent a possibility to distinguish between models with MFV and the RS model with custodial protection. However, we have to be aware that this investigation would be quite complicated because of the problems in the extraction of the SD contribution to $K_L \to \mu^+\mu^-$ from the experiments (see Sec. 4.2.10). Still future theoretical and experimental developments in the decay could open the road to a better

understanding of the non-MFV nature of the RS model with custodial protection.

It is instructive to investigate how these results would look like if the custodial protection of the RS model was not present. In particular we are interested in inferring if the difficulty in distinguishing models with MFV from the RS model is a peculiar problem of the model with custodial protection or, more generally, of the RS model itself. With this purpose in mind, in Fig. 5.10 we show the correlation between $\mathrm{Br}(B_s \to \mu^+\mu^-)$ and $\mathrm{Br}(B_d \to \mu^+\mu^-)$ once that the custodial protection is removed from the model (see also end of Sec. 3.1.4 or Sec. 4.2.9 for the details on the particular procedure adopted).

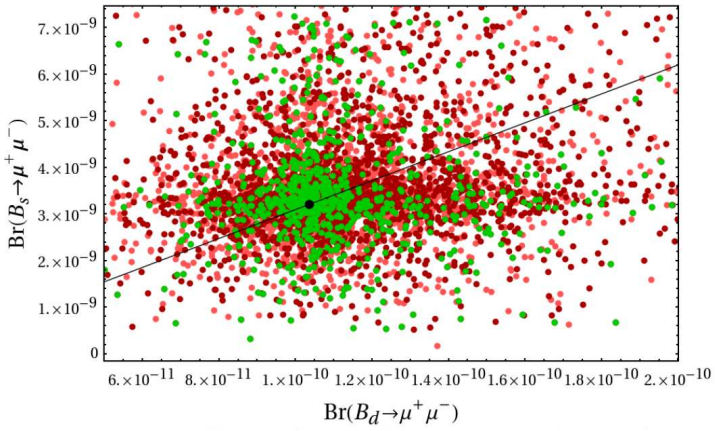

Figure 5.10: $\mathrm{Br}(B_s \to \mu^+\mu^-)$ versus $\mathrm{Br}(B_d \to \mu^+\mu^-)$ in the RS model *without* custodial protection. The straight line represents the MFV prediction ($r = 1$ in Eq. (5.23)) and the black point is the SM prediction (note that they are slightly different than the updated values we put in Tab 4.6; in fact the point in the plot represents the SM prediction at the time of our numerical analysis (Dec 2008)).

From the figure, we note that, removing the protection, large NP contributions in the two rare B decay branching ratios are now possible: $B_d \to \mu^+\mu^-$ and $B_s \to \mu^+\mu^-$ typically get up to a 50% and 80% of NP effects, respectively (to compare with the 20% and 10% obtained in the case of the model with custodial protection, in Fig. 5.7). Evidently, in the case of no custodial protection, the deviations from the MFV prediction (straight line in the figure) is quite sizable and could in principle be measured by next experiments.

It is worth to remind the theoretical reason for which the NP effects in rare B decays are largely enhanced in the case of removal of the custodial protection (see also Sec. 4.2.9). As we have shown in Fig. 3.4, without the custodial protection, the flavor violating couplings $\Delta_L^{ij}(Z)$ are larger than the corresponding right handed couplings $\Delta_R^{ij}(Z)$. This enforces the predominance of the contribution of the Z boson (coupled this time with left handed down quarks) on the branching ratios of the several rare B (and K) decays. Additionally, contrary to the case of custodial protection, $\Delta_L^{ij}(Z)$ exhibit a similar hierarchy as the CKM factors $\lambda_t^{(q)}$, $\lambda_t^{(K)}$ and hence relative NP effects of roughly equal size are expected in K and B decays. In few words, the main effect of removing the custodial protection is the enhancement of the NP effects in B physics.

We can conclude this section with the main message: the difficulty in distinguishing between MFV frameworks and the RS model resides exclusively in the custodial protection of the model, which reduces the NP effects in rare B decays. Still we have to point out that a comparative study of rare K and B decays can give the possibility to discriminate between the two frameworks, even in the presence of the custodial protection.

5.3.4 Rare K and B decays in the Susy flavor models

In this section we analyze the rare K and B decays in the framework of the abelian AC model and of the non abelian RVV2 model, with the aim to show clear patterns to distinguish the two Susy flavor models from the RS model with custodial protection. As for the RS model, the essential channels for our scope are

- $K \to \pi\nu\bar{\nu}$;
- $B_q \to \mu^+\mu^-$;
- Their correlation with the CP violating asymmetry $S_{\psi\phi}$.

The most immediate difference between the RS model and the Susy flavor models concerns the theoretically clean decays $K \to \pi\nu\bar{\nu}$. In Sec. 4.2.3 we have shown that, in Susy, large NP effects can arise only through

1. *Chargino/up squark loops* in the presence of sizable flavor changing trilinear couplings of the up squarks (see Eq. (4.73));
2. *Charged Higgs/top quark loops* in the presence of sizable right-right down MIs, both in the $1-3$ sector and in the $2-3$ sector (see Eq. (4.74)).

However, the Susy flavor models we have analyzed in this thesis do not satisfy neither the first, nor the second condition. Thus we expect the branching ratios of the $K \to \pi\nu\bar{\nu}$ decays to be mostly SM-like. This is indeed confirmed by our numerical analysis. The NP contributions are at the percent level in both models, with slightly larger effects in the non abelian model due to its larger $(\delta_d^{RR})_{13,23}$ mass insertions.

Comparing the NP contributions to the SM predictions reported in Tab. 4.6, we can conclude that the Susy effects on the K branching ratios are well within the theoretical errors and thus uninteresting. For this reason, we decided not to give plots of these decays here, contrary to what we have done for the RS model (Fig. 5.5 and 5.6).

The clear message from the rare K decays is that, if the upcoming experiments NA62, K0TO and Project-X will decrease the experimental error on the measurement of $\mathrm{Br}(K^+ \to \pi^+\nu\bar{\nu})$ and will, at the same time, confirm the present central value for that branching ratio ($\sim 1.73\cdot 10^{-10}$), then the Susy flavor models discussed in this thesis will be put under serious pressure and disfavored compared to the RS model with custodial protection. The same conclusion arises if the experiments will detect the decay $K_L \to \pi^0\nu\bar{\nu}$ and will set a central value significantly larger than the SM prediction. Vice versa, if the central value of $\mathrm{Br}(K^+ \to \pi^+\nu\bar{\nu})$ will decrease with the future measurements, and also

$\mathrm{Br}(K_L \to \pi^0 \nu\bar{\nu})$ will turn out to be SM-like, then no clear message will originate from these rare decay modes.

The discussion of the decays $B_q \to \mu^+\mu^-$ is a bit more involved and will show a different pattern for the abelian and the non abelian model.

First of all, it is of primary interest to investigate if the correlation between $\mathrm{Br}(B_s \to \mu^+\mu^-)$ and $\mathrm{Br}(B_d \to \mu^+\mu^-)$ predicted by models with MFV, and discussed by us in Sec. 5.3.2, is highly violated or, as it occurs in the RS model with custodial protection, does not supply a powerful tool to distinguish the Susy flavor models from the MFV framework.

Already from the relevant MIs predicted by the two models, we could assert that probably the correlation is strongly broken, mainly because of the very large effects in the branching ratio of $B_s \to \mu^+\mu^-$. Indeed this expectation is confirmed by Fig. 5.11 where we present the result of our numerical investigation for the two rare B decays, in the left panel for the abelian model and in the right panel for the non abelian one.

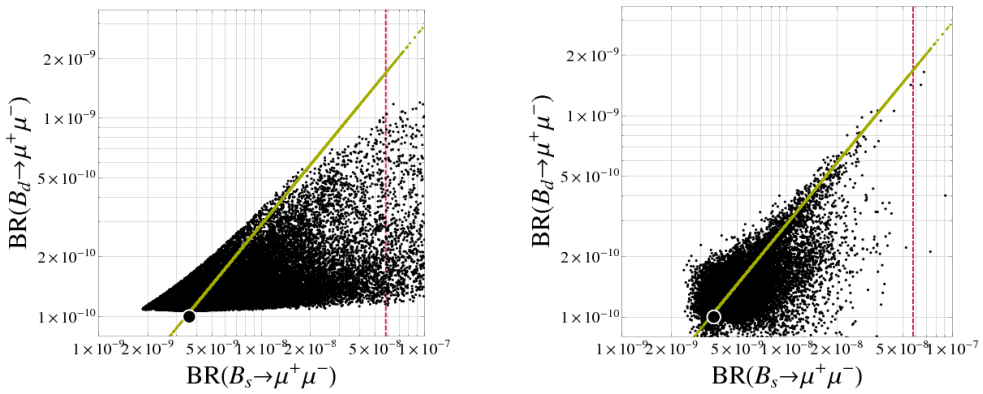

Figure 5.11: Left: correlation between $\mathrm{Br}(B_s \to \mu^+\mu^-)$ and $\mathrm{Br}(B_d \to \mu^+\mu^-)$ in the abelian AC model. Right: the same for the non abelian RVV2 flavor model. In both panels the dot represents the SM prediction (note that they are slightly different than the updated values we put in Tab 4.6; in fact the point in the plot represents the SM prediction at the time of our numerical analysis (Sept 2009)), the straight green line the prediction of MFV frameworks. Finally the red vertical line represents the experimental upper bound on the branching ratio of $B_s \to \mu^+\mu^-$.

Several messages can be read from the two plots

- An order of magnitude enhancement is possible for the two branching ratios. In the abelian model $\mathrm{Br}(B_s \to \mu^+\mu^-)$ can even reach easily its experimental upper bound.
- The two models predict very striking deviations from the MFV prediction. More specifically, since the NP flavor structure of the two models affects mainly (or at least more strongly) the $b \to s$ sector than the $b \to d$ sector, then the ratio $\mathrm{Br}(B_d \to \mu^+\mu^-)/\mathrm{Br}(B_s \to \mu^+\mu^-)$ is dominantly below its MFV prediction. The feature is noticeable especially in the abelian model in which the $b \to d$ sector is not affected

by beyond MFV structures and hence the ratio can be even much smaller than the MFV prediction.

- As a consequence of the previous point, the two decay channels can offer to LHCb a perfect tool to investigate and eventually to disprove the MFV hypothesis.
- Finally, one should note the striking difference between the above features and the pattern of prediction of the RS model with custodial protection on the two rare B decays, in which the NP effects are at the level of $(10-20)\%$.

From the above discussion it is evident that for the two Susy flavor models the $B_s \to \mu^+\mu^-$ (and $B_d \to \mu^+\mu^-$) decay and $S_{\psi\phi}$ are the two golden channels in the quark sector (in addition to be two of the main golden channels for the future experiments). It is then worth to investigate if there is a correlation between the two observables. In Fig. 5.12 we represent the branching ratio of $B_s \to \mu^+\mu^-$ versus the CP violating asymmetry $S_{\psi\phi}$ in the abelian flavor model (left panel) and in the non abelian flavor model (right panel).

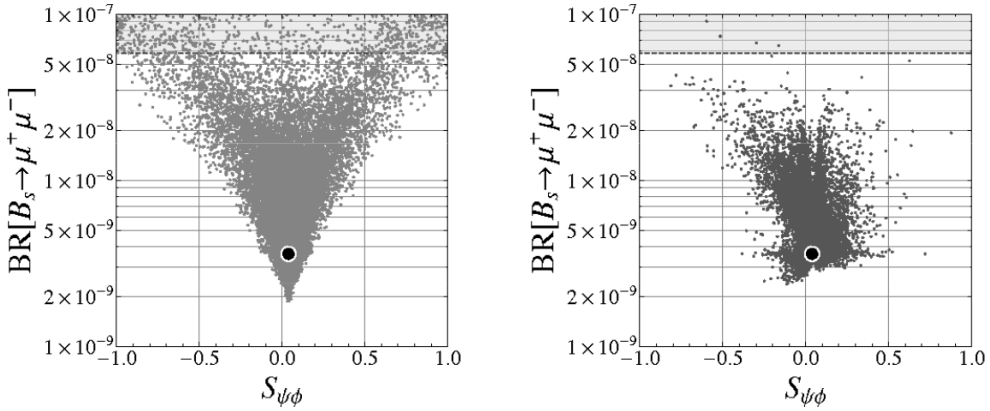

Figure 5.12: Left: correlation between $\mathrm{Br}(B_s \to \mu^+\mu^-)$ and $S_{\psi\phi}$ in the abelian AC model. Right: the same for the non abelian RVV2 flavor model. In both panels the dot represents the SM prediction for the two observables (note that they are slightly different than the updated values we put in Tab 4.6; in fact the point in the plot represents the SM prediction at the time of our numerical analysis (Sept 2009)), the horizontal dashed line represents the experimental upper bound on the branching ratio of $B_s \to \mu^+\mu^-$.

The two plots show a basic difference: the AC abelian model exhibits a strong correlation between $\mathrm{Br}(B_s \to \mu^+\mu^-)$ and $S_{\psi\phi}$, in the RVV2 non abelian model instead the correlation is washed out, although both observables can differ spectacularly from their SM predictions. More specifically in the AC abelian model large effects in $S_{\psi\phi}$ predict a lower bound on $\mathrm{Br}(B_s \to \mu^+\mu^-)$ at the level of $\mathrm{Br}(B_s \to \mu^+\mu^-) > 10^{-8}$ for $|S_{\psi\phi}| \geq 0.3$ (the converse is obviously not true).

To understand the theoretical reason for this correlation, one has to recall our analysis of the Susy contributions to the two observables of Secs. 4.1.4 and 4.2.7. We have explicitly shown that the main NP effects in $\mathrm{Br}(B_s \to \mu^+\mu^-)$ arise (if present) from the Higgs penguins of Fig. 4.9 that contribute to the scalar and pseudoscalar operators Q_S and Q_P

(and the corresponding $\tilde{Q}_S$, $\tilde{Q}_P$). The situation for $S_{\psi\phi}$ is a bit more involved. In principle both the double Higgs penguins of Fig. 4.5 and the gluino boxes of Fig. 4.4 can give sizable NP effects. However, the most relevant difference between the two contributions is that, contrary to the gluino boxes, the double Higgs penguins do not decouple with the Susy mass scale $\tilde{m}$.[5]
Additionally, in the AC model the huge NP contributions to the $D^0 - \bar{D}^0$ system force the Susy mass spectrum ($\tilde{m}$) to be relatively heavy, in order to be in agreement with the experiments on $D^0 - \bar{D}^0$ mixing. Consequently, the double Higgs penguins bring the dominant NP contribution to $S_{\psi\phi}$ and hence large NP effects in $S_{\psi\phi}$ correspond to large NP effects in the branching ratio of $B_s \to \mu^+\mu^-$.

In the RVV2 model, the absence of the $D^0 - \bar{D}^0$ constraints, as well as the more complicated flavor structure of the model (as for instance the presence of left handed currents carrying new sources of CPV) washes out the above correlation as shown in the right panel of Fig. 5.12.

The different role of the constraints from the $D^0 - \bar{D}^0$ system in the two Susy flavor models is also shown by Fig. 5.13 in which we present the plane for the lightest stop mass ($m_{\tilde{t}_1}$) vs. the lightest chargino mass ($m_{\tilde{\chi}_1^\pm}$) on the first row and the plane for the charged Higgs mass ($M_{H^\pm}$) vs. $\tan\beta$ on the second row. The plots in the first column correspond to the abelian AC model, the ones in the second column to the non abelian RVV2 model. From the plots in the first column (for the abelian model), we can clearly read that large effects in $S_{\psi\phi}$ (darker colors) are only possible for a heavy spectrum, even beyond the LHC reach, but for a relatively light Higgs boson (and large $\tan\beta$). This feature confirms once more the special role of the double Higgs penguins in generating large NP effects in $S_{\psi\phi}$ in the abelian model. From the plots in the second column (for the non abelian model), we can instead recognize that the importance of a heavy spectrum and of a light Higgs boson is weaker: the gluino boxes acquire in fact more relevance.

Beyond the importance of the double Higgs penguin contribution, from the left upper panel in Fig. 5.13 a very important message arises: there exist regions of the Susy parameter space at the border or even beyond the LHC reach where we can expect clear non-standard signals in flavor processes, such as in $S_{\psi\phi}$. In these regions, flavor phenomena represent the most powerful tool to shed light on NP.

5.4 Comparison and future prospective to distinguish

The main aim of this thesis is to supply a way to distinguish the RS model with custodial protection from the two Susy flavor models, using only few low energy flavor observables. We therefore complete this chapter with a summary of the main numerical results that clearly show different patterns of predictions of the two frameworks.

- All the three models can predict large new physics effects in the CP violating asymmetry $S_{\psi\phi}$. However, the new physics effects in the RVV2 non abelian flavor model

[5] Another important feature is that, contrary to the gluino box contribution, the double Higgs contribution is enhanced by $\tan\beta$ to the fourth power.

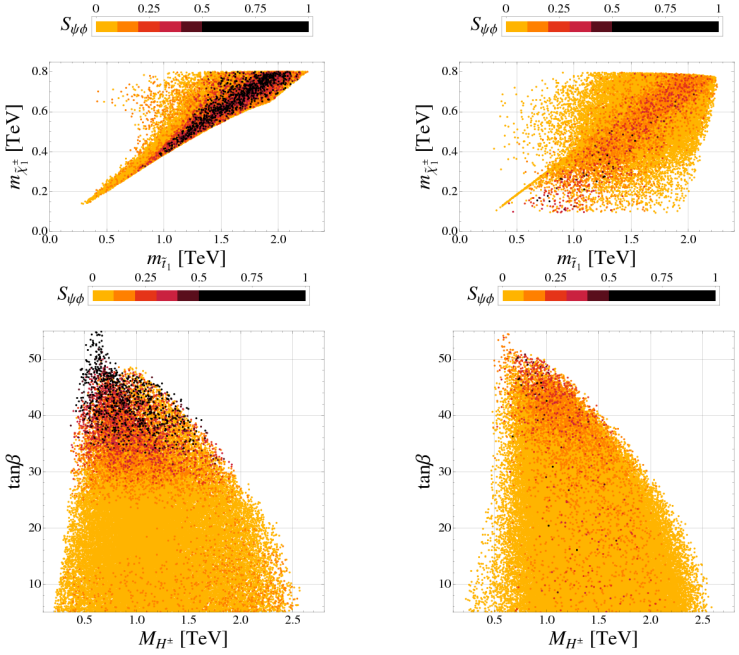

Figure 5.13: First row: The plane of the lightest stop mass ($m_{\tilde{t}_1}$) vs. the lightest chargino mass ($m_{\tilde{\chi}_1^\pm}$). Second row: the plane of the charged Higgs mass $M_{H^\pm}$ vs. $\tan\beta$. The first column corresponds to the AC model; the second to the RVV2 model. The different colors show the possible values for $S_{\psi\phi}$ in these models as indicated in the overall bar.

cannot be so large to cover the entire range for $S_{\psi\phi}$ ($-1 < S_{\psi\phi} < 1$). Hence we can write

$$(S_{\psi\phi})^{\max}_{\rm RVV2} < (S_{\psi\phi})^{\max}_{\rm RS} \approx (S_{\psi\phi})^{\max}_{\rm AC}\,. \tag{5.25}$$

- While $\mathrm{Br}(B_s \to \mu^+\mu^-)$ in the two supersymmetric flavor models can get huge NP contributions, the enhancements of $\mathrm{Br}(B_s \to \mu^+\mu^-)$ in the RS model with custodial protection do not exceed 10%. The feature is strongly connected to the custodial protection of some of the Z boson couplings (see Sec. 5.3.3).

- The opposite pattern is found for the $K \to \pi\nu\bar{\nu}$ decays. In the two supersymmetric flavor models, $\mathrm{Br}(K \to \pi\nu\bar{\nu})$ are basically SM-like. On the other hand in the RS model the $\mathrm{Br}(K \to \pi\nu\bar{\nu})$ can be enhanced by as much as a factor 1.6 (for $\mathrm{Br}(K^+ \to \pi^+\nu\bar{\nu})$) and 2.5 (for $\mathrm{Br}(K_L \to \pi^0\nu\bar{\nu})$).

- Particularly interesting would be the consequences of a confirmation of a large value for the CP violating asymmetry $S_{\psi\phi}$ by future experiments:

  – The AC abelian model would imply a lower bound on $\mathrm{Br}(B_s \to \mu^+\mu^-)$ significantly higher than possible values that the RS model with custodial protection can reach. Consequently simply the measurement of $\mathrm{Br}(B_s \to \mu^+\mu^-)$ could distinguish the two models.

	AC	RVV2	RS
$D^0 - \bar{D}^0$	★★★	★	?
ε_K	★	★★★	★★★
$S_{\psi\phi}$	★★★	★★★	★★★
$A_{\rm CP}\,(B \to X_s\gamma)$	★	★	?
$B_s \to \mu^+\mu^-$	★★★	★★★	★
$B_d \to \mu^+\mu^-$	★★★	★★★	★
$K^+ \to \pi^+\nu\bar{\nu}$	★	★	★★★
$K_L \to \pi^0\nu\bar{\nu}$	★	★	★★★
$\mu \to e\gamma$	★★★	★★★	★★★

Table 5.4: "DNA" of flavor physics effects for the flavor observables studied in this thesis in the two Susy flavor models and in the RS model with custodial protection. ★★★ signals large effects and ★ implies that the given model does not predict sizable effects in that observable. Finally with "?" we indicate those flavor observables that are not studied in the literature yet.

  - The RS model with custodial protection would exclude the possibility to have large NP contributions in the $\mathrm{Br}(K \to \pi\nu\bar{\nu})$ decays. Hence in that case, it would be really difficult to distinguish the RS model from the two Susy flavor models. However, this prediction of the RS model could provide the possibility to future experiments on the rare K decays to put under pressure the model, in the case of a discovery of a non-SM K decay branching ratio.

- The AC abelian model and the RVV2 non abelian model predict an opposite pattern for the observables of the $D^0 - \bar{D}^0$ mixing system: a strong enhancement is in general predicted by the AC model, a SM-like $D^0 - \bar{D}^0$ mixing is predicted by the RVV2 model. As noticed in Secs. 5.2.4, 5.2.5, this feature is a general feature of abelian and non abelian flavor models, independently of their characteristics (e.g., flavor group, pattern of flavor symmetry breaking). Possibly, this different prediction of abelian and non abelian flavor models could be tested by a SuperB factory [234, 235].

We conclude this chapter with Tab. 5.4, which reports a summary of the potential size of deviation from the SM results allowed for the observables considered in the text, when all existing constraints from the well measured observables of Tabs. 4.5 and 5.3 are taken into account. We distinguish among

- large effects (three *red* stars),
- vanishingly small effects (one *black* star).

This table can be considered as the collection of the DNA's for various models. These DNA's will be modified as new experimental data will be available and in certain cases will allow us to declare certain models to be disfavored or even ruled out.

The table does not take into account possible correlations among the observables listed there. As we have explained above, the correlations are additional informations that can be really useful in order to distinguish between the different models. We have shown in fact that in some models, it is not possible to obtain large effects simultaneously for certain pairs or sets of observables and consequently future measurements of a few observables listed in Tab. 5.4 will have an impact on the patterns for the other observables shown in this DNA table. It will be really interesting to monitor the changes in this table when the future experiments will provide new results on flavor observables.

Chapter 6

Summary and outlook

The Randall-Sundrum model with custodial protection and the MSSM based on a flavor symmetry are two of the most sound theories beyond the Standard Model. They represent two very interesting possibilities to address both the gauge hierarchy problem and the Standard Model flavor puzzle in generating strongly hierarchical quark masses and mixing angles. While the starting point of the MSSM is a *symmetry principle*, the one of the RS model is *geometry*. In fact, while in Susy flavor models the gauge hierarchy problem is solved by relating bosonic and fermionic degrees of freedom through Supersymmetry, in the RS model it is addressed by the virtue of the warped background metric. Analogously, while in Susy flavor models the generation of a hierarchical quark spectrum relies on abelian or non abelian flavor symmetries á la Froggatt-Nielsen, in the RS model it is achieved by the non-uniform localization of the quark field shape functions along the fifth dimension.

However the general MSSM exhibits a severe difficulty in being in agreement with the experiments on flavor changing neutral observables, since the New Physics effects in flavor changing neutral currents are generically too large to be in accordance with the data which amazingly confirm the Cabibbo-Kobayashi-Maskawa picture of the Standard Model. Nevertheless, implementing a flavor symmetry in the MSSM softens naturally the problem. Abelian flavor symmetries enforce indeed an approximate alignment between down type squark masses and down Yukawa couplings. Non abelian flavor symmetries instead accomplish an approximate degeneracy between the several squark masses (both of the up type and down type). Both effects (alignment and degeneracy) induce a strong reduction of the off-diagonal entries in the squarks soft mass matrices and hence a limitation of the New Physics effects in flavor changing neutral currents, that will appear as functions of small flavor symmetry breaking parameters. Thus, Susy flavor models can address the New Physics flavor problem.

In parallel, also the RS model suffers in general from too large New Physics contributions to flavor changing neutral transitions. In fact, as a byproduct of the non-uniform localization of the SM fermions in the fifth dimension, flavor changing neutral currents appear in the model already at the tree level. However, the effects are strongly related to the difference in mass of the SM quarks involved in the transition. Hence flavor changing transitions involving the first two generation quarks will be protected from too large

New Physics effects (*RS-GIM mechanism*). Additionally, the RS model with custodial protection, namely with an additional $SU(2)_R \times P_{LR}$ gauge symmetry in the bulk, can ameliorate the NP flavor problems thanks also to the protection of several off-diagonal couplings of the SM Z boson with quarks.

After having discussed quantitatively how to address the NP flavor puzzle in the two frameworks, we analyzed in detail several flavor observables with the main aim to show some possible recipes to distinguish the two Susy flavor models analyzed by us from the RS model with custodial protection with the use of low energy observables, once that new data will be available. Quite importantly, we decided to fix a not too high NP energy scale in both frameworks, in order not to compromise the possibility to have direct detection of new particles at the LHC. In particular in the RS model we have set $M_{\rm KK} \simeq (2-3)\,\text{TeV}$, while in the Susy flavor models we have scanned over the soft Susy scale $m_0 < 2\,\text{TeV}$. Our study was twofold: first we investigated the New Physics effects on meson-antimeson oscillation observables; secondly, we analyzed the possible implications in the rare K and B decays. For both sets of observables, we first derived analytic expressions in the two frameworks, hinting already on the possible numerical results, and subsequently we performed a global numerical analysis.

In the $\Delta F = 2$ sector we focused mainly on the mass differences ΔM_K, ΔM_s and ΔM_d of the $K^0 - \bar{K}^0$, $B_s^0 - \bar{B}_s^0$ and $B_d^0 - \bar{B}_d^0$ systems, respectively, and on the CP violating asymmetries ε_K and $S_{\psi K_s}$, with the main purpose to constrain the parameter space of the two frameworks, imposing the strict experimental bounds coming from these observables. Subsequently we analyzed the NP effects on the CP violating observable of the $B_s^0 - \bar{B}_s^0$ system, $S_{\psi\phi}$, showing explicitely the possibility of having large NP contributions, while being compatible with the several constraints coming from the other $\Delta F = 2$ observables. This is certainly an important message from both NP frameworks, in the light of the recent hints of CDF and D0 on the presence of NP effects in $S_{\psi\phi}$. Finally we have studied the role of the $D^0 - \bar{D}^0$ mixing in the Susy flavor models. Here a summary of our main findings in the $\Delta F = 2$ sector

- In the RS model with custodial protection

  1. $K^0 - \bar{K}^0$ oscillations are dominated by the chirality-flipping operator $\mathcal{Q}_2^{LR}$ which is strongly chiral and QCD enhanced. Only KK gluons are responsible for that operator and hence the KK gluons bring the most important contribution.
  2. In the $B_{s,d}^0 - \bar{B}_{s,d}^0$ systems the SM operator $\mathcal{Q}_1^{VLL}$ is competitive with $\mathcal{Q}_2^{LR}$, since the latter is weaker QCD and chirally enhanced in the B system than in the K system. Hence the EW gauge bosons Z_H and Z' and the KK gluons are equally important.
  3. The strongest constraint is represented by the CP violating observable ε_K. Our fine-tuning analysis shows that to have agreement with the data, with an average of fine-tuning smaller than 20 and completely anarchical 5D Yukawa couplings, a $M_{\rm KK}$ scale of around 20 TeV would be required. However, even for $M_{\rm KK} \simeq (2-3)\,\text{TeV}$, the constraint from ε_K can be satisfied with a moderate fine-tuning, if the assumption of strictly anarchic Yukawa couplings is slightly

relaxed. No particular problem arises in fitting all the other well measured $\Delta F = 2$ observables with a low level of fine-tuning.

4. Having imposed all the $\Delta F = 2$ constraints, large NP effects in the CP asymmetry $S_{\psi\phi}$ are still possible, such that the entire range $-1 < S_{\psi\phi} < 1$ can be reached. Because of the strong correlation with the semileptonic asymmetry $A^s_{\rm SL}$, also the latter observable can be highly enhanced (by two orders of magnitude), when compared to the SM prediction.

- In the two Susy flavor models

1. Both $K^0 - \bar{K}^0$ and $B^0_{s,d} - \bar{B}^0_{s,d}$ oscillations are dominated by the chirality-flipping operator $\mathcal{Q}_2^{LR}$ because of a strong QCD enhancement and a large loop function.
2. In the abelian flavor model the constraints coming from $D^0 - \bar{D}^0$ mixing are quite severe and impose the soft Susy mass scale m_0 to be relatively high. Vice versa, in the non abelian flavor model the $D^0 - \bar{D}^0$ mixing does not represent a serious restriction, and hence also lighter soft Susy mass scales are acceptable.
3. In the abelian flavor model no other important constraint is arising from $\Delta F = 2$ transitions. Vice versa, in the non abelian flavor model the CP violating observable ε_K can receive in general sizable NP contributions, both coming from gluino boxes and from double Higgs penguins. However, the constraint coming from the data can be accommodated by the model relatively easily.
4. Concerning the B_s meson mixing system, in the abelian flavor model effects are coming mainly from double Higgs penguins that are not suppressed by the Susy mass scale m_0. Contrary, in the non abelian flavor model the effects of the double Higgs penguins are comparable to those arising from the gluino boxes. In both models large values of the CP violating asymmetry $S_{\psi\phi}$ can be reached, with in general slightly larger effects in the abelian model than in the non abelian one.
5. Finally, especially in the case of the abelian flavor model, large effects in $S_{\psi\phi}$ can be possible also for a quite heavy spectrum. Hence, there exist regions of the SUSY parameter space at the border or even beyond the LHC reach where we can expect clear non-standard signals in flavor processes.

It is also important to notice that the points 2.-3. are always valid, independently of the particular flavor model analyzed. They are simply a result of abelian and non abelian flavor symmetries.

Subsequently we determined the size of NP effects in various rare B and K decays that remain possible after imposing all existing constraints from the $\Delta F = 2$ transitions analyzed previously and from other relevant constraints such as from $\mathrm{Br}(b \to s\gamma)$ in the Susy flavor models. We considered for both frameworks the branching ratios of the decay modes $K^+ \to \pi^+\nu\bar{\nu}$, $K_L \to \pi^0\nu\bar{\nu}$, $B_{s,d} \to \mu^+\mu^-$ and finally of $K_L \to \mu^+\mu^-$ in the RS model. More specifically we investigated first the several branching ratios and secondly the possible correlations between them and together with $S_{\psi\phi}$. Here we summarize the main results we obtained

- In the RS model with custodial protection

  1. The main contributions, both in rare K and B decays, are coming from the exchange at the tree level of the SM Z boson, coupled with right handed down quarks.
  2. Strong enhancements are possible in the rare K decays. Vice versa, quite small effects (up to $(10-20)\%$) are found for the rare B decays. This opposite pattern of K and B decays is a result of the custodial protection of the model, that affects more the B sector than the K sector.
  3. The CP asymmetry $S_{\psi\phi}$ is strongly correlated with the rare K decay branching ratios. Simultaneous large enhancements in both systems are strongly disfavored.
  4. Because of the quite small NP effects in rare B decays, the possibility to distinguish the RS model from models with Minimal Flavor Violation using only rare B decays (such as the correlation predicted by MFV models between the branching ratios of $B_s \to \mu^+\mu^-$ and of $B_d \to \mu^+\mu^-$) is quite unlikely. More promising is the investigation of correlations between rare B and K decays, such as between $K_L \to \mu^+\mu^-$ and $B_s \to \mu^+\mu^-$.

- In the two Susy flavor models

  1. The rare K decay branching ratios are SM-like.
  2. The rare B decay branching ratios can get huge NP effects, thanks to the Higgs penguin contribution. In particular in the abelian model the experimental bound on the branching ratio of $B_s \to \mu^+\mu^-$ can be reached.
  3. A strong correlation between the asymmetry $S_{\psi\phi}$ and $\mathrm{Br}(B_s \to \mu^+\mu^-)$ arises in the abelian model: the confirmation of a non SM-like $S_{\psi\phi}$ at future experiments would lead to a quite high lower bound on the braching ratio of $B_s \to \mu^+\mu^-$, at the level of 10^{-8}.
  4. The prediction of MFV models for the correlation between $\mathrm{Br}(B_s \to \mu^+\mu^-)$ and $\mathrm{Br}(B_d \to \mu^+\mu^-)$ can be strongly broken in both Susy flavor models, opening the possibility to distinguish between them and the MFV framework as soon as new data on rare B decays will be available.

This summary shows that the simultaneous study of various flavor violating processes can allow us to distinguish the two New Physics frameworks. For this reason, we proposed a DNA-flavor test that will help us to shed light on the "correct" New Physics model, once that new data on flavor observables will be available.

In particular we have shown the big role of $S_{\psi\phi}$ and of the braching ratio of $B_s \to \mu^+\mu^-$ in distinguishing between the three models analyzed throughout this thesis. It will be of course of great interest to monitor the future results of LHCb and of Tevatron on the two observables, in order to start to disentangle between the several New Physics theories, using low energy observables.

In conclusion, flavor physics might prove itself again to be one of the big actors in particle physics and it can play a major role in letting us understand whether nature possesses supersymmetry, or whether other scenarios like the Randall-Sundrum model with custodial protection are realized in nature.

Appendix A

Basic notation and formulae for WED models

In this Appendix we report the main formulae and concepts of warped extra dimensional models, that were not introduced in the main text, since they were not crucial for the main line of this thesis.

Neglecting the possible brane kinetic terms for gauge bosons, the action of a free gauge boson in a warped metric is given by

$$S_V = \int d^4x \int_0^L dy \sqrt{G} \left(-\frac{1}{4} F_{MN} F^{MN} \right) + h.c. \,, \tag{A.1}$$

where $F^{MN} = \partial^M V^N - \partial^N V^M$ is the field strength tensor.

The variation principle $\delta S_V = 0$ yields to the equation of motion [47]

$$\left[-e^{-2ky} \eta^{\mu\nu} \partial_\mu \partial_\nu + e^{2ky} \partial_5 \left(e^{-2ky} \partial_5 \right) \right] V_\alpha(x^\mu, y) = 0 \,. \tag{A.2}$$

To solve this differential equation, we make use of the KK decomposition, employed already for the fermion fields in Eq. (2.9)

$$V_\alpha(x^\mu, y) = \frac{1}{\sqrt{L}} \sum_{n=0}^{\infty} V_\alpha^{(n)}(x^\mu) f_V^{(n)}(y) \,. \tag{A.3}$$

Inserting then this KK tower of fields inside the equation of motion (A.2), one finds

$$\left[\partial_5^2 - 2k\partial_5 + e^{2ky} m_n^2 \right] f_V^{(n)}(y) = 0 \,, \tag{A.4}$$

where m_n is the mass of the n-th KK mode gauge boson, given by

$$\eta^{\mu\nu} \partial_\mu \partial_\nu V_\alpha^{(n)}(x^\mu) = m_n^2 V_\alpha^{(n)} \,. \tag{A.5}$$

As discussed for the fermion fields in Sec. 2.2.1, in order to solve the equation of motion for the gauge bosons, one has to specify the BCs. Usually, the BCs adopted are

- Dirichlet BC $(-)$: $f_V^{(n)}(y)\Big|_{\text{brane}} = 0$,

- Neumann BC (+): $\partial_5 f_V^{(n)}(y)\Big|_{\text{brane}} = 0$.

The solutions of the equation of motion (A.4) are then given by

$$f_V^{(0)}(y) = 1\,, \tag{A.6}$$

$$f_V^{(n)}(y) = \frac{e^{ky}}{N_n}\left[J_1\left(\frac{m_n}{k}e^{ky}\right) + b_1(m_n)Y_1\left(\frac{m_n}{k}e^{ky}\right)\right] \qquad (n = 1, 2, ...)\,, \tag{A.7}$$

where J, Y are the Bessel function of first and second kind, respectively, N_n is the normalization factor of the gauge field set by the condition

$$\frac{1}{L}\int_0^L dy\, f_V^{(n)}(y) f_V^{(m)}(y) = \delta_{mn}\,, \tag{A.8}$$

and where, as in the case of fermions, the zero mode $f_V^{(0)}$ exists only for (++) BCs and it corresponds to a SM gauge boson. An interesting and phenomenologically important feature is that all KK excitation gauge bosons are strongly peaked towards the IR brane as can be seen from the exponential factor in front of (A.7).
The coefficient $b_1(m_n)$ and the mass of the n-th KK state m_n depend on the boundary conditions on the branes. For (++) fields one obtains [47]

$$b_1(m_n) = -\frac{J_1(m_n/k) + m_n/k\, J_1'(m_n/k)}{Y_1(m_n/k) + m_n/k\, Y_1'(m_n/k)} = b_1(m_n e^{kL})\,, \tag{A.9}$$

which can be solved numerically. However, for the first excited state the approximate expression

$$m_1(++) \simeq 2.45 f \tag{A.10}$$

holds (where f was defined in Sec. 2.2.1).

For (−+) fields instead one obtains [47]

$$b_1(m_n) = -\frac{J_1(m_n e^{kL}/k) + m_n e^{kL}/k\, J_1'(m_n e^{kL}/k)}{Y_1(m_n e^{kL}/k) + m_n e^{kL}/k\, Y_1'(m_n e^{kL}/k)} = -\frac{J_1(m_n/k)}{Y_1(m_n/k)}\,. \tag{A.11}$$

For the first excited state the approximate expression

$$m_1(-+) \simeq 2.40 f \tag{A.12}$$

holds.

Appendix B

Couplings and charge factors in the RS model

In this Appendix we list all the couplings and the charge factors that were used in this thesis. They can be easily worked out using the formulae of Eqs. (3.40), (3.41), and the quantum numbers of the several fermions presented in Eqs. (2.34)-(2.36). However, for completeness, we report here the explicit form.

First, we give the charge factors in the couplings of SM down quarks (both left and right handed) to the Z and Z_X gauge bosons

$$g^{4D}_{Z,L}(d) = \frac{g^{4D}}{\cos\psi}\left[-\frac{1}{2}+\frac{1}{3}\sin^2\psi\right], \quad g^{4D}_{Z,R}(d) = \frac{g^{4D}}{\cos\psi}\left[\frac{1}{3}\sin^2\psi\right], \tag{B.1}$$

$$\kappa^{4D}_{Z,L}(d) = \frac{g^{4D}}{\cos\phi}\left[-\frac{1}{2}-\frac{1}{6}\sin^2\phi\right], \quad \kappa^{4D}_{Z,R}(d) = \frac{g^{4D}}{\cos\phi}\left[-1+\frac{1}{3}\sin^2\phi\right]. \tag{B.2}$$

Analogously, the charge factors in the couplings of SM up quarks (both left and right handed) to the Z and Z_X gauge bosons read

$$g^{4D}_{Z,L}(u) = \frac{g^{4D}}{\cos\psi}\left[\frac{1}{2}-\frac{2}{3}\sin^2\psi\right], \quad g^{4D}_{Z,R}(u) = \frac{g^{4D}}{\cos\psi}\left[-\frac{2}{3}\sin^2\psi\right], \tag{B.3}$$

$$\kappa^{4D}_{Z,L}(u) = \frac{g^{4D}}{\cos\phi}\left[-\frac{1}{2}-\frac{1}{6}\sin^2\phi\right], \quad \kappa^{4D}_{Z,R}(u) = \frac{g^{4D}}{\cos\phi}\left[-\frac{2}{3}\sin^2\phi\right]. \tag{B.4}$$

Finally, the charge factors in the couplings of the additional vector-like fermion fields (χ^{u^i}, χ^{d^i}, U'^i, U''^i and D'^i) to the Z, Z_X gauge bosons are given by

$$g_Z^{4D}\left(\chi^u\right) = \frac{g^{4D}}{\cos\psi}\left[\frac{1}{2}-\frac{5}{3}\sin^2\psi\right], \quad \kappa_Z^{4D}\left(\chi^u\right) = \frac{g^{4D}}{\cos\phi}\left[\frac{1}{2}-\frac{7}{6}\sin^2\phi\right], \tag{B.5}$$

$$g_Z^{4D}\left(\chi^d\right) = \frac{g^{4D}}{\cos\psi}\left[-\frac{1}{2}-\frac{2}{3}\sin^2\psi\right], \quad \kappa_Z^{4D}\left(\chi^d\right) = \frac{g^{4D}}{\cos\phi}\left[-\frac{1}{2}+\frac{5}{6}\sin^2\phi\right], \tag{B.6}$$

$$g_Z^{4D}\left(U'\right) = \frac{g^{4D}}{\cos\psi}\left[-\frac{2}{3}\sin^2\psi\right], \quad \kappa_Z^{4D}\left(U'\right) = \frac{g^{4D}}{\cos\phi}\left[-\frac{2}{3}\sin^2\phi\right], \tag{B.7}$$

$$g_Z^{4D}(U'') = \frac{g^{4D}}{\cos\psi}\left[-\frac{2}{3}\sin^2\psi\right], \quad \kappa_Z^{4D}\left(U''\right) = \frac{g^{4D}}{\cos\phi}\left[-\frac{2}{3}\sin^2\phi\right], \tag{B.8}$$

$$g_Z^{4D}\left(D'\right) = \frac{g^{4D}}{\cos\psi}\left[-1+\frac{1}{3}\sin^2\psi\right], \quad \kappa_Z^{4D}\left(D'\right) = \frac{g^{4D}}{\cos\psi}\left[\frac{4}{3}\sin^2\phi\right]. \tag{B.9}$$

Appendix C

Explicit expressions for the loop functions

C.1 Loop functions for the $\Delta F = 2$ mixing amplitudes

SM contribution

$$S_0(x) = \frac{4x - 11x^2 + x^3}{4(1-x)^2} - \frac{3x^3 \log x}{2(1-x)^3}\,, \tag{C.1}$$

$$S_0(x,y) = x\left(\log\frac{y}{x} - \frac{3xy}{4(1-y)} - \frac{3y^2\log y}{4(1-y)^2}\right)\,. \tag{C.2}$$

Gluino box contribution

$$g_1(x) = -\frac{11 + 144x + 27x^2 - 2x^3}{108(1-x)^4} - \frac{x(13+17x)}{18(1-x)^5}\log x\ , \tag{C.3}$$

$$g_2(x) = \frac{17x(x^3 - 9x^2 - 9x + 17)}{108(x-1)^5} + \frac{17x(1+3x)}{18(x-1)^5}\log x\ , \tag{C.4}$$

$$g_3(x) = -\frac{3}{17}g_2(x) = -\frac{x(x^3 - 9x^2 - 9x + 17)}{36(x-1)^5} - \frac{x(1+3x)}{6(x-1)^5}\log x\ , \tag{C.5}$$

$$g_4(x) = \frac{2 - 99x - 54x^2 + 7x^3}{18(1-x)^4} - \frac{x(5+19x)}{3(1-x)^5}\log x\ , \tag{C.6}$$

$$g_5(x) = -\frac{10 + 117x + 18x^2 - x^3}{54(1-x)^4} - \frac{x(11+13x)}{9(1-x)^5}\log x\ , \tag{C.7}$$

$$g_4'(x) = -\frac{11(-x^3 - 9x^2 + 9x + 1)}{54(x-1)^5} + \frac{11x(1+x)}{9(x-1)^5}\log x\ , \tag{C.8}$$

$$g_5'(x) = \frac{15}{11}g_4'(x) = -\frac{15(-x^3 - 9x^2 + 9x + 1)}{54(x-1)^5} + \frac{15x(1+x)}{9(x-1)^5}\log x\ . \tag{C.9}$$

Double Higgs penguin contribution

$$h_1(x) = \frac{4(1+x)}{3(1-x)^2} + \frac{8x}{3(1-x)^3}\log x\ , \tag{C.10}$$

$$h_2(x) = -\frac{4(2+5x-x^2)}{9(1-x)^3} - \frac{8x}{3(1-x)^4}\log x\ , \tag{C.11}$$

$$h_3(x) = -\frac{1}{2(1-x)} - \frac{x}{2(1-x)^2}\log x\ , \tag{C.12}$$

$$h_4(x,y) = -\frac{1}{(1-x)(1-y)} + \frac{x}{(1-x)^2(y-x)}\log x + \frac{y}{(1-y)^2(x-y)}\log y. \tag{C.13}$$

Chargino box contribution

$$f_1(x) = -\frac{x+1}{4(1-x)^2} - \frac{x}{2(1-x)^3}\log x\ , \tag{C.14}$$

$$f_3(x) = \frac{x^2-6x-17}{6(1-x)^4} - \frac{3x+1}{(1-x)^5}\log x\ . \tag{C.15}$$

C.2 Loop functions for the rare decays $K \to \pi\nu\bar{\nu}$

SM contribution

$$X(x) = \frac{x}{8}\left(\frac{x+2}{x-1} + \frac{3x-6}{(x-1)^2}\log x\right)\ . \tag{C.16}$$

Higgs penguin contribution

$$f_H(x) = \frac{x}{4(1-x)} + \frac{x}{4(1-x)^2}\log x\,, \tag{C.17}$$

$$H_2(x_1,x_2) = \frac{x_1\log x_1}{(1-x_1)(x_1-x_2)} + \frac{x_2\log x_2}{(1-x_2)(x_2-x_1)}\,, \tag{C.18}$$

$$H_3(x_1,x_2,x_3) = \frac{H_2(x_1,x_2)-H_2(x_1,x_3)}{x_2-x_3}\,. \tag{C.19}$$

Chargino box contribution

$$\ell_c(x) = -\frac{1-5x-2x^2}{6(1-x)^3} + \frac{x^2}{(1-x)^4}\log x\,. \tag{C.20}$$

C.3 Loop functions for the rare decays $B_q \to \mu^+\mu^-$

SM contribution

$$Y(x) = \frac{x}{8}\left(\frac{x-4}{x-1} + \frac{3x}{(x-1)^2}\log x\right), \tag{C.21}$$

$$Z(x) = -\frac{1}{9}\log x + \frac{18x^4 - 163x^3 + 259x^2 - 108x}{144(x-1)^3} + \frac{32x^4 - 38x^3 - 15x^2 + 18x}{72(x-1)^4}\log x\,. \tag{C.22}$$

C.4 ϵ resummation factor

$$f(x) = \frac{1}{1-x} + \frac{x}{(1-x)^2}\log x\ . \tag{C.23}$$

Bibliography

[1] E. Gildener, "Gauge Symmetry Hierarchies," *Phys. Rev.* **D14** (1976) 1667.

[2] E. Gildener and S. Weinberg, "Symmetry Breaking and Scalar Bosons," *Phys. Rev.* **D13** (1976) 3333.

[3] J. Wess and B. Zumino, "A Lagrangian Model Invariant Under Supergauge Transformations," *Phys. Lett.* **B49** (1974) 52.

[4] N. Arkani-Hamed, S. Dimopoulos, and G. R. Dvali, "The hierarchy problem and new dimensions at a millimeter," *Phys. Lett.* **B429** (1998) 263–272, `arXiv:hep-ph/9803315`.

[5] L. Randall and R. Sundrum, "A large mass hierarchy from a small extra dimension," *Phys. Rev. Lett.* **83** (1999) 3370–3373, `arXiv:hep-ph/9905221`.

[6] L. Susskind, "Dynamics of Spontaneous Symmetry Breaking in the Weinberg-Salam Theory," *Phys. Rev.* **D20** (1979) 2619–2625.

[7] N. Arkani-Hamed, A. G. Cohen, and H. Georgi, "Electroweak symmetry breaking from dimensional deconstruction," *Phys. Lett.* **B513** (2001) 232–240, `arXiv:hep-ph/0105239`.

[8] N. Arkani-Hamed, A. G. Cohen, E. Katz, and A. E. Nelson, "The littlest Higgs," *JHEP* **07** (2002) 034, `arXiv:hep-ph/0206021`.

[9] H. P. Nilles, "Supersymmetry, Supergravity and Particle Physics," *Phys. Rept.* **110** (1984) 1–162.

[10] M. Kobayashi and T. Maskawa, "CP Violation in the Renormalizable Theory of Weak Interaction," *Prog. Theor. Phys.* **49** (1973) 652–657.

[11] S. L. Glashow, J. Iliopoulos, and L. Maiani, "Weak Interactions with Lepton-Hadron Symmetry," *Phys. Rev.* **D2** (1970) 1285–1292.

[12] M. K. Gaillard and B. W. Lee, "Rare Decay Modes of the K-Mesons in Gauge Theories," *Phys. Rev.* **D10** (1974) 897.

[13] P. J. Franzini, "B anti-B Mixing: A Review of Recent Progress," *Phys. Rept.* **173** (1989) 1.

[14] F. Jegerlehner and A. Nyffeler, "The Muon g-2," *Phys. Rept.* **477** (2009) 1–110, arXiv:0902.3360 [hep-ph].

[15] A. Lenz and U. Nierste, "Theoretical update of $B_s - \bar{B}_s$ mixing," *JHEP* **06** (2007) 072, arXiv:hep-ph/0612167.

[16] **UTfit** Collaboration, M. Bona *et al.*, "First Evidence of New Physics in $b \longleftrightarrow s$ Transitions," *PMC Phys.* **A3** (2009) 6, arXiv:0803.0659 [hep-ph].

[17] N. Cabibbo, "Unitary Symmetry and Leptonic Decays," *Phys. Rev. Lett.* **10** (1963) 531–533.

[18] A. J. Buras and D. Guadagnoli, "Correlations among new CP violating effects in Δ F = 2 observables," *Phys. Rev.* **D78** (2008) 033005, arXiv:0805.3887 [hep-ph].

[19] A. J. Buras and D. Guadagnoli, "On the consistency between the observed amount of CP violation in the K^- and Bd-systems within minimal flavor violation," *Phys. Rev.* **D79** (2009) 053010, arXiv:0901.2056 [hep-ph].

[20] E. Lunghi and A. Soni, "Possible Indications of New Physics in B_d -mixing and in sin(2 beta) Determinations," *Phys. Lett.* **B666** (2008) 162–165, arXiv:0803.4340 [hep-ph].

[21] E. Lunghi and A. Soni, "Hints for the scale of new CP-violating physics from B-CP anomalies," *JHEP* **08** (2009) 051, arXiv:0903.5059 [hep-ph].

[22] **UTfit** Collaboration, M. Bona *et al.*, "The UTfit collaboration report on the status of the unitarity triangle beyond the standard model. I: Model- independent analysis and minimal flavour violation," *JHEP* **03** (2006) 080, arXiv:hep-ph/0509219.

[23] **CKMfitter Group** Collaboration, J. Charles *et al.*, "CP violation and the CKM matrix: Assessing the impact of the asymmetric B factories," *Eur. Phys. J.* **C41** (2005) 1–131, arXiv:hep-ph/0406184.

[24] K. G. Wilson, "Nonlagrangian models of current algebra," *Phys. Rev.* **179** (1969) 1499–1512.

[25] K. G. Wilson, "The Renormalization Group and Strong Interactions," *Phys. Rev.* **D3** (1971) 1818.

[26] M. K. Gaillard and B. W. Lee, "Delta I = 1/2 Rule for Nonleptonic Decays in Asymptotically Free Field Theories," *Phys. Rev. Lett.* **33** (1974) 108.

[27] G. Altarelli and L. Maiani, "Octet Enhancement of Nonleptonic Weak Interactions in Asymptotically Free Gauge Theories," *Phys. Lett.* **B52** (1974) 351–354.

[28] E. Witten, "Short Distance Analysis of Weak Interactions," *Nucl. Phys.* **B122** (1977) 109.

[29] B. Guberina and R. D. Peccei, "Quantum Chromodynamic Effects and CP Violation in the Kobayashi-Maskawa Model," *Nucl. Phys.* **B163** (1980) 289.

[30] G. Buchalla, A. J. Buras, and M. E. Lautenbacher, "Weak decays beyond leading logarithms," *Rev. Mod. Phys.* **68** (1996) 1125–1144, arXiv:hep-ph/9512380.

[31] A. J. Buras, "Weak Hamiltonian, CP violation and rare decays," arXiv:hep-ph/9806471.

[32] G. Isidori, Y. Nir, and G. Perez, "Flavor Physics Constraints for Physics Beyond the Standard Model," arXiv:1002.0900 [hep-ph].

[33] R. Franceschini and S. Gori, "Solving the mu problem with a heavy Higgs boson," arXiv:1005.1070 [hep-ph].

[34] K. Agashe, A. Delgado, and R. Sundrum, "Grand unification in RS1," *Ann. Phys.* **304** (2003) 145–164, arXiv:hep-ph/0212028.

[35] K. Agashe and G. Servant, "Warped unification, proton stability and dark matter," *Phys. Rev. Lett.* **93** (2004) 231805, arXiv:hep-ph/0403143.

[36] K. Agashe, A. Falkowski, I. Low, and G. Servant, "KK Parity in Warped Extra Dimension," *JHEP* **04** (2008) 027, arXiv:0712.2455 [hep-ph].

[37] K. Agashe and G. Servant, "Baryon number in warped GUTs: Model building and (dark matter related) phenomenology," *JCAP* **0502** (2005) 002, arXiv:hep-ph/0411254.

[38] G. Panico, E. Ponton, J. Santiago, and M. Serone, "Dark Matter and Electroweak Symmetry Breaking in Models with Warped Extra Dimensions," *Phys. Rev.* **D77** (2008) 115012, arXiv:0801.1645 [hep-ph].

[39] G. Nordstrom, "Über die Möglichkeit, das elektromagnetische Feld und das Gravitationsfeld zu vereinigen," *Physikalische Zeitschrift* **15** (1914) 1762351.

[40] T. Kaluza *Sitzungsber. Preuss. Akad. Wiss. Berlin (Math. Phys.)* (1921) 966972.

[41] O. Klein *Zeitschrift fr Physik a Hadrons and Nuclei* **37 (12)** (1926) 895906.

[42] I. Antoniadis, "A Possible new dimension at a few TeV," *Phys. Lett.* **B246** (1990) 377–384.

[43] I. Antoniadis, N. Arkani-Hamed, S. Dimopoulos, and G. R. Dvali, "New dimensions at a millimeter to a Fermi and superstrings at a TeV," *Phys. Lett.* **B436** (1998) 257–263, arXiv:hep-ph/9804398.

[44] N. Arkani-Hamed, S. Dimopoulos, and G. R. Dvali, "Phenomenology, astrophysics and cosmology of theories with sub-millimeter dimensions and TeV scale quantum gravity," *Phys. Rev.* **D59** (1999) 086004, arXiv:hep-ph/9807344.

[45] H. Davoudiasl, J. L. Hewett, and T. G. Rizzo, "Bulk gauge fields in the Randall-Sundrum model," *Phys. Lett.* **B473** (2000) 43–49, arXiv:hep-ph/9911262.

[46] A. Pomarol, "Gauge bosons in a five-dimensional theory with localized gravity," *Phys. Lett.* **B486** (2000) 153–157, arXiv:hep-ph/9911294.

[47] T. Gherghetta and A. Pomarol, "Bulk fields and supersymmetry in a slice of AdS," *Nucl. Phys.* **B586** (2000) 141–162, arXiv:hep-ph/0003129.

[48] S. Chang, J. Hisano, H. Nakano, N. Okada, and M. Yamaguchi, "Bulk standard model in the Randall-Sundrum background," *Phys. Rev.* **D62** (2000) 084025, arXiv:hep-ph/9912498.

[49] Y. Grossman and M. Neubert, "Neutrino masses and mixings in non-factorizable geometry," *Phys. Lett.* **B474** (2000) 361–371, arXiv:hep-ph/9912408.

[50] S. J. Huber, "Flavor violation and warped geometry," *Nucl. Phys.* **B666** (2003) 269–288, arXiv:hep-ph/0303183.

[51] K. Agashe, G. Perez, and A. Soni, "Flavor structure of warped extra dimension models," *Phys. Rev.* **D71** (2005) 016002, arXiv:hep-ph/0408134.

[52] T. Appelquist, H.-C. Cheng, and B. A. Dobrescu, "Bounds on universal extra dimensions," *Phys. Rev.* **D64** (2001) 035002, arXiv:hep-ph/0012100.

[53] S. J. Huber and Q. Shafi, "Higgs mechanism and bulk gauge boson masses in the Randall-Sundrum model," *Phys. Rev.* **D63** (2001) 045010, arXiv:hep-ph/0005286.

[54] C. Csaki, J. Erlich, and J. Terning, "The effective Lagrangian in the Randall-Sundrum model and electroweak physics," *Phys. Rev.* **D66** (2002) 064021, arXiv:hep-ph/0203034.

[55] G. Burdman, "Constraints on the bulk standard model in the Randall- Sundrum scenario," *Phys. Rev.* **D66** (2002) 076003, arXiv:hep-ph/0205329.

[56] C. Csaki, C. Grojean, H. Murayama, L. Pilo, and J. Terning, "Gauge theories on an interval: Unitarity without a Higgs," *Phys. Rev.* **D69** (2004) 055006, arXiv:hep-ph/0305237.

[57] S. Casagrande, F. Goertz, U. Haisch, M. Neubert, and T. Pfoh, "Flavor Physics in the Randall-Sundrum Model: I. Theoretical Setup and Electroweak Precision Tests," arXiv:0807.4937 [hep-ph].

[58] C. D. Froggatt and H. B. Nielsen, "Hierarchy of Quark Masses, Cabibbo Angles and CP Violation," *Nucl. Phys.* **B147** (1979) 277.

[59] M. Blanke, A. J. Buras, B. Duling, S. Gori, and A. Weiler, "$\Delta F = 2$ Observables and Fine-Tuning in a Warped Extra Dimension with Custodial Protection," *JHEP* **03** (2009) 001, arXiv:0809.1073 [hep-ph].

[60] K. Agashe, A. Delgado, M. J. May, and R. Sundrum, "RS1, custodial isospin and precision tests," *JHEP* **08** (2003) 050, arXiv:hep-ph/0308036.

[61] C. Csaki, C. Grojean, L. Pilo, and J. Terning, "Towards a realistic model of Higgsless electroweak symmetry breaking," *Phys. Rev. Lett.* **92** (2004) 101802, arXiv:hep-ph/0308038.

[62] K. Agashe, R. Contino, and A. Pomarol, "The Minimal Composite Higgs Model," *Nucl. Phys.* **B719** (2005) 165–187, arXiv:hep-ph/0412089.

[63] M. S. Carena, E. Ponton, J. Santiago, and C. E. M. Wagner, "Light Kaluza-Klein states in Randall-Sundrum models with custodial $SU(2)$," *Nucl. Phys.* **B759** (2006) 202–227, arXiv:hep-ph/0607106.

[64] K. Agashe, R. Contino, L. Da Rold, and A. Pomarol, "A custodial symmetry for $Zb\bar{b}$," *Phys. Lett.* **B641** (2006) 62–66, arXiv:hep-ph/0605341.

[65] G. Cacciapaglia, C. Csaki, G. Marandella, and J. Terning, "A New Custodian for a Realistic Higgsless Model," *Phys. Rev.* **D75** (2007) 015003, arXiv:hep-ph/0607146.

[66] A. Djouadi, G. Moreau, and F. Richard, "Resolving the A_{FB}^b puzzle in an extra dimensional model with an extended gauge structure," *Nucl. Phys.* **B773** (2007) 43–64, arXiv:hep-ph/0610173.

[67] R. Contino, L. Da Rold, and A. Pomarol, "Light custodians in natural composite Higgs models," *Phys. Rev.* **D75** (2007) 055014, arXiv:hep-ph/0612048.

[68] M. Bauer, S. Casagrande, L. Grunder, U. Haisch, and M. Neubert, "Little Randall-Sundrum models: ϵ_K strikes again," *Phys. Rev.* **D79** (2009) 076001, arXiv:0811.3678 [hep-ph].

[69] M. Bauer, S. Casagrande, U. Haisch, and M. Neubert, "Flavor Physics in the Randall-Sundrum Model: II. Tree- Level Weak-Interaction Processes," arXiv:0912.1625 [hep-ph].

[70] M. E. Peskin and T. Takeuchi, "Estimation of oblique electroweak corrections," *Phys. Rev.* **D46** (1992) 381–409.

[71] S. J. Huber, C.-A. Lee, and Q. Shafi, "Kaluza-Klein excitations of W and Z at the LHC?," *Phys. Lett.* **B531** (2002) 112–118, arXiv:hep-ph/0111465.

[72] J. L. Hewett, F. J. Petriello, and T. G. Rizzo, "Precision measurements and fermion geography in the Randall-Sundrum model revisited," *JHEP* **09** (2002) 030, arXiv:hep-ph/0203091.

[73] M. S. Carena, A. Delgado, E. Ponton, T. M. P. Tait, and C. E. M. Wagner, "Precision electroweak data and unification of couplings in warped extra dimensions," *Phys. Rev.* **D68** (2003) 035010, arXiv:hep-ph/0305188.

[74] M. S. Carena, A. Delgado, E. Ponton, T. M. P. Tait, and C. E. M. Wagner, "Warped fermions and precision tests," *Phys. Rev.* **D71** (2005) 015010, arXiv:hep-ph/0410344.

[75] K. Agashe *et al.*, "LHC Signals for Warped Electroweak Neutral Gauge Bosons," *Phys. Rev.* **D76** (2007) 115015, arXiv:0709.0007 [hep-ph].

[76] M. S. Carena, E. Ponton, J. Santiago, and C. E. M. Wagner, "Electroweak constraints on warped models with custodial symmetry," *Phys. Rev.* **D76** (2007) 035006, arXiv:hep-ph/0701055.

[77] A. D. Medina, N. R. Shah, and C. E. M. Wagner, "Gauge-Higgs Unification and Radiative Electroweak Symmetry Breaking in Warped Extra Dimensions," *Phys. Rev.* **D76** (2007) 095010, arXiv:0706.1281 [hep-ph].

[78] M. E. Albrecht, M. Blanke, A. J. Buras, B. Duling, and K. Gemmler, "Electroweak and Flavour Structure of a Warped Extra Dimension with Custodial Protection," *JHEP* **09** (2009) 064, arXiv:0903.2415 [hep-ph].

[79] Y. A. Golfand and E. P. Likhtman, "Extension of the Algebra of Poincare Group Generators and Violation of p Invariance," *JETP Lett.* **13** (1971) 323–326.

[80] D. V. Volkov and V. P. Akulov, "Possible universal neutrino interaction," *JETP Lett.* **16** (1972) 438–440.

[81] J. Wess and B. Zumino, "Supergauge Transformations in Four-Dimensions," *Nucl. Phys.* **B70** (1974) 39–50.

[82] M. T. Grisaru, W. Siegel, and M. Rocek, "Improved Methods for Supergraphs," *Nucl. Phys.* **B159** (1979) 429.

[83] L. Girardello and M. T. Grisaru, "Soft Breaking of Supersymmetry," *Nucl. Phys.* **B194** (1982) 65.

[84] G. 't Hooft, "Naturalness, chiral symmetry, and spontaneous chiral symmetry breaking," *NATO Adv. Study Inst. Ser. B Phys.* **59** (1980) 135.

[85] M. Leurer, Y. Nir, and N. Seiberg, "Mass matrix models: The Sequel," *Nucl. Phys.* **B420** (1994) 468–504, arXiv:hep-ph/9310320.

[86] L. Wolfenstein, "Parametrization of the Kobayashi-Maskawa Matrix," *Phys. Rev. Lett.* **51** (1983) 1945.

[87] H. K. Dreiner, "An introduction to explicit R-parity violation," arXiv:hep-ph/9707435.

[88] M. Misiak, S. Pokorski, and J. Rosiek, "Supersymmetry and FCNC effects," *Adv. Ser. Direct. High Energy Phys.* **15** (1998) 795–828, arXiv:hep-ph/9703442.

[89] J. Rosiek, "Complete set of Feynman rules for the MSSM – ERRATUM," arXiv:hep-ph/9511250.

[90] W. Altmannshofer, A. J. Buras, S. Gori, P. Paradisi, and D. M. Straub, "Anatomy and Phenomenology of FCNC and CPV Effects in SUSY Theories," *Nucl. Phys.* **B830** (2010) 17–94, arXiv:0909.1333 [hep-ph].

[91] S. P. Martin, "A Supersymmetry Primer," arXiv:hep-ph/9709356.

[92] S. Dimopoulos and D. W. Sutter, "The Supersymmetric flavor problem," *Nucl. Phys.* **B452** (1995) 496–512, arXiv:hep-ph/9504415.

[93] A. H. Chamseddine, R. L. Arnowitt, and P. Nath, "Locally Supersymmetric Grand Unification," *Phys. Rev. Lett.* **49** (1982) 970.

[94] S. P. Martin and M. T. Vaughn, "Two loop renormalization group equations for soft supersymmetry breaking couplings," *Phys. Rev.* **D50** (1994) 2282, arXiv:hep-ph/9311340.

[95] K. Agashe and C. D. Carone, "Supersymmetric flavor models and the $B \to \Phi K(S)$ anomaly," *Phys. Rev.* **D68** (2003) 035017, arXiv:hep-ph/0304229.

[96] Y. Nir and N. Seiberg, "Should squarks be degenerate?," *Phys. Lett.* **B309** (1993) 337–343, arXiv:hep-ph/9304307.

[97] E. Dudas, S. Pokorski, and C. A. Savoy, "Soft scalar masses in supergravity with horizontal $U(1)_X$ gauge symmetry," *Phys. Lett.* **B369** (1996) 255–261, arXiv:hep-ph/9509410.

[98] Y. Nir and G. Raz, "Quark squark alignment revisited," *Phys. Rev.* **D66** (2002) 035007, arXiv:hep-ph/0206064.

[99] A. Pomarol and D. Tommasini, "Horizontal symmetries for the supersymmetric flavor problem," *Nucl. Phys.* **B466** (1996) 3–24, arXiv:hep-ph/9507462.

[100] R. Barbieri, G. R. Dvali, and L. J. Hall, "Predictions From a U(2) Flavour Symmetry In Supersymmetric Theories," *Phys. Lett.* **B377** (1996) 76–82, arXiv:hep-ph/9512388.

[101] R. Barbieri, L. J. Hall, S. Raby, and A. Romanino, "Unified theories with U(2) flavor symmetry," *Nucl. Phys.* **B493** (1997) 3–26, arXiv:hep-ph/9610449.

[102] R. Barbieri, L. J. Hall, and A. Romanino, "Consequences of a U(2) flavour symmetry," *Phys. Lett.* **B401** (1997) 47–53, arXiv:hep-ph/9702315.

[103] S. F. King and G. G. Ross, "Fermion masses and mixing angles from SU(3) family symmetry," *Phys. Lett.* **B520** (2001) 243–253, arXiv:hep-ph/0108112.

[104] S. F. King and G. G. Ross, "Fermion masses and mixing angles from SU(3) family symmetry and unification," *Phys. Lett.* **B574** (2003) 239–252, arXiv:hep-ph/0307190.

[105] G. G. Ross, L. Velasco-Sevilla, and O. Vives, "Spontaneous CP violation and non-Abelian family symmetry in SUSY," *Nucl. Phys.* **B692** (2004) 50–82, arXiv:hep-ph/0401064.

[106] S. Antusch, S. F. King, and M. Malinsky, "Solving the SUSY Flavour and CP Problems with SU(3) Family Symmetry," *JHEP* **06** (2008) 068, arXiv:0708.1282 [hep-ph].

[107] L. Calibbi *et al.*, "FCNC and CP Violation Observables in a SU(3)-flavoured MSSM," *Nucl. Phys.* **B831** (2010) 26–71, arXiv:0907.4069 [hep-ph].

[108] A. Delgado, A. Pomarol, and M. Quiros, "Electroweak and flavor physics in extensions of the standard model with large extra dimensions," *JHEP* **01** (2000) 030, arXiv:hep-ph/9911252.

[109] F. del Aguila and J. Santiago, "Universality limits on bulk fermions," *Phys. Lett.* **B493** (2000) 175–181, arXiv:hep-ph/0008143.

[110] A. J. Buras, B. Duling, and S. Gori, "The Impact of Kaluza-Klein Fermions on Standard Model Fermion Couplings in a RS Model with Custodial Protection," *JHEP* **09** (2009) 076, arXiv:0905.2318 [hep-ph].

[111] F. del Aguila, M. Perez-Victoria, and J. Santiago, "Effective description of quark mixing," *Phys. Lett.* **B492** (2000) 98–106, arXiv:hep-ph/0007160.

[112] F. del Aguila, M. Perez-Victoria, and J. Santiago, "Observable contributions of new exotic quarks to quark mixing," *JHEP* **09** (2000) 011, arXiv:hep-ph/0007316.

[113] W. Buchmuller and D. Wyler, "Effective Lagrangian Analysis of New Interactions and Flavor Conservation," *Nucl. Phys.* **B268** (1986) 621.

[114] C. Arzt, M. B. Einhorn, and J. Wudka, "Patterns of deviation from the standard model," *Nucl. Phys.* **B433** (1995) 41–66, arXiv:hep-ph/9405214.

[115] A. J. Buras, M. V. Carlucci, S. Gori, and G. Isidori, "Higgs-mediated FCNCs: Natural Flavour Conservation vs. Minimal Flavour Violation," arXiv:1005.5310 [hep-ph].

[116] K. Agashe and R. Contino, "Composite Higgs-Mediated FCNC," *Phys. Rev.* **D80** (2009) 075016, arXiv:0906.1542 [hep-ph].

[117] A. Azatov, M. Toharia, and L. Zhu, "Higgs Mediated FCNC's in Warped Extra Dimensions," *Phys. Rev.* **D80** (2009) 035016, arXiv:0906.1990 [hep-ph].

[118] B. Duling, "A Comparative Study of Contributions to ϵ_K in the RS Model," arXiv:0912.4208 [hep-ph].

[119] K. Agashe, G. Perez, and A. Soni, "B-factory signals for a warped extra dimension," *Phys. Rev. Lett.* **93** (2004) 201804, arXiv:hep-ph/0406101.

[120] C. Csaki, A. Falkowski, and A. Weiler, "The Flavor of the Composite Pseudo-Goldstone Higgs," *JHEP* **09** (2008) 008, arXiv:0804.1954 [hep-ph].

[121] G. Cacciapaglia *et al.*, "A GIM Mechanism from Extra Dimensions," *JHEP* **04** (2008) 006, arXiv:0709.1714 [hep-ph].

[122] A. L. Fitzpatrick, G. Perez, and L. Randall, "Flavor from Minimal Flavor Violation & a Viable Randall- Sundrum Model," arXiv:0710.1869 [hep-ph].

[123] C. Csaki, A. Falkowski, and A. Weiler, "A Simple Flavor Protection for RS," *Phys. Rev.* **D80** (2009) 016001, arXiv:0806.3757 [hep-ph].

[124] G. F. Giudice, M. Nardecchia, and A. Romanino, "Hierarchical Soft Terms and Flavor Physics," *Nucl. Phys.* **B813** (2009) 156–173, arXiv:0812.3610 [hep-ph].

[125] L. J. Hall, V. A. Kostelecky, and S. Raby, "New Flavor Violations in Supergravity Models," *Nucl. Phys.* **B267** (1986) 415.

[126] F. Gabbiani, E. Gabrielli, A. Masiero, and L. Silvestrini, "A complete analysis of FCNC and CP constraints in general SUSY extensions of the standard model," *Nucl. Phys.* **B477** (1996) 321–352, arXiv:hep-ph/9604387.

[127] K. Blum, Y. Grossman, Y. Nir, and G. Perez, "Combining $K - \bar{K}$ mixing and $D - \bar{D}$ mixing to constrain the flavor structure of new physics," *Phys. Rev. Lett.* **102** (2009) 211802, arXiv:0903.2118 [hep-ph].

[128] G. F. Giudice and R. Rattazzi, "Theories with gauge-mediated supersymmetry breaking," *Phys. Rept.* **322** (1999) 419–499, arXiv:hep-ph/9801271.

[129] G. D'Ambrosio, G. F. Giudice, G. Isidori, and A. Strumia, "Minimal flavour violation: An effective field theory approach," *Nucl. Phys.* **B645** (2002) 155–187, arXiv:hep-ph/0207036.

[130] A. J. Buras, P. Gambino, M. Gorbahn, S. Jager, and L. Silvestrini, "Universal unitarity triangle and physics beyond the standard model," *Phys. Lett.* **B500** (2001) 161–167, arXiv:hep-ph/0007085.

[131] R. S. Chivukula and H. Georgi, "Composite Technicolor Standard Model," *Phys. Lett.* **B188** (1987) 99.

[132] L. J. Hall and L. Randall, "Weak scale effective supersymmetry," *Phys. Rev. Lett.* **65** (1990) 2939–2942.

[133] L. Mercolli and C. Smith, "EDM constraints on flavored CP-violating phases," *Nucl. Phys.* **B817** (2009) 1–24, arXiv:0902.1949 [hep-ph].

[134] S. Dimopoulos and G. F. Giudice, "Naturalness constraints in supersymmetric theories with nonuniversal soft terms," *Phys. Lett.* **B357** (1995) 573–578, arXiv:hep-ph/9507282.

[135] A. G. Cohen, D. B. Kaplan, and A. E. Nelson, "The more minimal supersymmetric standard model," *Phys. Lett.* **B388** (1996) 588–598, arXiv:hep-ph/9607394.

[136] G. F. Giudice, M. Nardecchia, and A. Romanino, "SUSY contributions to $\phi(B(s))$ from hierarchical sfermions," *J. Phys. Conf. Ser.* **171** (2009) 012059.

[137] R. Barbieri, E. Bertuzzo, M. Farina, P. Lodone, and D. Pappadopulo, "A Non Standard Supersymmetric Spectrum," arXiv:1004.2256 [hep-ph].

[138] H.-C. Cheng, J. L. Feng, and N. Polonsky, "Super-oblique corrections and non-decoupling of supersymmetry breaking," *Phys. Rev.* **D56** (1997) 6875–6884, arXiv:hep-ph/9706438.

[139] **ARGUS** Collaboration, H. Albrecht *et al.*, "Observation of B0 - anti-B0 Mixing," *Phys. Lett.* **B192** (1987) 245.

[140] **CLEO** Collaboration, M. Artuso *et al.*, "B0 anti-B0 Mixing at the Upsilon (4S)," *Phys. Rev. Lett.* **62** (1989) 2233.

[141] S. Herrlich and U. Nierste, "Enhancement of the $K(L) - K(S)$ mass difference by short distance QCD corrections beyond leading logarithms," *Nucl. Phys.* **B419** (1994) 292–322, arXiv:hep-ph/9310311.

[142] A. J. Buras, M. Jamin, and P. H. Weisz, "LEADING AND NEXT-TO-LEADING QCD CORRECTIONS TO epsilon PARAMETER AND B0 - anti-B0 MIXING IN THE PRESENCE OF A HEAVY TOP QUARK," *Nucl. Phys.* **B347** (1990) 491–536.

[143] S. Herrlich and U. Nierste, "The Complete $|\Delta S| = 2$ Hamiltonian in the Next-To-Leading Order," *Nucl. Phys.* **B476** (1996) 27–88, arXiv:hep-ph/9604330.

[144] A. J. Buras and R. Fleischer, "Quark mixing, CP violation and rare decays after the top quark discovery," *Adv. Ser. Direct. High Energy Phys.* **15** (1998) 65–238, arXiv:hep-ph/9704376.

[145] G. Burdman, "Flavor violation in warped extra dimensions and CP asymmetries in B decays," *Phys. Lett.* **B590** (2004) 86–94, arXiv:hep-ph/0310144.

[146] G. Moreau and J. I. Silva-Marcos, "Flavour physics of the RS model with KK masses reachable at LHC," *JHEP* **03** (2006) 090, arXiv:hep-ph/0602155.

[147] S. Chang, C. S. Kim, and J. Song, "Constraint of $B^0_{d,s} - \bar{B}^0_{d,s}$ mixing on warped extra- dimension model," *JHEP* **02** (2007) 087, arXiv:hep-ph/0607313.

[148] A. J. Buras, S. Jager, and J. Urban, "Master formulae for $\Delta(F) = 2$ NLO-QCD factors in the standard model and beyond," *Nucl. Phys.* **B605** (2001) 600–624, arXiv:hep-ph/0102316.

[149] M. Ciuchini *et al.*, "Next-to-leading order QCD corrections to Delta(F) = 2 effective Hamiltonians," *Nucl. Phys.* **B523** (1998) 501–525, arXiv:hep-ph/9711402.

[150] A. J. Buras, M. Misiak, and J. Urban, "Two-loop QCD anomalous dimensions of flavour-changing four-quark operators within and beyond the standard model," *Nucl. Phys.* **B586** (2000) 397–426, arXiv:hep-ph/0005183.

[151] R. Babich *et al.*, "$K_0 - \bar{K}_0$ mixing beyond the standard model and CP- violating electroweak penguins in quenched QCD with exact chiral symmetry," *Phys. Rev.* **D74** (2006) 073009, arXiv:hep-lat/0605016.

[152] D. Becirevic, V. Gimenez, G. Martinelli, M. Papinutto, and J. Reyes, "B-parameters of the complete set of matrix elements of $\Delta(B) = 2$ operators from the lattice," *JHEP* **04** (2002) 025, arXiv:hep-lat/0110091.

[153] C. Aubin, J. Laiho, and R. S. Van de Water, "The neutral kaon mixing parameter B_K from unquenched mixed-action lattice QCD," *Phys. Rev.* **D81** (2010) 014507, arXiv:0905.3947 [hep-lat].

[154] V. Lubicz and C. Tarantino, "Flavour physics and Lattice QCD: averages of lattice inputs for the Unitarity Triangle Analysis," *Nuovo Cim.* **123B** (2008) 674–688, arXiv:0807.4605 [hep-lat].

[155] C. Hamzaoui, M. Pospelov, and M. Toharia, "Higgs-mediated FCNC in supersymmetric models with large tan(beta)," *Phys. Rev.* **D59** (1999) 095005, arXiv:hep-ph/9807350.

[156] A. J. Buras, P. H. Chankowski, J. Rosiek, and L. Slawianowska, "$\Delta M_{d,s}, B^0_{d,s} \to \mu^+\mu^-$ and $B \to X_s\gamma$ in supersymmetry at large $\tan\beta$," *Nucl. Phys.* **B659** (2003) 3, arXiv:hep-ph/0210145.

[157] L. J. Hall, R. Rattazzi, and U. Sarid, "The Top quark mass in supersymmetric SO(10) unification," *Phys. Rev.* **D50** (1994) 7048–7065, arXiv:hep-ph/9306309.

[158] M. S. Carena, M. Olechowski, S. Pokorski, and C. E. M. Wagner, "Electroweak symmetry breaking and bottom - top Yukawa unification," *Nucl. Phys.* **B426** (1994) 269–300, arXiv:hep-ph/9402253.

[159] D. Becirevic *et al.*, "$B_d - \bar{B}_d$ mixing and the $B_d \to J/\psi K_s$ asymmetry in general SUSY models," *Nucl. Phys.* **B634** (2002) 105–119, arXiv:hep-ph/0112303.

[160] **Particle Data Group** Collaboration, W. M. Yao *et al.*, "Review of particle physics," *J. Phys.* **G33** (2006) 1–1232.

[161] A. J. Buras, D. Guadagnoli, and G. Isidori, "On ϵ_K beyond lowest order in the Operator Product Expansion," *Phys. Lett.* **B688** (2010) 309–313, arXiv:1002.3612 [hep-ph].

[162] Z. Ligeti, M. Papucci, and G. Perez, "Implications of the measurement of the $B_s^0 - \bar{B}_s^0$ mass difference," *Phys. Rev. Lett* **97** (2006) 101801, arXiv:hep-ph/0604112.

[163] M. Blanke, A. J. Buras, D. Guadagnoli, and C. Tarantino, "Minimal Flavour Violation Waiting for Precise Measurements of ΔM_s, $S_{\psi\phi}$, A_{SL}^s, $|V_u b|$, γ and $B_{s,d}^0 \to \mu^+\mu^-$," *JHEP* **10** (2006) 003, arXiv:hep-ph/0604057.

[164] **CDF** Collaboration, T. Aaltonen *et al.*, "First Flavor-Tagged Determination of Bounds on Mixing- Induced CP Violation in $B_s^0 \to J/\psi\phi$ Decays," *Phys. Rev. Lett.* **100** (2008) 161802, arXiv:0712.2397 [hep-ex].

[165] **D0** Collaboration, V. M. Abazov *et al.*, "Measurement of B_s^0 mixing parameters from the flavor-tagged decay $B_s^0 \to J/\psi\phi$," *Phys. Rev. Lett.* **101** (2008) 241801, arXiv:0802.2255 [hep-ex].

[166] **The D0** Collaboration, V. M. Abazov *et al.*, "Evidence for an anomalous like-sign dimuon charge asymmetry," arXiv:1005.2757 [hep-ex].

[167] **Heavy Flavor Averaging Group** Collaboration, E. Barberio *et al.*, "Averages of $b-$hadron and $c-$hadron Properties at the End of 2007," arXiv:0808.1297 [hep-ex].

[168] Talk by Louise Oakes at the Flavor Physics and CP Violation Conference (FPCP 2010) in Turin, May 25-29, 2010.

[169] **Particle Data Group** Collaboration, C. Amsler *et al.*, "Review of particle physics," *Phys. Lett.* **B667** (2008) 1.

[170] M. Ciuchini, E. Franco, V. Lubicz, F. Mescia, and C. Tarantino, "Lifetime differences and CP violation parameters of neutral B mesons at the next-to-leading order in QCD," *JHEP* **08** (2003) 031, arXiv:hep-ph/0308029.

[171] **CDF** Collaboration, A. Abulencia *et al.*, "Observation of $B_s^0 - \bar{B}_s^0$ oscillations," *Phys. Rev. Lett.* **97** (2006) 242003, arXiv:hep-ex/0609040.

[172] **UTfit** Collaboration, M. Bona *et al.*, "The unitarity triangle fit in the standard model and hadronic parameters from lattice QCD: A reappraisal after the measurements of $\Delta(m(s))$ and BR($B \to \tau\nu_\tau$)," *JHEP* **10** (2006) 081, arXiv:hep-ph/0606167. Updates available on http://www.utfit.org/.

[173] M. Blanke, A. J. Buras, B. Duling, K. Gemmler, and S. Gori, "Rare K and B Decays in a Warped Extra Dimension with Custodial Protection," *JHEP* **03** (2009) 108, arXiv:0812.3803 [hep-ph].

[174] G. Buchalla and A. J. Buras, "The rare decays $K \to \pi\nu\bar{\nu}$, $B \to X\nu\bar{\nu}$ and $B \to \ell^+\ell^-$: An update," *Nucl. Phys.* **B548** (1999) 309–327, arXiv:hep-ph/9901288.

[175] A. J. Buras, M. Gorbahn, U. Haisch, and U. Nierste, "The rare decay $K^+ \to \pi^+ \nu\bar{\nu}$ at the next-to-next- to-leading order in QCD," *Phys. Rev. Lett.* **95** (2005) 261805, arXiv:hep-ph/0508165.

[176] A. J. Buras, M. Gorbahn, U. Haisch, and U. Nierste, "Charm quark contribution to $K^+ \to \pi^+ \nu\bar{\nu}$ at next-to-next-to-leading order," *JHEP* **11** (2006) 002, arXiv:hep-ph/0603079.

[177] A. J. Buras, F. Schwab, and S. Uhlig, "Waiting for precise measurements of $K^+ \to \pi^+ \nu\bar{\nu}$ and $K_L \to \pi^0 \nu\bar{\nu}$," *Rev. Mod. Phys.* **80** (2008) 965–1007, arXiv:hep-ph/0405132.

[178] Y. Nir and M. P. Worah, "Probing the flavor and CP structure of supersymmetric models with $K\pi\nu\bar{\nu}$ decays," *Phys. Lett.* **B423** (1998) 319–326, arXiv:hep-ph/9711215.

[179] A. J. Buras, A. Romanino, and L. Silvestrini, "$K \to \pi\nu\bar{\nu}$: A model independent analysis and supersymmetry," *Nucl. Phys.* **B520** (1998) 3–30, arXiv:hep-ph/9712398.

[180] G. Colangelo and G. Isidori, "Supersymmetric contributions to rare kaon decays: Beyond the single mass-insertion approximation," *JHEP* **09** (1998) 009, arXiv:hep-ph/9808487.

[181] A. J. Buras, G. Colangelo, G. Isidori, A. Romanino, and L. Silvestrini, "Connections between epsilon'/epsilon and rare kaon decays in supersymmetry," *Nucl. Phys.* **B566** (2000) 3–32, arXiv:hep-ph/9908371.

[182] G. Isidori and P. Paradisi, "Higgs-mediated $K \to \pi\nu\bar{\nu}$ in the MSSM at large tan(beta)," *Phys. Rev.* **D73** (2006) 055017, arXiv:hep-ph/0601094.

[183] A. J. Buras, T. Ewerth, S. Jager, and J. Rosiek, "$K^+ \to \pi^+ \nu\bar{\nu}$ and $K(L) \to \pi^0 \nu\bar{\nu}$ decays in the general MSSM," *Nucl. Phys.* **B714** (2005) 103–136, arXiv:hep-ph/0408142.

[184] G. Isidori, "Flavor physics with light quarks and leptons," arXiv:hep-ph/0606047.

[185] C. Smith, "Theory review on rare K decays: Standard model and beyond," arXiv:hep-ph/0608343.

[186] A. J. Buras, R. Fleischer, S. Recksiegel, and F. Schwab, "Anatomy of prominent B and K decays and signatures of CP- violating new physics in the electroweak penguin sector," *Nucl. Phys.* **B697** (2004) 133–206, arXiv:hep-ph/0402112.

[187] F. Mescia and C. Smith, "Improved estimates of rare K decay matrix-elements from K(l3) decays," *Phys. Rev.* **D76** (2007) 034017, arXiv:0705.2025 [hep-ph].

[188] G. Isidori, F. Mescia, and C. Smith, "Light-quark loops in $K \to \pi\nu\nu$," *Nucl. Phys.* **B718** (2005) 319–338, arXiv:hep-ph/0503107.

[189] P. H. Chankowski and L. Slawianowska, "$B^0_{d,s} \to \mu^-\mu^+$ decay in the MSSM," *Phys. Rev.* **D63** (2001) 054012, arXiv:hep-ph/0008046.

[190] M. Gorbahn and U. Haisch, "Charm quark contribution to $K(L) \to \mu^+\mu^-$ at next-to- next-to-leading order," *Phys. Rev. Lett.* **97** (2006) 122002, arXiv:hep-ph/0605203.

[191] B. Duling, *The Custodially Protected Randall-Sundrum Model: Global Features and Distinct Flavor Signatures*. PhD thesis, Technische Universitaet, Munich, 2010.

[192] **E949** Collaboration, A. V. Artamonov *et al.*, "New measurement of the $K^+ \to \pi^+\nu\bar{\nu}$ branching ratio," *Phys. Rev. Lett.* **101** (2008) 191802, arXiv:0808.2459 [hep-ex].

[193] **E391a** Collaboration, J. K. Ahn *et al.*, "Experimental study of the decay $K^0_L \to \pi^0\nu\bar{\nu}$," *Phys. Rev.* **D81** (2010) 072004, arXiv:0911.4789 [hep-ex].

[194] Y. Grossman and Y. Nir, "$K(L) \to \pi^0\nu\bar{\nu}$ beyond the standard model," *Phys. Lett.* **B398** (1997) 163–168, arXiv:hep-ph/9701313.

[195] J. Brod and M. Gorbahn, "Electroweak Corrections to the Charm Quark Contribution to $K^+ \to \pi^+\nu\bar{\nu}$," *Phys. Rev.* **D78** (2008) 034006, arXiv:0805.4119 [hep-ph].

[196] A. Antonelli *et al.*, "The NA62 rare kaon decay experiment photon veto system," *J. Phys. Conf. Ser.* **160** (2009) 012020.

[197] H. Nanjo, "J-PARC E14 K0TO experiment for $K_L \to \pi^0\nu\bar{\nu}$," *PoS* **KAON09** (2009) 047.

[198] **CDF** Collaboration, T. Aaltonen *et al.*, "Search for $B^0_s \to \mu^+\mu^-$ and $B^0_d \to \mu^+\mu^-$ decays with $2fb^{-1}$ of $p\bar{p}$ collisions," *Phys. Rev. Lett.* **100** (2008) 101802, arXiv:0712.1708 [hep-ex].

[199] **D0** Collaboration, V. M. Abazov *et al.*, "Search for $B_s \to \mu^+\mu^-$ at D0," *Phys. Rev.* **D76** (2007) 092001, arXiv:0707.3997 [hep-ex].

[200] G. Punzi, "Flavour physics at the Tevatron," arXiv:1001.4886 [hep-ex].

[201] A. J. Buras *et al.*, "Patterns of Flavour Violation in the Presence of a Fourth Generation of Quarks and Leptons," arXiv:1002.2126 [hep-ph].

[202] **LHCb** Collaboration, H. Ruiz, "Rare B decays at LHCb," *J. Phys. Conf. Ser.* **171** (2009) 012057.

[203] **E791** Collaboration, A. Heinson *et al.*, "Measurement of the branching ratio for the rare decay $K0(L) \to \mu^+\mu^-$," *Phys. Rev.* **D51** (1995) 985–1013.

[204] T. Inagaki *et al.*, "Measurement of the branching ratio of the decay $K0(L) \to \mu\mu$," *Phys. Rev. Lett.* **67** (1991) 2618–2621.

[205] G. Isidori and R. Unterdorfer, "On the short-distance constraints from $K(L,S) \to \mu^+\mu^-$," *JHEP* **01** (2004) 009, arXiv:hep-ph/0311084.

[206] M. Byrd, "The Geometry of SU(3)," arXiv:physics/9708015.

[207] K. Agashe, A. Azatov, and L. Zhu, "Flavor Violation Tests of Warped/Composite SM in the Two- Site Approach," *Phys. Rev.* **D79** (2009) 056006, arXiv:0810.1016 [hep-ph].

[208] C. Jarlskog and R. Stora, "Unitarity Polygons and CP Violation Areas and Phases in the Standard Electroweak Model," *Phys. Lett.* **B208** (1988) 268.

[209] U. Nierste, "Three Lectures on Meson Mixing and CKM phenomenology," arXiv:0904.1869 [hep-ph].

[210] Flavianet, "Precise tests in kaon decays," 2010. Available from http://www.lnf.infn.it/wg/vus/.

[211] S. Herrlich and U. Nierste, "Indirect CP violation in the neutral kaon system beyond leading logarithms," *Phys. Rev.* **D52** (1995) 6505–6518, arXiv:hep-ph/9507262.

[212] J. Urban, F. Krauss, U. Jentschura, and G. Soff, "Next-to-leading order QCD corrections for the B0 anti-B0 mixing with an extended Higgs sector," *Nucl. Phys.* **B523** (1998) 40–58, arXiv:hep-ph/9710245.

[213] **UTfit** Collaboration, M. Bona *et al.*, "Model-independent constraints on Δ F=2 operators and the scale of new physics," *JHEP* **03** (2008) 049, arXiv:0707.0636 [hep-ph].

[214] U. Chattopadhyay and P. Nath, "Probing supergravity grand unification in the Brookhaven g-2 experiment," *Phys. Rev.* **D53** (1996) 1648–1657, arXiv:hep-ph/9507386.

[215] J. Prades, "Standard Model Prediction of the Muon Anomalous Magnetic Moment," *Acta Phys. Polon. Supp.* **3** (2010) 75, arXiv:0909.2546 [hep-ph].

[216] J. A. Casas and S. Dimopoulos, "Stability bounds on flavor-violating trilinear soft terms in the MSSM," *Phys. Lett.* **B387** (1996) 107–112, arXiv:hep-ph/9606237.

[217] R. Barbieri and G. F. Giudice, "Upper Bounds on Supersymmetric Particle Masses," *Nucl. Phys.* **B306** (1988) 63.

[218] M. S. Carena, A. Menon, R. Noriega-Papaqui, A. Szynkman, and C. E. M. Wagner, "Constraints on B and Higgs physics in minimal low energy supersymmetric models," *Phys. Rev.* **D74** (2006) 015009, arXiv:hep-ph/0603106.

[219] W. Altmannshofer, A. J. Buras, and D. Guadagnoli, "The MFV limit of the MSSM for low tan(beta) : Meson mixings revisited," *JHEP* **11** (2007) 065, arXiv:hep-ph/0703200.

[220] M. Gorbahn, S. Jager, U. Nierste, and S. Trine, "The supersymmetric Higgs sector and $B-$ Bbar mixing for large tan β," `arXiv:0901.2065 [hep-ph]`.

[221] M. Ciuchini *et al.*, "D - $\bar{D}$ mixing and new physics: General considerations and constraints on the MSSM," *Phys. Lett.* **B655** (2007) 162–166, `arXiv:hep-ph/0703204`.

[222] M. Artuso *et al.*, "B, D and K decays," *Eur. Phys. J.* **C57** (2008) 309–492, `arXiv:0801.1833 [hep-ph]`.

[223] **MEGA** Collaboration, M. L. Brooks *et al.*, "New Limit for the Family-Number Non-conserving Decay $mu^+ \to e^+\gamma$," *Phys. Rev. Lett.* **83** (1999) 1521–1524, `arXiv:hep-ex/9905013`.

[224] B. C. Regan, E. D. Commins, C. J. Schmidt, and D. DeMille, "New limit on the electron electric dipole moment," *Phys. Rev. Lett.* **88** (2002) 071805.

[225] M. Pospelov and A. Ritz, "Electric dipole moments as probes of new physics," *Annals Phys.* **318** (2005) 119–169, `arXiv:hep-ph/0504231`.

[226] C. A. Baker *et al.*, "An improved experimental limit on the electric dipole moment of the neutron," *Phys. Rev. Lett.* **97** (2006) 131801, `arXiv:hep-ex/0602020`.

[227] M. Misiak *et al.*, "The first estimate of $B(\bar{B} \to X_s\gamma)$ at $O(\alpha(s)^2)$," *Phys. Rev. Lett.* **98** (2007) 022002, `arXiv:hep-ph/0609232`.

[228] **BABAR** Collaboration, B. Aubert *et al.*, "Measurement of the $B \to X_s\ell^+\ell^-$ branching fraction with a sum over exclusive modes," *Phys. Rev. Lett.* **93** (2004) 081802, `arXiv:hep-ex/0404006`.

[229] **Belle** Collaboration, M. Iwasaki *et al.*, "Improved measurement of the electroweak penguin process $B \to X_s l^+ l^-$," *Phys. Rev.* **D72** (2005) 092005, `arXiv:hep-ex/0503044`.

[230] T. Huber, E. Lunghi, M. Misiak, and D. Wyler, "Electromagnetic logarithms in $\bar{B} \to X_s l^+ l^-$," *Nucl. Phys.* **B740** (2006) 105–137, `arXiv:hep-ph/0512066`.

[231] V. Tisserand, "CKM fits as of winter 2009 and sensitivity to New Physics," `arXiv:0905.1572 [hep-ph]`.

[232] M. Blanke, "Insights from the Interplay of $K \to \pi\nu\bar{\nu}$ and ϵ_K on the New Physics Flavour Structure," *Acta Phys. Polon.* **B41** (2010) 127, `arXiv:0904.2528 [hep-ph]`.

[233] A. J. Buras, "Relations between $\Delta M(s,d)$ and B$(s,d) \to \mu\bar{\mu}$ in models with minimal flavor violation," *Phys. Lett.* **B566** (2003) 115–119, `arXiv:hep-ph/0303060`.

[234] T. E. Browder, T. Gershon, D. Pirjol, A. Soni, and J. Zupan, "New Physics at a Super Flavor Factory," `arXiv:0802.3201 [hep-ph]`.

[235] T. Aushev *et al.*, "Physics at Super B Factory," `arXiv:1002.5012 [hep-ex]`.